The Development of Condition Monitoring Strategies and Techniques appropriate to Mechanical Structures

Gordon Drummond

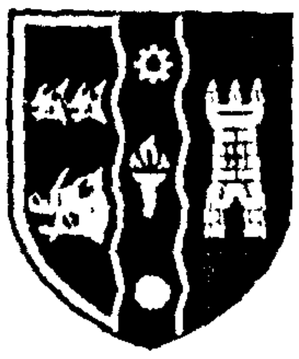

THE
ROBERT GORDON
UNIVERSITY
ABERDEEN

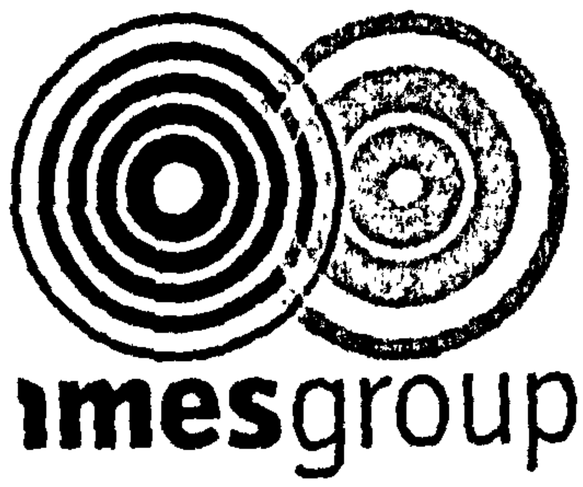

THESIS CONTAINS CD

The Development of Condition Monitoring Strategies and Techniques appropriate to Mechanical Structures

A thesis submitted in partial fulfilment of the requirements
of The Robert Gordon University
for the degree of Doctor of Philosophy

This research programme was carried out
in collaboration with Imes Group

November 2004

Acknowledgements

I would like to express my sincere gratitude to all those who were a part of formulation and compilation of this work. The acknowledgements are probably slightly longer than would be anticipated for a submission of this type as much of the work was conducted in an industrial environment and many experiments on an industrial scale.

My first acknowledgements must go to the programme sponsor, my academic supervisor and to my colleagues within the R & D unit at Imes. The programme sponsor is Melfort Campbell, Chief Executive of Imes Group, an individual of extraordinary self belief and commitment to this programme. His belief has never wavered that the work put into this programme would one day yield commercial benefits particularly to a subsidiary of Imes, WaterWeights™. Professor John Watson, my academic supervisor, has provided support and encouragement throughout the duration of the research without which it would never have been completed. Finally, my colleagues within Imes R & D, Kevin Fraser, Chris Mills, Dr. Dave McMinn, Nick Pashley, Lynn Barclay, Jon Gill and John Little during his time here, but now returned to RGU. The R & D unit have all been part of a bigger dream: the development of condition monitoring strategies and techniques, of which this work is a subset. I wish them well with their future careers.

For the experimental work documented in chapter three, my gratitude goes to laboratory technicians at Robert Gordon University, Doug Thom and Kevin Fraser. (now of Imes)

For the field tests described in chapter four, I am grateful to the Imes test team Bryce Lewis, Duncan Mitchell, Eric Laing and Roger Jamieson for their assistance in attaining the data that allowed this testing to be conducted on the pad-eyes. Thank you also to Ministry of Defence (MoD) for the provision of a dispensation that permitted the load test procedure to be amended to allow for two consecutive proof tests instead of the customary one. With regard to crane testing I would particularly like to thank Kevin Barnes (MoD) for both the financial assistance and knowledge in support of this work, and the dispensation to revise the MoD load test procedures to accommodate the AE tests for the testing of the Carrier cranes. Equally, the author would particularly like to thank Pat McCrory of BP for both the financial assistance and knowledge in support with the pedestal crane test. Thanks to Sparrows Offshore Ltd who as BP's major crane contractor provided both the three point bend test rig and general support. Offshore Crane Engineering provided the crane boom section, my gratitude to them also.

Additionally, the author would like to extend a special thanks to Chris Mills for his construction of the PUMA software, which was especially effective in reducing the laborious task of data analysis in the crane's destruction test. Thank you to my fellow employment colleagues, Kevin Fraser and John Little who both assisted with the practicalities and logistics with conducting a test of this magnitude.

For the tests conducted on the underwater vehicle pressure hull, I am grateful to Fraser Livingstone and his team at QinetiQ, Rosyth, who provided the facilities for such a trial and who additionally conducted the ACPD and ToFD NDT. And finally to Peter

Campbell, Sea Technology Group, DPA, MoD and James Bentley, MSX IPT, DPA, MoD, the programme sponsors.

During chapter 5 the investigation returns to the laboratory, my thanks to Graeme Budge, the current technician at RGU. Graeme kept both a cool head and judgement during the period of fatigue and critical stress intensity factors.

During the course of my career in the practice of AE implementation I have been indebted to a number of individuals who have provided both guidance and advice to me on the correct use of Acoustic Emission as a technology. The individuals who I feel have contributed to enhancing my knowledge are Phil Cole of Physical Acoustics Ltd, Adrian Pollock of Physical Acoustics Corporation and Hal Dunegan of DEC Inc.

Finally my thanks to my wife who undertook the thankless task of proof reading the thesis, a piece of work she described as dull! I hope she takes no offence to that fact that I have chosen not to take her advice of an insertion of a little sex and violence between chapters three and four 'just to spice it up a little'.

ABSTRACT

Recent legislation, LOLER, removed the compulsion of periodical proof testing of lifting equipment to ascertain its "fitness for purpose". It has become the responsibility of a competent person to assess equipment's fitness for purpose and ability for continued safe use. This thesis reviews the technologies available to the competent person to enable him/her to come to an informed decision regarding the condition of mechanical structures. It was identified that an optimal methodology would interrogate structural integrity whilst the equipment performed its intended function. Coupling a means of assessment with the equipment's operation allows the investigator to focus on only defective conditions that will limit the future operation. Such an approach of condition monitoring structural integrity as opposed to employing traditional methods of inspection that are essentially failure finding tasks permits the discrimination between benign and malignant defects. Restorative and replacement activities can therefore take place based upon the likelihood of equipment's functional failure.

The supplementary monitoring of Acoustic Emission (AE), with the established industrial practice of proof testing, was considered to provide data to monitor structural integrity and provide the basis upon which a structure can be re-qualified for future service. The nature of failure of engineering materials was examined which identified failure modes such as corrosion, creep and fatigue resulted in a progressive degradation of a localised area. The AE is a proportion of energy released during such deterioration. Further it was determined that the rate at which the deterioration increased was non-linear.

Within a laboratory environment wire ropes with seeded faults were subjected to a simulated life during which the qualitative and quantitative nature of the AE was investigated. It was found that the quantity of the emission generated during proof tests was indicative of the severity of the induced defect. This substantiated the claim that AE could be used to enhance the proof test and provide a means by which a condition assessment could be made at intervals through out the life of a structure.

A series of five case studies explored the use of AE on a variety of differing in-service mechanical structures, mostly lifting equipment. The case studies were conducted on pad-eyes, link-plates, cranes, both Electrical Overhead Travelling (EOT) and pedestal cranes and finally, an underwater vehicle pressure hull. The approach of using the combination of AE with a proof test was verified in the cases of pad-eyes and EOT cranes. In the instance of link plates, simultaneous measurement of strain and AE during a load test demonstrated the ability of AE to detect localised yielding. During the destruction test of a pedestal crane boom section, various conventional methods of AE evaluation were utilised to investigate which would provide the most reliable condition indicator; it was found that Intensity Analysis generated the most effective trendable measurement.

A study on a pressure hull with known fatigue cracks that were subjected to both static and dynamic testing whilst monitoring with AE was conducted. The fatigue cracks were sized pre and post the trial using Time of Flight Diffraction (ToFD). During the trial

Alternating Current Potential Drop (ACPD) was used to detect any growth as it occurred. Such techniques were used to substantiate claims AE could detect a propagating defect. When the AE is viewed in conjunction with ACPD results and the measurements attained with the ToFD it was clear that all three techniques concluded that crack growth occurred at two sites.

Finally the investigation returns to a laboratory to examine the robustness of the technique through the life of a mechanical structure. The objective being to identify if periodical measurement of AE taken during the course of the life of the structure would repetitively generate information pertaining to the identification of the flaw as well as the severity of the flaw as it initiates and propagates through to failure. A power law was fitted to the data acquired during the proof tests. The use of a power law was considered appropriate due to the previously identified non-linear nature of material failure. A Scanning Electron Microscope was used to visually examine the fracture surfaces. It was found that increasing increments between striations on the fracture surface illustrated the non-linear increase of crack extensions during fatigue and corroborated the appropriateness of fitting a power law to the proof test data.

Such an investigation permitted the conclusion that the approach of fitting a power law to the discrete energies from sequential proof tests is an appropriate method of attaining a trendable condition indicator. The competent person could employ such a methodology for the purposes of attaining information upon which an informed decision can be made on the continued safe use of mechanical structures.

1. **Drummond G.R; Watson J.F; & Taylor R.M (2001) "The Non Destructive Evaluation of Wire ropes – utilizing Acoustic Emission Techniques" Fleet Maintenance Symposium, San Diego, USA**
2. **Drummond G.R; Fraser K.F; Little J.L; Watson J.F; & Campbell P; (2002) "Assessing the Structural Integrity of Crane Booms using Acoustic Emission" 25th European Conference on Acoustic Emission Testing, Prague Czech Republic**
3. **Drummond G.R; Mills C.J; Watson J.F; & Walter T; (2003) "Using Wide Band Acoustic Emission to determine the condition of rolling element bearings" MFPT Society, 57th meeting, Impact of prognostics on organisational success, Virginia Beach USA**
4. **Drummond G.R; Campbell M; & Watson J.F; (2003) "Talking Structures" International Conference of Maintenance Societies, Perth Australia**
5. **Drummond G.R; (2004) "Assessing the structural performance of cranes" 9th North Sea Offshore Cranes Conference, Aberdeen, Scotland**
6. **Drummond G.R; & Watson J.F; (2004) "An investigation into the comparison of maintenance strategies past, present and future by enhancing periodic proof testing with Acoustic Emission to generate reliable through life structural integrity assurance" 26th European Conference on Acoustic Emission Testing, Berlin, Germany**

CHAPTER 1: Introduction

1.1 Overview

1.1.1 Thesis objectives

"The Development of Condition Monitoring Strategies and Techniques appropriate to Mechanical Structures" encapsulates a broad range of concepts. This work initially began as Government sponsored DTI scheme, the TCS (Teaching Company Scheme), which subsequently became the KTP (Knowledge Transfer Partnership.) These schemes provide technology transfer between academia and industry and as such tend to concentrate their attentions on successful market ready implementation and commercialisation. The initial focus of this thesis was consequently the implementation and validation of existing technology in an industrial environment. The investigation was subsequently extended into a research theme and presents a unique scientific contribution.

The initial TCS objectives were described as "for critical structures such as cranes and bridges, the development of a suite of PC measurement systems to monitor the stress induced during load testing. This will provide previously unavailable data to continuously monitor structural integrity".

The objectives further state that "Load testing legislation is moving away from statutory testing on a regular basis and putting the onus on the owner of the structure/equipment to ensure fitness for purpose and capability for safe operation. A complete system will give the owner comprehensive data on how the structure is performing under real load conditions, thus enabling informed decisions to be made on the asset's safety. The system will allow measurements to be taken either continuously or on a regular basis which will allow charting of the deterioration of the structure and planning of preventative maintenance."

The premise for such ambition is generated from two commercial drivers; the move away from prescriptive legislation towards a goal setting approach by the Health and Safety Executive (HSE) and additionally the introduction of the Lifting Operations and Lifting Equipment Regulations, LOLER.

LOLER,[1] came into force on December 5th 1998. Its accompanying code of practice states that it is now a matter for the competent person to determine the necessity and nature of any test. So whereas it had been previously compulsory to load test most lifting equipment,[2,3,4,5,6] this statutory instrument revoked all of the compulsion and shifted the responsibility on to the competent person to determine the applicability and usefulness of any load test.

With load testing having been previously mandatory on a periodic basis there was an identifiable need for research to investigate the means by which better information on the

health or well being of a mechanical structure could be attained. This would assist the competent person to come to an informed decision with respect to future preventative maintenance for mechanical structures.

The goal of this thesis was to review existing techniques and strategies of condition monitoring that may be applicable to mechanical structures and to determine a suitable approach which can be validated in laboratory tests and subsequently trial the technique in field. The intent is the provision of a supplementary tool for the competent person to assess structural integrity. The investigation ultimately focuses on proving that the technique acts as robust condition indicator that is indicative of damage progression throughout the life of mechanical structures.

The objectives can be summarised as:

- Conduct a review of condition monitoring approaches appropriate to mechanical structures in order to select an optimum technique
- Conduct a deeper review of precedence of the selected technique and formulate a research theme
- Verify the qualitative and quantitative nature of the selected technique in a laboratory environment
- Conduct field trials and highlight any benefits and limitations. Use complimentary methods to verify of results where possible
- Identify a programme of experimentation that will permit the formulation of an evaluation criterion for structural integrity assurance, thereby generating a unique scientific contribution

1.1.1.1 The development of condition monitoring strategies and techniques appropriate to mechanical structures – a definition

This section reviews the different methodologies by which mechanical structures can be monitored, examined or interrogated that can potentially forewarn of incipient failure. Such information can be used to implement a maintenance strategy that may involve remedial action. The remedial action may take many forms for example, instigating a repair, limiting the duty cycle or alternatively decommissioning the structure. This thesis will confine itself to provision of the information that enables the decision. Making recommendations on remedial action based upon the outcome of measurement is beyond the scope of this work.

A definition of condition monitoring is given, by Courney as "The assessment on a continuous or periodic basis of the mechanical and electrical condition of machinery, equipment and systems from the observations and/or recording of selected measured parameters".[7]

Condition monitoring has been applied widely to dynamic machinery applications where the well-being or health of the machine is interrogated on a continuous or periodic basis. Maintenance decisions are prioritised based upon the informed judgement provided by

measurements that are indicative of potentially problematic symptoms. Examples of measurements taken as conditional indicators are vibration analysis in rotating machinery and particle analysis of the oil on reciprocating engines. Such technologies enjoy widespread commercial acceptance. Condition monitoring is a well-established tool for the provision of information to maintainers and permits them to decide whether to provide a restorative or replacement task or indeed take no remedial action.

1.1.2 Thesis structure

Firstly, the history and philosophies of maintenance are explored to establish what is anticipated from a condition monitoring strategy or technique. An overview of the current tools and techniques that could be used for condition monitoring of structural health succeeds this.

Having reviewed the existing technology, chapter two examines the feasibility of using the conjunction of Acoustic Emission (AE) and periodic proof testing as a means of defect detection in mechanical structures.

The results of a series of trials on wire ropes are presented, in chapter three, demonstrating that the combination of the two technologies can identify structurally significant defects. Exploration of the qualitative and quantitative nature of the outputs shows that identification of defect severity is additionally possible. This work is documented in chapter three.

With successful demonstration in laboratory trials, the combination of the two technologies was implemented in the field. In field trials differing methods of verifying the results were employed. The successful field demonstrations illustrated a capability to enhance the currently available information for decision-making. Chapter four presents the results of the field trials in a series of case studies. The case studies predominately focus on the condition assessment of lifting equipment to which LOLER is applicable.

Chapter five extends the investigation in a laboratory to determine the robustness of the technology through the life of equipment. Specimens were subjected to cyclical three point bending fatigue and their longevity recorded, their structural performance was monitored throughout using AE. In contrast, a further series of samples were subjected to cyclical fatigue, but their lifetimes punctuated by periodic proof tests. The effect on the lifetimes of these proof tests was investigated by comparison with the lifetimes of those specimens without proof tests. Such an investigation permitted the compromise between longevity and empirical condition assessment to be explored. Preceding the introduction of LOLER, prescriptive legislation, statutory instrument 1019 [4] made it compulsory to periodically conduct proof testing. The specimen set that has its life punctuated with periodic proof tests replicates such an approach.

Chapter six reviews the investigation in its entirety and draws together the conclusive remarks and suggests manners in which the investigation might be elaborated upon.

1.2 Maintenance strategies

1.2.1 Introduction

The earliest recorded maintenance strategy [8] was known as breakdown or run to failure maintenance. One of the perceived drawbacks of such a strategy is that an extensive inventory of spares must be maintained to cater for all conceivable types of breakdowns to ensure downtime is minimised. This approach can equally result in high overtime costs of engineers and technicians required to conduct the repair. Such high levels of unplanned maintenance can also impact on the cost of loss of production. This strategy is utilised predominately when a mechanism is highly simplistic and not process or safety critical; in certain critical circumstances it may be employed, but is generally complimented with the use of redundancy. In some instances this particular maintenance strategy provides the most cost effective solution to industry.

Preventative or planned maintenance came about largely due to World War II, a period in which there was a reduced availability of skilled personnel who were available for repair and renewal tasks. During this period there was a corresponding increase in mechanisation in industrial practices. The mechanisation resulted in an increase in the sophistication of manufacturing plant and equally an increase in the dependency upon it. The premise of this strategy is one of periodic replacement of parts that are most likely to fail. Examples of such replacement components are seals, bearings and wear rings. This strategy was the logical development to breakdown maintenance, where historically the knowledge of which components failed most frequently had been established. Replacement could take place as a precautionary measure to reduce the probability of failure. Such a strategy is employed by industry predominately on machines that are process critical i.e. failure directly results in loss of production. The interludes between these routine maintenance periods are statistically determined from the mean time between failures (MTBF). The principle drawbacks are that new parts do not always improve reliability. In fact, conversely, the intrinsic nature of the replacement can drastically reduce reliability. Additionally, a part being replaced prior to the end of their useful lives is not an optimal use of resource.

The most recently developed strategy is that of predictive maintenance. Predictive maintenance involves the detection of small changes in a physical parameter that are known to have a direct correlation with degradation of the item. Changes in the measured parameter are used as a means of diagnosing the health of the equipment. Analysis of this data allows scheduled maintenance to take place prior to failure, whilst optimising the usage from the asset.

As knowledge has increased regarding maintenance strategies there has also been a corresponding change in the views of the manner in which equipment is anticipated to fail.[8,9] It is important to recognise the manner in which equipment fails as when employing a predictive maintenance strategy the selection and measurement of suitable parameter must be directly matched to the nature of the failure.

1.2.2 The changing views of failure

The changing views of failure are summarised diagrammatically in figure 1.1

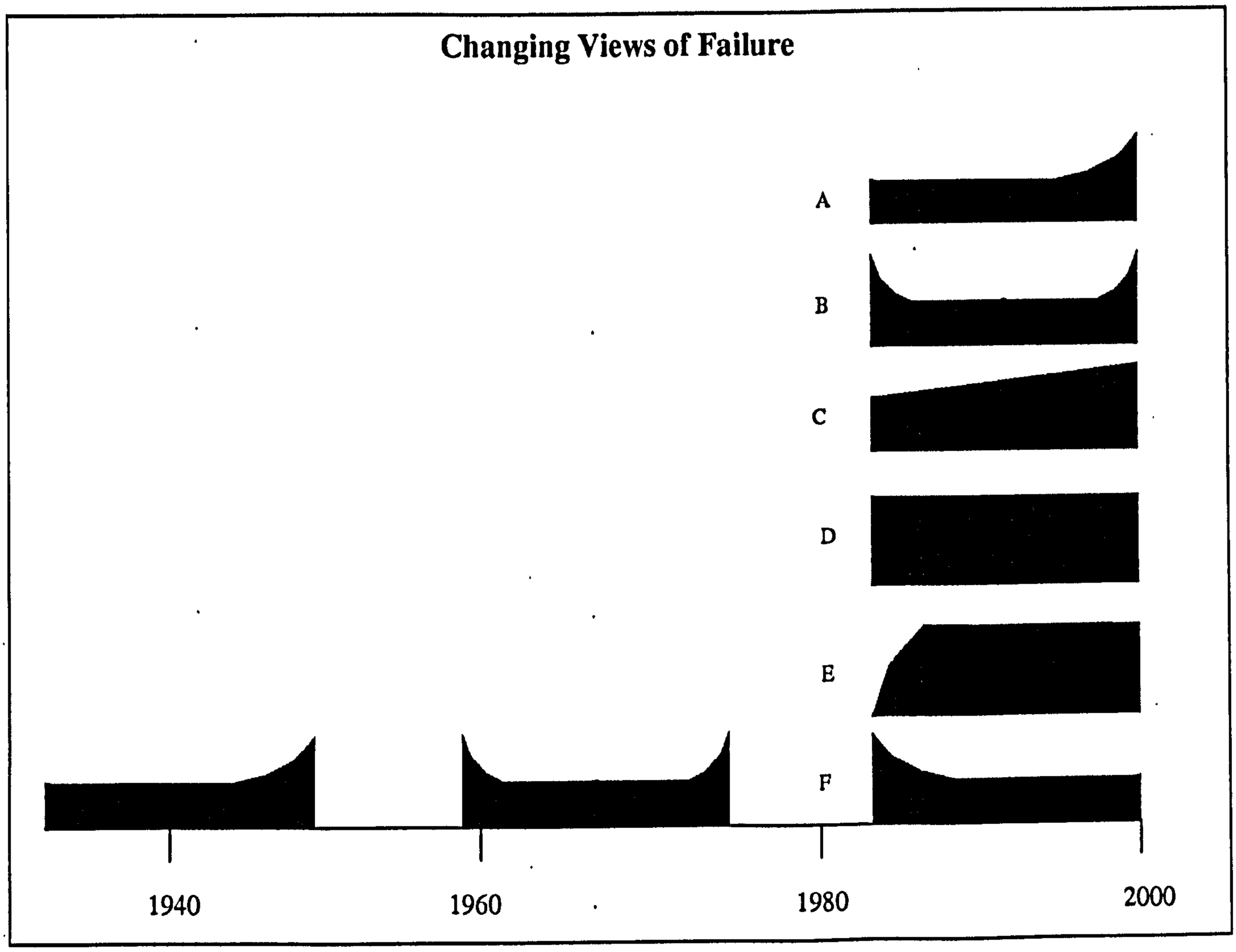

Figure 1.1: The changing views of failure [8,9]

The earliest view of failure was simply that as equipment aged the more likely it was to fail. This was superseded with the traditional bathtub curve, which took account of the "burn-in" phase of life where new items were found to fail early in their design life. The reasons that new parts fail may be due to poor quality controls at the manufacturing stage or alternatively erroneous replacement. Recent research suggests that there are in fact six different failure patterns as illustrated by figure 1.1. The first three types of failure, A, B, and C are all considered to be age related whereas D, E and F are considered to be random.[10]

A: Depicts an age related failure where the probability of failure increases as design life approaches

B: Bathtub curve, takes account infant mortality as well as the age related profile at the end of design of life

C: Age related failure that increases with increasing usage

D: A totally random failure distribution bearing no relationship to usage

E: Known as the "J" curve, depicts few failures during burn in, but failures become random after an initial wearing in period

F: Known as the reverse "J" curve and is understood to be the most common failure characteristic. Demonstrates a higher proportion of failures at the start of life, but becomes random in nature after an initial wear in period

From the evolution of the understanding of failure patterns and maintenance strategies grew a concept known as Reliability-Centred Maintenance (RCM), which is the marrying of a maintenance strategy to both the nature of failure and criticality of the machine. The original ideas, as cited, of RCM [8] were developed by Nowlan and Heap in 1978 and were derived from a study of failure and maintenance strategies employed in the aircraft industry. Their study showed that only 11% of failures were age related and challenged the necessity for planned maintenance. They suggested that if failures were largely independent of usage, then the merits of periodic replacement were questionable.

In 2001, the U.S Navy completed a similar investigation into the nature of failures on submarines and found that the proportion of age related failures they experienced was as high as 29%. They concluded that the higher percentage of age related failures was, in part due to the corrosive environment and rigorous pre-service component testing which virtually eliminated initial wear in failures. They supported the original findings of Nowlan and Heap that reliability and overhaul time were not directly related. Therefore as a strategy the U.S Navy would no longer prescribe time directed component renewal tasks, but would advocate the use of condition monitoring strategies to maintain safe operation and required asset functionality.[10]

Condition monitoring is a tool in service of maintenance and as such it is appropriate to outline the philosophy of reliability centred maintenance more fully to determine the role of condition monitoring in industrial practice and thus generate a context for this investigation.

1.2.3 Reliability-centred maintenance

RCM [8] achieves its aims through a consensus reached by a group of people, specifically the operator, the maintainer and those with the hands on experience of the equipment under review. The philosophy is to establish a hierarchical breakdown of equipment in terms of its consequence to the functional performance of the plant as a whole. The plant is assigned a top line functional objective, which is then distilled to individual systems, consisting of a series of machines and ultimately reduced to a component level that makes up the machine. Each component can then be ranked in terms of its contribution to the plant performance. Their relative importance is therefore quantitatively assessed

and subsequent care and attention in terms of maintenance can be matched appropriately to the consequence of failure. This prioritises maintenance to areas that are most likely to be problematic and ensures that the most appropriate types of inspection and testing are focussed at the identified modes of failure.

The process of assessment for a maintenance strategy may be divided into nine sequential steps. The complete breakdown of the steps can be viewed in Appendix I. It can be summarised as the identification and isolation of systems and the associated interface boundaries. A functional description is given for each system in numeric terms where possible. An analysis of the threat incurred by the consequence of a system failing is conducted, specifically identifying the risk in terms of both safety and productivity. There then follows a process of task selection by directly marrying maintenance activities to the functional failure.

Issues of the age and reliability relationship for the identified failure are examined. Where there exists a defined correlation between age and reliability scheduled restoration and discard tasks may be performed, often these are carried over from traditional schedules or because statutory legislation requires it. Alternatively, an on–condition task may be advised, as the name suggests, this comprises of condition monitoring tasks. The purpose is to establish a record of the asset's material state thus enabling a trend to be identified such that future performance can be predicted. Such preventative tasks are selected to limit in-service failures. RCM advocates that if the nature of failure is not known then "on condition tasks" should be implemented until such times as trends can be established that will ultimately allow forecasting of the failure.[8]

In the event that a preventative task cannot be found, the RCM analysis may conclude that a failure finding task is appropriate, a failure finding task is a proactive search for hidden defects. Other outcomes of the RCM analysis may suggest a redesign proposal that may involve changes in procedures to minimise the risks to personnel and the environment to an acceptable level. In some cases the analysis may suggest that a conscious decision be made to employ no scheduled maintenance. This may occur when the consequences of failure are either acceptably low or when there is no definable life. In such instances if the failure is process critical then redundancy may be employed.

RCM therefore employs all of the previously described approaches to maintenance, specifically, run to failure (no scheduled maintenance), planned (scheduled restoration and discard) and predictive (on condition).

The perceived benefits of employing RCM [8] are documented as being:

1) Increased plant availability
   - The required spares and expertise are available on hand at the time of scheduled downtime.
   - The time between overhauls can be maximised.

- The planned overhaul time is reduced as the nature of the failure is known.

2) Reduced maintenance costs. (for the reasons stated above)
3) Improved operator and end user safety.
   - The lead-time given by condition monitoring allows machinery to be stopped prior to a catastrophic failure.
4) More efficient plant operation.
   - The output of the plant can be matched to its condition.
5) More effective negotiations with repairers.
   - No longer are operators dependent on the availability of repairers because they can inform their suppliers of a lead-time.
6) Better customer relations.
   - Inconvenient breakdowns causing promises on delivery times to be broken no longer occur.
7) Operators can specify and design better systems.
   - Because operators have historically recorded machinery performances they can therefore select the most suitable product for the application, and feedback their knowledge to designers.

The strategy derived for RCM as outlined above is highly generic due to the fact that RCM must address a vast array of differing functional types of equipment and their associated failure modes.

TEAMM, (Techno-Economic Ageing and Maintenance Management) is an extension of RCM that has all the same essential features, but additionally combines probabilistic risk assessment within the standard framework of RCM. This maintenance model is currently employed within the UK Nuclear Power Industry. The new method is based on the assumption that there already exists a maintenance strategy that satisfies all the safety requirements and its purpose is to minimise the frequency of inspections without compromising safety.[11]

Work within the microelectronics industry suggests a new means of developing models for failure time based on newly developed statistical models.[12] There are in fact many hybrids of RCM which constitute different maintenance strategies for different industrial sectors, however they are all essentially derived from the previous principles.

It is suggested that RCM has enjoyed such widespread acceptance because all data is empirically derived and as such it is difficult to discredit. Based upon the assumption that maintenance should be prioritised on the condition of the equipment, the worthiness of this approach to generate condition monitoring strategies and techniques that are appropriate to mechanical structures becomes apparent. This investigation will review the options open to maintainers in order to ascertain the condition of mechanical structures and will additionally seek ways to forecast their failure.

The following section falls naturally into two types of approach for the interrogation of structural health or diagnostics: on condition tasks and failure finding tasks. This is considered to have evolved from both a historical perspective and mechanical design philosophies.

Structures are designed in two ways either for a safe life or to be damage tolerant. Both types of design have separate philosophies dependent on the structure's function and value. Safe life design utilises the material properties to ensure that there will be, as implied, a minimum acceptable service life, upon completion of which, such items are subjected to a scheduled discard and replacement task. Damage progression rates tend to be rapid post crack initiation, suggesting that periodical condition monitoring or inspection would be useless unless conducted with high frequency. Damage tolerance design uses materials that are environmentally durable and have long crack propagation durations permitting inspection intervals to be set based upon the fastest growth of failure mode. Such items are assessed for their fitness for service by a branch of science known as Non Destructive Testing (NDT). NDT in most instances uses an active means of seeking out defects and flaws and therefore falls within the definition of the RCM nomenclature of being typical of a failure finding task. This is in contrast to passive techniques, which become alerted to the degradation of the equipment through changes in the measurement of a physical parameter and could be described as on condition tasks.

1.3 Non-destructive testing and Non-destructive evaluation

1.3.1 Definitions

A broad definition of non-destructive testing that covers most uses is: the testing of a specimen that determines its serviceability without damage that could prevent its intended use.[14] Inversely, destructive testing is when the specimen is destroyed and it can no longer be used for the purpose for which it was intended. The rational behind destructive testing is that if the specimen fails a predetermined criterion then the destroyed specimen was unsatisfactory for the intended purpose.

NDT is the examination of an object or material with technology that does not affect its future usefulness. NDT can be used without destroying or damaging a product or material because it allows inspection without interfering with a product's final use. It provides the balance between quality control and cost-effectiveness. It may be used on all of a specimen group or used on randomly selected specimens to give a uniformity check without incurring the cost of testing them all.

The term "NDT" includes many methods that can:

- Detect internal or external imperfections
- Determine structure, composition, or material properties
- Measure geometric characteristics

Non-destructive evaluation (NDE) differs from NDT in that the evaluation determines the significance of the NDT findings. For example, virtually every structure or component contains cracks, defects or flaws inherently. Their significance hinges on factors such as material characteristics, operating temperature, tensile stress level, type of service involved and the environment. An objective of crack detection procedure (NDT) is to determine the location, size and shape of the defect whereas the implication of the defect upon equipment life would be deemed the evaluation. [13]

There is a vast range of NDT methods currently in use that can evaluate structural integrity to greater or lesser extents. Some are used only in laboratories, some are only suitable for specific geometries or materials and some methods are highly experimental with little documentary evidence to support them.

Good reasons for employing NDT include economic advantages, avoidance of physical injury, freedom from liability damages, and the desire for corporate bodies to be recognised for producing goods of the highest quality and reliability. Materials, products and equipment that fail to achieve design requirements or projected life due to undetected defects may require expensive repair or early replacement. Such defects may also be the cause of an unsafe condition possibly resulting in catastrophic failure, as well as loss of revenue due to unplanned plant shutdown.

NDT can be used throughout the process of manufacture both before and after production of raw materials such as ingots and castings, before and after fabrication, and before and after assembly of parts into a completed product. Applied at each stage of an item's construction prevents the inclusion of a defective component within an assembly, which may be impossible to identify after completion. Materials and welds can be examined and either accepted, rejected or repaired. NDT techniques can then be used to monitor the integrity of the item or structure throughout life.

To conclude, NDT may be as simple as looking at a part or counting the number of components going into a package before it is passed to the consumer. NDT may be far more sophisticated and expensive, but only if the cost or safety implications demand it.

For the purposes of this investigation, the methodologies described in the subsequent section are confined to the more traditional methods that could be realistically employed in industrial practice to assess structural integrity.

1.3.2 NDT Techniques

1.3.2.1 Overview

The following sections describe NDT methods. These are divided into methods that employ optical, magnetic, electrical, radiographic techniques and then in to methods that measure strain or the effect of strain. Each method is sub divided into headings of *Principle and Process,* which includes all salient and unique points to the subject matter, succeeded by comments on *Typical Items and Materials tested,* any perceived *Benefits* and finally in accordance with RCM nomenclature whether it is deemed to be *on condition task* or a *failure finding* task.

The objective of this section is to identify a technique or series of techniques that can be used to identify the degradation processes experienced by mechanical structures. It was previously stated that many techniques are failure finding and therefore are reliant upon active methods of inspection. Given that all structures contain inherent flaws, it is logical to assume that with increasing capabilities offered by active techniques the sizes and nature of reportable defects will only increase with technological development. Many structures exist through life with inherent defects that never propagate or contribute to a loss of strength.[14] For this reason it is preferable to employ a method that is passive and therefore susceptible to the detection of defects that result directly in a loss of strength i.e. ideally an on conditional task should be specified. Failure finding tasks using an active technique employed periodically that trend the propagation of a degradation process could equally be considered a condition monitoring task.

1.3.2.2 Visual Inspection

Visual inspection techniques range from being simplistic to sophisticated. This section explores general visual inspection followed by some visual inspection enhancement methods.

1.3.2.2 (a) General (VI)

Principle and Process

Almost any specimen can be visually examined to determine correctness of size, completeness and the accuracy of fabrication. In many cases visual inspection is used as the first form of NDT, in that if a specimen fails visual inspection then there is no need for more sophisticated techniques to be applied. Visual testing may also select portions of the specimen that should be inspected further by other techniques. Visual inspection for defect detection is assisted by the fact that the most serious defects are surface breaking.[15]

There are various mechanical and optical aids that assist with visual testing, these include, but are not limited to: [15]

- Measuring rules and tapes
- Callipers and micrometers
- Squares and angle measuring devices
- Thread, pitch, and thickness gauges
- Level gauges (liquid and laser) and plumb lines
- A variety of weld gauges

Initial visual inspection may confirm that the correct numbers of components are present, but mechanical aids may be required in order to check dimensions.

Optical aids for visual testing range from a simple mirror or magnifying glasses to sophisticated devices such as closed circuit television (CCTV) and coupled fibre optic scopes. A list of most optical aids currently in use are:

- Mirrors (especially small, angled mirrors)
- Magnifying glasses, multi-lens magnifiers, measuring magnifiers
- Microscopes (optical and electron)
- Optical flats (for surface flatness measurement)
- Boroscopes and fibre optic boroscopes
- Optical comparators
- Photographic records
- Closed circuit television (CCTV) systems (alone and coupled to boroscopes / microscopes)
- Machine vision systems
- Positioning and transport systems (often used with CCTV systems)
- Image enhancement (computer analysis and enhancement).

As the need increases to see smaller and smaller defects, the eyes need optical aids to enhance the image. In most instances, the greater the magnification, the smaller the area that can be seen in a single instance and the longer it takes to examine.

Mirrors allow vision in inaccessible areas to see around corners or past obstructions. Boroscopes are the combination of lenses placed in rigid tubes enabling inspection inside machinery such as jet engines or complex piping.

Optical fibres made up of flexible bundles can often permit access to areas, which a rigid boroscope cannot. Care must be taken to ensure the fibres are in exactly the same position at the inlet and outlet of the bundle to keep the image intact. Also, the fibres must be small to provide the optimum clarity. They may be connected to CCTV systems so that larger images can be generated and the inspection recorded on a storage medium. When such video systems are combined with computers, images can be enhanced and details not observable on the original image viewed. Before any mechanical or optical aids are used, the specimen should be well illuminated and its surface cleaned.

Typical items tested and Materials types
Visual inspection is not limited to any particular item or material.

Benefits
Often the inspection identifies areas where other NDT techniques need to be applied, or areas where the mechanical and optical aids may provide better inspection. Frequently visual inspection examination can eliminate the need for further, expensive testing procedures.

This can be considered both *failure finding task* as well as an *on condition task*, scheduled periodic inspection to investigate the functionality and condition is in essence a failure finding task in that it involves pro-action. However the use of machine vision systems where perhaps some expert recognition of a fault condition is programmable can be considered an "on condition task".

1.3.2.2 (b) Liquid Penetrant Testing

Principle and Process
Again, this method is limited to surface breaking defects, but is viewed as an enhancement to visual testing in that it can cover large areas quickly, cheaply and effectively.

After surface preparation, it is a four-step[16] process consisting of:

1. A coloured penetrant or dye is sprayed over the surface area being inspected
2. It is then wiped clean leaving no dye visible to the human eye

3. A developer (typically a dry powder) is then sprayed over the treated area and left to dry
4. The penetrant, when applied to the surface is retained in the indentation occupied by defects. The developer acts as a blotter, and highlights the defects by contrast. The indications are much bigger than the actual flaw size making them more easily visible

The technique may utilise a variety of differing types of penetrant. Maximum sensitivity is achieved through the use of a penetrant that is visible under ultra violet light. Sensitivity to crack sizes are documented as having a dependency on the surface roughness of the item under inspection, with polished surfaces, defects as small as 0.6 microns wide and 5 microns deep are reportable, whereas with rough cast surfaces the limit is in the region of 0.6 microns wide and 30 microns deep. Realistically, defects of dimensions with depths exceeding 30 microns and 0.5mm in length will be reliably detected.[17]

Typical Items and Materials Tested
Liquid penetrant Inspection is most often used on materials made from steel, particularly stainless. Liquid penetrant inspection can be performed on most non-porous clean materials. It is unsuitable for dirty materials or materials with a high surface roughness.

Benefits
Such technology has been fully automated using robotic handling and CCTV recording of the outputs with pattern recognition methods used to identify and categorise flaws.

With the exception of the described automated process, this technique can only be described as a *failure finding task.*

1.3.2.2 (c) Thermography

Principle and Process
All objects above the temperature of absolute zero produce thermal radiation, some of which is within the infra-red portion of the electromagnetic spectrum. Thermography is the process of detecting the invisible infra-red radiation and converting the energy detected into visible light. The resultant image depicts and quantifies the energy being radiated and reflected from the test object. The normal method is to use cameras with an infra-red sensitive detector and a transmitting lens.[18]

Thermography allows visualisation of the differences of radiated infra-red energy across the test object and shows those differences in either greyscale or pseudo-colour. An example is shown below.[19]

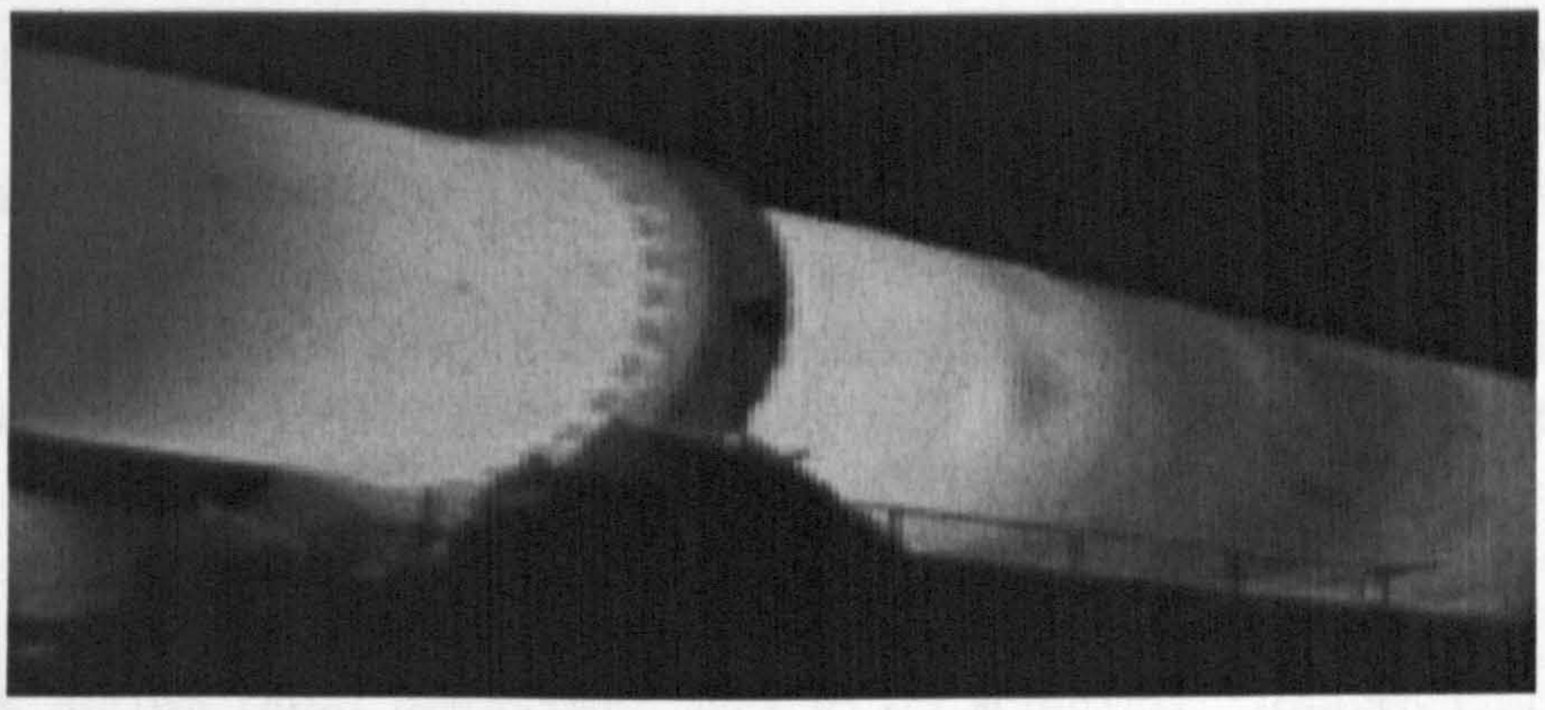

Figure 1.2: Thermographic Image

Using specialist cameras the technology can resolve temperature differences of 0.2°C.[18] Thermal images can be stored on an electronic storage medium or videotape and can be then overlaid on an image of the same scene in order to assist with interpretation.

A schematic of the process is shown below:

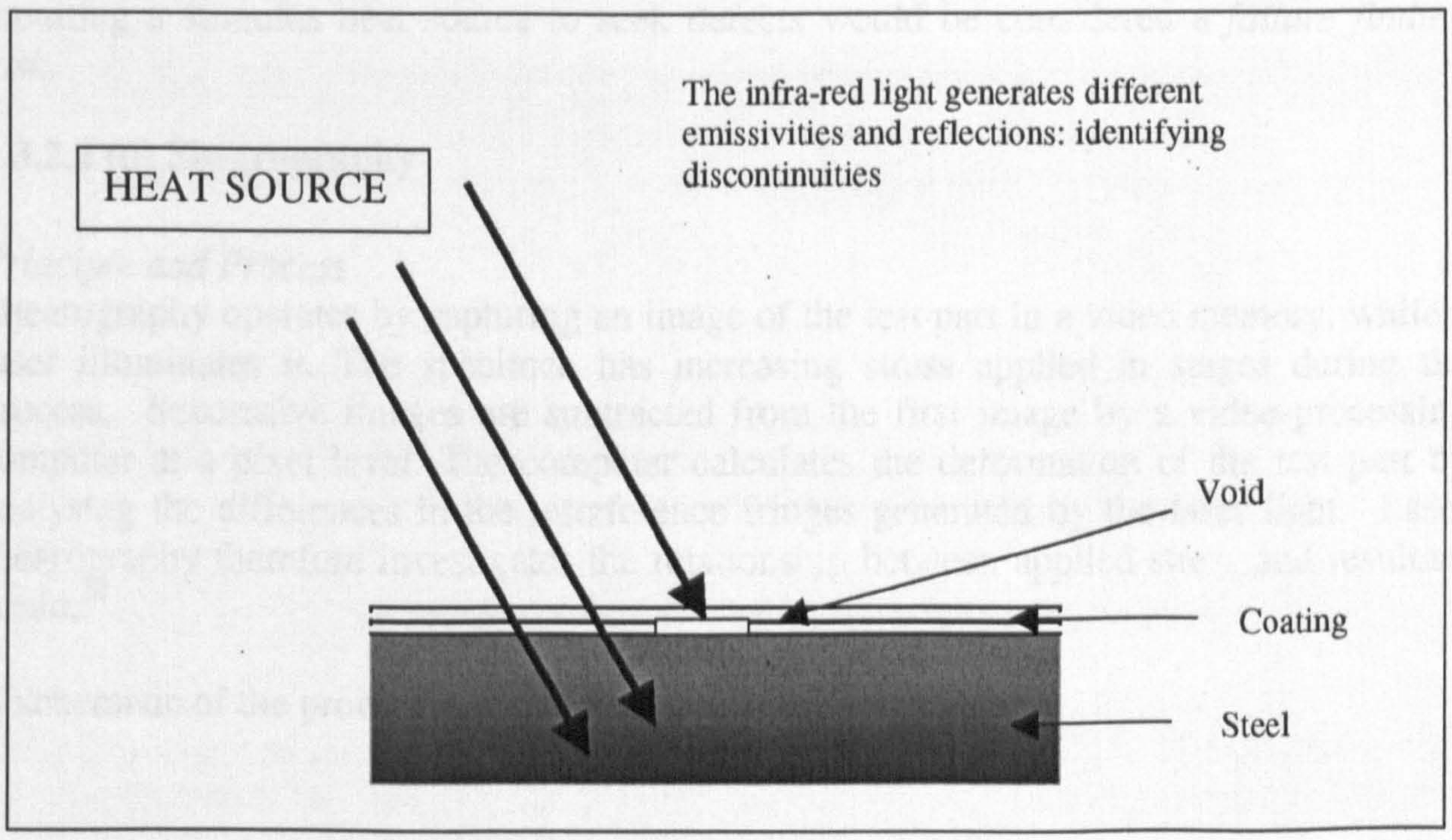

Figure 1.3: Principle of Thermography[18]

Typical items and Materials tested

The range of possible applications is enormous, but the two main applications are:

- Detection of heat leaks,[18] heat leaks occur during the assessment of insulation on boilers and steam pipes and from poor connections in electrical equipment.

- The provision of a heat source on one side of a specimen and examination of the other side. Non-uniformities in the infra-red emission correspond to internal inhomogeneities or large flaws

The majority of the work is carried out to date has been on coated materials or composite materials like Glass Reinforced Plastics (GRP), honeycombed and sandwich constructions.

Benefits
The technique allows rapid inspection rates to be achieved. Images can be stored on video tape and analysed by computer. Interpretation of images is straightforward as the extent and shape of defect is illustrated. Thermal imaging equipment is both non-contact and non-intrusive. A significant advantage is that the technology can be used during operating conditions and images can be subsequently averaged to give an empirical assessment of the material's behaviour under the dynamic condition.

Due to the nature of being able to conduct the assessment of the dynamic condition and the ability to detect changes this could be considered an *on condition task*, but the use of inputting a stimulus heat source to seek defects would be considered a *failure finding task*.

1.3.2.2 (d) Shearography

Principle and Process
Shearography operates by capturing an image of the test part in a video memory, while a laser illuminates it. The specimen has increasing stress applied in stages during the process. Successive images are subtracted from the first image by a video-processing computer at a pixel level. The computer calculates the deformation of the test part by analysing the differences in the interference fringes generated by the laser light. Laser shearography therefore investigates the relationship between applied stress and resultant strain.[20]

A schematic of the process is shown below: [21]

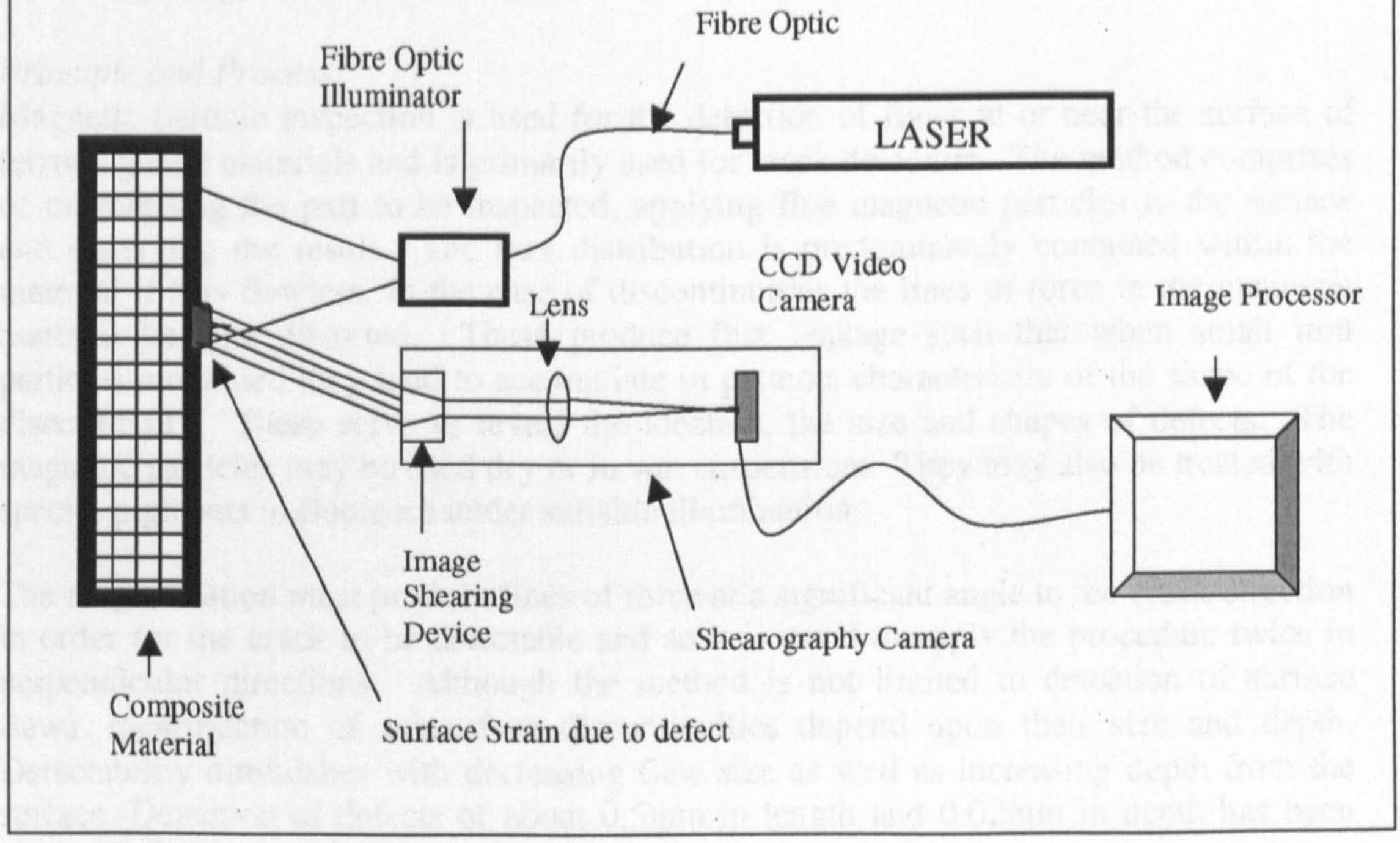

Figure 1.4: Principle of Shearography

Typical items and Materials tested

It can detect effectively impact damage in graphite epoxy structures, find delamination and bond defects in composite honeycomb or foam structures, and is sometimes used to validate repairs in composite constructions.[22] It has also been used on metallic jet engine components.

Benefits

The technique is non-contact and non-contaminating and is not affected by the part shape. The inspection rate is high. Again, it illustrates how the structure or component behaves under the loaded condition. The measured strains derived from a defect can be fed directly into a finite element system, which can perform fatigue analysis for lifetime prediction.[21]

Due to the nature of being able to conduct the assessment of the dynamic condition and detect changes this can be considered an *on condition task*.

1.3.2.3 Magnetic Methods

1.3.2.3 (a) Magnetic Particle Inspection (MPI)

Principle and Process
Magnetic particle inspection is used for the detection of flaws at or near the surface of ferromagnetic materials and is primarily used for crack detection. The method comprises of magnetising the part to be inspected, applying fine magnetic particles to the surface and observing the result. The flux distribution is predominately contained within the material if it is flawless. In the case of discontinuities the lines of force in the magnetic material become distorted. These produce flux leakage such that when small iron particles are added they tend to accumulate in patterns characteristic of the shape of the discontinuity. These serve to reveal the location, the size and shapes of defects. The magnetic particles may be used dry or in wet suspensions. They may also be treated with special pigments to fluoresce under suitable illumination.

The magnetisation must produce lines of force at a significant angle to the crack direction in order for the crack to be detectable and so it is usual to apply the procedure twice in perpendicular directions. Although the method is not limited to detection of surface flaws, identification of subsurface discontinuities depend upon their size and depth. Detectability diminishes with decreasing flaw size as well as increasing depth from the surface. Detection of defects of about 0.5mm in length and 0.02mm in depth has been reported.[23]

Typical Items and Materials tested
This method is limited to ferrous materials and does not tend to be used on austenitic steels [24] (generally low in iron composition and consequently has poor magnetic properties).

Benefits
This method enjoys widespread industrial acceptance.

Again, this would be considered a *failure finding task* as it involves a proactive search for defects.

1.3.2.3 (b) Magnetic Flux leakage Methods

Principle and Process
This method is not dissimilar to the previously outlined method of MPI in that the specimen must be magnetised either locally or globally, but in this case it is reliant on a Hall effect detector coil (physical phenomena when a specific type of crystal is placed within magnetic field and a potential difference is created across faces of the crystal). The detector coil reads the change in the magnetic flux between the magnetising poles. The signal generated is proportional to the magnetic flux leakage.[25, 26]

Typical Items and Materials tested
This technique is confined to ferrous materials.

Benefits
Unlike MPI this method is not sensitive to just surface or near surface flaws, but actually becomes increasing sensitive to far field flaws.

This is considered to be a *failure finding task* due to the necessity of seeking out flaws.

1.3.2.4 Electrical Methods

1.3.2.4 (a) Eddy Current Inspection

Principle and Process

Eddy current testing is an electromagnetic technique. Applications range from crack detection, to the rapid sorting of small components for flaws, size or material variations. When an energised coil is brought in close proximity to a conducting surface, circulating (eddy) currents are induced into the specimen. These currents set up a field that opposes the primary magnetic field. The eddy currents in the specimen are distorted by the presence of the flaws or material variations and consequently the impedance in the coil is altered to give discernable changes in current flow. This change is measured and can be displayed in a manner indicative of the type of flaw or material condition. [27]

This principle is illustrated below in figure 1.5. Consider a deep crack in the surface immediately underneath the coil. This will interrupt or reduce the eddy current flow, thus decreasing the loading on the coil and increasing its effective impedance.

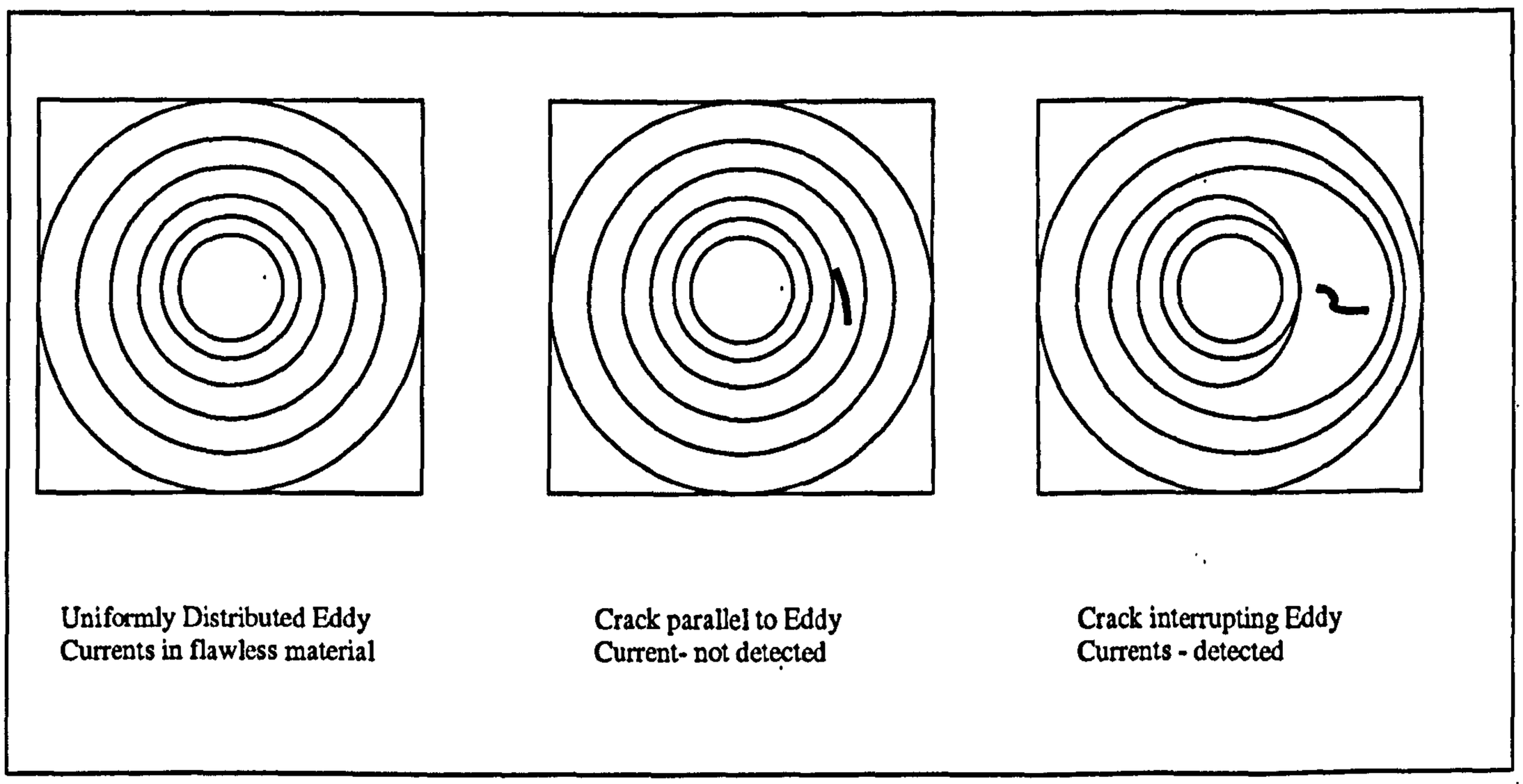

Figure 1.5: Principle of Eddy Current Technique

Note that the crack must interrupt the surface eddy current flow in order to be detected. Cracks lying parallel to the current path will not cause any significant interruption and will be undetected. Factors that affect the response are the material conductivity, magnetic permeability, the oscillating frequency, the geometry and the distance of the probe to the specimen.

The eddy current density, and thus the strength of the response from a flaw, is greatest at the surface of the metal being tested and diminishes with depth. The detection limits of eddy current testing depend upon the surface condition of the piece being inspected. It is

not normally possible to detect defects that are smaller than about three times the surface roughness of the component. Limits of detection on components with very good surface finish are of the order of 0.05 to 0.1mm deep[28].

Typical Items and Materials tested.
Commonly it is used in the aerospace, automotive, marine and manufacturing industries. Since no direct contact between the part and the induction coil is necessary, the method is well adapted to mechanised production applications for inspecting welded pipe, tubing, bars, billets, and cables. It can only be used on conductive materials.

Benefits
It experiences widespread industrial acceptance.

Unless automated, this is a pro-active search for flaws and therefore constitutes a *failure finding task.*

1.3.2.4 (b) Alternating Current Potential Difference Flaw Detection (ACPD)

Process and Principle
The potential difference can be used to measure crack depth. A reference for a material is established by determining the potential drop over a known distance. Comparison of the drop in potential can then be made with the potential difference across the width of a crack and hence a crack depth can be determined. Readings can be affected when the crack contains conductive particles such as corrosion products as this effectively shortens the conductive path.[29]

The principle is shown schematically in figure 1.6:

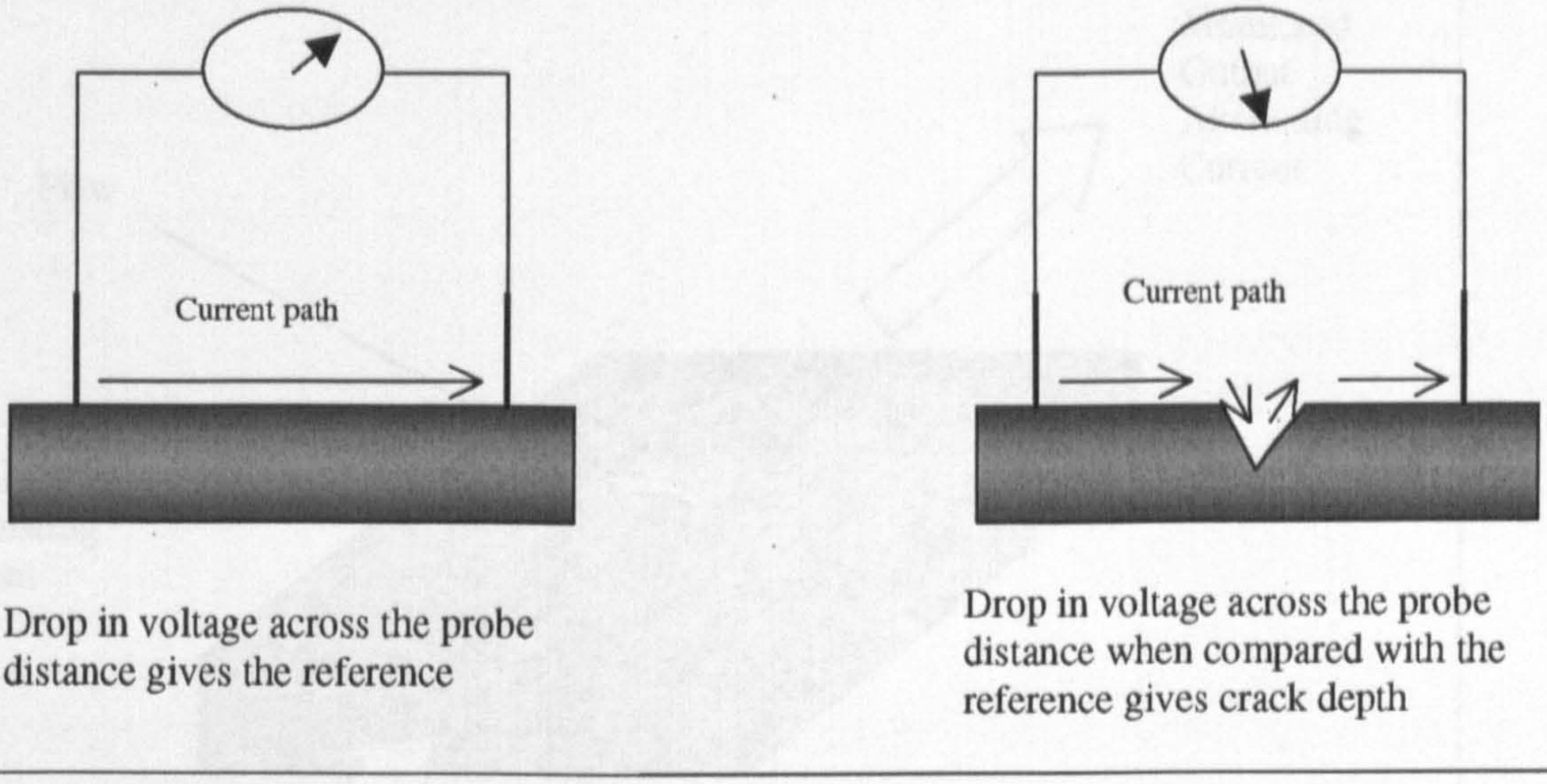

Figure 1.6: Principle of Potential Difference Technique

Typical Items and Materials Tested
This method tends to be used in applications when the crack has already been found by some other means and accurate sizing is required for NDE purposes. Potential drop method is limited to conductive materials only.

Benefits
ACPD is one of the few methods that can size the flaw depth accurately. An advantage is that instruments can be made to be small and portable.

Such a proactive approach of crack sizing would be considered a *failure finding task.*

1.3.2.4 (c) Alternating Current Field Measurement (ACFM)

Principle and Process
The alternating current (AC) field measurement is capable of detecting both the length and depth of a defect. The basis is that AC flows in a "skin" near to the surface of any conductor. The introduction of a uniform current through the component under test will result in an undisturbed field. In the event of discontinuities the uniform current flow is disturbed. The magnetic field associated with the electrical field is additionally disturbed and can be measured using magnetic field sensors.[30]

The principle is shown schematically in figure 1.7:

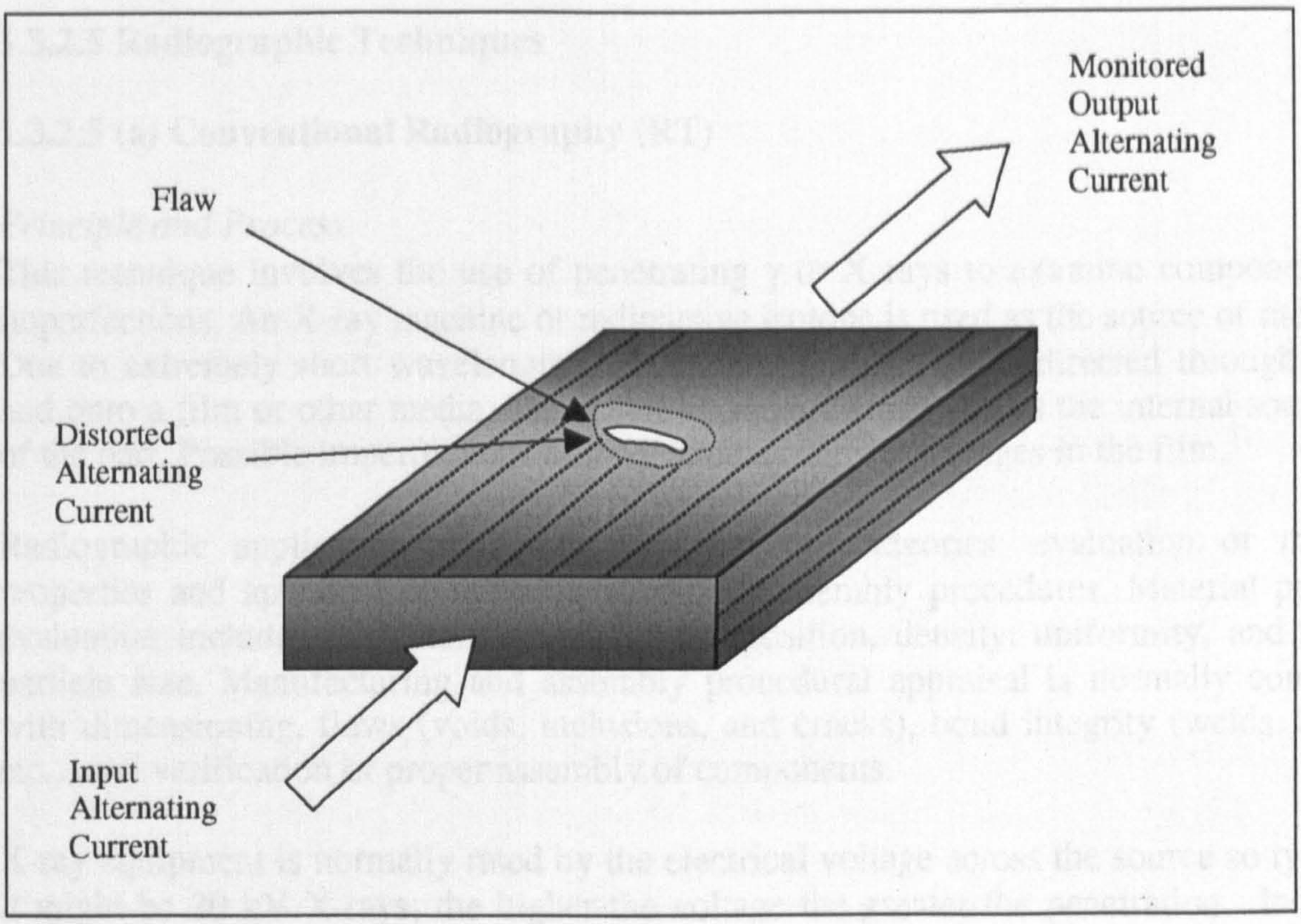

Figure 1.7: Principle of Alternating Current Field Measurement

Typical Items and Materials tested
The technique is mostly used to inspect welded and threaded connections. The materials must be conductive.

Benefits
The technique has been successfully automated in some sub-sea applications.

The intrusive point-by-point interrogation necessary to use this technique classifies this method as a *failure finding task.*

1.3.2.5 Radiographic Techniques

1.3.2.5 (a) Conventional Radiography (RT)

Principle and Process

This technique involves the use of penetrating γ or X rays to examine components for imperfections. An X-ray machine or radioactive isotope is used as the source of radiation. Due to extremely short wavelengths involved, radiation can be directed through a part and onto a film or other media. The resulting shadowgraph shows the internal soundness of the part. Possible imperfections are indicated as density changes in the film.[31]

Radiographic applications fall into two distinct categories: evaluation of material properties and appraisal of manufacturing and assembly procedures. Material property evaluation includes the determination of composition, density, uniformity, and cell or particle size. Manufacturing and assembly procedural appraisal is normally concerned with dimensioning, flaws (voids, inclusions, and cracks), bond integrity (welds, brazes, etc.), and verification of proper assembly of components.

X-ray equipment is normally rated by the electrical voltage across the source so typically it might be 20 kV X-rays; the higher the voltage the greater the penetration. Industrial equipment ranges from 20 kV to 20 MV and can penetrate up to 500mm thickness. The technique has the obvious drawback of being hazardous due to the presence of radiation.

The principle is shown schematically in figure 1.8:

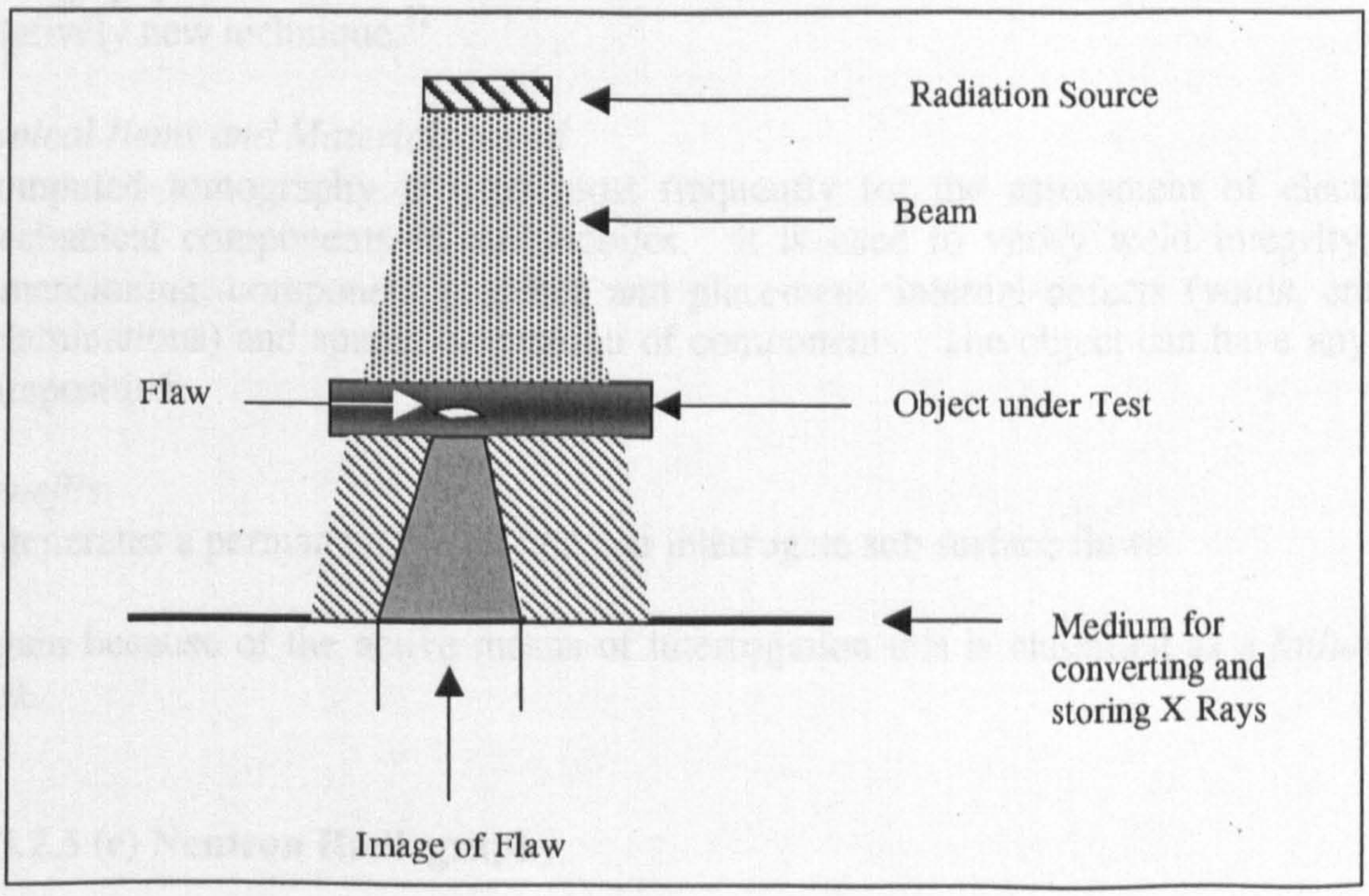

Figure 1.8: Principle of Radiography

For the technique to be effective the flaw must be normal to the radiating source. Flaws parallel to the source can go undetected.

Typical Items and Materials Tested
This type of testing is generally used on items such as: boiler tubing, steam piping, pressure vessel welds, castings and forgings and small components. This type of inspection can be performed on most materials.

Benefits
It can detect sub-surface defects and provides the operator with a permanent record of the inspection in the form of a film. It enjoys widespread commercial acceptance and is often used in conjunction with ultrasonic testing.

The point-by-point interrogative nature of this inspection type constitutes this a *failure finding task.*

1.3.2.5 (b) Computed Tomography (CT)

Principle and Process
Computed Tomography can be described as a three-dimensional X-ray inspection method. Moving the test object through the beam in a number of different directions and storing the measured absorption achieves this. The absorption or attenuation is approximately proportional to the materials density. A computer image is created that resembles the component if it were cross-sectioned at any location. Computed tomography is used to examine the internal structure of many items and is still a relatively new technique.[32]

Typical Items and Materials tested
Computed tomography is used most frequently for the assessment of electrical and mechanical components in automobiles. It is used to verify weld integrity, internal dimensioning, component presence and placement, internal defects (voids, cracks, and delaminations) and spatial orientation of components. The object can have any material composition.

Benefits.
It generates a permanent record and can interrogate sub surface flaws.

Again because of the active means of interrogation this is classified as a *failure finding task.*

1.3.2.5 (c) Neutron Radiography

Principle and Process
Neutron radiography is a non-destructive testing technique that is widely used in the nuclear and aerospace industries. It is similar to X-radiography in so far as both

techniques use beams of penetrating radiation to interrogate an object and generate an image. This permits visualisation of areas that attenuate the beam differently from neighbouring areas. However, neutrons are attenuated very differently from X-rays, and therein lies the difference.

Matter attenuates neutrons, either by scattering from the nucleus of a target atom or through absorption by the nucleus, which is unlike X-rays, which interact predominantly with the outer-shell electrons. Clearer images are generated from samples where the majority of the attenuation is through absorption, meaningful neutron radiographs can still be generated where scattering is the predominant mode.

Creation of images from the attenuated neutron beam can be accomplished in a variety of ways. The most frequently used method today is the direct method using X-ray film and a suitable conversion screen. The conversion screen selected depends upon the application.

Typical Items and Materials tested

Neutron Radiography has been successfully used in the inspection of nuclear fuel elements, the continuity of explosive detonator cords and in complex castings such as turbine blades.[33] Any material can be tested by this means.

Benefits

Again, as with all of the radiographic applications a permanent record is available for storage and the method is not restricted to surface flaws.

The nature of having to scan the structure constitutes this technique as a *failure finding task.*

1.3.2.5 (d) X-ray Diffraction

X ray diffraction is a radiographic method, but can additionally be used as a means of stress measurement. X ray diffraction will therefore be covered in the section titled "Stress-strain measurement".

1.3.2.6 Mechanical Waves

1.3.2.6 (a) Ultrasonic testing (UT)

Principle and Process

Ultrasonic testing or inspection involves directing a series of high frequency mechanical waves (vibration) into a test part. These waves are of short wavelengths, typically 1 – 10 mm, at a frequency ranging from 0.2 – 20 MHz. The most common method is the pulse echo method. The pulses impinge upon obstructions or the back wall of the part, which are parallel or nearly so to the pulse initiation surface and are reflected back. These reflected signals are detected by the transducer and are amplified and displayed on a screen. The same electronic equipment transmits the original sound pulses and detects their echoes.[34] A range of angled probes are used for the interrogation of welds and this allows the transmitted and therefore the reflected wave to follow the weld preparation profile.

The principle is shown schematically in figure 1.9:

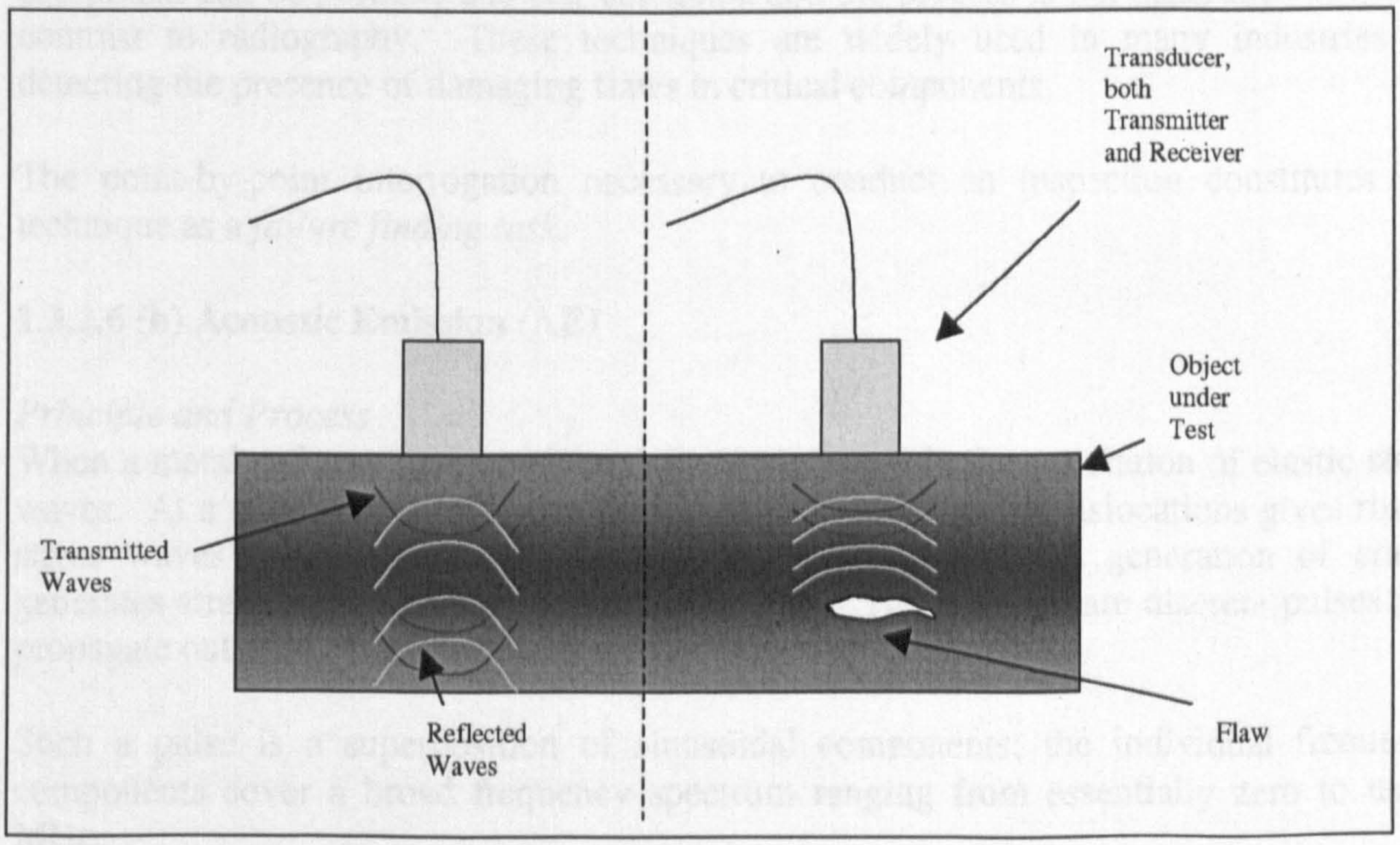

Figure 1.9: Principle of Ultrasonic Testing

In the pulse echo straight beam mode, the time interval between signal bursts or pulses permits the reflected sound pulses to be returned to the transducer and processed. Since the sound propagates in solid materials at a known velocity, typically 5960m/s in steel, this characteristic can be used as the basis for determining the distance from the echo and hence identify flaws and discontinuities. The pulse echo is displayed on a time base on an oscilloscope and through comparisons of amplitudes of the displayed discontinuity

signals can be compared to a reference standard. Both location and size of the flaw can be estimated. This process is known as an 'A' scan. Two-dimensional images can also be produced which when displaying a cross-sectional view is known as 'B' scan. The plan view is known as a 'C' scan.

This method is most sensitive to delamination or cracks whose planar surfaces lie normal to the direction of the propagating sound. So in the event of utilising angled probes the method is most sensitive under conditions where radiography is least sensitive and so these two are often used concurrently.

Typical Items and Materials tested
UT is used in almost every industrial sector. The attenuation and the scattering of the reflected wave are dependent on the grain size. Materials like austenitic steel weldments and copper castings are difficult to inspect by this technique, forged steels are however comparatively easy.

Benefits
Ultrasonic inspection provides higher sensitivity and greater accuracy than most other NDT methods in identifying and characterising internal discontinuities. Testing equipment can be portable and self contained and the process is not hazardous to use, in contrast to radiography. These techniques are widely used in many industries for detecting the presence of damaging flaws in critical components.

The point-by-point interrogation necessary to conduct an inspection constitutes this technique as a *failure finding task.*

1.3.2.6 (b) Acoustic Emission (AE)

Principle and Process
When a metal deforms various internal processes result in the generation of elastic stress waves. At a microscopic level, the formation and movement of dislocations gives rise to stress waves at low amplitude; at the macroscopic level, the generation of cracks generates stress waves at much larger amplitudes. These waves are discrete pulses that propagate outward from a localised source.

Such a pulse is a superposition of sinusoidal components; the individual frequency components cover a broad frequency spectrum ranging from essentially zero to many MHz.

The detection of Acoustic Emission from a propagating crack using a transducer has proven to be practical. It is important to recognise that the output from such a transducer is not in general a precise reproduction of the elastic stress wave impinging on it but when the transducer is excited by a stress wave the detector is simply shocked into vibration at its natural frequency. It has been experimentally demonstrated that the rate of emission of the stress wave pulses increases with the rate of macroscopic crack

propagation in a variety of materials. By measuring the differences in the times of arrival of the signals at the transducers the source may be located by triangulation. [35]

Typical Items and Materials tested

Major applications to date have been on large storage tanks and nuclear reactor pressure vessels during proof tests. Unlike many of the previously mentioned techniques AE is responsive to stress applied to the material. It is not particularly material sensitive, but generally the more brittle the more prolific it is as an emitter.

Benefits

It is sensitive to discontinuities that propagate under an applied stress and can be used to globally monitor a structure. It is both non-intrusive and non contaminating.

The fact that global monitoring can be achieved by an array of transducers, without the necessity of a point-by-point interrogation this is deemed an *on condition task.*

1.3.2.7 Strain and Stress Measurement

Generic Principle and Process
All solid objects undergo changes in geometrical configuration when subjected to mechanical loading. These are expressed in terms of stresses and the corresponding changes in configuration are expressed in strains. An unrestrained body can also undergo strains due to other changes in its physical state such as temperature.

1.3.2.7 (a) Brittle Coatings

Principle and Process
The use of brittle coatings is based on the principle that when strained only very slightly a brittle substance will crack in the direction of maximum tensile strain. These coatings can be made such that they will only crack over and above a pre-determined level. It is one of the simplest means of locating regions of high strain concentrations.

Typical items and Materials tested
Both tensile and compressive strains can be investigated and quantitative strain values within about ± 10% accuracy are possible. There are three types of coatings used: resin, lacquer and ceramic. Each has associated advantages and disadvantages. The resin and lacquer coatings are sensitive to humidity and temperature changes and are easily scratched limiting the potential to where they can be applied. Additionally, lacquer coatings must employ a solvent that is not only highly flammable, but poisonous making the technique hazardous. Ceramic-based coatings require that the test specimen be heated to approximately 1000°F, the glazing temperature, prohibiting its use in many applications. On thin sections this method is only qualitative since the reinforcing and loading effects of the coating itself are difficult to determine accurately. It can be used on any material that can be spray-painted.[36]

Benefits
The simple nature makes the technique easy to apply and interpret.

This is an *on condition task* in that defects that are active under the stimulus of stress are detectable.

1.3.2.7 (b) Photo elastic coatings

Principle and Process
The use of these coatings is concerned with a strain-optical property (birefringence) of certain materials. A birefringent coating (normally a plastic) is applied to the surface to be inspected and illuminated with polarised light. When the coating is viewed through a second polarising lens (analyser), interference fringes are seen. The pattern viewed is dependent on the type of light and the relative orientation of the polariser and analyser. The magnitudes and directions of the principle stresses can be ascertained from these observed fringes, but generally it requires more than one measurement.[37]

Typical Items and Materials Tested
Measurements can be made under a variety of environmental conditions, but applications are limited to the areas of interest being accessible by the polarised light. Photo Elastic coatings can be applied to most structural materials.

Benefits
Photo Elastic coatings provide rapid locations of high strain concentrations on the surface of the specimen, giving the overall picture of the principle strain difference. Large strains are measurable making it possible to determine the onset of yielding in the specimen under test.

Like brittle coatings such a technique is an *on condition task.*

1.3.2.7 (c) Strain Gauges

Principle and Process
Electric strain gauges operate by the interaction of electrical energy with the strain field of the sensor. A resistance strain gauge consists of a wire or foil grid which, when rigidly bonded to the structure, undergoes changes in electrical resistance in direct proportion to the changes in the strain in the structure. There are a variety of differing types of gauges; the most sensitive are semiconductor gauges, which are usually made of a piezo-resistive material in which the electric resistance is extremely sensitive to small changes in strain. Resistance changes from gauges are usually measured using a Wheatstone bridge arrangement or by amplifying the signal from the gauge and displaying it on a readout. It should be noted that resistance strain gauges indicate the strain at a point and does not show the strain gradient in the field. The strain resistance effect is not completely linear, especially at higher elongations for a given wire length. Semiconductor types are inherently non-linear although it is possible to compensate with additional electronics.[38]

Typical Items and Materials Tested
All sorts of structures are tested by this means such as pressurised and mechanical load bearing structures. It is frequently used during prototype testing to provide confirmation to the design engineer that the structural performance is as anticipated. They can be used on almost all materials.

Benefits
Strain gauges are well accepted industrially and are relatively simple. Care should be taken in the bonding of a gauge to a surface as the epoxies are affected by the cleanliness. Interpretation must always consider that the readings are a local representation of the strain measured across the gauge length and are rarely typical of the global stress distribution.

Again, this is a direct measure of structural performance and therefore could be considered as a passive method and an *on condition task.*

1.3.2.7 (d) X-ray Diffraction

Principle and Process

As X-rays have wavelengths comparable to the atomic spacing in a crystal, surface diffraction occurs and interference patterns are obtained that contain information on the atomic spacing within the material. The crystal lattice is a regular three-dimensional distribution (cubic, rhombic, etc.) of atoms in space. These are arranged so that they form a series of parallel planes separated from one another by a distance *d*, which varies with material. For any crystal, planes exist in a number of different orientations, each with its own specific *d* spacing. Measurements of radiation intensities in the diffraction pattern can be made from exposed and developed photographic film, or by using a goniometer in conjunction with X-radiation intensity measuring devices.

The pattern reveals the relative location of atoms in the crystal structure. Changes in the pattern can be used to calculate the strain in the test piece. The "diffractogram" shows the changes in the atomic spacing associated with the applied stress. Stress is determined by recording the angular shift of a given Bragg reflection as a function of sample tilt. In the presence of an applied stress in the sample there is a change in the atomic spacing (*d*). The stress can then be calculated by plotting the change in *d* spacing and the sample tilt.[39]

Typical Items and materials tested

Used frequently in research applications for material characterisation and composition, but has industrial uses in the measurement of residual stresses particularly in welded specimens. X- ray diffraction is applicable to crystalline and polycrystalline materials only.

Benefits

X-ray diffraction is non-intrusive to the specimen under test.

Failure finding task, but could be used as an *on condition task* due to the ability to detect stress.

1.3.2.7 (e) Extensometers

Principle and Process

The method in which extensometers are used differs from the aforementioned strain-measuring methods in that the quantity measured is the change in length (ΔL) of a discrete macroscopic segment of the test specimen. If the segment is of length (L) the average strain (ε) in the segment is calculated as

$$\varepsilon = \Delta L / L$$

Many types of extensometer have been developed. Pneumatic, acoustical, mechanical, electrical or optical methods have all been used as a means of detecting and magnifying

the change in separation between two points of the test specimen under the applied stress. Some general categories into which these may be divided and examples of each are:

1) Mechanical levers (screw micrometers)
2) Optical levers (deflection of a light beam by a mirror)
3) Optical interferometry (interference holography)
4) Electrical extensometers (differential transformers)
5) Grid systems (Moiré fringe methods)
6) Acoustic gauges (sensing the frequency of a vibrating wire)[40]

Typical Items and materials Tested
This technique has been largely applied where the properties of elasticity are of paramount interest, items such as bungee ropes and springs. This technique is applicable to most types of material.

Benefits
This technique has the ability to monitor the dynamic condition.

Again because of the ability to monitor the dynamic condition this is an *on condition task.*

1.3.2.7 (f) Proof load testing

Principle and Process
This technique can be viewed either as a destructive test or as a non-destructive testing technique depending on the outcome. The principle is that if a test object is subjected to a stress greater than that the test object is ever likely to experience in service then it has been empirically proven that all inherent flaws are sub critical, otherwise the specimen would fail.[41]

Typical items and materials tested
Items that are tested by this technique are lifting equipment, cranes and pressurised systems. This technique is not sensitive to particular material type.

Benefits
This technique enjoys widespread industrial acceptance.

An *on condition task* because it involves the proving of the structure.

1.4 Chapter Discussion

The preceding section has reviewed the applicable non-destructive techniques that may be appropriate for the purposes of an integrity assessment of mechanical structures. It is unlikely that any singular technique will suffice in the provision of a solution for all structural integrity assessments for all material compositions and constructions, but for the purposes of this investigation it is necessary to attain an optimal solution that is applicable in the most instances.

In order to achieve this it is necessary to prioritise what are the most salient characteristics for the design of a monitoring procedure to observe the behavioural characteristics of a structure whilst subjected to an induced stress. The initial objectives stated the technique should operate in conjunction with a load test and therefore be able to assess the structural performance under its applied stress.

The implication of using the load test means any solution should address the measurement of the structure's performance to sustain the applied load. This, in turn, suggests the use of an on condition task as opposed to a failure finding task. Many of the failure finding tasks make use of a point-by-point interrogation of the structure in order to identify the presence of defects that may or may not become active under an applied load. The use of such active techniques involve the monitoring of a resultant energy output from an inputted source is considered non-applicable to a condition monitoring strategy, as these outputs are not always indicative of the presence of a defect that will propagate under load conditions.

The contentious issue of what is important in the condition monitoring of structural integrity is within the definition of integrity or what threatens the integrity of mechanical structures. The method employed to identify this, follows the questions that the RCM philosophy asks of an asset.

What are its functions and performance standards? In the case of the mechanical structures cited in the objectives, examples being a bridge, a crane's supporting structure or a pressurised system; it is easy to observe that there is a huge diversity in their functionality. The performance standard is more recognisable, generically; the performance standard can be identified as the ability to support a mechanical load. Such structures are subjected to mechanical stresses, which they must endure without failing.

In which case, the next step in the RCM process can be asked; what causes functional failure?

Traditional steel structures degrade in various ways:

1. Corrosion. The conversion of metal to a hydrated oxide that has the consequence of eating away the material reducing its volume and therefore its ability to carry load.

2. Stress corrosion. The interaction of corrosion with a material that is experiencing micro-structural changes due to carrying mechanical load. This condition can result in a fine array of short, but sharp cracks in stressed material. These can link up and constitute failure.
3. Fatigue. Cyclic loading that initiates new cracks or extends existing manufacturing defects by small increments with repetitive load cycles. It is particularly important at points of stress concentrations such as changes in the sectional thickness and jointed areas. Cyclical stresses induced by alternating temperature are equally considered as fatigue.
4. Creep. A time dependent mechanism particularly applicable to structures that either continuously or near continuously sustain a static load and is most apparent in high temperature environments. It produces plastic, irreversible deformation.
5. Plastic collapse. Loading that exceeds the material yield stress resulting in either permanent deformation, or in a gross overload condition that results in complete failure.
6. Negligence. In many cases and it is almost impossible to prevent, a structure will be subjected to damage through impacts with other objects that can result in permanent deformation or holes that thereafter act as stress concentrations.

Composite materials; a composite is defined as being two or more materials meshed, generally, (in the form of a resin and fibre), so as to act as a single material. Such materials suffer degradation in the following ways:

1. Matrix cracking are micro-cracks that take place throughout the resin as the material is stressed, but they do not propagate or join up as aggressively as they do in metals. Composites are therefore recognised as having good fatigue properties as they can sustain an enormous amount of accumulated micro-damage, but still remain intact. If the matrix cracking is severe and localised, then splitting of the material can result.
2. Delamination is the process where the plies start to separate as the stress on the material increases. This could be due to poor adhesion of the plies because of some inherent manufacturing defect or the stress being greater than its designed working load.
3. Fibre or matrix debonding. This effect is known also as fibre pull-out and occurs when the fibres part from the resin when the stress is greater than the interfacial strength of the fibre or matrix.
4. Fibre fracture. The fibres in a composite material are the main load bearing elements so when fibre fracture occurs it is normally associated with delamination or fibre pull-out.

In the above defined failure modes, the nature of failure almost exclusively commences at a localised area and propagates through thickness until failure occurs. The exception to this is plastic collapse. Plastic collapse as stated will occur during gross overload. Gross overload is only likely to occur in instances when either the structure is under designed

for its stated function or alternatively is subjected to a purpose for which it was never intended i.e. negligence. In both of these instances condition monitoring of the structure is unlikely to yield any benefit, as the failure is likely to be instantaneously catastrophic.

For the purposes of this investigation it is considered that defining the nature of the defect is of less consequence than its effect on the structure. That is if a defect is present it may or may not threaten the integrity; it is recognised that no materials is flawless and in many cases flaws lie dormant for the life of the structure.[14] This investigation will concentrate on the effects of the failure modes on mechanical structures, that is it will seek to monitor malignant as opposed to benign flaws. It is concerned with ascertaining the maintainability and reliability of mechanical structures through life and therefore seeks a means of measurement that is appropriate in measuring the outcome of defects and not their inherent presence.

This is considered to be in keeping with the RCM philosophy of marrying the preventative task to the failure mode.

To reach an encompassing conclusion a matrix has been constructed with issues that are considered the most appropriate in the monitoring of structural integrity. Each issue is given an equal weighting and these are plotted against the various NDT methods. A conclusion can then be drawn as to a single technique that is most applicable in the majority of circumstances.

The issues that are believed to be important in formulating an optimised solution are:

1. The technique must be already accepted commercially as implementation would be otherwise difficult. The previously described techniques have confined themselves to those that are commercially available and could not be described as fledgling technologies. The presence of existing codes and standards are considered to be indicative of commercial acceptance.
2. It should have the ability to detect as many of the previously described failure modes as possible, both in composites and metals.
3. It would be preferable to monitor the structure in its entirety i.e. globally, as opposed to having to use a technique that could be described as a point-by-point interrogation.
4. It should not have any adverse effect on the structures future performance, for example weakening of the material or paint and coating removal should be avoided.
5. The technique should be applicable to all materials and have the potential to detect dynamic failure modes. That is it must address the structure's performance under its loaded condition. The technique should therefore be discriminatory between benign and malignant flaws.
6. The information should lend itself to being stored as a permanent electronic record.
7. The technique should not be dependent on the assessor's opinion; as subjectivity cannot be measured.

8. The technique should not present any health, safety or environmental issues.

With these factors in mind a decision matrix was formulated to evaluate the relative suitability of the techniques for the condition monitoring of mechanical structures.

		Commercial Acceptance	Suitability to all failure modes	Ability To Monitor Globally	Operates with a loaded condition	Applicable to most Materials	Electronic Storage Capability	Non Subjective	No H/S/E Issues	TOTAL
Visual Inspection	General	1	1	0	0	1	0	0	1	4
	Liquid Penetrant	1	0	0	0	1	1	0	1	4
	Thermography	0	1	1	1	1	1	1	1	7
	Shearography	0	1	1	1	1	1	1	1	7
Magnetic Methods	Magnetic Particle	1	0	0	0	0	0	0	1	2
	Magnetic Flux Leakage	0	0	0	0	0	0	0	1	1
Electrical Methods	Eddy Current Inspection	1	0	0	0	0	0	0	1	2
	AC Potential Drop	0	0	0	1	0	1	1	1	4
	AC Field Measurement	0	0	0	1	0	1	1	1	4
Radiographic Techniques	Conventional	1	0	1	0	0	1	0	0	3
	Computed Tomography	0	0	1	0	0	1	0	0	2
	Neutron Radiography	0	0	1	0	0	1	0	0	2
Mechanical Waves	Ultrasonic Inspection	1	0	1	0	0	1	1	1	5
	Acoustic Emission	1	1	1	1	1	1	1	1	8
Strain Measurement	Brittle Coatings	0	1	1	1	1	0	1	0	5
	Photo Elastic Coatings	0	1	1	1	1	0	1	0	5
	Strain Gauges	1	1	0	1	1	1	1	1	7
	X Ray Diffraction	0	0	0	1	1	1	0	0	3
	Extensometers	0	1	1	1	1	0	1	1	6
	Proof Testing	1	1	1	1	1	0	1	0	6

1.5 Chapter Conclusion

From the decision matrix it can established that the highest scoring types of inspection that fulfil the requirements is acoustic emission, followed closely by strain gauging, thermography and shearography.

Examining the latter two first, thermography appears to offer many benefits as it can monitor large areas of the structure under the conditions of the load test. It lends itself to an electronic storage capacity and interpretation is highly instinctive as changes in colour are representative of severity. Therefore, as a through life condition indicator, the image becomes increasingly intense as the damage more progressive and end of life approaches. It is considered, however that areas of interest could be masked by other elements of structure during the image capture. A specific methodology of identical site location for image capture would have to be established for any application. The consequences of the environment are a detrimental factor making like with like temperature correlations arduous when image capture is likely to be effected by the ambient conditions. This could lead to a possible misinterpretation of a trend. Temperature as a through life trendable condition indicator is considered an unlikely candidate for further investigation as it may prove unreliable, particularly on large outdoor infrastructure. Although thermography is quite well established there are as yet no standards for the implementation of the technology.

Shearography, like thermography, detects changes in a physical parameter that is attributable to a state change experienced during a dynamic condition. An especially attractive attribute of this technique is the ability to measure the structural performance with respect to changes in applied load. The resultant output can then be compared directly to the applied stress and areas of high local stress concentrations become identifiable. The perceived drawbacks are that the laser can only be subjected to reasonably small areas at any given time and therefore one is reduced to conducting a point-by-point interrogation if the structure is large. It is felt that it would be preferable to have a technique that would permit global interrogation. Again, no standards exist for this practice.

One of the highest scores was attained by strain gauging which, with initial observation, would illustrate the most logical approach to the assessment of structural integrity. It provides an output in terms of measured strain that is readily convertible into principal stresses, the language of mechanical engineering structural design. In an environment with increasing reliance on finite element models, a correctly deployed array of strain gauges would serve to validate models and confirm assumptions about the structures global performance. The disadvantages of such an approach is that the surface finish of the area upon which the gauge is to be affixed must be good, which may include the removal of paint. The gauges are notoriously frail and awkward to bond. Mechanical design assumes homogeneity of materials and freedom from defects, which in reality is not the case. Design compensates for the assumptions by the introduction of factors of safety. These safety factors are essentially over design multiples that reduce the likelihood of any inherent defect becoming sufficiently stressed as to either initiate or

propagate. The deficiency of the approach of using strain gauge to monitor structural integrity is that the gauge detects the localised strain beneath its gauge length. A structure may experience stresses below the acceptable homogenous stress, but in local areas the stresses may exceed the maximum permissible stress. The nature of failure of mechanical structures is initiated from highly localised stress concentrations that propagate and ultimately contribute to catastrophic failure. The likelihood of being able to ensure that the gauge length lies over the local stress concentration is considered small and as such this methodology would fail to detect the mechanisms that ultimately contribute to catastrophic failure.

The other technique that scored the highest value was Acoustic Emission (AE), this technique offers global structural integrity monitoring and differs from the strain gauge in that it can pickup the dynamic motions of highly localised discontinuities as the applied load excites them without requirement that the transducers are mounted directly on the defect. The rate of the emission is proportional to rate of the degradation process, a valuable feature when ultimately it is sought to generate a means of mapping the progressive deterioration. The facility of using triangulation to source locate a site of interest is important, if an active site requires further investigation then a complimentary technique could be utilised in order to generate further information about a defect. The perceived disadvantage is that due to the sensing element being shocked at its own resonant frequency the actual characteristics of the materially generated signal are lost, and differentiation of different source mechanisms is unlikely to be achieved.

Considering the factors above, acoustic emission was selected for further investigation and the subsequent documentation is restricted to this.

CHAPTER 2: Review of Acoustic Emission and proof load testing

2.1 Chapter Introduction

The chapter is structured such that initially there is a review of the challenge given matched by the justification of the choice of the selected topic for further research. Deeper discussion concentrates on the nature of failure of mechanical structures and a review of the effects of proof testing is conducted. There follows some examples of the successful industrial applications of AE. A more detailed examination into the sources of AE is described and the interpretation and evaluation of the generated signals are examined. The chapter concludes with the formulation of a programme of research based upon the results of previous investigative work.

2.2 Review

The preceding chapter concluded that the chosen approach for the investigation was Acoustic Emission in conjunction with proof load testing. The factors that affected that particular choice can be summarised as:

The initial objectives cited that the technique should enable measurement in conjunction with a load test and therefore be able to assess the structural performance under its applied stress. The consequence of being able to interrogate the structure in a dynamic condition has the advantage of selecting a method that will differentiate between benign and malignant flaws and thus achieve a true measure of structural integrity. Ideally, the chosen approach should not involve a point-by-point interrogation, but should be capable of global monitoring.

The technique should be commercially acceptable with existing codes and standards and demonstrate a proven ability to detect failure modes. With industrial practices becoming increasingly dependent on quality, health, safety and environmental issues, it is important that the integrity assessment does not adversely effect the future performance of the item of interest, therefore the means of measurement should be non-intrusive. The traceability of monitoring records is considered imperative and should where possible be non-subjective. The use of existing codes and practices should permit that the interpretation of results be conducted in a repeatable manner and give guidance on AE interpretation and defect categorisation.

2.3 Acoustic Emission as compared with other NDT Methods

In contrast with most the previously described NDT methods AE detects motion whereas other methods detect geometric discontinuities. Acoustic Emission differs from most other non-destructive methods in two significant respects. Firstly, the energy that is detected is released from within the test object as opposed to being externally supplied by

the non-destructive method.[35] The flaw generates its own signal that is responsive to the applied stress; static discontinuities will not generate Acoustic Emission signals. The passive means of measurement should ensure that the results are truly representative of the integrity of the structure by differentiating between benign and malignant defects.

Secondly, the Acoustic Emission method is capable of detecting the dynamic processes associated with the degradation of structural integrity. Such dynamic processes, include crack growth and plastic deformation both of which are major sources of AE. Discontinuities that enlarge under load are active sources of AE and by the virtue of their size, location or orientation are the most significant in terms of structural integrity.[14]

Acoustic Emission can detect and evaluate discontinuities throughout an entire structure during a single test. A carefully deployed array of transducers can be employed to conduct global monitoring, since only limited access is required for sensor deployment. [42] Historically, structures have been re-qualified by the use of a proof test,[14,42] complementing the proof test with a screening technique to permit the detection of an active conditional source is considered advantageous.

Any indications that result from the AE monitoring may influence the deployment of a supplementary failure finding task that can size and orientate the symptom for further evaluative purposes. This prevents the necessity of conducting a point-by-point interrogation of the entire structure and focus can be directed at active sources that are representative of structural degradation.

A further benefit of the use of Acoustic Emission is that the method may employed to prevent catastrophic failure of systems with unknown defects as it has the ability to evaluate a structure in real time, thereby enhancing safety during the proof test itself. There exist a number of codes and standards to assist the practitioner with the set up, test implementation and analysis of AE, for the most part such standards are published by the American Society for the Testing of Materials. (ASTM)

2.4 The nature of failure of engineering materials

The nature of failure of engineering materials can be segregated into two types, brittle and ductile fractures. These are relative terms that describe the nature of failure dependent on the materials ability to sustain plastic deformation.[43] Ductile materials exhibit substantial plastic deformation with high energy absorption before fracture, however ductility is dependent on factors such as temperature, the straining rate and nature of the imposed stress. Any fracture involves two processes: crack initiation and crack propagation, a ductile material will exhibit plastic deformation ahead of the advancing crack tip and the crack progression is relatively slow. In contrast, a brittle material generates very little plastic behaviour and the crack progresses rapidly. In the design of mechanical structures the use of ductile materials is favoured as a preventative measure can often be employed to forewarn of failure.

In chapter 1, the failure modes of engineering materials were reviewed. Engineering materials were classified as either composite or metallic structures. There has been considerable emphasis put on the monitoring of composite structures by the Acoustic Emission community and there are many published papers, codes and standards developed for such practices. [44,45] One of the most significant findings of the AE community for composite evaluation was the discovery of the knee in the curve. During a destruction test of a composite material observation of the cumulative acoustic energy generated reveals that at approximately 70 % of the failure load the AE becomes exponential. This change in the behaviour is sometimes referred to as the knee of the curve. [46]

Composite structures have evolved due to a greater comprehension of materials and their properties. Their use is becoming increasingly more widespread as compromises are found for certain unique applications that benefit from the combined action of two materials. Within the transportation sector, some cylinders are favoured as a composite structure due to the high strength to weight ratio that can be achieved through material composition. This enables better fuel consumption by limiting weight. To date, structural engineering constructions have for the most part been fabricated from metal and as such it is considered that for the development of a condition monitoring strategy focus should be directed at metallic structures. The historic dependence on metal as the load bearing component of structures means that metallic structures are closer to approaching the end of their design lives and would more readily benefit from any development in condition monitoring.

Chapter 1 concluded that in almost all instances a localised area is subjected to a degradation process that is progressive and ultimately constitutes structural failure. The six structural failure modes identified for metallic structures were corrosion, stress corrosion, fatigue, creep, plastic collapse and negligence. It was stated that neither plastic collapse nor negligence could be avoided through the employment of a condition monitoring strategy. Examining each of these failure modes in more detail permits the investigation to determine the suitability of using Acoustic Emission in conjunction with proof testing as a means of defect detection.

It is estimated that the effects of corrosion and corrosion prevention makes up 5% of the nations income.[43] There are eight recognised forms of corrosion; uniform, galvanic, crevice, pitting, inter-granular, selective leaching, erosion and stress corrosion. It has been chosen to encompass the second failure mode of stress corrosion within corrosion as a generalised heading.

1. Uniform corrosion occurs in areas that are subjected to environmental attack.
2. Galvanic corrosion occurs when two dissimilar materials are electrically coupled and exposed to an electrolyte.
3. The same electrochemical mismatch can result in two localities of the same material when a crevice holds a stagnant solution and consumes the local area through reduction.

4. Pitting is a common corrosive type where small holes penetrate through the thickness of the material until there is no residual.
5. Inter-granular corrosion results in material disintegration along the grain boundaries, it is particularly prevalent at welded connections on stainless steels.
6. Selective leaching results in the removal of one of the alloying components in a material along the grain boundaries and has the effect of reducing the mechanical properties.
7. Erosive corrosion is a combined mechanical and chemical process, mechanical motion may break down a materials protective film leaving the material susceptible to chemical attack.
8. Stress corrosion results in the small cracks that adjoin to form a larger crack that ultimately propagates through the material.

A common theme of each of these corrosive mechanisms is that they result in a degradation of the strength of material in a localised area. Obviously the size of the localisation is contentious particularly with respect to uniform corrosion, but it can be envisaged that uniform corrosion will be dispersed principally in areas exposed to the environment or in the direction of the prevailing wind.

Creep is a time and temperature dependent mechanism, which results in permanent deformation when a material is subjected to a constant stress. When the material is subjected to a constant stress the material instantaneously deforms, however, the deformation occurs at different rates. It is recognised that there are three stages of progressive deterioration. Primary creep acts as an initial increase in the deformation rate with respect to time. The rate diminishes as the material strain hardens and deformation becomes more difficult during secondary creep. Finally, during tertiary creep there is further acceleration in the rate of deformation. This ultimately results in failure. The nature of the failure is grain boundary separations that form internal cracks that propagate through the thickness of the material.[43]

Fatigue makes up almost 90% of metallic failures.[43] Fatigue is experienced by structures that are subjected to repetitive fluctuating loadings.[47] It involves the generation of a crack that grows under fluctuating loads. The use of ductile materials in structural design is a measure employed to improve the detection of such incipient failure.

2.4.1 Crack initiation and propagation

Cracks almost always initiate on the surface of a material in the region of a stress concentration.[43] Sites of geometric changes such as holes, keyways, and sharp fillets act as stress raisers which magnify the local stresses and exceed the material's resistance. Crack propagation is considered as a three-phase process. During Stage I, as a crack initiates it progresses very slowly along the lines of high shear stress. The crack advances over several grains during this early stage. During Stage II, the crack direction changes until it is perpendicular to the applied stress and the extension rate increases dramatically. The first two stages are shown diagrammatically in figure 2.1.

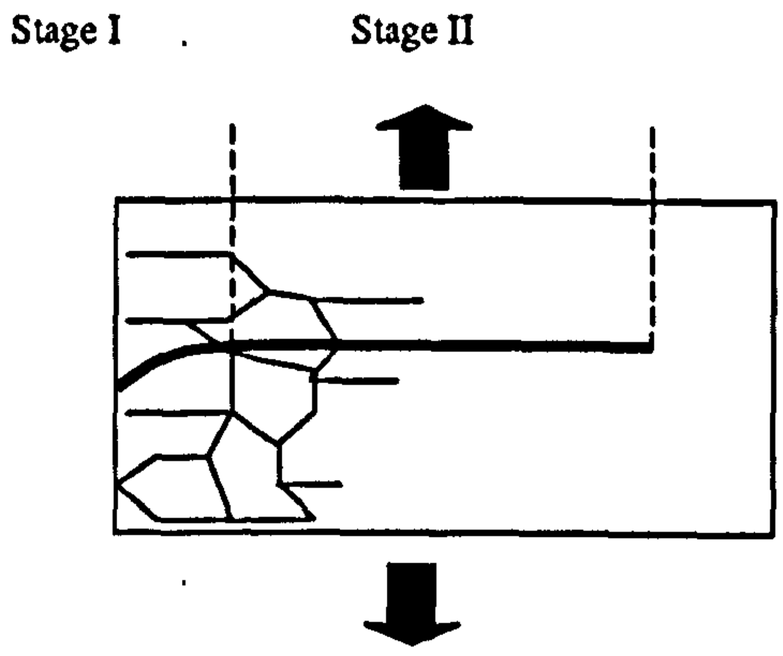

Figure 2.1: Stage I and II of crack growth

During Stage II, propagation progresses by a repetitive plastic bluntening and sharpening process induced by the fluctuating stresses. The stresses act along the lines of slip at 45^0 to the crack as shown by figure 2.2a. As the crack widens with increasing loading the effect is a bluntening of the tip, figure 2.2b. During the load removal/reversal, figure 2.2c, there is a corresponding reversal in the directions of the shear stresses at the tip, which returns the crack to its sharpened state. During one load evolution the crack advances an increment until the dimensions of the crack become such that a critical state is reached. When the crack dimensions are deemed "critical", the third and final stage of growth is reach, which culminates in fast fracture and ensuing failure.

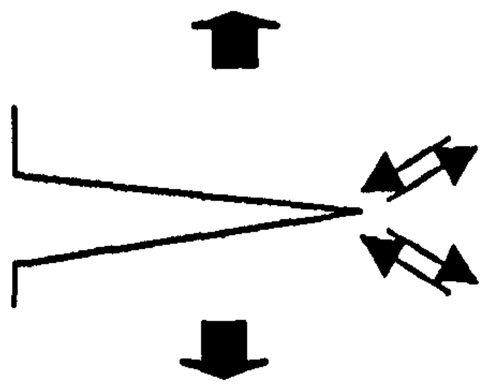

a) Shear stresses acting at 45^0 to the applied load

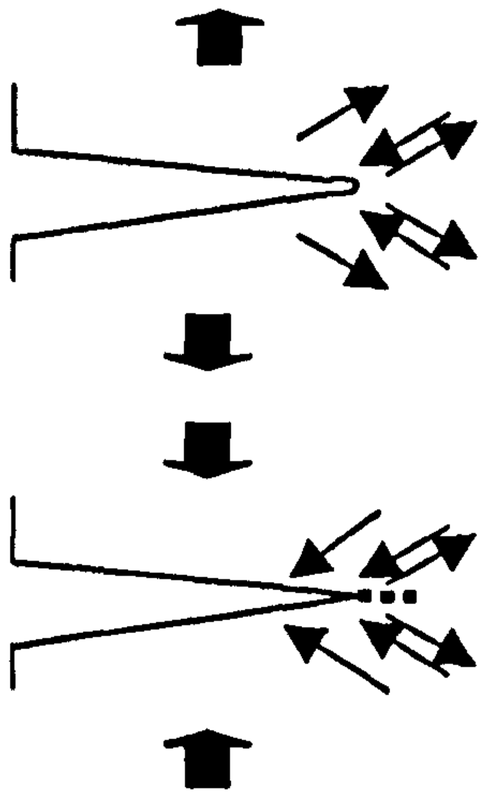

b) At maximum load the crack bluntens

c) During load reversal / removal the stresses reverse and the crack is returned to its sharpened state but has progressed a small increment

Figure 2.2: Crack progression during one cycle of fatigue

Conventionally mechanical engineering characterises fatigue crack growth in three regions (Region I, II, III) on a cross plot of the fatigue crack growth rate and the range in the stress intensity factor, figure 2.3. Region II is expressed mathematically by a power law relationship.[43] Paris, 1961, as cited by Varkoly [48] initially put the equation forward and currently a number of different iterations exist which take account of other factors, which are known to effect fatigue lives such as surface roughness and environmental factors. A feature of a power law is that on a log-log plot it becomes linear. An example is shown in figure 2.3 and the explanation of Paris's equation succeeds it.

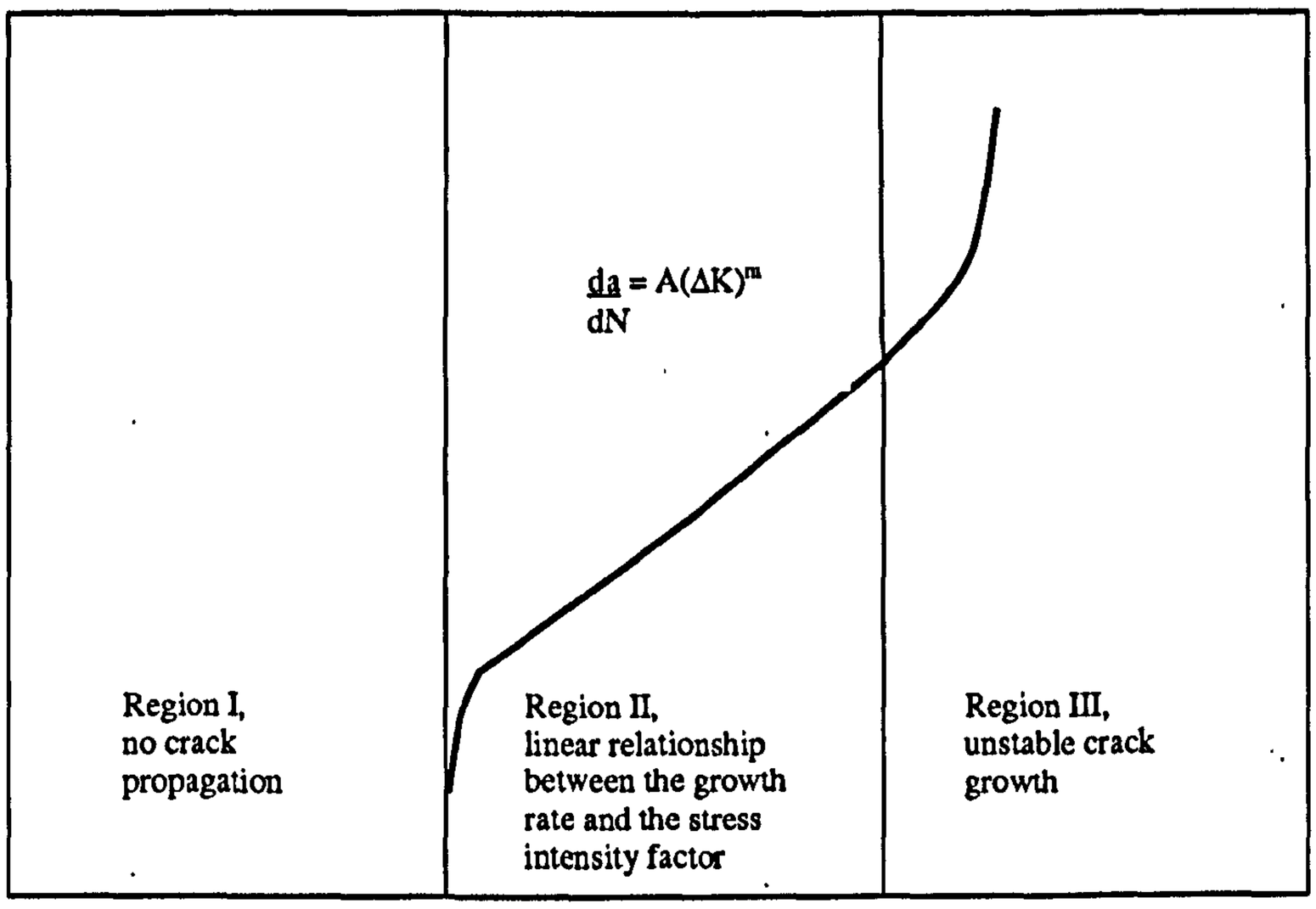

Figure 2.3: Regional separation of crack growth behaviours

The equation:

$$\frac{da}{dN} = A(\Delta K)^m$$

Where:

$\frac{da}{dN}$ = the crack growth rate where a is the crack length and N is the number of cycles

$A \& m$ = are material constants which depend on environment, frequency and stress ratio

ΔK = the range in the stress intensity factor

This mathematical representation of crack growth permits the structural analyst to calculate the crack extension for a given number of cycles and if experimental data is available, the point at which a critical state is reached. Determination of the stress intensity factors and the material constants, however, is a laborious procedure involving

significant experimentation. If conducted the critical value can be used to select an appropriate NDT method, which is known to have a favourable probability of detection for identification of flaws of the critical size for both the specific material and geometry.

There are three recognised forms of cracking that can occur in engineering materials. These are known as Mode I, Mode II and Mode III. The forces required to generate such modes are shown diagrammatically in figure 2.4.

Mode I

K_I
Strictly growth (opening)

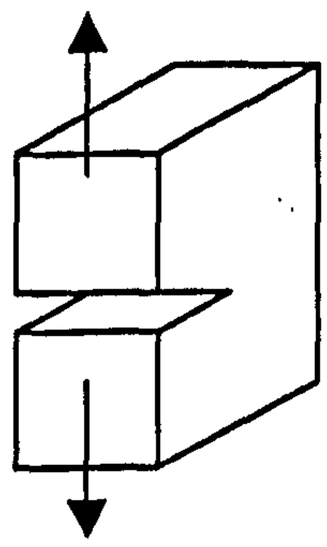

Mode II

K_{II}
Sliding

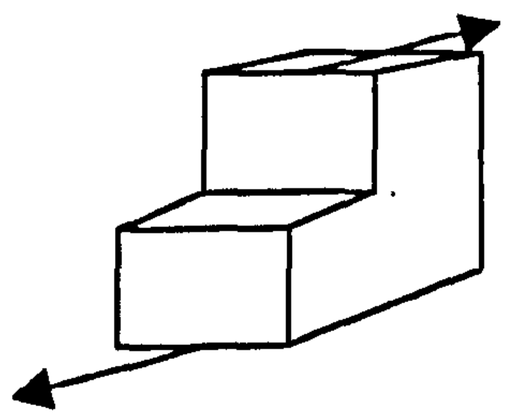

Mode III

K_{III}
Tearing

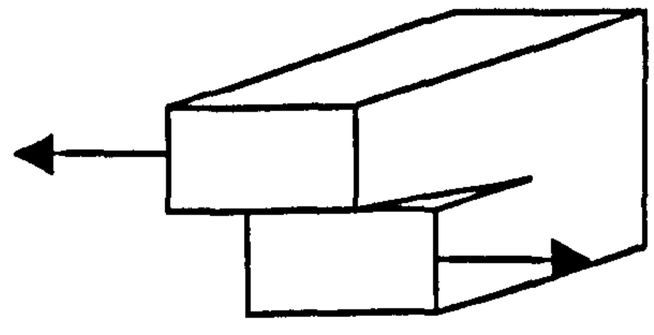

Figure 2.4: Modes of crack growth

It can be assumed that what ever mode of cracking exists then it will still behave in a manner that can be described by the regional separations illustrated in figure 2.3 and by the Paris equation.

2.5 Load Testing

Design of structures utilises the mechanical properties of materials to ensure safe operation. In general when designing a structure to endure anticipated in-service stresses a safety factor is used, and it is common to discuss structures with respect to their inherent factor of safety. The safety factor ensures that the material is operated within its linearity or elastic limit. The factor of safety is normally related to the ultimate strength. During normal operating conditions the structure is expected to operate at what is known as the safe working load (SWL) or sometimes referred to as the rated load. The loads anticipated by designers are frequently doubled in order that they will be less than half of the material failure load or ultimate strength.[49] It is more probable, however, that the factors of safety employed can be as high as seven or eight times the maximum anticipated in-service loads to minimise the risk of material imperfections and the effect of local stress concentrations, which magnifying the stresses.[50]

Many mechanical structures are periodically re-qualified by a test condition. Under test conditions the structure is subjected to some overload condition a percentage increment above the SWL. Typically, in wire ropes this is 200%, in cranes 125% and in pressurised systems 150% of the rated load. In all circumstances, the test load or proof load, as it is more commonly known, is beneath the material yield point confining both operations and testing to within the elastic limit. This ensures no plastic deformation is ever incurred. Proof testing is employed periodically as a means of proving a structure. The principle is if the structure contains a critically significant flaw then during the test condition the structure will catastrophically fail and if performed at periodic intervals can be used to eliminate weak structures. The literature varies widely in its opinion of proof testing.

Contradictions exist that proof testing is a detrimental to the structure under test. Formby strongly opposed the use of repeat proof testing in simple welded structures.[51] Moubary suggested that proof testing often provides an unfounded sense of confidence in a structure.[8] Shoup et al reported that proof testing substantially increased fatigue lives, at least in chains. [52] It was the original work of Elber, 1972, who was credited with the discovery of crack retardation through plastically induced crack closure. He showed that fatigue cracks could be arrested through the use of overloads, which transmitted compressive forces on to the crack faces suppressing growth. [53]

This concept is illustrated diagrammatically in figure 2.5.

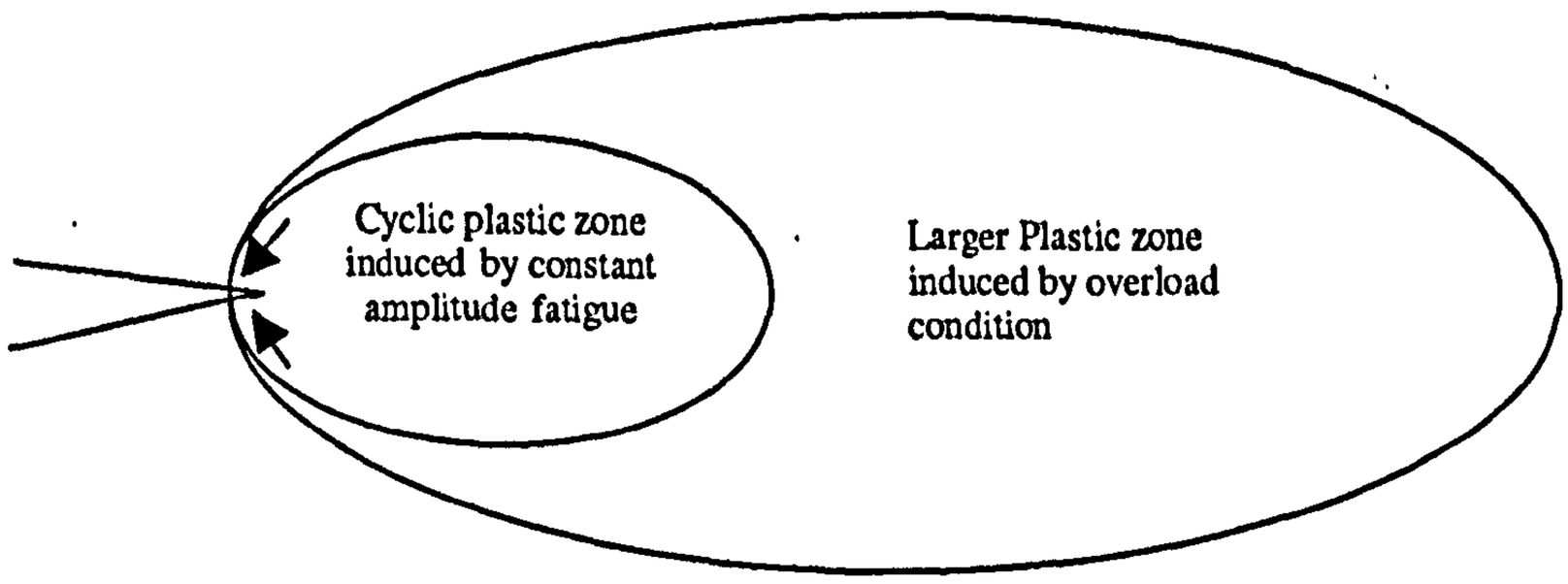

Figure 2.5: Plastic zone formation

The plastic zone exerts compressive forces on the faces of the crack tip preventing or suppressing growth. Crack growth can only occur when the forces on the faces are in a tension-tension condition. If initial compressive forces must be first overcome before a tension-tension condition is reached then the load at which growth can recommence is increased. Much of the research into crack closure and the effects of the overload interactions were conducted in the aircraft industry and studies predominantly focussed on Aluminium and Titanium alloys and some high strength aircraft steels.

Newman at Langley Research centre continued much of the work initiated by Elber and in a paper that he co-authored with Dewicke commenced a fracture mechanics approach of determining a safe life based on the maximum size of a defect that could be present having survived a proof test. The relationship between the magnitude of the proof test and the number of cycles post the proof tests to failure was evaluated. [53]

Skorupa, 1999, showed that load interaction effects found in Aluminium alloys differed from structural steels. Fatigue tests on polish structural steels demonstrated that crack retardation effects were present in all specimens tested. The conclusions were that the crack retardation effect increased with the size of the overload and that multiple overloads applied sequentially additionally increased the retardation effect.[54] Skorupa, 1999, conducted an extensive literature review on the effects of load interactions, which was published in two parts. Conclusions reached included that the conditions under which various load interaction effect fatigue crack growth are insufficiently recognised and that the underlying causes are not necessarily similar for different groups of metals e.g. Steels of various classes and Aluminium and Titanium alloys. [55]

The effects of proof tests on fatigue lives are examined in chapter 5

2.6 The Technology of Acoustic Emission

2.6.1 Successful AE applications

A summary of the successful of Acoustic Emission applications are given below: [42]

1. Mechanical property testing and characterisation
2. Pre service proof testing
3. In service (re-qualification) testing
4. On line monitoring
5. Weld monitoring
6. Mechanical signature analysis
7. Leak detection and location
8. Geological applications

The successful applications of pre-service proof testing and in-service re-qualification are the most salient to this investigation. The investigation is focussed on the delivery of an additional tool to supplement the information generated during proof testing of mechanical structures.

2.6.2 Definition of Acoustic Emission

The American Society for the Testing of Materials (ASTM) has been involved with AE testing since its outset. Their definition of Acoustic Emission is "the class of phenomena whereby transient elastic stress waves are generated by the rapid release of energy from localised sources within a material." [56, 57] This particular definition is the most frequently cited and almost certainly has its origin from the initial pioneers on the sub committees for establishing a glossary of terms set up by Spanner and Green. [58]

Weavers offers a further definition "Acoustic Emission is a naturally occurring phenomenon within materials and the term AE is used to define the resulting transient elastic waves when the strain energy is released suddenly within a material due to the occurrence of micro-structural changes in a material." [59]

2.6.3 Overview of AE Process

The elastic stress wave is detected by the use of a piezoelectric crystal element within a transducer. The crystal develops an electric voltage across its faces as it is excited by the stress waves. A pre-amplifier, usually within the sensor, amplifies this voltage and the signal is carried to the main processor via a cabled link. The operator can monitor in real time the acquired data and determine the location of the Acoustic Emission activity. The operator can view the AE and how it varies with respect to time and load. A representation of the AE process can be viewed in figure 2.6.

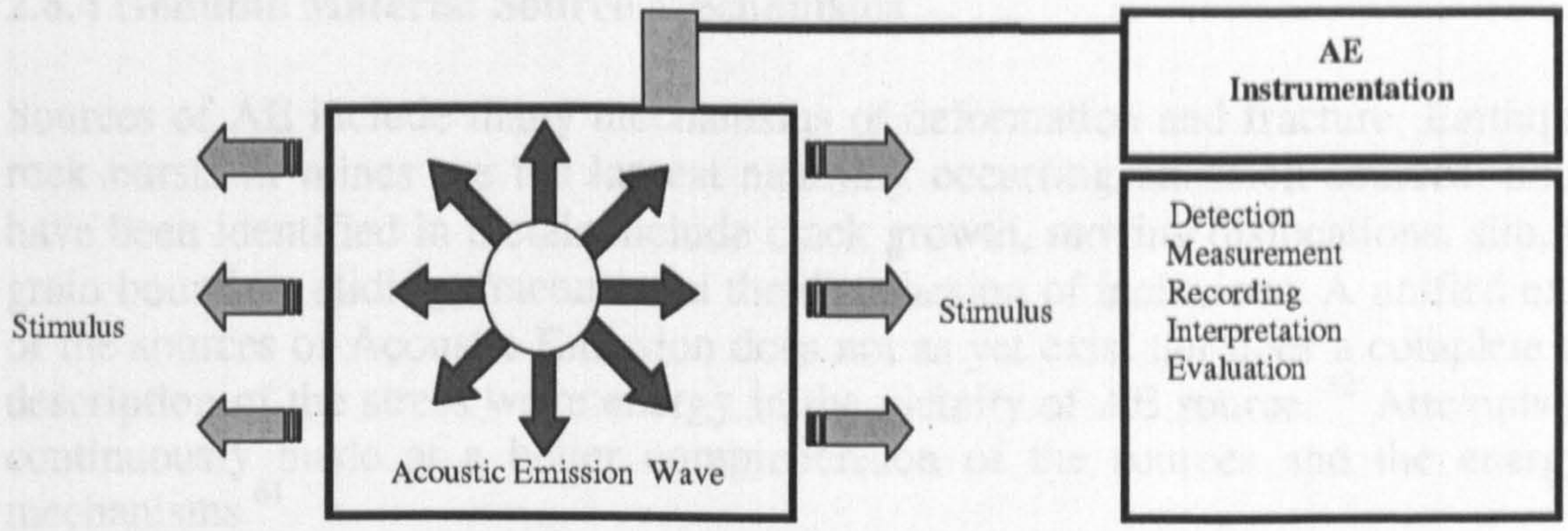

Figure 2.6: Overview of AE process [60]

Each wave has a unique signature composed of counts, amplitude, rise-time, duration, energy and relative time of arrival. The details of these unique features of the signal are discussed in the section entitled "measurement". Full analysis of the emission can be used to determine the features of the detected emission and assist in characterising the significance of any source.

Most Acoustic Emission sources function as point source emitters that radiate energy in spherical wave fronts. [42] Therefore, a sensor located in the locality of the source can detect the resulting AE irrespective of the direction of source. This contrasts with the other methods of non-destructive testing previously outlined, which depend on prior knowledge of the probable location of the flaw so that the local area might be interrogated.

The logical manner in which to describe Acoustic Emission would be to breakdown the process in to the constituent parts of detection, measurement, recording, interpretation and evaluation as illustrated in the above diagram, figure 2.6. Within Appendix II, there is a discussion regarding the signal as it is followed through the material and the factors that might affect it en route to the sensor are described. It was felt that whilst factors such as the discrimination against noise, wave propagation and attenuation are paramount to successful AE implementation, their relative importance in the context of this work constituted their inclusion as an appendix as opposed to containment within the main document. Equally, the signal's path into the sensor face and its amplification such that it can travel up the cabled link into the computer are documented in Appendix II.

Focus in this section is confined to the review the recognised material related sources of AE and subsequent description of the measured features of the waveform; the digitised representation of the signal. Definitions are given for terms and techniques that are used latterly in the investigation. Attention is directed at the evolution and successful implementation of AE in conjunction with proof testing.

2.6.4 Genuine Material Source Mechanisms

Sources of AE include many mechanisms of deformation and fracture. Earthquakes and rock bursts in mines are the largest naturally occurring emission sources. Sources that have been identified in metals include crack growth, moving dislocations, slip, twinning, grain boundary sliding, fracture and the discohesion of inclusions. A unified explanation of the sources of Acoustic Emission does not as yet exist nor does a complete analytical description of the stress wave energy in the vicinity of AE source. [42] Attempts are being continuously made at a better comprehension of the sources and the energy release mechanisms.[61]

Research shows that AE can be attributed to many different sources. The investigative work conducted by Heiple and Carpenter, 1987, is regarded as and one of the most influential papers to date on the sources of AE in metals and successfully identified one of the AE sources during deformation of metallic materials originates from dislocations. They described that the energy released from a single dislocation was too small to be detectable, but detection of AE signals was most likely generated from the motion of large numbers of dislocations within a small material volume.[62] Dislocation motion occurs prolifically during material yield and successful detection of yield is important in the detection of progressive deterioration. Slip can be described as a micro–yield phenomena, which involves the simultaneous motion of large numbers of dislocations has been shown by researchers to improve detectability of the AE.[63]

Metals contain impurities either unintentionally or purposefully through the inclusion of compounds to improve their properties. Such compounds are usually harder and more brittle than the parent material, because the mechanical properties of the inclusion are different from the parent, substantial stress concentrations build up during straining within and around an inclusion and their fracture or crack growth along the inclusion boundary – discohesion, were found to be good sources of emission.[64]

AE research built on such fundamentals and many papers into material behaviour characterisation have been since published.

2.6.5 History of Acoustic Emission

The chronological evolution of key concepts in AE is given to explain how the competent person can use AE in order to assess structural integrity. There are diverse uses of the AE in geological, biological and engineering applications. This review will confine its attention to assessment of structural integrity.

2.6.5.1 Kaiser Effect -1953

An important phenomenon affecting AE applications is the irreversible nature of the emission from most materials. On the initial application of a given load there is corresponding AE associated with stabilisation of the material to accommodate the stress. After that has ceased, further emission will not occur until that stress level is surpassed,

even if the load is completely removed and subsequently reapplied. This behaviour has been named the Kaiser effect in honour of the researcher who first reported it. [42,58,62,65] Drouillard states that there is perhaps no other AE research that has yielded a generalisation of comparable power. [58]

Graph 2.1 demonstrates the Kaiser effect. The cross hairs are aligned at the maximum peak load that was achieved on the initial rising load at approximately 1470 seconds and emission is apparent, but on the second rising load at 1620 seconds it is observable that only after the maximum previous load has been surpassed there is new emission. The solid line is proportional to the applied load and the AE is illustrated by the dots.

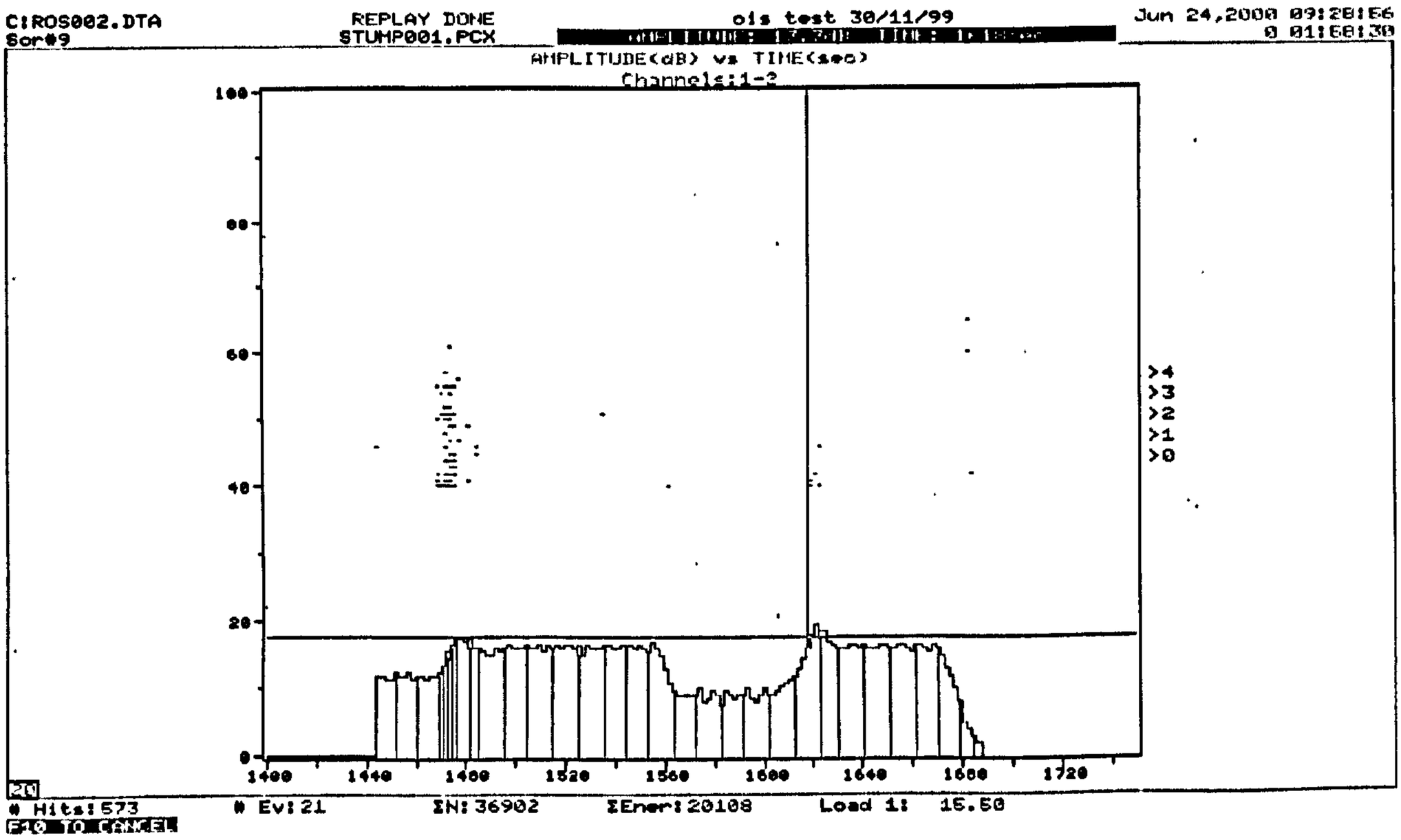

Graph 2.1: Kaiser effect

The degree to which the Kaiser effect is present varies between materials and may even disappear completely. This absence of irreversible behaviour is particularly applicable to materials that exhibit appreciable room temperature annealing characteristics. Some materials may not exhibit any measurable Kaiser effect at all, although this is not considered the norm. [58]

From such a phenomenon it can be determined that Acoustic Emission testing is disadvantaged when compared to other techniques as most techniques can be applied repeatedly without effecting either the structure or the discontinuity. Due to the Kaiser effect, each acoustic signal may occur only once and this has a pronounced effect on the manner by which AE testing may be implemented. AE testing must be conducted at predetermined times that are well planned and executed as the Kaiser effect can negate the usefulness of the test. Almost all structural AE applications are reliant is some respect on the Kaiser effect.

Pollock, redefined the Kaiser effect slightly with the Kaiser principle, it is a modern slant on the existing concept "Materials only emit under an unprecedented stress."[66] This explanation of the Kaiser effect has a greater significance to true material behaviour when expressed in terms of a stress as opposed to load. The Kaiser effect is true only if the magnitude of the load is applied in the same direction as the previously applied maximum. Stresses can be considered as a vector component in that there is significance in the direction of the stress. It is commonplace to talk of a tensile or compressive stress, but load is not always applied in a downward direction and therefore may be considered as a scalar quantity.

The Kaiser principle becomes particularly important during this investigation, as much of the successful commercial applications to date have been applied to interrogation of pressurised systems in which the directionality of the applied stress is well understood and is easily replicated. However, in mechanical handling equipment, to which LOLER is applicable, the creation of an identical stress condition is more difficult.

2.6.5.2 Dunegan Corollary - 1968

Dunegan compiled a strategy for the use of AE in conjunction with periodic proof testing. It is reliant on the Kaiser effect and can be summarised as the AE experienced during proof testing reveals damage incurred during the preceding operational period. Essentially, it means that should a structure suffer no damage during a particular operational period, then on a subsequent proof load no emission will be observed i.e. it will obey the Kaiser effect. However, in the event of a change of state during a working period then on a subsequent proof load, emission will be observed, as the discontinuity will be subjected to a higher and therefore unprecedented stress than previously. It also states that the amount of emission experienced on a proof load is a measure of the damage induced within the preceding operational period.[42] Almost all of the industrial practices are based on this approach; there exists American Society of Mechanical Engineers (ASME) and ASTM standards that incorporate the monitoring of the structural integrity of pressure vessels with a hydro-test. [67,68]

With the exception of two of the ASTM standards, Acoustic Emission for Insulated Aerial personnel devices[69] and Acoustic Emission monitoring of structures during controlled simulation,[70] all existing standards concentrate on the inspection of pressurised systems.

It is the validation and enhancement of Dunegans concept that this investigation will primarily focus to generate a more appropriate condition monitoring strategy for mechanical structures in conjunction with the proof test.

2.6.5.3 Fowler 1977

Fowler, one of the recognised AE pioneers, offers the following relationship between AE and the well-understood stress strain behaviour of metals.

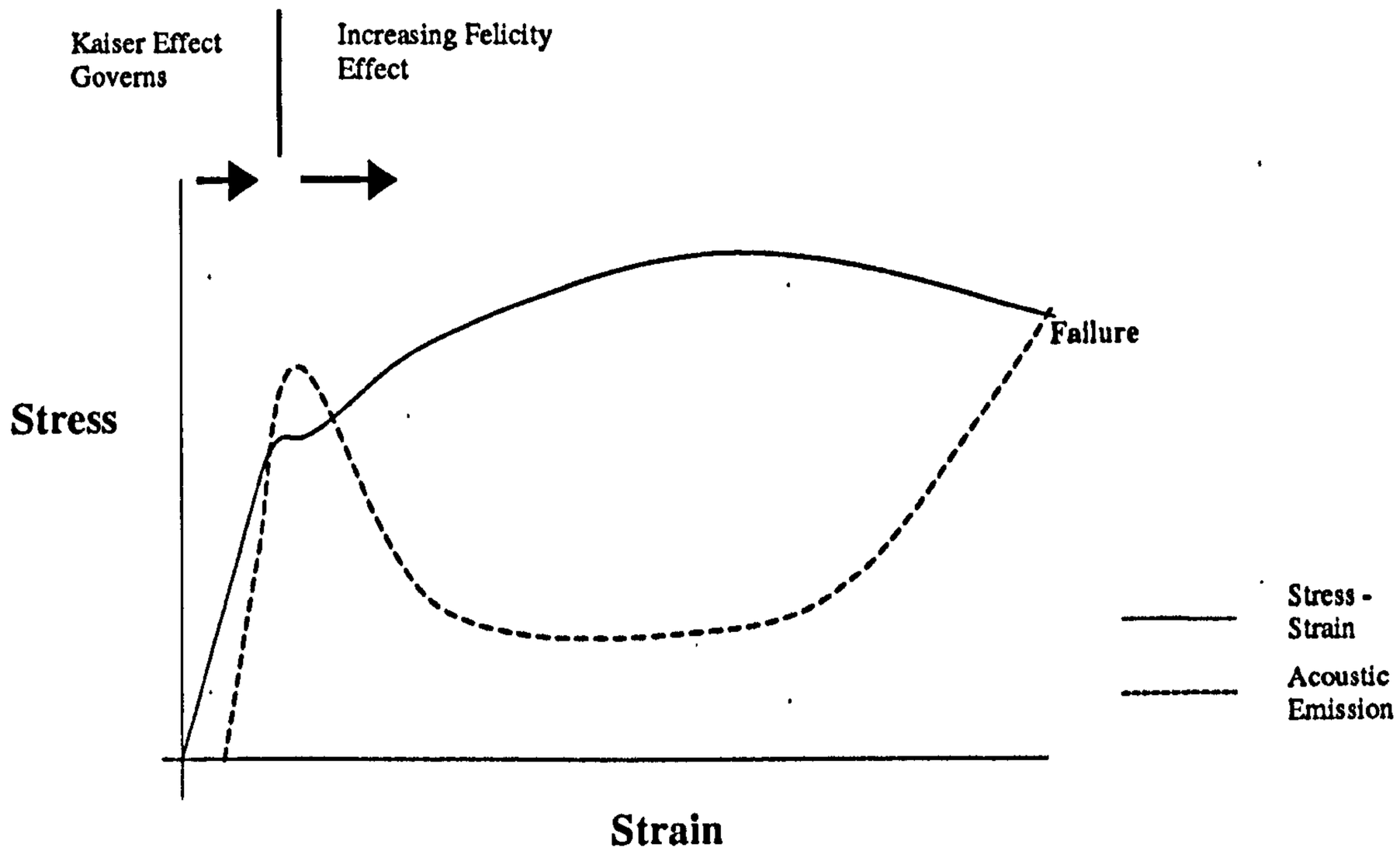

Figure 2.7: The relationship of AE with stress and strain

When the Acoustic Emission output is viewed superimposed on the stress strain relationship it is observed that the majority of the Acoustic Emission occurs at the yield point, this is due to the presence of the alignment of slip planes and with the generation of dislocations. Fowler goes on to state the following observations with respect to AE and metallic stress strain behaviours.[71]

- No emission will occur until a threshold strain is reached which in steels is generally approximately 60% of the yield stress
- If the strain is increased at a constant rate then the rate of emission will increase from zero at the threshold strain to a maximum at the yield stress
- The rate of emission will decrease as the strain is increased beyond yield
- As the metal is further strained the rate of AE will again begin to increase corresponding to the point at which work hardening occurs
- Fracture will generate large bursts of high-energy emission
- If the strain is held constant above the threshold strain then emission will continue to occur, but will eventually cease
- If the stress is held constant at a strain above the threshold strain, emission will continue to occur for as long as the strain increases or until failure
- The Kaiser effect will normally hold true for values of strain below the yield strain.
- The Felicity effect is indicative of a severe structural defect. The Felicity effect will be discussed fully within the section entitled "Evaluation and Interpretation".

2.6.6 Measurement

This section outlines the measurement process, Within Appendix II, it has been discussed that an epicentre source generates a mechanical wave that hits the piezoelectric crystal whose properties translate the mechanical wave into a voltage. It is amplified within the sensor and driven up a cabled connection into the computer. On arrival in the computer, features of the waveform are measured. Such features can be used to derive information about the source such as its activity and intensity. The measured features assist with interpretation and evaluation of the significance of the signals. The waveform is described by a number of measured features. The means by which these are calculated is illustrated in figure 2.8, and there follows a detailed explanation of each of these measurements and their relative importance to the process of interpreting and evaluating the signals. At this point it is important to differentiate between two types of AE, burst or continuous emission.

2.6.6.1 Burst and Continuous Type AE

Acoustic Emission sources can be segregated into two distinct classifications; [72] burst, discrete or intermittent sources and continuous sources. Examples of burst signals source mechanisms are cracks jumping, fibres breaking in composite materials and frictional sources. The processing techniques therefore make use of "Hit based" analysis and the associated features of the waveform, specifically, amplitude, duration, counts, energy and rise-time. (subsequently described)

Examples of continuous sources are leaks and the yielding of materials. Continuous emission is a considerable number of burst emissions that occur over a short period of time giving the effect of a continuous signal. Additionally, background or white noise can be categorised as a continuous source. The processing techniques utilised are Root Mean Square of the signal (RMS), Average Signal Level (ASL) and frequency analysis.

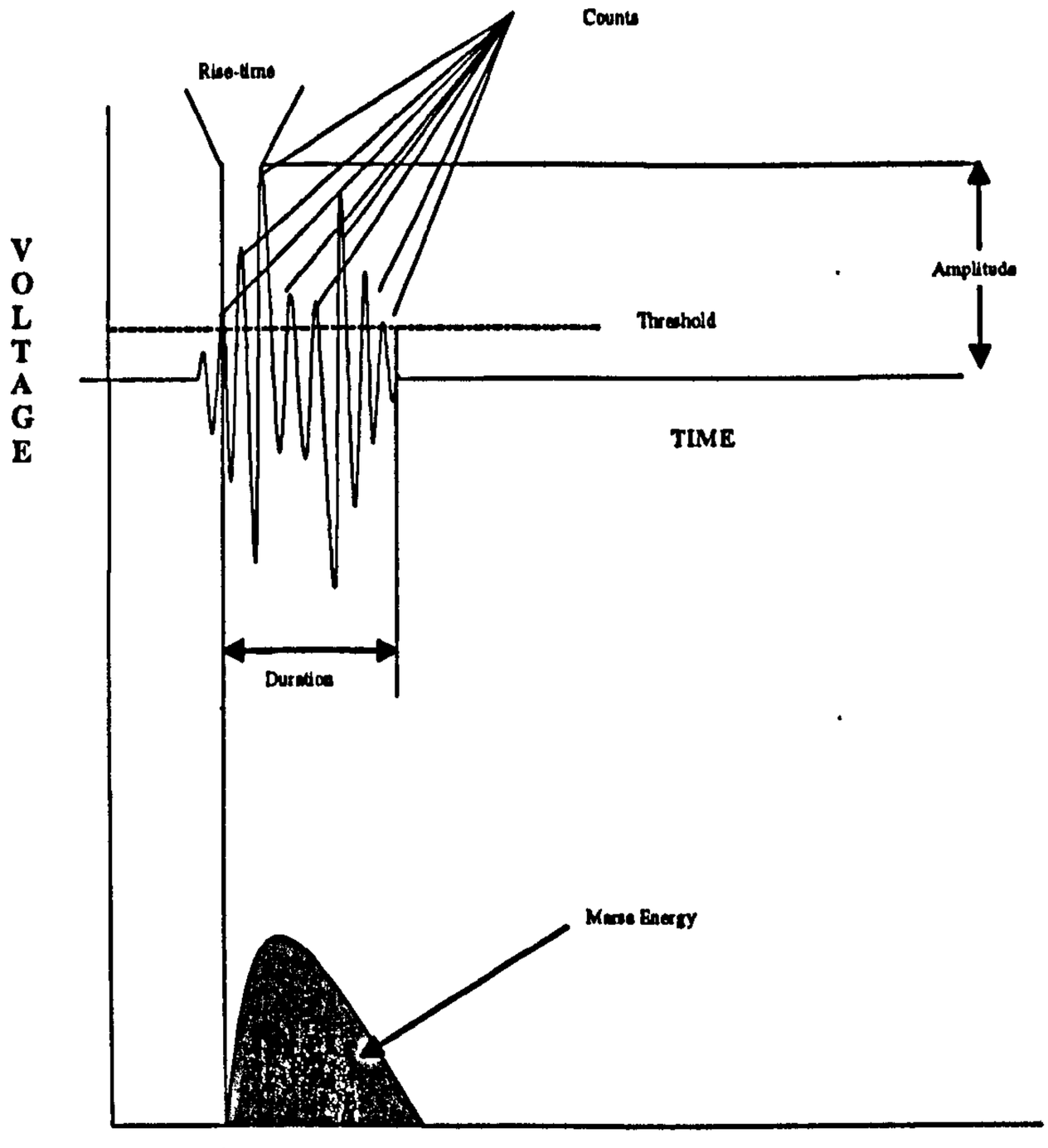

Figure 2.8: The measurement process from the waveform

2.6.6.2 AE Signal Features and their Significance

Hits / Events

The waveform shown in figure 2.8 is called a hit in that it hits a sensor. When a source mechanism generates a signal that arrives at two or more transducers the source can be located by comparison of their relative time of arrivals. A group of hits that permit a source to be located are known as an event. The number of hits or events is a good measure of activity and is often used in the creation of accept/reject criteria in certain test procedures. This terminology of a hit and an event is unique to a certain AE instrumentation manufacturer. [83] It generates confusion, in that an event in normal signal processing terminology would be equivalent of a hit. For definition purposes and relevance to this investigation a hit is defined, as a single transducing elements signal and an event is a source located physical mechanism. Therefore, an event must comprise of greater than a single hit.

Signal Amplitude

The first key feature of an AE signal is its amplitude, i.e. the highest voltage at any point on the voltage-time waveform. In order to handle the very wide range of signal Amplitudes found in practice, it is convenient to describe Amplitudes on a simple 0-100

decibel scale, this scaling that has become industrially accepted. It is important to realise that the Amplitude is referenced with respect to zero volts and not the threshold crossing value.

The signal amplitude in dB is calculated as follows:

$$A(dB_{AE}) = 20\log\frac{V_p}{V_{ref}}$$

Where V_p is the peak voltage at the preamplifier input with respect to the reference voltage, which is the same as the transducing elements output.

Amplitude is the key to the detectability of the signal. It is best used for attenuation measurements and characterisation of failure mechanisms. It is a good measure of the intensity of the source mechanism. It is one of the basic components utilised in pattern recognition of deformation mechanisms through its interrelationships with other parameters on various cross-plots. Peak Amplitude measurements are generally performed using a logarithmic amplifier to provide accurate measurement of both large and small signals.

Signal Strength / Marse Energy / Absolute Energy
Since the generation of signals can be attributed to the rapid release of energy from within a material, the energy content of the signals can be directly related to this energy release. The true energy is directly proportional to the area encapsulated by the waveform and is referred to as signal strength. Another means of measuring energy is the "Measured Area under the Rectified Signal Envelope" is known as the MARSE energy, it is dimensionless quantity of Energy. A further measure of energy is the Absolute energy, the absolute energy is the integral of waveform at the sensor preamplifier input and is measured in atto ($1*10^{-18}$) joules. The energy content of the signal is best for summing the measure of activity. The use of energy has essentially replaced the former measure of activity, counts, which was a convenient measurement with relatively primitive electronics. It is frequently used in the determination of accept and rejection criterions.

Counts
This is one of the oldest and simplest features for summing the measure of activity. Traditionally, the number of threshold crossings, counts, was a reasonably straightforward parameter to measure with analogue equipment. The drawback is that it tends to emphasise acoustic and instrument factors at the expense of source factors, as it is dependent on the resonance of the transducing element. It has largely been superseded by the measure of energy, but still remains useful for crossplots.

Duration
It is a valuable quantity for signal qualification by crossplots with other parameters. One such application is the recognition of the delamination process in composites.

Rise-time
Rise-time is useful for both signal qualification and rejection of noise sources.

Average frequency
The average frequency is a calculated feature comprising of the number of counts divided by the duration.

Hit time i.e. the time at which the hit occurs
This is the key external parameter for source location and analysis.

Parametric Input (Load etc)
The measurement of other external parameters assists in attributing the signals to material deformation processes. The simultaneous measurement of the stimulus and the AE greatly increases comprehension and are very useful for both data interpretation and evaluation.

RMS / ASL
The Root Mean Square (RMS) and Average Signal Level (ASL) are used for quantifying continuous emissions such as leak detection and bearing fault detection, but are not generally used in burst type emission analysis.

2.6.7 Interpretation and Evaluation

Once the features of the waveform are measured they can be displayed graphically in a number of formats. The first approach in Acoustic Emission data analysis is the systematic removal of any known noise source. This involves the correct interpretation that the signals are from the material prior to any evaluation of the signals significance. Table 2.1 summarises how each of signal features is best used for either interpretative or evaluative purposes. [72]

	Events	Hits	Amplitude	Energy	Duration	Counts	Rise-time
Interpretation	√		√ (with duration and counts)		√ (with Amplitude)	√ (with Amplitude)	√ (determines noise like leaks)
Evaluation	√	√	√ (e.g. fibre breakage in composites >70dB)	√√	(√) (can be weighted in favour of small events)	√	

Table 2.1: Signal feature appropriateness for either interpretation or evaluation

2.6.7.1 Interpretation

Perhaps the most important feature in the interpretation of AE signals is the discrimination of noise. Noise is defined as an acoustic source that is not flaw related sources such as mechanical friction or perhaps flow noise in process systems. There are a number of approaches utilised for the identification and removal of noise, many of which use the appearance of the data, particularly counts as a means of recognising a noise source. Noise sources can often be recognised in a data set by its dissimilarity to the rest of the data. Fowler proposed identification of data with high numbers of counts that appeared intermittently could be attributable to noise, figure 2.9.[71] One traditional method for assessing the quality of data is that it should form a tightly bound curve on a cross-plot of either Counts or Duration with Amplitude, as shown by figure 2.10. Deviations from the tightly bound distribution are often recognisable as sources that are not materially related.[73]

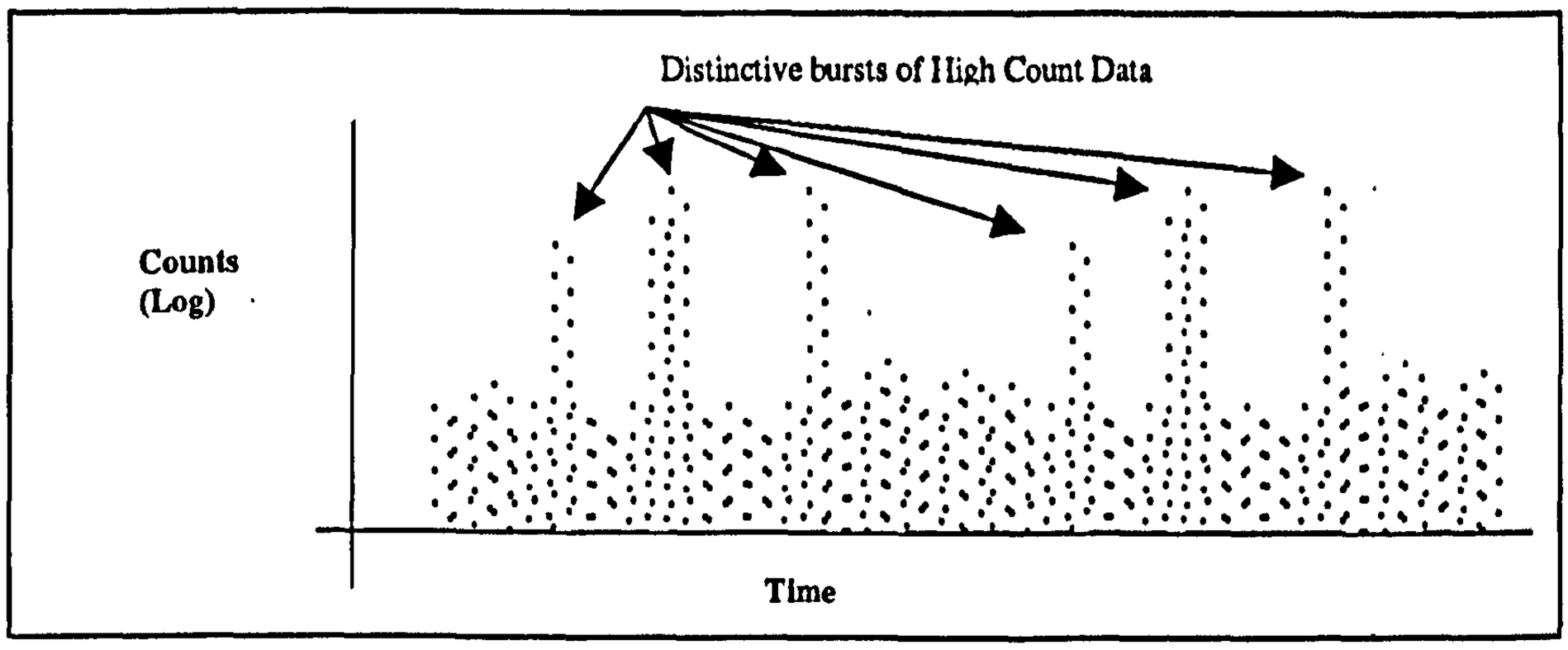

Figure 2.9: Fowlers noise recognition

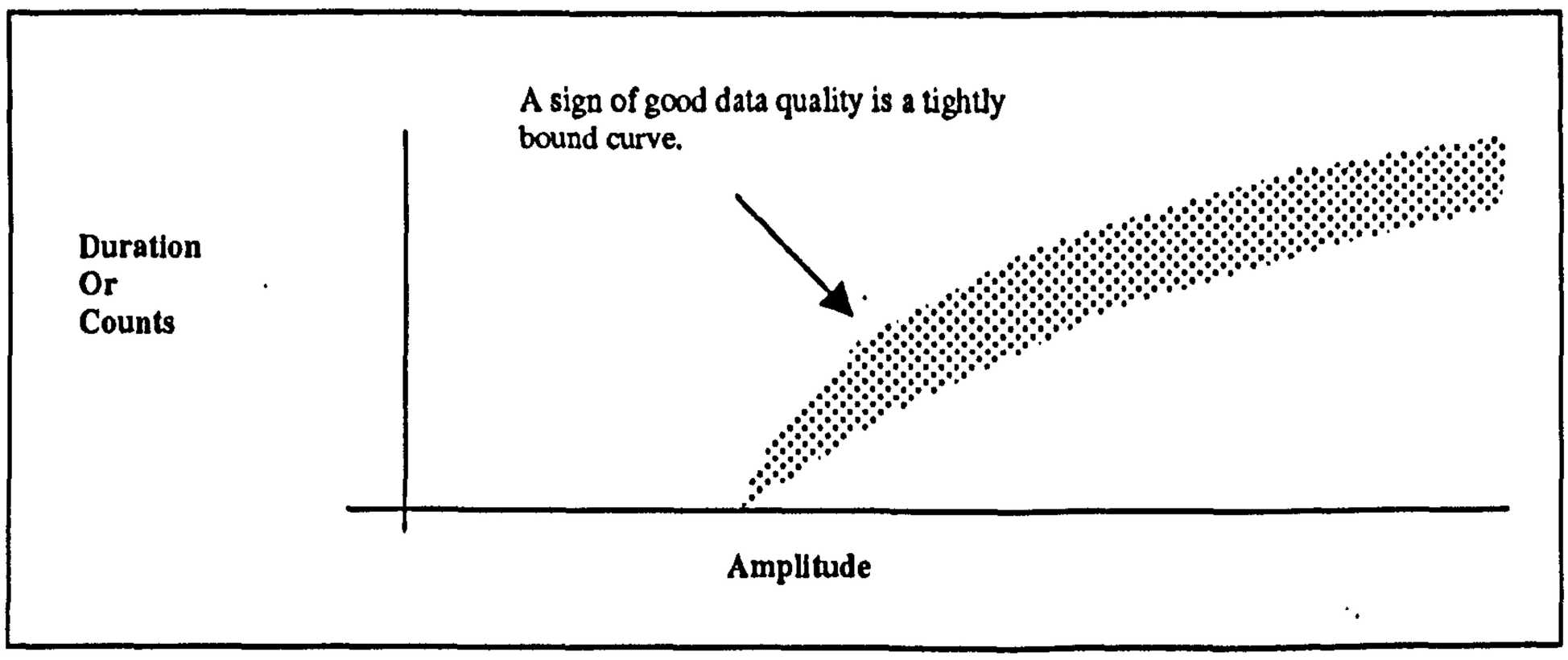

Figure 2.10: A tightly bound grouping of data on a counts or duration versus amplitude

One established procedure used in structural integrity evaluation elaborates on an approach of the appearance duration amplitude distributions, the procedure for Railroad tank cars [74] describes the effects of noise sources and its appearance on a Duration Amplitude cross-plot. This is shown in figure 2.11.

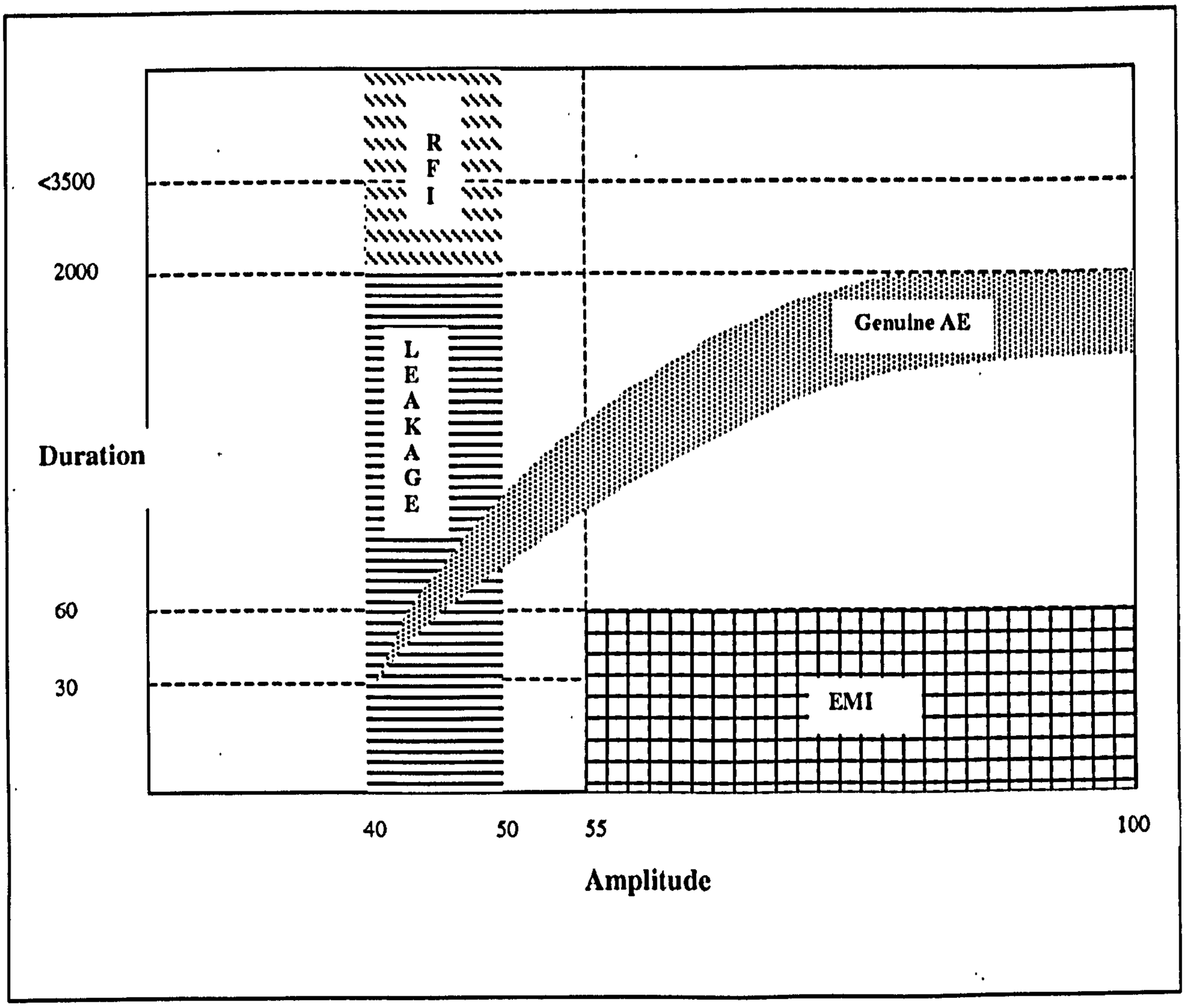

Figure 2.11: Recognition of AE sources from Railroad tank cars

Genuine AE is characterised by hits concentrated in the 30-2000 microsecond range. As the amplitude increases so to does the duration. This gives the data a banded appearance. Low amplitude, long duration hits may indicate sliding or rubbing at metal surfaces and are not indicative of structural damage. Leakage can be found to be a narrow band of long duration in the 40-50 dB range. Electromagnetic Interference (EMI) often causes hits greater than 55 dB that have short durations less than 60 microseconds. Radio Frequency Interference (RFI) appears as long duration hits usually greater than 3.5 milliseconds, but of low amplitude typically 40-50 dB.

Mechanical noise has characteristics that help distinguish it from genuine AE signals or cracks. Noise signals are relatively low frequency with large rise-times. The Acoustic Emission bursts from cracks generally have rise-times (from threshold to peak) less than 25 microseconds if the sensor is near the source. Mechanical noise rarely has such a fast rise-time. The rise-time of both noise and Acoustic Emission signals increases with the source to sensor distance because of the attenuation of the high frequency components. In some cases, a rise-time discriminator can be effective in isolating Acoustic Emission

from mechanical noise, but the frequency discrimination is usually a more reliable approach. [73]

There is a wide range of potential noise sources associated with Acoustic Emission monitoring. Before performing a test, it is vital to check for the background noise levels. This check should include all equipment and machinery operated during the test. Noise should be eliminated either at source or by analysis from the written test log taken by the operator during acquisition and the test data.

After discriminating against noise there are a number of methods that can be employed for evaluative purposes.

2.6.7.2 Evaluation methods

The evaluation methods outlined have been previously used in the assessment of structural integrity. Such methods can be employed for determining the significance of an active source from the monitored outputs generated during a proof test.

2.6.7.2 a) Felicity Ratio

Fowler, (1977) was responsible for one of the most well used evaluation criterions used in AE testing. He named the presence of genuine AE at lower loads than the previous maximum, the Felicity effect, after his daughter. The Felicity effect may be described as the opposite or breakdown of the Kaiser effect. The Felicity effect is attributed to instabilities in the material. [42]

A ratio can be obtained.

$$\text{Felicity Ratio} = \frac{\text{Load at which AE Recommences}}{\text{Previous Max load}}$$

Felicity ratios of below 95% is one of the rejection criterions for Fibre Reinforced Plastic tanks and vessels. [45] The Felicity Ratio is used as a measure of the severity of damage induced in a structure. An example of the breakdown of the Kaiser effect or the Felicity effect is shown in graph 2.2.

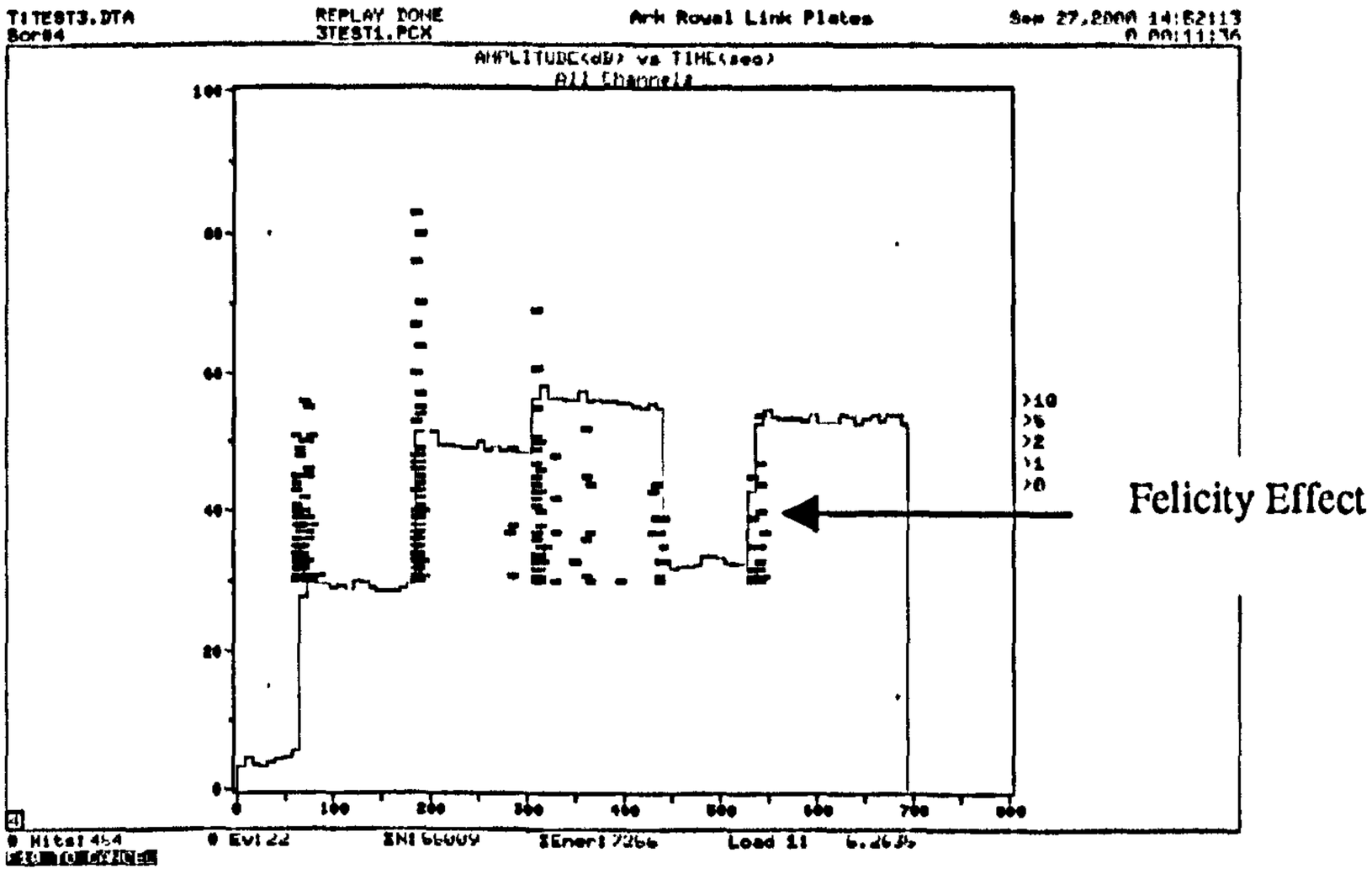

Graph 2.2: Felicity Effect

The incremental, increasing load steps shown by the solid line between 50 and 450 seconds show the presence of AE coincident with each increase. There follows a partial relaxation of the load between 450 and 550 seconds and a reapplication back up to the previous maximum. The load reapplication should result in no further emission in accordance with the Kaiser effect. The presence of AE prior to exceeding the previous maximum is known as the Felicity effect.

2.6.7.2 b) Amplitude distributions

Pollock [75] proposed the β Value as a method of evaluation. This criterion operates on the premise that with increasing load, in the event of a discontinuity, there will be corresponding increase in the signal amplitudes. Therefore, on a normalised logarithmic plot of the sum of the hits against amplitude a change in the gradient (β) is anticipated as the signal amplitudes become greater. Pollock suggested that with increasing load the linear regression should reduce in steepness and the gradient should approach zero. The method is shown diagrammatically in figure 2.12.

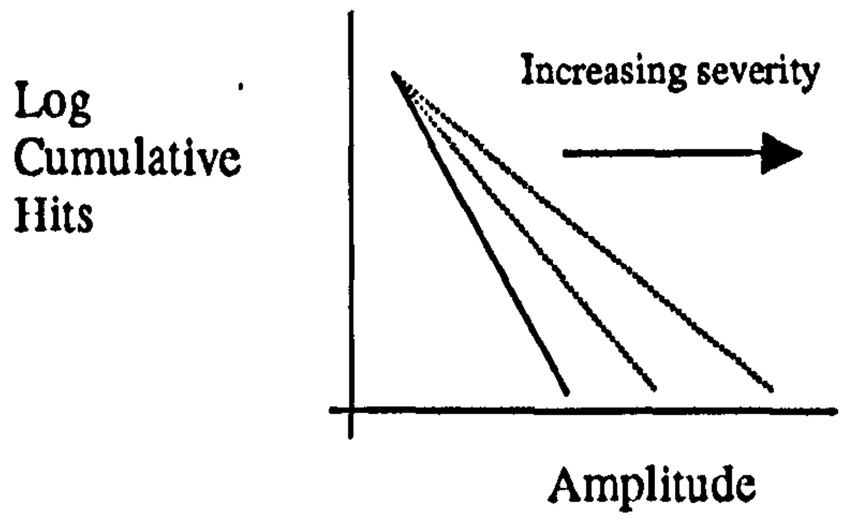

Figure 2.12: Change in the gradient of the hits amplitude plot

2.6.7.2 c) Persistence

Persistence is a measure of how long a source continues to emit whilst subjected to a constant load.[76] If the emission is considered analogous to complaining about an ensuing stress then it is conceived that the "persistence" of the emission will give information regarding the severity of the distress suffered by the structure. Persistence is the time taken until the emission ceases during a period of sustained loading.

2.6.7.2 d) ASTM method for data evaluation

Frequently evaluative procedures refer to the AE in terms of its activity and its intensity these have been derived from the standard for monitoring of structures during controlled simulation. [70] The significance of the measured parameters and how they relate to activity and intensity are summarised in table 2.2.

	Events	Hits	Amplitude	Energy	Duration	Counts	Risetime
Activity	√	√		√√		√	
Intensity			√√	√			

Table 2.2: Signal feature appropriateness for either activity and intensity

The standard elaborates into the creation of classes of both activity and intensity. These classifications are inactive, active and critically active, equally for intensity, low intensity, intense and critically intense. Such evaluations tend to be conducted on a per channel basis and are evaluated with respect to either load or time. Figure 2.13 illustrates the means for differentiation. In this instance the Y-axis reference to "cumulative event counts" means hits as the evaluation is conducted on a per channel basis.

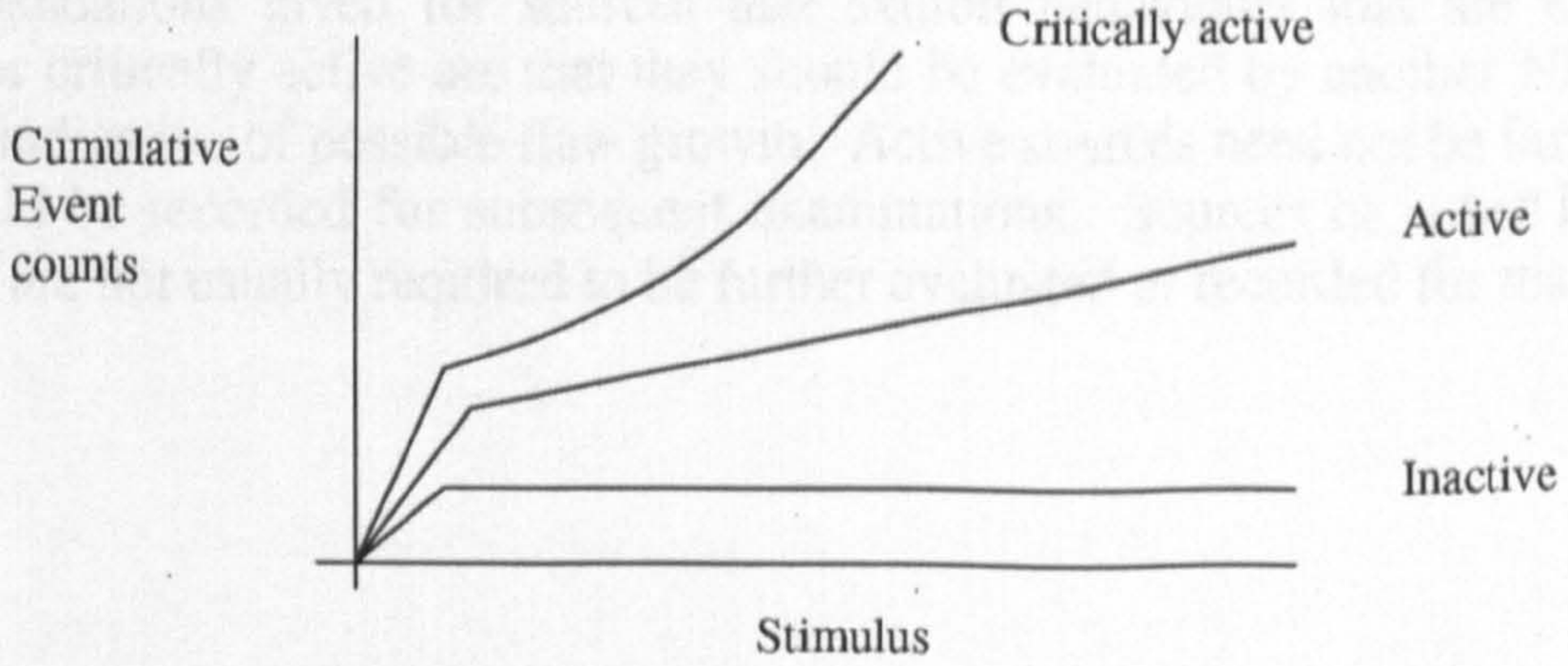

Figure 2.13: Change in the gradients of the cumulative event counts

An inactive classification gives no increase in AE with increasing load. An active source shows an increase in AE with either constant or increasing load and a critically active source shows a consistent increase of its rate of change with either a constant or increasing stimulus.

Again, Intensity is plotted against stimulus. Intensity is measured as either the energy or amplitude of a hit.

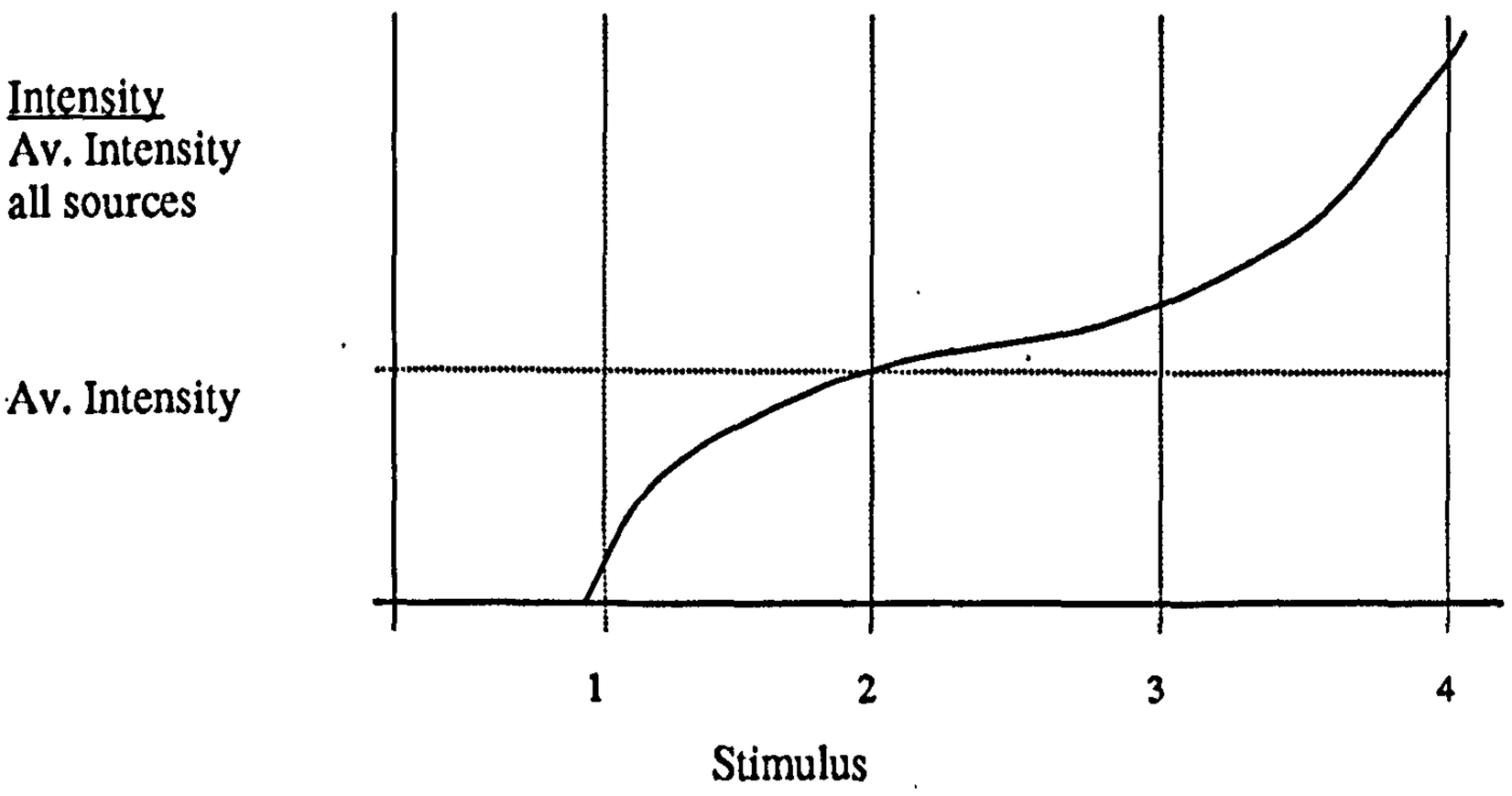

Figure 2.14: Intensity average

A source is deemed to have a low intensity if it is less than the average of all intensities as shown between the periods 0 – 2 in figure 2.14. After period 2, the intensity exceeds the average and is referred to as an intense source as it increases by a specified amount with increasing load. Between periods 3 – 4, the energy increases consistently with increasing stimuli.

Recommendations given for sources that exhibit behaviours that are either critically intense or critically active are that they should be evaluated by another NDT method, as they are indicative of possible flaw growth. Active sources need not be further evaluated, but should be recorded for subsequent examinations. Sources of either low activity or intensity are not usually required to be further evaluated or recorded for reassessments.

2.6.7.2 e) Leaird's evaluation method

Leaird [77] proposed a very similar method of evaluation broadly based on this standard, but discriminates critical sources from active sources through the recognition of an exponential increase as opposed to linear increase with respect to the stimulus. He additionally formulated an A through to E grading scale based on the relationship between the activity and intensity.

INTENSITY	Inactive	Active	Critically Active
Critically Intense	A Minor No action	D Severe defect Immediate NDT	E Critical defect Terminate test
Intense	A Minor No action	C Defect Implement NDT	D Severe defect Immediate NDT
Low Intensity	A Minor No action	B Possible crack Note for future use	C Defect Implement NDT
Inactive	A Minor No action	A Minor No action	B Possible crack Note for future use

ACTIVITY

Table 2.3: Leairds grading scale

2.6.7.2 f) Intensity Analysis

MONPAC is possibly the most widespread evaluation criterion applied in industrial practices, it is a proprietary evaluation method applied to pressure vessels. The method for calculating historic index and severity was discussed by Fowler in the MONPAC system. [73] Calculations of two parameters, historic index and severity are conducted and a cross-plot generated. Depending on where the distribution of hits falls on the cross-plot, a grade is assigned. The grades range from A through to E, E being the most severe condition. The grade is applied on a per channel basis. The A through to E scale is shown in figure 2.15

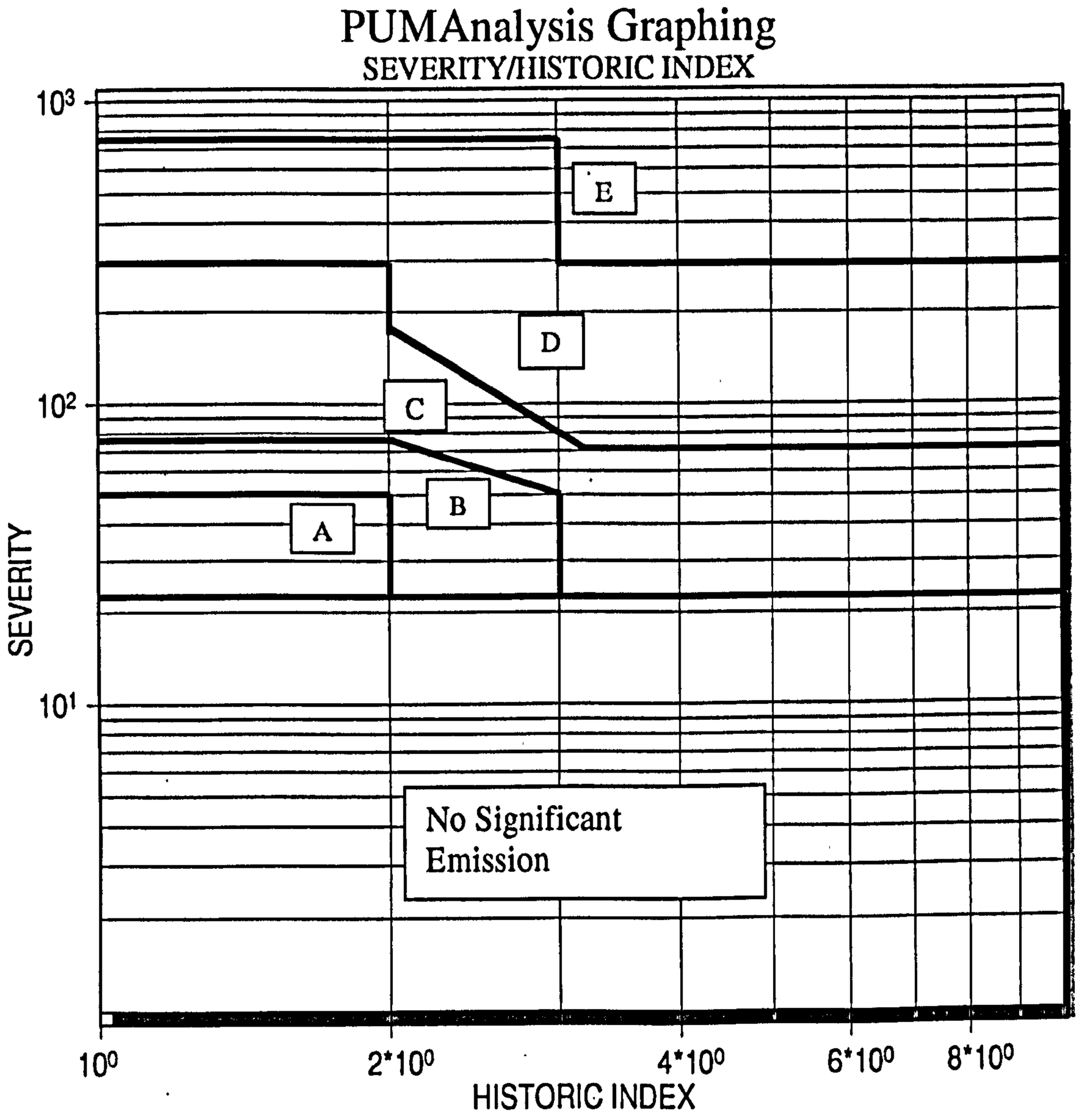

Figure 2.15: Intensity analysis cross plot

2.7 Chapter discussion

The nature of failure of engineering materials has been reviewed and identified that corrosion, creep and fatigue were dominant modes of failure that a condition monitoring approach should address. Each of these failure types resulted in a progressive degrading process of a localised area. During both fatigue and creep, engineering recognises distinctive phases of the damage progression that result ultimately in a rapid acceleration in the progression of the damage prior to the end of life. It can be envisaged that a staged process could also describe corrosion, that of initiation, successive material reduction to a point when there is a sudden and rapid acceleration in the deteriorative process. In the instance of cracking a power law was used to describe stable crack growth. The power law implies a non-linear deterioration characteristic suggestive that with increased crack length the crack extensions become increasingly larger. All of the aforementioned failure modes could act in such a manner.

The practices of load testing were examined. Conflicting evidence was presented on the perceived benefits. In some circumstances it appears that load testing may arrest crack growth and contribute to an increase in material durability.

The sources of AE were addressed and it was found that the sources of the elastic waves were attributable to the degradation processes that occur in engineering materials. The AE is a proportion of energy released during deterioration. The phenomenon of the Kaiser effect was described. It was explained how the Kaisier effect can be used as a method, which under the maximum stress condition of a proof test can be used to periodically re-qualify structures. Dunegan's work was described illustrating how the approach is not only qualitative, but also quantitative as the amount of AE generated during the proof test is a measure of the damage severity. Reference was made to the standards that are used in the inspection and testing of predominately pressurised systems.

A variety of evaluative techniques were discussed and how they are used as a means of defect detection in structures. A common feature of some of evaluative techniques was the recognition the non-linear nature of the AE to determine the significance of any defect. Both, the ASTM and Leaird's methods described the identification of an exponential increase in the cumulative AE to determine the presence of a critical defect. Pollack's amplitude distribution does the same in the respect that the change in gradient of the amplitude distribution is an exponential increase if expressed as an antilogarithm.

It is apparent that the deterioration of mechanical structures, particularly fatigue crack growth is a non linear process. During the deterioration one of the mechanisms by which energy is released is through the generation of elastic waves that are detectable by acoustic transducers. Previous research and validated industrial practices illustrate that the methods of evaluating the significance of sources uses recognition of a non linearity in the stress wave signals. Mathematically the procedure of fitting a power law to model the crack behaviour suggests that as the AE energy is a component of the energy released, the fitting of a power law to AE data may be appropriate. If the power law was fitted to

data that was acquired periodically throughout the life of the structure it may generate a conditional indicator that is trendable. This may generate supplementary information from which the competent person can come to a more informed decision regarding a structures capability for continued safe operation.

Morton et al, 1973, first used the concept of fitting a power law to AE data during fatigue. They additionally observed AE at the minimum load, which they considered to be from crack surface interference.[78] They found a strong relationship between the stress intensity factor and the AE generated at peak loads. Harris and Dunegan in the following year reported the relationship, which is very similar to the Paris equation for modelling fatigue crack growth: [79]

$$N' = A(\Delta K)^n$$

Where:

$N' =$ the AE count rate per cycle

$A \& n =$ are constants

$\Delta K =$ the range in the stress intensity factor

More recently, 2002, research conducted at Cardiff University by Roberts and Talebzadeh, explored the relationships between crack propagation rates, Acoustic Emission count rates and the stress intensity factors for the development of a means of estimating remaining fatigue lives on steel girders. [80]

2.8 Chapter conclusion

From the results of this review a comprehensive testing programme was determined which sought to determine the suitability of employing AE supplementary to proof tests. The competent person could use the AE to attain better information on the condition of structures and be therefore enabled to come to a more informed decision regarding the continued safe use and future preventative maintenance strategy of structures.

The programme of work can be summarised as:

Initial verification of the approach in a laboratory, the advantages of laboratory trials are that in-service components cannot as readily be subjected to a simulated life. The results of such experiments are reported in chapter three.

1. Verification of the Dunegan corollary on a component to which LOLER is applicable.
2. Investigation into the qualitative and quantitative nature of the AE generated during proof tests
3. Continuous monitoring of a component during a fatigue trial to observe the progressive nature of failure of engineering materials and observe the applicability of a power law relationship

Field trials were conducted to investigate the effectiveness of AE as means of detecting defects on in-service structures. The results from field trials are reported in chapter four as a series of case studies.

1. Trials were conducted on equipment re-qualified by the use of a proof test; verification of the Kaiser effect was sought on non defective lifting equipment to which LOLER is applicable.
2. An experimental procedure was conducted on defective lifting equipment to identify AE's suitability for defect identification.
3. Cranes both defective and non defective were investigated and the previously described evaluative methods were applied.
4. An underwater vehicle was tested using complimentary NDT techniques. It was subjected to both a proof test and fatigue and the use of other methods of measurement were used to substantiate claims that AE would detect a propagating defect.

Finally, the investigation returns to the laboratory and focuses on using the results attained during only proof tests to identify the non linear nature of failure in fatigue cracking as a means of establishing a through life trendable condition indicator. The results conducted on notched specimens subjected to fatigue until failure is reported in chapter five. The effect of the proof tests on the lifetimes is additionally investigated.

CHAPTER 3: Laboratory investigation of load testing and Acoustic Emission as a suitable condition indicator

3.1 Chapter Introduction

In order to investigate the feasibility the chosen approach to successfully identify defects in mechanical structures, a series of tests was designed. Initially evidence was sought on the applicability of the Dunegan corollary to wire ropes with seeded faults. A population of wire ropes with induced flaws of known severity was subjected to a loading pattern that simulated normal operational conditions. The objective of this investigation was to demonstrate the methodology that could be used for the non destructive evaluation of wire ropes, an example of lifting equipment to which LOLER is applicable. Acoustic Emission was monitored throughout the test, however the points in conjunction with a proof load test were of the most interest. The Acoustic Emission generated during the proof test would verify the suitability of the methodology for periodic inspection during which information about the ropes condition could be attained. Diagnosis of the severity of damage that had been induced was also investigated.

A wire rope with an induced flaw was subjected to constant amplitude fatigue until failure. During the trials to investigate the Dunegan corollary, an audible cracking noise and the failure of single wires that make up the rope were observed to coincide. As a result the investigation sought to identify singular wire breaks from other AE sources. To achieve this it was necessary to isolate such sources of AE from other mechanisms that generate AE during the test. The description of how differentiation from other sources that can occur during the stressing of the rope was accomplished is discussed. It was found that the almost simultaneous fracture of a number of singular wires meant that isolation of a classifier that could be used to identify individual wire breaks proved impossible. Within any given hit there could occur numerous wire breaks and so the classification was changed from the identification of wire breaks to merely identifying damage related AE from non damage related AE. This classifier was then used for the generation of a filter that was used to identify the damage that occurred during a fatigue test.

3.2 Investigation into the feasibility of using the Dunegan corollary as means of defect detection in wire ropes

Wire ropes, figure 3.1, are mechanical structures that are traditionally re-qualified by a periodic proof test. For this investigation such a methodology was incorporated into the testing regime and evidence that the Dunegan corollary could be used as a means of reliable defect detection during the simulated life of a rope was sought. The tests endeavoured to replicate the life of a typical rope. Initially, the rope was commissioned with the application of a pre-stressing proof load. Such a procedure would be conducted prior to the rope going into service. During service, the operator utilises the rope at the predetermined safe working load (SWL), usually a proportion of the proof load for a

specific period of time. In accordance with current maintenance regimes, after the specified usage time, a periodic inspection takes place by the further application of a proving load. Current industrial practice dictates that if the structure withstands a stated percentage overload from its safe working load then that structure is deemed 'fit for purpose' and safe for continued use.

In this study, differing degrees of damage were introduced into a wire rope population by means of a saw cut. In order to determine the levels of severity of the respective saw cuts a light illuminated the specimens enlarging the image of the flaw on to a screen. Measuring the proportionality of the magnified flaw to the magnified shadow area generated by the rope assisted in accurately identifying the differing degrees of damage severity introduced. This approach is shown diagrammatically in figure 3.2.

These tests were designed to replicate reality and therefore the damage in the ropes was introduced mid way through the life. Thereafter it was assumed that the operator would continue to use the rope without any awareness of the inherent defect. A periodic inspection was then conducted in conjunction with Acoustic Emission monitoring at the scheduled point of periodic re-qualification.

The investigation sought to determine that the generation of AE on the proof test is indicative of the presence of a flaw in the rope. Equally, it was investigated if the quantity of AE generated was indicative of the severity of the flaw. Thus both the qualitative and quantitative nature of the AE generated on proof tests was examined.

In summary and in keeping with current practices that are applied industry wide a wire rope is likely to experience distinct stages during its life. These are:

1. During commissioning the rope would be subjected to a proving load to essentially pre-stress the rope.
2. It would then under go an operational period in which the operator utilises the rope at a SWL for a predetermined period.
3. It is then subjected to periodic proof test. In the event that the rope does not fail the proof test verification is achieved and it is safe for continued safe use.
4. The rope is then be returned to service for a further fixed interval, until the next test.

The technique outlined by Dunegan should prove suitable for integrity assessment in wire ropes. If the rope contains an integrity threatening flaw, it will grow under the application of the proof load and AE will result, as the rope will experience an unprecedented stress during the proof load.

A number of researchers have focused on the non-destructive testing of wire ropes utilising Acoustic Emission techniques. Harris and Dunegan (1974) conducted both rising load tests and fatigue tests on wire ropes and found that ample warning was given of impending failure under both conditions.[81] Additionally, they stated that the continuous AE monitoring of wire rope whilst in service would be prohibitively expensive and the

likely commercial application of AE monitoring would be in conjunction with a periodic proof test. This part of the investigation is largely an elaboration of their work and makes use of the phenomenon described some years earlier by Dunegan and subsequently referred to by Pollack[82] as the "Dunegan Corollary". The penultimate chapter investigates how such a methodology can be used as a through life trendable conditional indicator.

Casey et al. (1985-97), [83,84,85,86,87,88] have been credited with a number of publications on the subject matter. Their focus was largely on the development of a wire break detector. They studied the AE amplitude distributions and the frequency components of singular wire fractures within a rope and were able to discriminate between genuine Acoustic Emission signals and background noise. They concluded that high amplitude hits could be associated with fractures and attained a one-to-one correlation between AE hits and wire breaks. They also suggested that the energy content of these associated wire break signals would not attenuate greatly over the length of a rope and that further work should show that detectability of signals from a distance of 30 metres was achievable.

Laura and Matthews[89] (1985) devised an instrument for the continuous monitoring of a mechanical cable utilising Acoustic Emission with some success.

Woodward[90] (1989) conducted a series of experiments at the Transport Research Laboratory on a variety of wires. A criterion was established whereby the detection of AE hits with signal features of high amplitude, long duration and a large numbers of counts could be attributed to wire breaks. Such hits were also likely to be coincidental with the maximum load. Due to both background noise and attenuation, confirmation was not attained.

The work of Harrop and Summerscales[91] (1989) suggested that the Kaiser effect may not be applicable on wire ropes as the inter wire fretting caused excessive low amplitude noise and hence interference. The authors did suggest that AE evaluation of wire rope had tremendous potential as a monitoring tool although significant development work was required.

3.2.1 Equipment and settings used

The wire rope specimens were made from 10mm steel wire rope, round strand of a configuration of 6 x 36(14/7 + 7/7/1) / IWRC. To explain this convention of a wire rope alphanumeric representation, the IWRC, is an abbreviation for Inner Wire Rope Core. The IWRC consists of a king wire, which is the most central wire, and wires are wound around the central king wire to produce a straight strand in a single helical form. A single helix is the helical curve whose axes are in a single plane. The rope consists of six outer strands comprising of thirty-six wires (6 x 36). Each one of the six strands is made up of three layers of wires wound around their central core wire. There are 14 wires in the outer layer, 14 wires of two alternating diameter (7+7) in the middle layer and seven wires in the innermost layer wrapped around a central core wire. The wire ropes cross section is shown diagrammatically in figure 3.1.

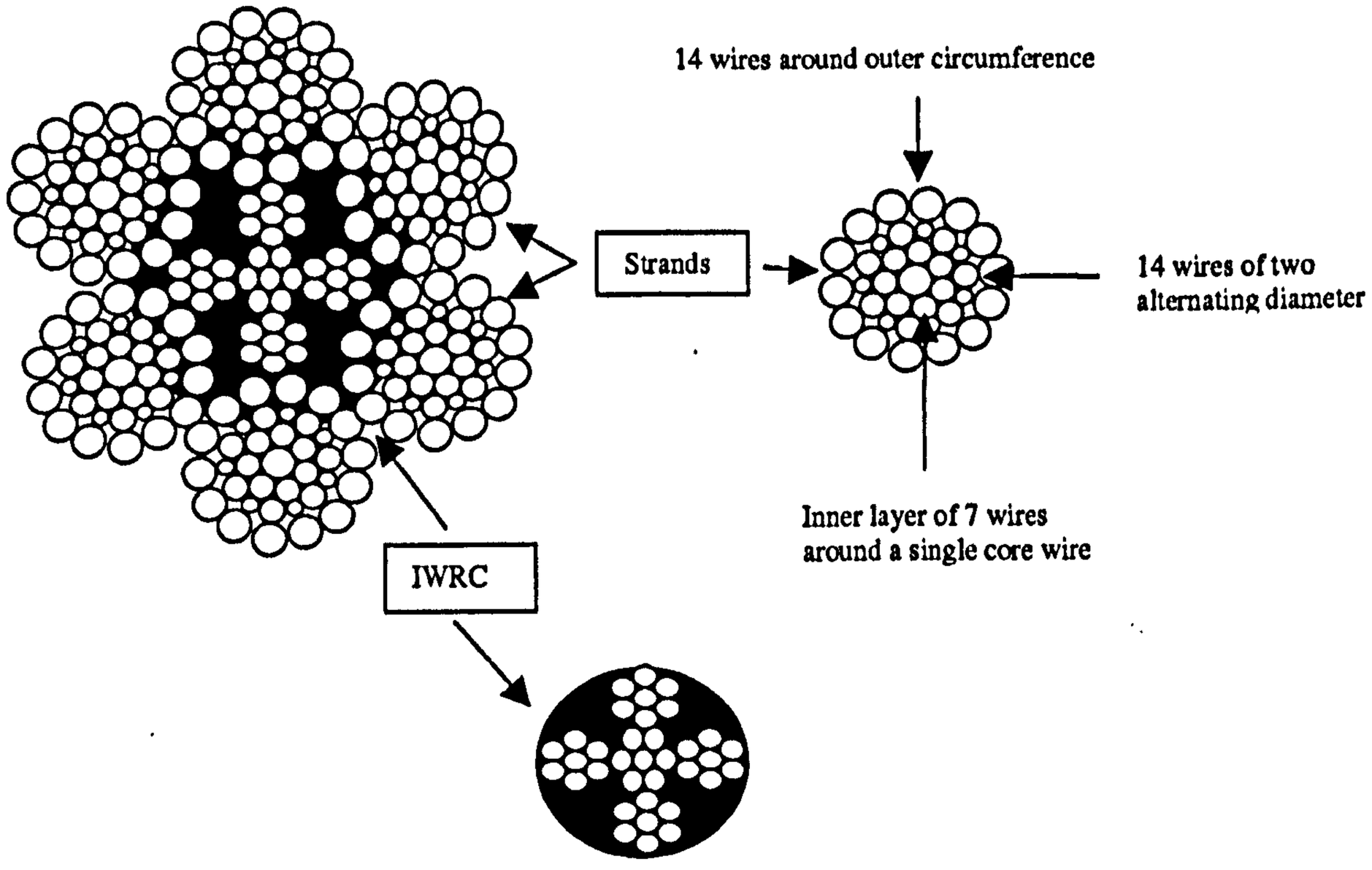

Figure 3.1: Wire Rope cross section

The associated certificate for the rope states a specified breaking force of 72.88 kN and the rope is certified to have a proof load of 2.6 Te (25.5 kN) and a SWL of 1.3 Te (12.75 kN). In simple terms, this wire has an inherent factor of safety built into it of approximately 6.

The rope specimens were made using the standard ferrule for this type of rope. In the manufacture of a lifting strop there would be the attachment of two ferrules whose purpose is to clamp the end of the wire back on to itself and create eyes at either end. For the purposes of this experiment four ferrules were attached. One ferrule was attached at either extremity to be griped within the loading machine. Two further ferrules were attached 50mm from each end, giving a gauge length of 550mm. The AE transducers were mounted on the inner ferrules.

The loading machine used was an Instron model No 1342 H 1031.

A camera and visual display unit was used for the purposes of magnifying the flaw so that the proportionality between the flaw and the rope was more discernible. Magnifying the image generated achieved a greater accuracy in quantifying the flaw size.

The AE equipment was manufactured by Physical Acoustics Corporation, a four channel AEDSP-32/16B with Mistras 2001 software. Only two of the available channels were used for the purposes of this test. The transducers were wide band with a frequency range from 0.1 to 1.2 MHz.

The instrument settings were set such that there was a fixed threshold level of 40 dB, a pre-amplifier gain of 40 dB, i.e. x 100, a sampling rate of 4 MHz and a software setting of a frequency bandpass of 100 kHz – 1.2 MHz. The applied load was also monitored and brought in to the instrument as an additional parametric input. This was achieved by a direct connection from the Instron loading machine.

Figure 3.2 depicts a schematic of the test set up.

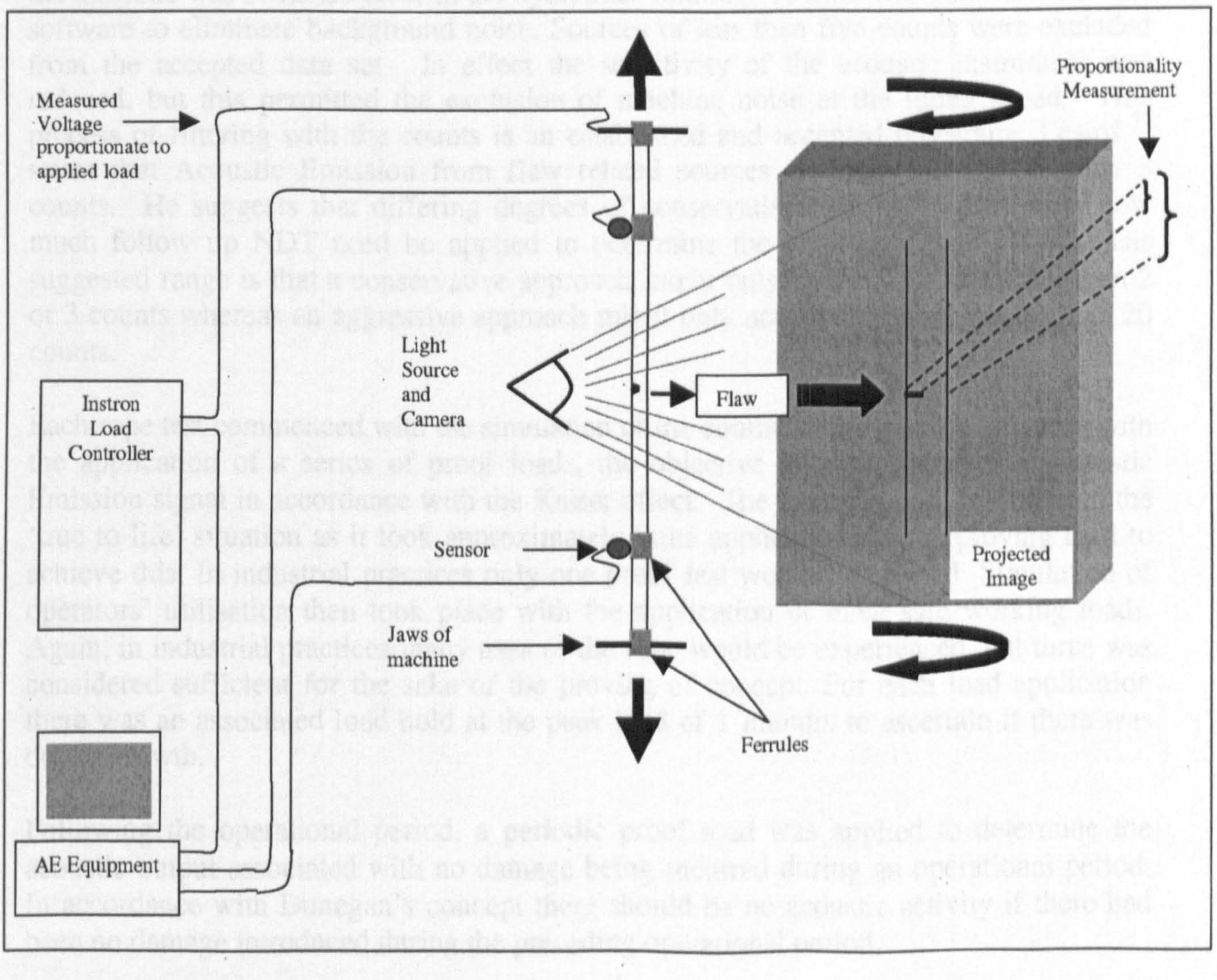

Figure 3.2: Test Set Up

3.2.2 Methodology

The transducers were mounted on the ferrules of the rope with industrial grease used as a coupling medium. They were secured by wrapping insulating tape around the transducer and the ferrule. Their sensitivities were checked using the Hsu-Neilson pencil source in accordance with standards.[92,93] The Hsu- Neilson pencil source involves the fracture of a mechanical pencil lead on the specimen under test. The fracture generates a stress wave that can be used to confirm the instruments sensitivity. The reported response should fall within a specified decibel range.

Prior to any testing, a background noise check was conducted with the rope secured within the grips of the loading machine for a period of one minute. During this period, the machine was switched on with the hydraulics running. A filter was created within the software to eliminate background noise. Sources of less than five counts were excluded from the accepted data set. In effect the sensitivity of the acoustic instrument was reduced, but this permitted the exclusion of machine noise at the idling speed. This process of filtering with the counts is an established and accepted procedure. Leaird [77] states that Acoustic Emission from flaw related sources generally have more than 3 counts. He suggests that differing degrees of conservatism can be applied as to how much follow up NDT need be applied to determine the significance of a flaw. His suggested range is that a conservative approach might only accept data of greater than 2 or 3 counts whereas an aggressive approach might only accept data with greater than 20 counts.

Each rope test commenced with the simulation of the commissioning of the structure with the application of a series of proof loads, the objective being to decay the Acoustic Emission signal in accordance with the Kaiser effect. The experiment departed from the 'true to life' situation as it took approximately three applications of the proving load to achieve this. In industrial practices only one proof test would be applied. Simulation of operators' utilisation then took place with the application of three safe working loads. Again, in industrial practices many uses of the rope would be experienced, but three was considered sufficient for the sake of the proving of concept. For each load application there was an associated load hold at the peak load of 1 minute, to ascertain if there was defect growth.

Following the operational period, a periodic proof load was applied to determine the acoustic output associated with no damage being incurred during an operational period. In accordance with Dunegan's concept there should be no acoustic activity if there had been no damage introduced during the preceding operational period.

The acoustic recording device was then paused and a saw cut was introduced into the rope. Various depths of saw cuts were applied to different ropes to achieve varying degrees of damage severity. The saw cut was measured by magnifying the flaw with the assistance of a camera and television screen. This flaw size is referred to as a percentage reduction in diameter. The calculated percentage reduction in diameter for the five wires was 12,18, 22, 22,and 32 % respectively.

The wires were assigned a unique identification number to which they will be subsequently referred to during the course of the investigation.

Rope I.D	Damage introduced (% reduction in diameter)	Damage Location(mm)
103	12%	120
105	32%	360
106	18%	440
107	22%	160
108	22%	180

Table 3.1: Ropes % damage and location

There were a number of weaknesses in the quantification of the flaw size, primarily because the image is sized on a flat screen. The method assumes that the flaw is introduced absolutely perpendicular to the camera which in practice is difficult to achieve. It also assumes that the flaw is introduced to the rope at the same orientation in each case. Due to the wire not being a true circular section, but a series of small circular sections arranged around a central core, it matters where the flaw is introduced. The effect is that the flaw can be induced by partially cutting a single strand or alternatively across two strands. This difficulty of achieving a repeatable orientation is shown diagrammatically in figure 3.3.

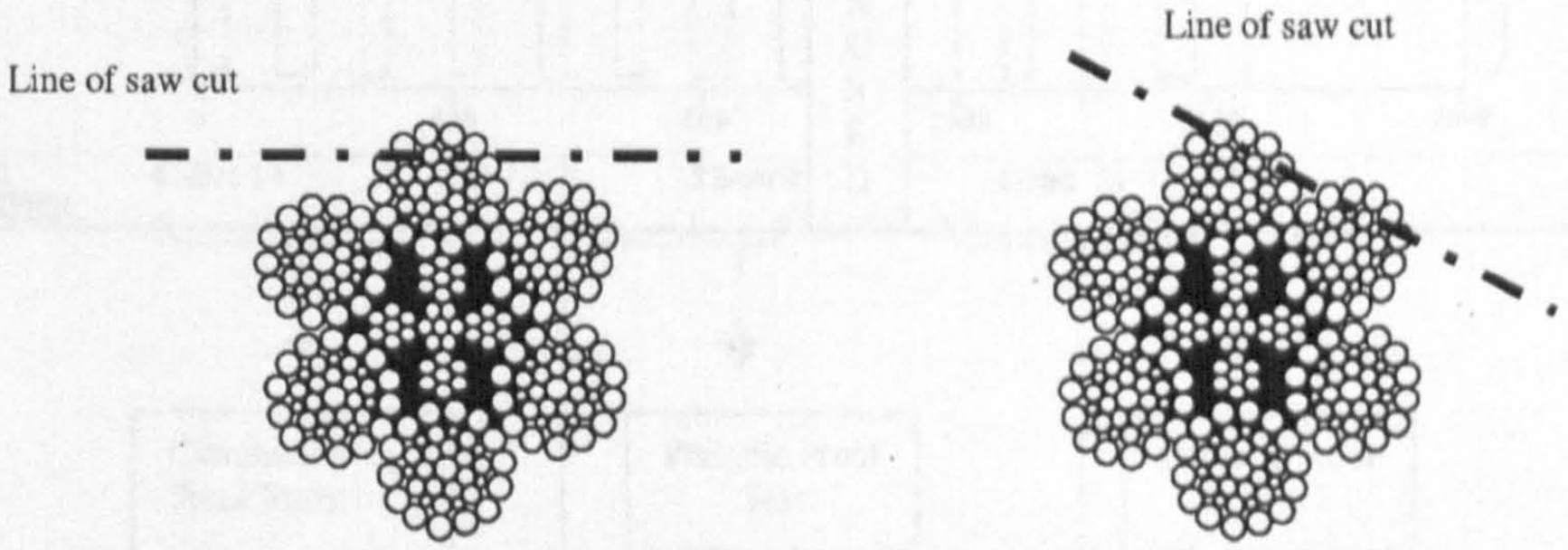

Figure 3.3: Discrepancy in the orientation of the rope

After introducing the damage into each rope the acoustic recording instrument was recommenced and lifetime simulation continued with three further applications of SWL.

This replicates the operator using the rope without an awareness of the defect. After the operational period, an inspection took place by the application of a proof load.

Graph 3.1 illustrates the AE and load characteristics for wire 106 with 18% damage induced and may be regarded as representative of a typical result set. The results of the other wire rope tests are given in Appendix III (A).

Results

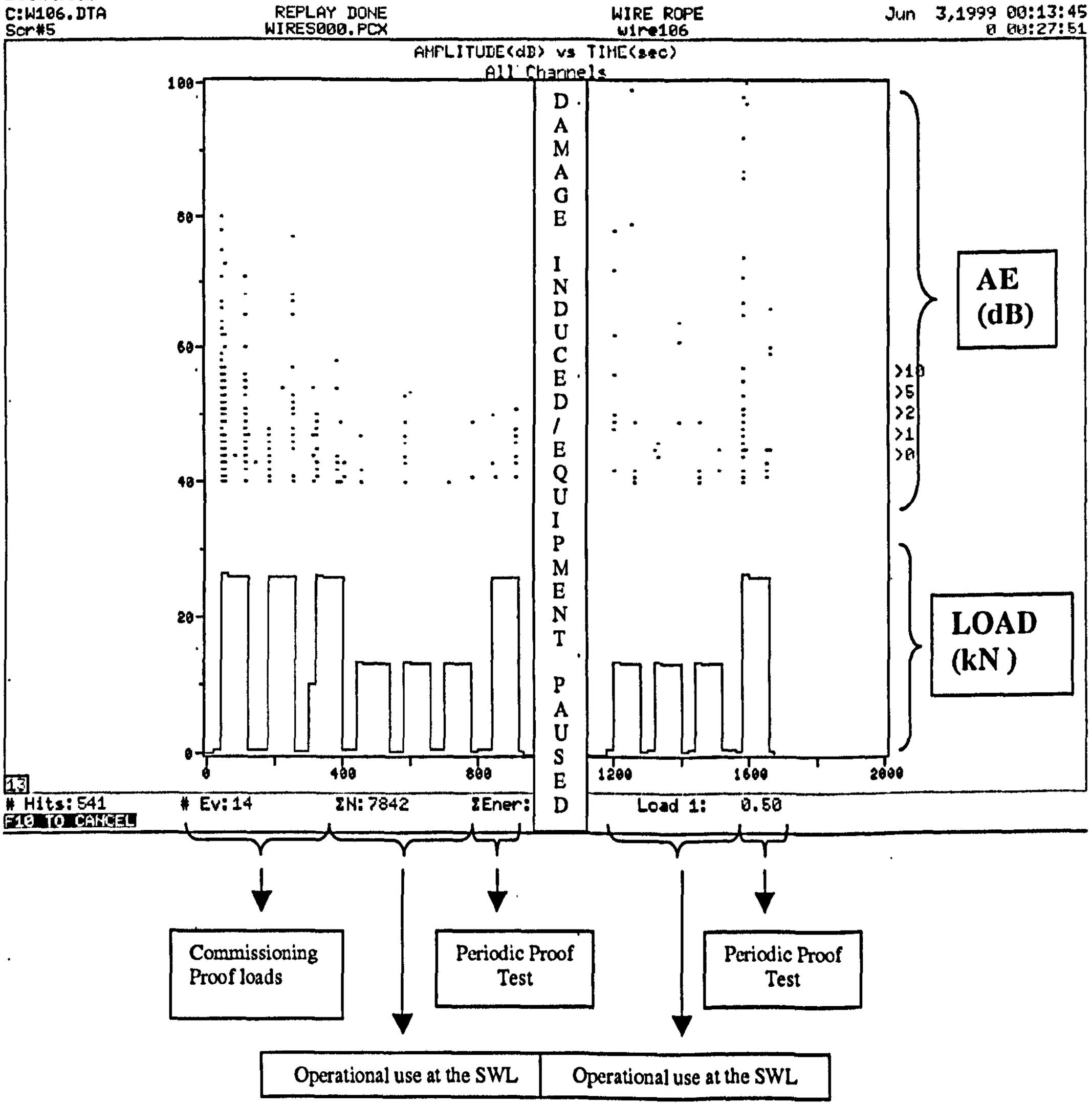

Graph 3.1: Acoustic Amplitude and load profiles against the time history of the test.

Discussion

Graph 3.1 shows both the loading profile and the associated acoustic activity over a time base of 2000 seconds. The load profile is shown by the line graph and the acoustic

activity by the dots. It is possible to differentiate between both the loading and unloading events. The commissioning phase is represented by the first 400 seconds where it is apparent that the acoustic activity decays with subsequent applications of load to the same stress level. This is in accordance with the Kaiser effect. Amplitude was chosen as the feature to best illustrate the acoustic activity. Amplitude is expressed over and above a threshold crossing, in this instance 40dB. This permits the load to be illustrated beneath and allows visualisation of the stimulus and the resultant output simultaneously without overlap.

Simulation of normal operation at the SWL takes place between 400 and 800 seconds and there is negligible acoustic activity. Note that during the hold periods there is an absence of acoustic activity suggesting that even on full load machine noise had been eliminated by the employed filtering technique.

The first of the periodic inspections occurred at 800 seconds and in accordance with the Dunegan Corollary there is no significant Acoustic Emission as there has been no damage incurred in the rope during the preceding operational period.

During the period between 900 and 1200 seconds the damage was induced in the rope, and the AE equipment was paused so as not to include the intervention in the data.

On restarting the recording equipment and applying the SWL it can be seen that there occurs new and significant emission. This is considered to be due to the redistribution of stress necessary to compensate for the change in load path now that some of the wires are no longer present. The emission can be observed to decay with subsequent loadings to the same stress level. This simulates the use of the structure by the operator without awareness of the defect. In normal operational circumstances the acoustic equipment would not be mounted on the wire during its service life, but for the purposes of laboratory work it assists in the comprehension of the acoustic behaviour by illustrating the irreversibility of AE - the Kaiser effect.

At 1550 seconds, the final periodic proof test occurs and as soon as the loading level surpasses the previously applied maximum load since the introduction of the damage, there is new and significant emission. Note, especially that there are a greater number of higher amplitude emission than in any of the previous loading cycles. These high amplitude hits are attributed to failures of individual wires that make up the strands of the rope. During the experiments there was a coincidence of the arrival of high amplitude hits and an audible cracking sound, which was observed to be the fracture of the individual wires.

These experiments demonstrated that it was possible to determine the condition of a wire rope by combining AE monitoring with the periodic application of proof tests permitting the identification of whether damage had been experienced and otherwise. The ropes condition can be ascertained without the necessity of monitoring through the life, but from periodic measurement. Of the five ropes tested, one of the 22% as well as the 32% damaged wires experienced a strand failure during the final application of the proof load.

Two wires received introduced damage of 22%, the reason why only one of the two experienced strand failure is because of the previously described orientation of the flaw. The wire that experienced a strand failure had the damage induced over a single strand. If the damage had been distributed over two of the strands then failure would have been less likely to occur. The 22% (107) damaged wire, that experienced a strand failure gave the same energy content as the 32% (105) damaged rope and therefore 107 was omitted from the subsequent analysis.

Graph 3.2 illustrates the capability of the technology to locate the source of the emission. This is achieved by time-of-arrival techniques. The flaw or AE source is given as a function of distance from the transducers. The results of the location plot are shown in graph 3.2 and reference is made to the test set up as illustrated by figure 3.3.

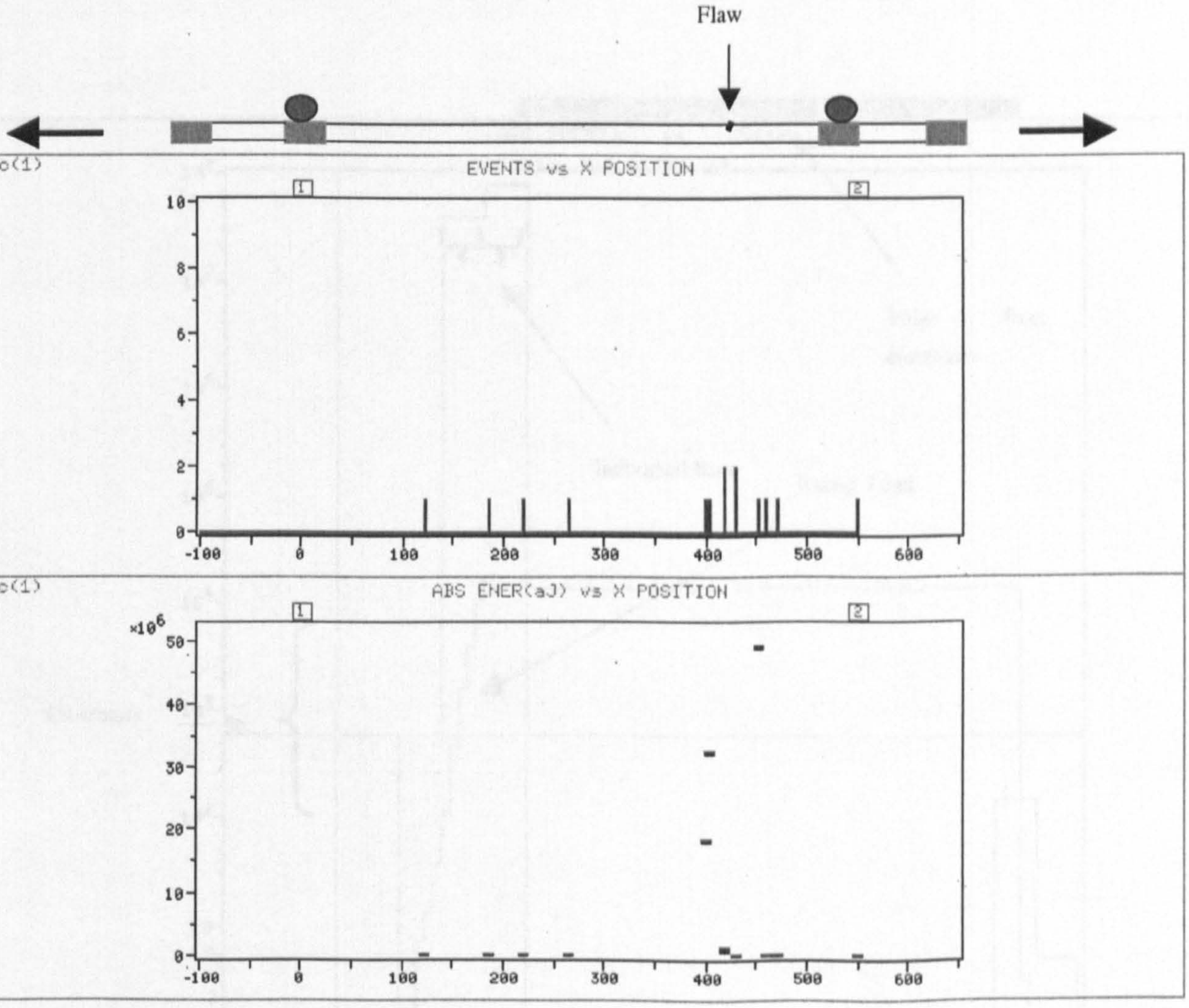

Graph 3.2 Location plots of both Events and Event Energy

The boxes at the top corners of each graphical display are representative of the transducers position over the gauge length of 550 mm. The source of the majority of the activity is shown in the region of 390-440 mm from transducer 1. The position of the

flaw was physically measured from transducer 1 and this was found to be 420 mm, in good agreement with the results in graph 3.2.

The software enables a single loading application to be separated and evaluated. The emission generated during the final proof test was isolated, and the sum of absolute energy identified by using the crosshairs to attain the exact value of each of the bins (bars on a Bar Chart). The bin quantities, measured in atto Joules, are displayed as white on black in upper section of graph 3.3. Only the hits experienced during rising load were summed. The relevance of isolating only the rising loads is that induced defect is stimulated by the increased stress and the falling loads are not considered to contribute damage progression.

Graph 3.3 illustrates the method by which the summing of the energy was achieved.

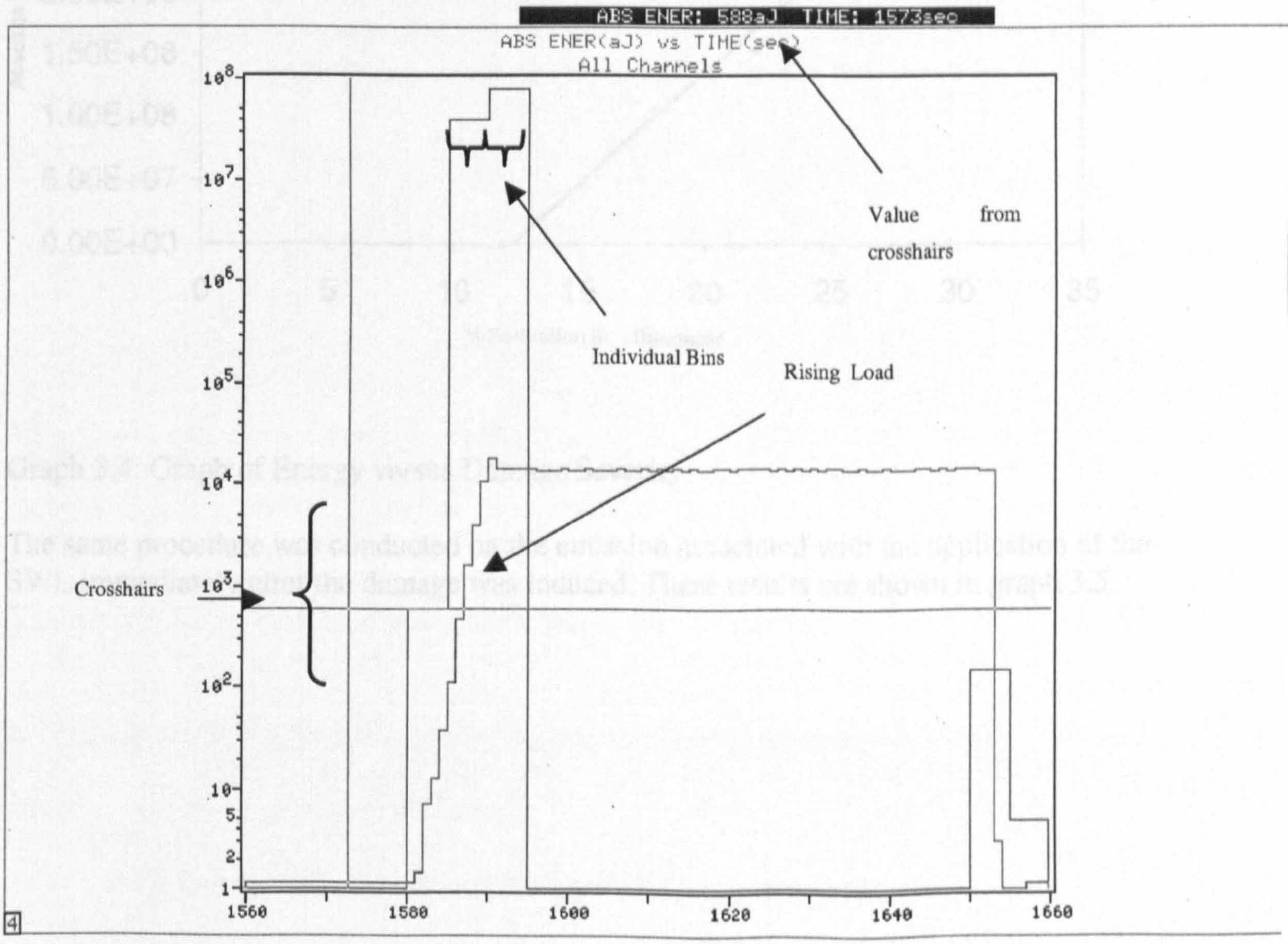

Graph 3.3: Measurement of the quantity of Energy emitted during a load

This procedure was conducted for each wire and the results were plotted against the percentage reduction in diameter. A line of best fit was obtained as well as the confidence (R^2) of the line fit to the data. The graph of this output is shown in graph 3.4.

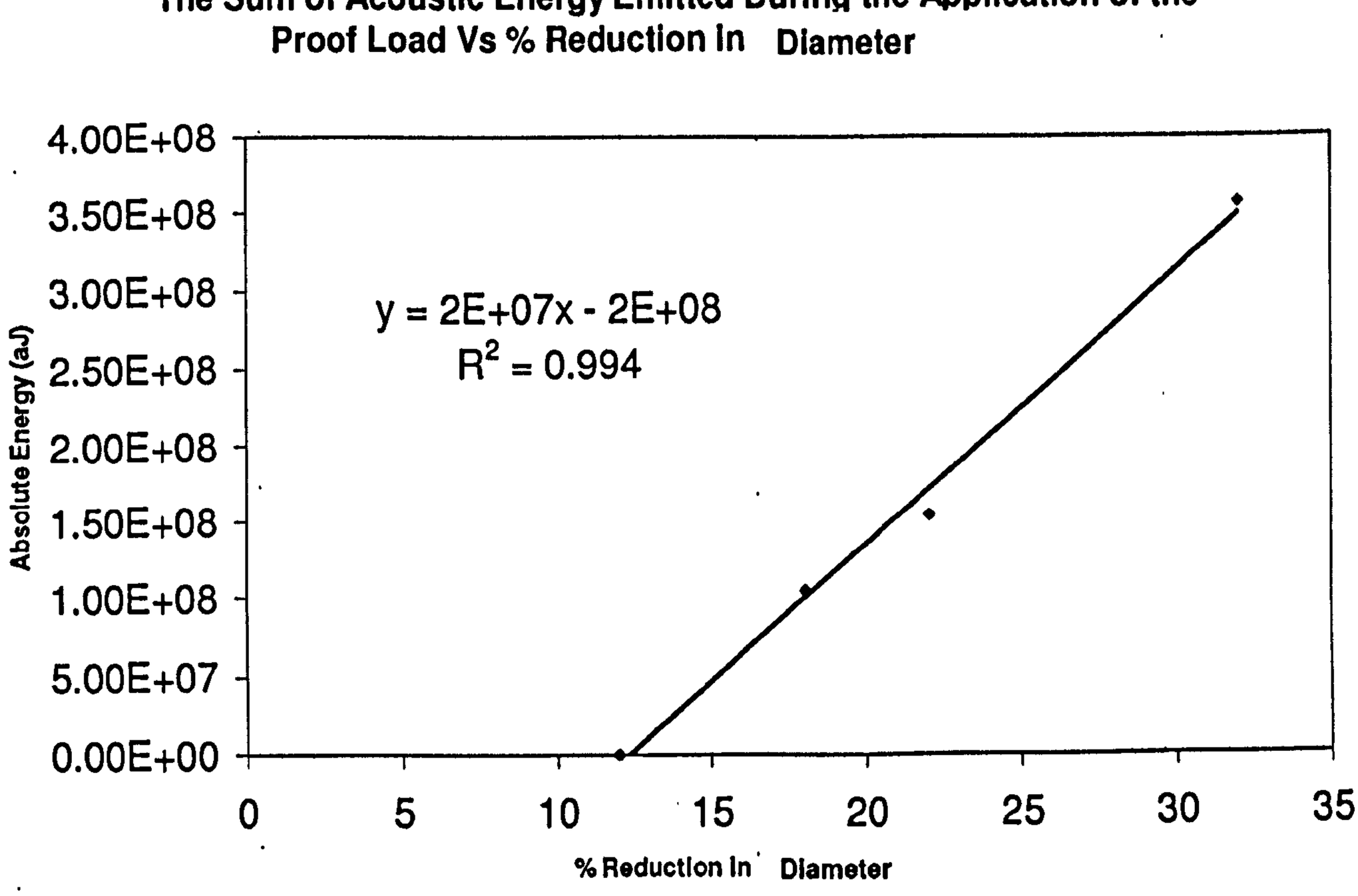

Graph 3.4: Graph of Energy versus Damage Severity

The same procedure was conducted on the emission associated with the application of the SWL immediately after the damage was induced. These results are shown in graph 3.5.

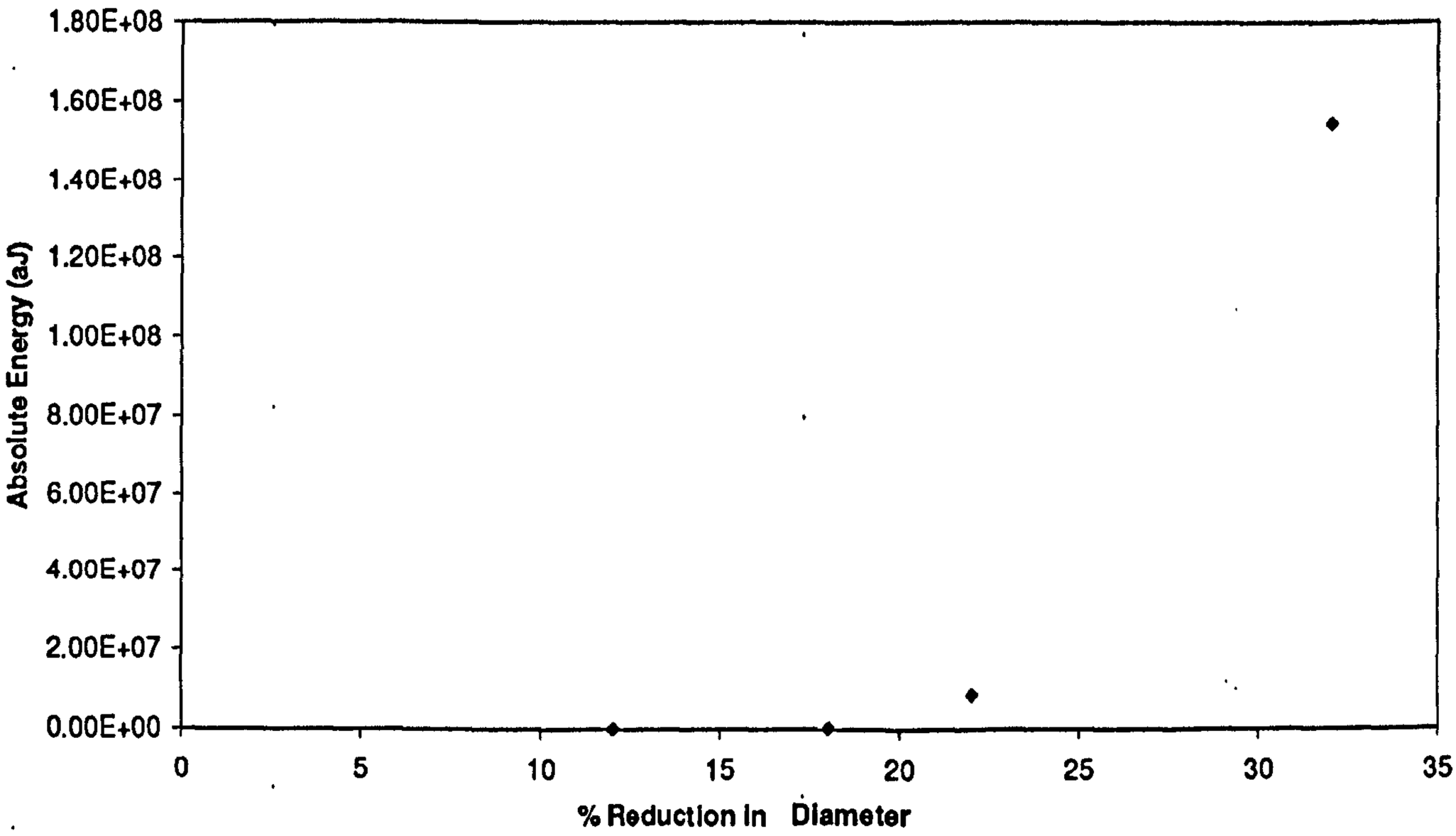

Graph 3.5: Graph of Energy versus Damage Severity

The results on the proving load application are indicative that there is a linear relationship, graph 3.4, between the energy content of the emission and the severity of the damage. Confirmation of Dunegan's corollary that the amount of emission is indicative of the level of damage has been achieved. However, the results from the AE attained on the application of the safe working load succeeding the introduction of the damage do not substantiate this. The suggested explanation for this is that the SWL application is a sixth of the load required to break an unflawed rope whereas the proving load is a third. Considering that Acoustic Emission are the resultant events of the integrity of the structure being threatened it is probable that the level of excitation of the SWL was not sufficient to threaten the ropes with the smaller defects. Small flaws with a limited stimulus cause no significant emission.

3.2.3 Conclusive remarks on the effectiveness of the Dunegan corollary

The significance of the test results shown suggest this concept could provide a means by which wire ropes could be non-destructively tested. If AE was used in conjunction with the industrial practice of the application of a proving load, flaws that did not necessarily result in the parting of the rope could be identified and their location established permitting further investigation. This would provided a significant enhancement to

industrial practices in that defects that were not sufficiently large as to cause the failure of the rope during proof testing could be identified sooner and a decision on whether they were safe for continued use determined.

The near perfect line fit of the acoustic energy to damage severity is not suggested as a definitive algorithm that can be used to assess this particular rope type because of the inadequacies of the quantification of flaw size. However, it can be stated that for increasing damage severity there is a corresponding increase in the energy content of the emission on the proof test.

This method could give the competent person the reassurance that the structure has no discontinuity growth at a prescribed loading level thus empirically proving the structure.

There are a number of issues pertaining to the above that raise questions and therefore are issues for further work The most concerning feature of this application is that the irreversibility of the acoustic activity could work equally well against the technique as it does to support it. Consider a situation where both damage as well as an overloaded condition occurred within the same operational period. During the periodic proof test the previous overload would mask the evidence of the change in state, if the overload was greater than proof test.

In this investigation only damage of a saw cut type flaw has been explored, other more natural failure modes of wire ropes should be explored. The wire ropes that made up the population set for the provision of these results are shown in Appendix III (A).

3.3 Classifying wire breaks

3.3.1 Introduction

The experimental procedure when conducted did not seek to create a means of identifying single wire breaks acoustically. The procedure aimed merely to illustrate the applicability of the Dunegan corollary as a means providing a suitable condition indicator. During the experiment no attempt was made to determine how many single wires the saw cut had severed. There was therefore no way after the experiments of correlating the signals to the number of wires broken during the loading regime. As a result, engineering intuition has been used to create a wire break discriminator that is based upon observations during the trials. From the observation that two of the ropes experienced a strand failure during the final proof test and that wires were broken during the stressing after the defect was introduced. It can conclude that the most likely load applications that are liable to generate wire breaks are the loads of the SWL after the damage, particularly the first one as well as the ultimate proof test. Additionally the most likely place for wires to break is at the site of damage.

3.3.2 Conventional AE analysis

This section of the investigation builds a means of identifying wire breaks from the data sets. In order to classify unique features that may differentiate between wire breaks and other sources a suite of pattern recognition plots were constructed, these are shown in Appendix III (B). Wire 106 is shown within this section as demonstrative of the approach taken to identify wire breaks. The constructed suite of plots that allow identification of single wire failures comprise of source location graphs, amplitude distributions and time histories.

Casey et al [84] suggested that the amplitude distributions and frequency components of the signals may provide the means of discovery of a unique characteristic that may permit the formulation of a wire rope classifier. Woodward[90] concluded that the criterion of high amplitude, long duration and a high number of counts and coincidence with the peak loading were likely to be wire breaks.

During the trials an audible noise was observed when straining some of the wires after the damage was introduced. This was considered to be single wires of the rope fracturing, as indeed others have reported. The instrument was observed in real time to be registering very high amplitude hits of the order of 95 dB coincident with these noises. 95dB is considerably higher than any hits that were generally observed during straining of ropes prior to the damage introduction.

The nature of the damage introduced into wire 106 can be observed in the plate 3.1, the damage can be viewed as break across the helical strand beneath the zero of 106.

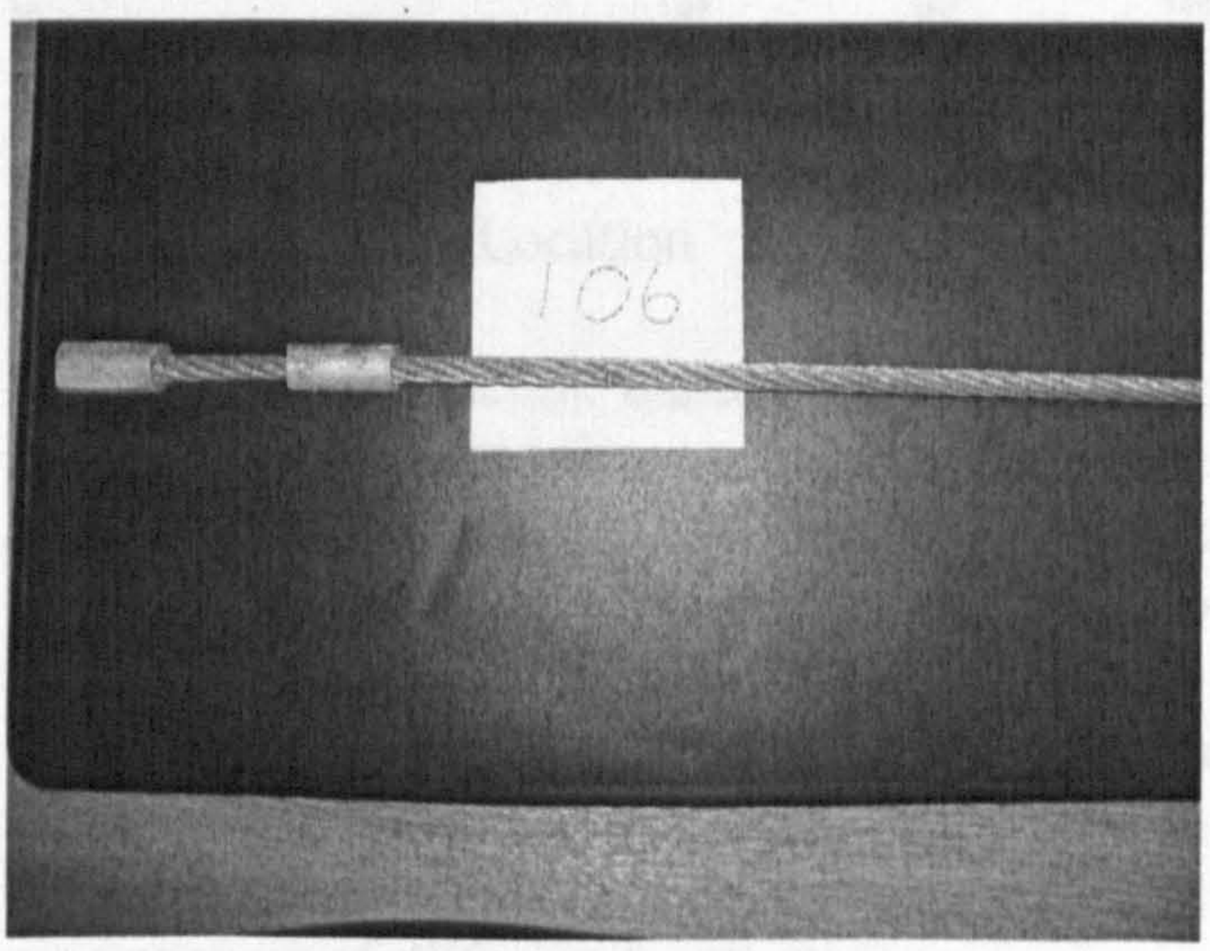

Plate 3.1: The damage on wire 106

It is felt that source location plots might additionally provide a useful means of identifying wire breaks from the data files. Wire breaks are most likely to occur in the

damaged region, as the stresses are highest at this point. Further, during the damage introduction some wires may be left partially severed and these would be the most likely to break during the applied excitation. Two-source location graphs are used, Events and Amplitude versus the X position measured in mm.

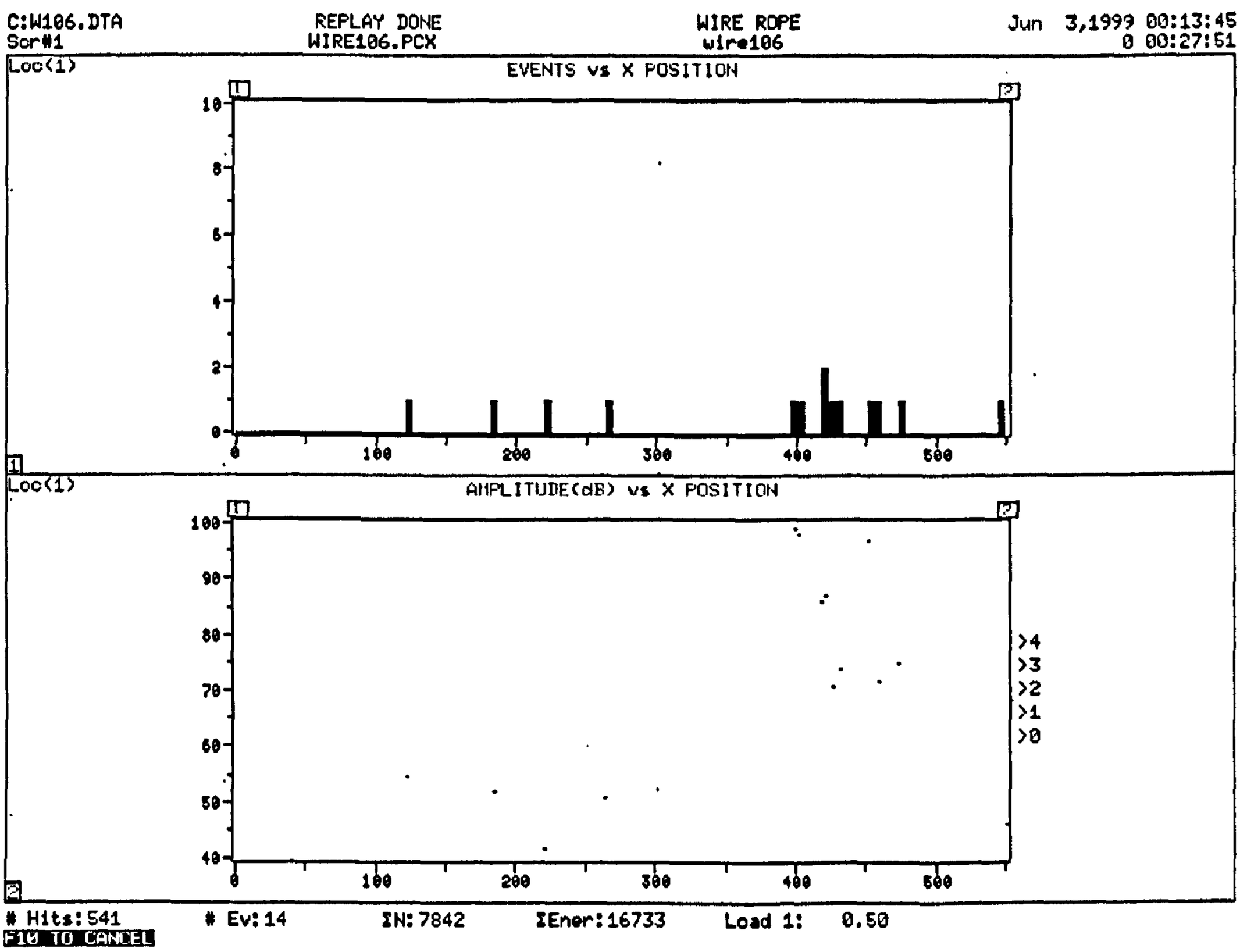

Graph 3.6: Source Location

In the proximity of the damage (420mm) the majority of the source located activity is observed. There are other events over the gauge length of the wire, but these are lower in amplitude. The slight spread of the source located activity within the damaged area is considered to be due to the different wave speeds travelling within the material, and additionally to the different paths along which the signal could travel. The signal may travel down either the straight central wire in the core of the strand or alternatively travel around the helical wires that are wrapped around the central core. This contributes to different lengths over which the signal would have to travel and hence the software reports them at different locations.

Examining both the amplitudes and energies of the signals emitted throughout the course of the test allows us to further identify the unique characteristics that may be attributable to single wire breaks.

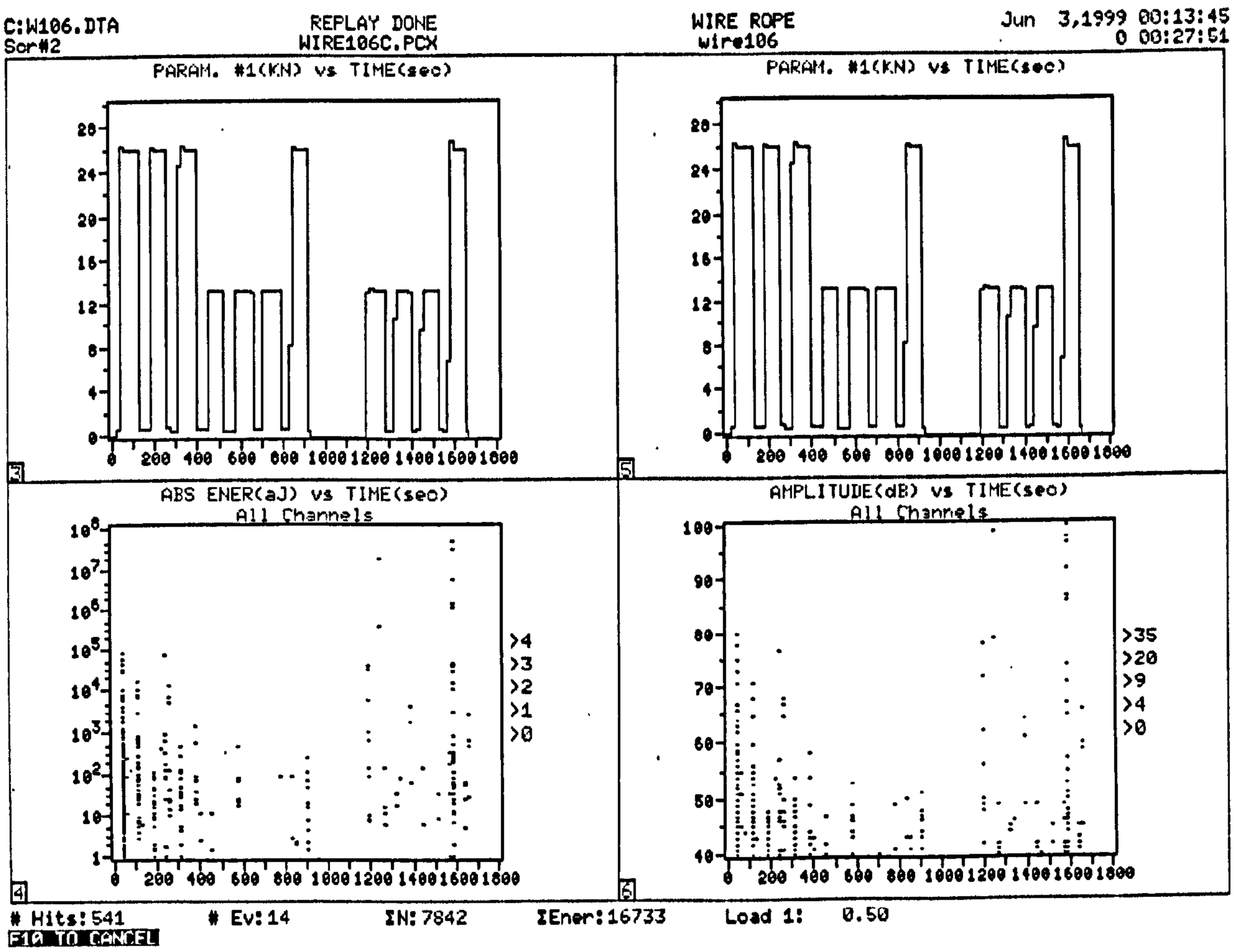

Graph 3.7: Load, Absolute Energy, Amplitude histories for Rope 106

The test logbook recounts that during the load hold of the initial application of the SWL after the introduction of the saw cut, there was an audible noise considered to be a wire break. The instrument reported this as a near 100dB hit which can be observed in the lower right graph at approximately 1250 seconds. In terms of energy content this exhibits a value of approximately $3*10^7$atto Joules.

The amplitudes and energies that occur on the applications of load after the damage introduction on both the initial SWL and on the final proof load are considerably greater than any amplitudes experienced during any other load application. It is at these points that wire breaks are most likely to occur.

One observable general characteristic of the AE generated in these trials is that the quantities of hits that occur on the initial commissioning proof load are significantly greater than any other load application. This information can be gleaned by observing the density of the hits on the graphs 3.7. It is most easily observed in the Absolute Energy graph, lower left side, by the high concentration of the AE on the initial proof test at 50 seconds.

Harrop et al.[91] suggested the Kaiser effect, may not exist within wire ropes due to low amplitude hits generated by inter-wire fretting. In these trials the Kaiser effect is seemingly not apparent in the strictest sense as on subsequent applications of the proof load, there is the presence of some acoustic activity, however, it decays with repetition. These emissions are likely to be associated with the stabilising of the rope, the strands and wires are likely to bite in to one another as they settle to find an arrangement from which they support the load.

On some of the SWL applications there is an absence of any AE indicative that the Kaiser effect is appropriate to wire ropes. One explanation for this low level activity that Summerscales reports was experienced during these trials. It was observed that whilst unloading to zero kN, the wire essentially tried to unwrap itself illustrating that torsional forces were present. The outcome is when the load is reapplied the orientation of rope cannot be guaranteed to be the same. The wire may therefore experience an unprecedented stress and hence the Kaiser principle rather than Kaiser effect may be more appropriate. If the wire is subjected to the loading whilst in a different orientation then it is likely that inter-wire fretting and stabilisation will reoccur giving rise to low-level emission. One means of avoiding this is to not fully unload the specimen and to ensure there is always some force on the rope and hence prevent the ropes from unwrapping.

Features of the signal were cross-plotted against the amplitude in order to investigate any unique characteristics that could be correlated with the arrival of wire breaks. These cross-plots are illustrated in graph 3.8.

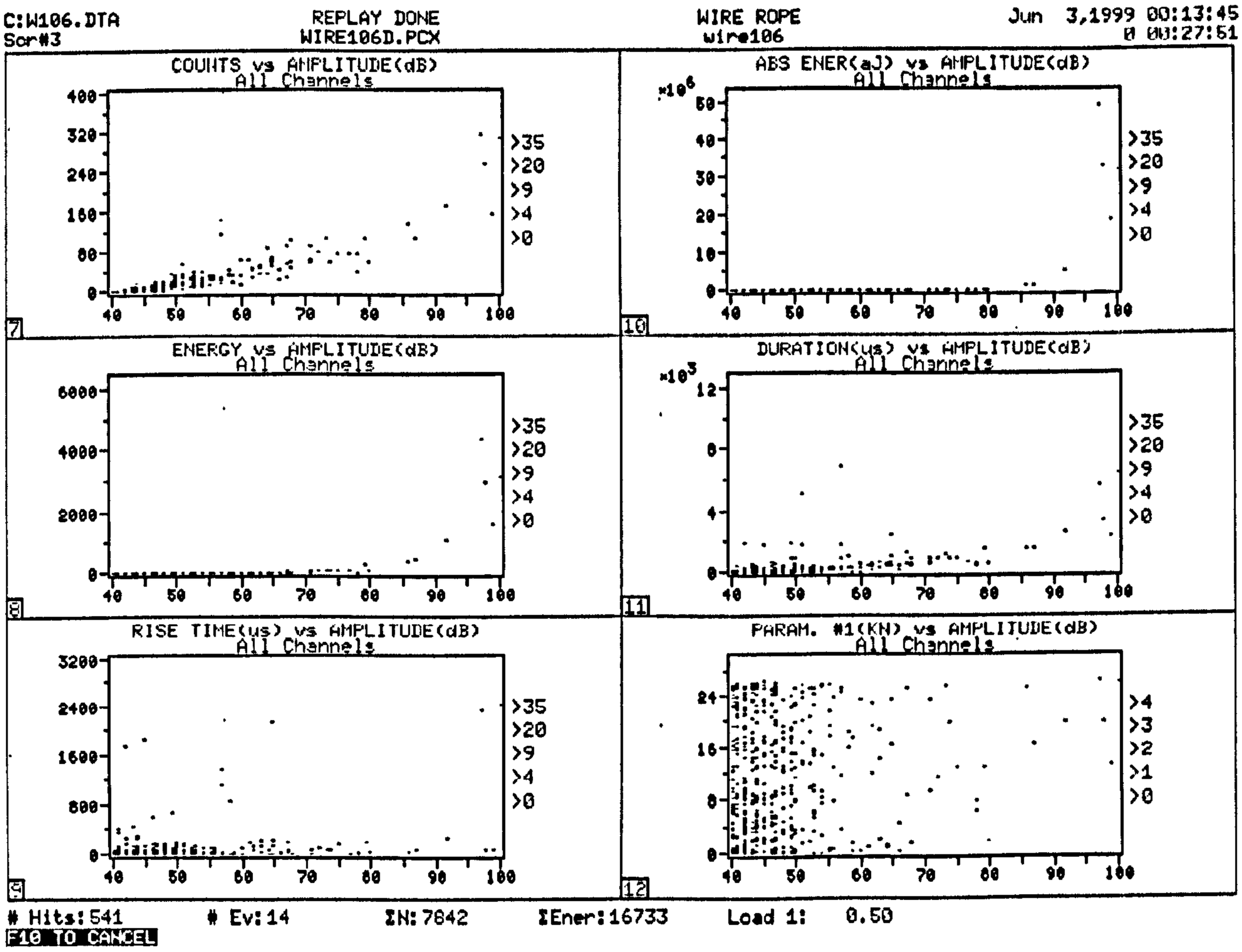

Graph 3.8: Amplitude distributions for Rope 106

Dealing with these sequentially the Counts versus Amplitude graph show with increasing Amplitude there is a corresponding increase in the number of counts. The Energy versus Amplitude graph shows all hits beneath 80dB have relatively low energy content, but after 80dB the energy content of the signals becomes more significant. The Rise-time versus Amplitude show the majority of hits have reasonably small rise times although some rise-times throughout the Amplitude range have highly variable values. Amplitudes approaching the 100 dB range have no consistency in their Rise-time.

The Absolute Energy versus Amplitude graph shows a very similar distribution to the previously described energy graph, a marked departure in significance at greater than 80 dB. An interesting observation of this graph, however is that the highest amplitude hit does not generate the highest energy and the range of energies from hits are enormous. One 98dB hit generates approximately 20 $*10^6$aJ and a 96dB hit generates in the region of 50 * 10^6aJ.

The Duration versus Amplitude graph has a similar distribution to the Counts versus Amplitude, as might be anticipated, although the inter-relationship between the features does not seem as pronounced. The Parametric verses Amplitude graph illustrates that most of the hits are of low Amplitude generally between 40 and 50 dB. The larger hits

(>80dB) occur mostly in the upper half of the load range. The wire break that was observed during the trial that gave rise to a 98dB hit can be observed at approximately 12kN. Viewing the time histories, figure 3.8, it can observed where the notable features occur during the loading sequence. It is useful to view the time histories in conjunction with the load history, which is shown in the extreme right graph, this permits one to view the acoustic behaviour with respect to the applied stimulus.

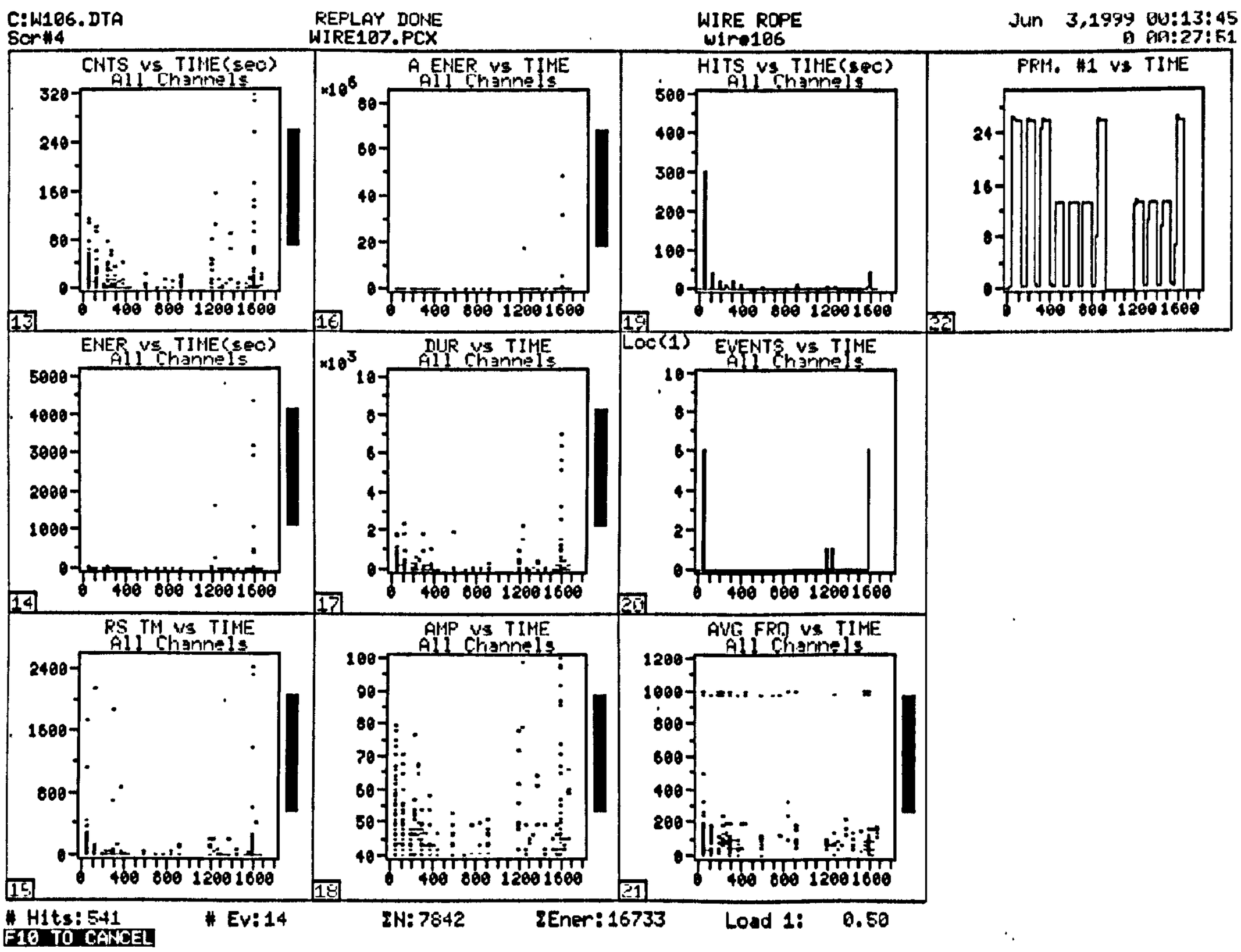

Graph 3.9: Time histories for Rope 106

Again, dealing with these sequentially, the counts history graph portrays relatively high numbers of counts on the initial commissioning loads. These subsequently decay until the damage is introduced after which hits occur with a high numbers of counts particularly on the application to the SWL and additionally on the final proof test. The Energy time graph illustrates that all the energy contents of the hits are comparatively small except when the damage has been introduced and the stress applied. The occurrence of high energy is coincident with the load application to SWL after the flaw introduction, 1200 seconds, and the load application of the final proof load, 1600 seconds.

Large Rise-times seem to occur predominantly at the beginning and end of the test, specifically on the initial proof test and on the final proof test. The Absolute Energy illustrates the same sort of distribution as the previously described energy graph, the energy content when the wire is stressed is significantly more after the introduction of the damage.

The duration history generates the same information as the counts history and no real additional value is attained from describing the graph. The amplitude time graph has been previously dealt with, but it can observe that where single wire fractures are anticipated i.e. after the damage has been introduced on the initial application of SWL and the proof test at the end of the load history. There occurs high Amplitudes hits of greater than 80 dB, a unique characteristic when compared with the remainder of the file.

Casey [87] stated that the frequency components could be used as a means of discriminating between wire breaks and noise so the inclusion of an average frequency history was considered salient in the suite of pattern recognition graphs. It shows the presence of high frequency hits, however these appear throughout the test history and are unlikely to assist in the formulation of a discriminator. The final graph is the load history and is included such that when viewing any of the other graphs one can observe the behaviour of the stimulus.

The pattern recognition graphs have been introduced and it can be observed that when using a number of these graphs in conjunction with one another, one can with the benefit of engineering judgement determine the characteristics that are most likely to assist in the formulation of a wire break classifier.

Wire breaks are most likely to occur after the damage has been induced, as the nature of the flaw is likely to give rise to partially severed wires at the site of a local stress concentration. From this it can be deduced that when seeking to identify unique characteristics of the signals that are likely to describe wire breaks their coincidence with load applications after the damage has been introduced provides a means of discrimination. The SWL that occurs after the introduction of the flaw therefore generates hits that are attributable to single wire breaks. In accordance with the Kaiser effect one might anticipate that the subsequent load applications to the SWL will not generate further emission as in principle the stress will have redistributed from the local stress concentration. The wire may additionally experience further wire breaks on the final proof test as a higher stimulus is applied. The likely presence of wire breaks on the final proof test is substantiated by the fact that during the trials two of the ropes experienced a strand failure on the final application of load. Strand failure can only occur through multiple wire fractures.

Based upon the judgements made from wire 106, the signal features that are considered most appropriate to differentiate wire breaks from other source mechanisms are hits that are of high Amplitude. Such hits additionally tend to have a large number of counts, long durations and significantly greater energy when compared to other sources that occur during the stressing of wire ropes.

The following section appraises the significant findings of the analysis of the remaining rope tests.

3.3.2.1 Wire Ropes 103, 105, 107 & 108

As previously mentioned the graphical outputs of these particular ropes acoustical behaviours can be viewed in the Appendix III (B). This section discusses any abnormalities found in the data.

3.3.2.1 (a) Wire rope 103

The least amount of damage was introduced into wire 103, 12%. The most observable characteristic about its data is that there is very little AE generated on SWL and PL after the introduction of the damage. It is difficult to differentiate the fact the wire is damaged when one compares the emission generated from the two evaluative proof tests. The proof test after the introduction of the damage shows little or no increase in emission from the proof test that succeeds the operational period when no damage had been experienced. It is considered that the damage was not severe enough to constitute an integrity threat to the rope at these levels of loading. It is considered that this data file contains no wire breaks. This is a useful feature as the acoustic behaviour that might be typical in a wire rope without a serious flaw is attained.

3.3.2.1 (b) Wire rope 105

This rope experienced a strand failure during the application of the final proving load and was subjected to the greatest level of damage, a 32% reduction in cross section. The initial commissioning proof load resulted in a hit greater than 90dB hit which could be a wire break, however the logical place for wire breaks to occur is after the introduction of the flaw. The 90 dB hit was only one isolated large hit and did not create an event (An event must be made up of at least two hits, one at each sensor in order the distance can be computed from the respective differences in the time of arrival). The source location plots show that all the events greater than 90dB occur in an area concentrated around 350mm from sensor 1, the area at which the damage was introduced. The hit and event graphs show a higher concentration of activity on the load applications after the defect was introduced. The greatest amount of source located events is apparent on the final proving load, which is when the strand failed. The Amplitude and Energy plots when viewed in conjunction with the applied loads illustrate that the higher values occur during the application to SWL and the proof test after the damage was present, indicative that wire breaks are both high in Amplitude and associated energy.

3.3.2.1 (c) Wire rope 107

This rope also experienced a strand failure during the final proof test. 22% damage was introduced into the rope. From the graphical output of both the Amplitude and applied load, one can observe that a slightly greater value of than the 25.5 KN has been applied

on the final proving load. This condition is considered to have arisen due to the failure of the strand near the peak load and with the strand failing the loading machine would be subjected to an instantaneous load relaxation until the load redistributed to the other strands. The loading machine strives to maintain a constant load and would continue to apply additional force until the load cell registered the overshoot.

The events are distributed over the length of the rope, although the area 150-200 mm has the greatest concentration in agreement with the damage site. It is considered that when a wire fails under the tension condition it will retract into the strand and may give rise to frictional activity during the retraction. When a strand fails the same behaviour may anticipated, but on a greater scale as the entire strand will unwrap itself from the helical configuration. Both ropes 105 and 107 exhibit quite distributed source located activity when compared to the concentrated activity generated by other ropes. The common feature of ropes 105 and 107 is they both experienced a strand failure during the final proof test. Two explanations are offered for the distributed source located activity: the aforementioned frictional source evident on the rope when it breaks under the tension and secondly the failure of multiple wires within the strand almost simultaneously will generate a burst of discrete signals that overlap on a time trace. The software is configured to anticipate discrete bursts whose duration are pre-determinately set, during which the features are measured. A number of overlapping discrete signals will appear as a continuous signal and will confuse the measurement process and not yield definitive results.

The hits that show relatively large energies with respect to the other hits are in this instance shown to occur at greater than 95dB as opposed to greater than 80dB as was the case in the analysis of rope 106. This is due to the relative scaling of the hits, in the case of rope 106 the maximum energy by a single hit was 5000 and in terms of absolute energy 50 $*10^6$aJ. However, in 107 we observe hits at 8000 and 320 $*10^6$aJ. This amplifies the dynamical range that can be experienced from AE hits.

Rope 107 illustrates the repetitive phenomenon that the majority of high amplitude and high energy AE appear at points of anticipated wire breaks specifically after the damage has been induced on the initial application to SWL and the final proof test.

3.3.2.1 (d) Wire rope 108

Rope 108 also had 22% damage induced, but did not experience a strand failure during the trial. Similar to rope 105, 108 has a rogue hit at greater than 90 dB on the initial commissioning proof test, but in this instance it did create a source located event.

The events appear to be universally distributed over the length of the wire, although it is known that the damage was introduced at 180mm where the highest amplitude events occur. The events occur on loads considered to cause the damage to propagate.

A further interesting characteristic of this data file is that not only are the high amplitude and high energy hits apparent on the initial load application after the introduction of the

damage, but equally on the second SWL there are two hits of greater than 95dB. This is a clear breakdown of the Kaiser effect. This is considered to be a further wire break. The third application of SWL results in a comparatively quiet load application indicative that the rope has stabilised.

3.3.2.3 Section Summary

Previous authors have described other discriminatory features that may be used to differentiate wire breaks from other acoustic source mechanisms that may be apparent whilst stressing a wire rope. These include the use of amplitude, frequency, duration, counts and the arrival of hits coincident with peak loads. Observation from the data attained in these trials is that all of these signal features could possibly be used as a means of producing a classifier for the identification of wire breaks. High amplitude, long duration and high energy hits with a large numbers of counts are all evident at the points in the trials where wire breaks might be anticipated. The range of values of the measured features, however, is large and it is difficult to discern a particular value, which could be used to discriminate a wire break from other sources.

3.3.3 Event filtering for wire breaks

With these factors in mind the data files were filtered with a view to attaining new files that only contained wire breaks. The load applications of the initial SWL after the damage introduction and the final proof test were isolated and the data that occurred on the rising load only, filtered to create independent files. The premise being that it is that at these instances a wire break is most likely to occur.

The files were filtered again in order to create only events, as opposed to hits. If the event occurs in proximity to the area where the damage was introduced then further confidence is gained in characterising such events as wire breaks. The outputs of the files of the wire breaks are shown in Appendix III (C).

To demonstrate the approach Wire 106 is used as the example. The file has been significantly reduced to 4 hits (2 events) apparent on the application to SWL and 12 hits (6 events) on the proof test. Formerly the file comprised of a total of 541 hits with 14 events.

Momentarily focusing on the levels of data reduction of the file size it is observed that a significant proportion of the data remains within the filtered file particularly in terms of the cumulative energy although the number of hits has been significantly reduced. The effect of the filter on the two rising loads is that the significant AE energy content remains in the filtered file. Table 3.2 illustrates the reduction experienced within each file, the reduction of hits, events, cumulative counts (N) and cumulative energy are shown. The quantities described by post filtering are made up of the sum of totals of both files of the SWL application after the flaw was introduced and the final proof test.

Wire ID	Pre-filtering				Post-filtering			
	Hits	Events	ΣN	ΣEnergy	Hits	Events	ΣN	ΣEnergy
103	814	12	8555	2696	0	0	0	0
105	1221	32	26557	68658	34	17	7543	55650
106	541	14	7842	16733	16	8	2026	14863
107	1189	42	30624	71415	42	21	7967	46212
108	849	13	10919	23365	10	5	1271	15061

Table 3.2: the effect on the files by filtering out the events from the SWL load and final proof load.

Reassessing these new files to determine if the events of the SWL post damage and the final proof test cluster in the vicinity of the damage site yield in the case of wire 106, graphs 3.10-3.11.

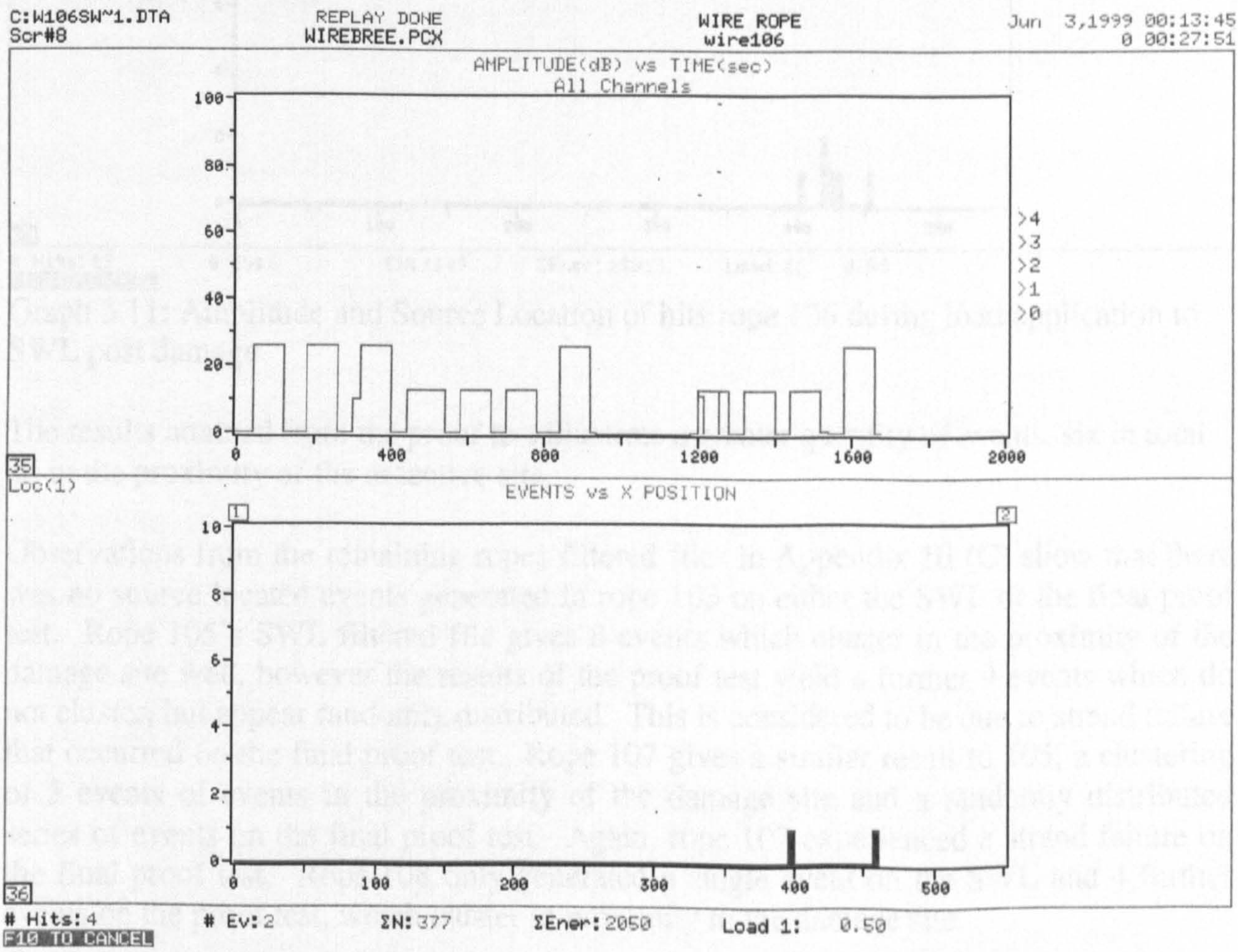

Graph 3.10: Amplitude and Source Location of hits rope 106 during load application to SWL post damage.

Only two events are evident on the application of load to the SWL after the damage has been introduced. These appear at the 400 and 460 mm from sensor 1.

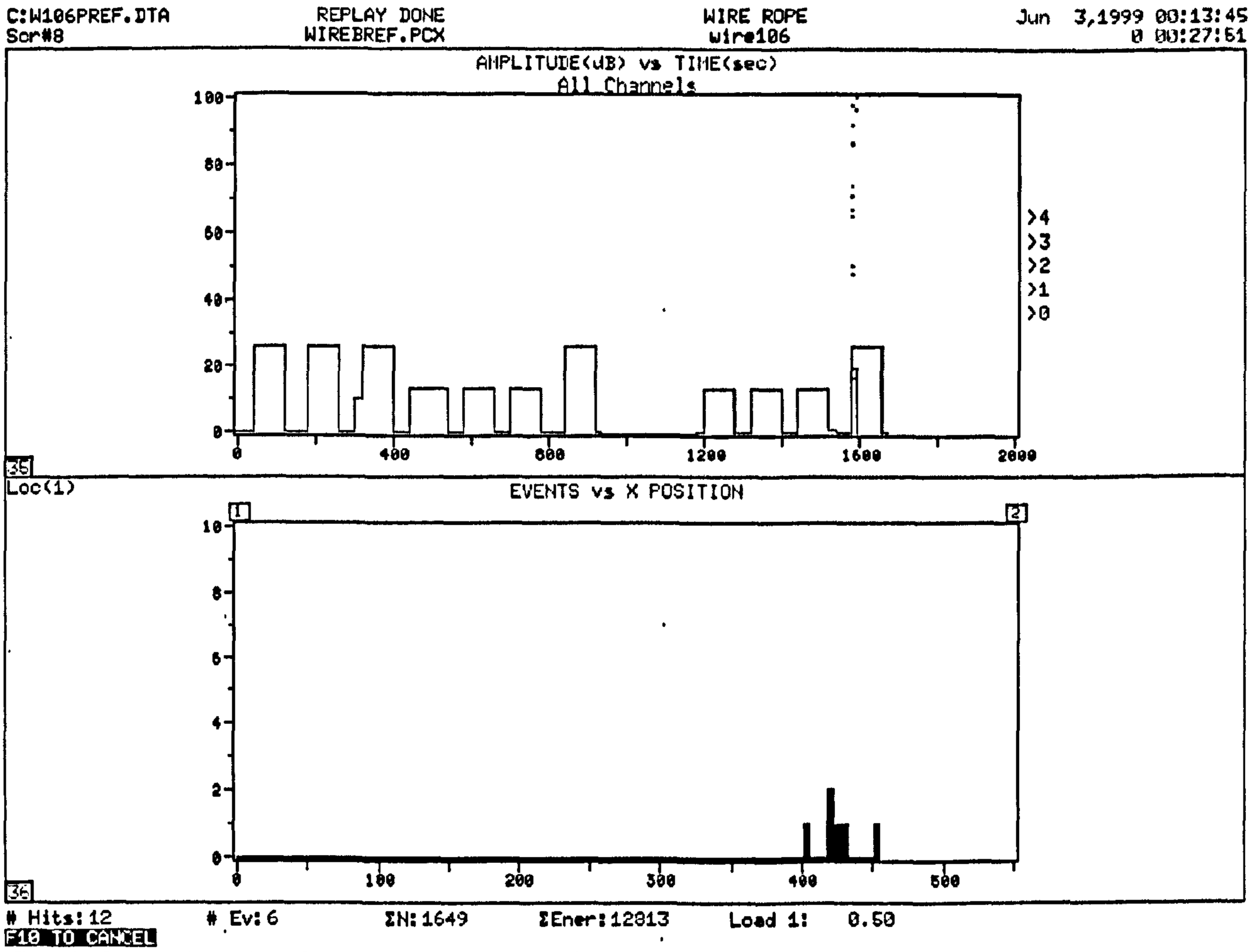

Graph 3.11: Amplitude and Source Location of hits rope 106 during load application to SWL post damage

The results attained from the proof test illustrate a greater quantity of events, six in total all in the proximity of the defective site.

Observations from the remaining ropes filtered files in Appendix III (C) show that there was no source located events generated in rope 103 on either the SWL or the final proof test. Rope 105's SWL filtered file gives 8 events which cluster in the proximity of the damage site well, however the results of the proof test yield a further 9 events which do not cluster, but appear randomly distributed. This is considered to be due to strand failure that occurred on the final proof test. Rope 107 gives a similar result to 105, a clustering of 5 events of events in the proximity of the damage site and a randomly distributed series of events on the final proof test. Again, rope 107 experienced a strand failure on the final proof test. Rope 108 only generated a single event on the SWL and 4 further events on the proof test, which cluster in proximity to the damage site.

3.3.3.1 Section summary

The isolation of the acoustic activity that occurs on the applications of loads that succeed the introduction of the damage assists in the identification of signals that are likely to include wire breaks. The fact that a further filter was introduced to include only hits that

created events and they tend to cluster in the proximity of the damage site adds confidence that wire breaks have been successfully isolated. The ruthlessness of the filter may have excluded other genuine wire breaks that may be contained within the data sets, however such a filter has created files small enough for further analysis to determine if there exists an interrelationship between the measured features that is statistically significant and can be used as a means of discriminating wire breaks from other sources.

The pattern recognition plots allow the identification of features that are attributable to wire failures, as previously discussed wire breaks have larger amplitudes, energies, counts and durations than other sources apparent within the file. However there is no single feature that enables a threshold to be set, such as amplitudes greater than 80 dB, that differentiate between wire breaks from other sources. There is overlap between signals generated from wire breaks and the other sources. Therefore further analysis was conducted into a statistical evaluation of the correlation between the signal features that would provide a discriminatory measure. In order to create a discriminator cross-plots all of the permeations of the signal features against one another could be created in order to determine if any particular combination would provide a unique characteristic. Instead of exploring all of the permeations, statistical analysis was conducted to focus attention on the most likely parameters that would yield a result.

3.3.4 Statistical analysis

The data was exported into text files such that it could be loaded into Microsoft Excel. Columns of data were created of the number of Counts, Duration, Amplitude and the two energies, both Absolute and Marse. The choice of the selection of these signal features was based upon the observations from the suite of pattern recognition graphs. Both Rise-time and average frequency were discarded from the analysis as both had shown significant variance in their consistency with amplitude.

With the data in this format the statistical process of correlation was conducted on the events generated from the initial proof test, from the SWL application after the damage had been induced and on the final proof test. Obviously if the correlation coefficients between features that were generated on the initial proof test was discernibly different from the events attained on the SWL and final proof test then there would exist a means for the establishment of a wire break classifier.

Rope 106 is again used as the vehicle for explaining the methodology. All results from other ropes are illustrated in the Appendix III (D). The text files were imported into Excel and subjected to correlation analysis. This statistical process measures the relationship between two data sets that are independently scaled. The calculation returns the covariance of the two data sets divided by the product of their standard deviations. The process determines whether large values of one set of data have correspondingly large values within another set. This results in a positive correlation. Alternatively small values in one set, which are associated with large values in another returns a negative correlation. A value of near zero indicates little or no correlation.

The output of the correlation analysis is a matrix, which numerically describes the signal features interrelationships. The outputs were then graphed on a radar plot to permit visualisation of any differences.

The matrix and corresponding radar plot, table 3.3 and graph 3.12, depicts the results generated from the initial proof test. The correlation coefficients generated from this are considered to be typical of AE from a wire rope without a wire failure, as it would not be expected that wire breaks occur on the initial commissioning load.

	Counts	*Energy*	*Duration*	*Amplitude*	*A Energy*
Counts	1				
Energy	0.936895	1			
Duration	0.901228	0.857674	1		
Amplitude	0.952283	0.978446	0.864592	1	
A Energy	0.800762	0.936457	0.631759	0.892676	1

Table 3.3 Correlation matrix for the initial commissioning proof test for rope 106

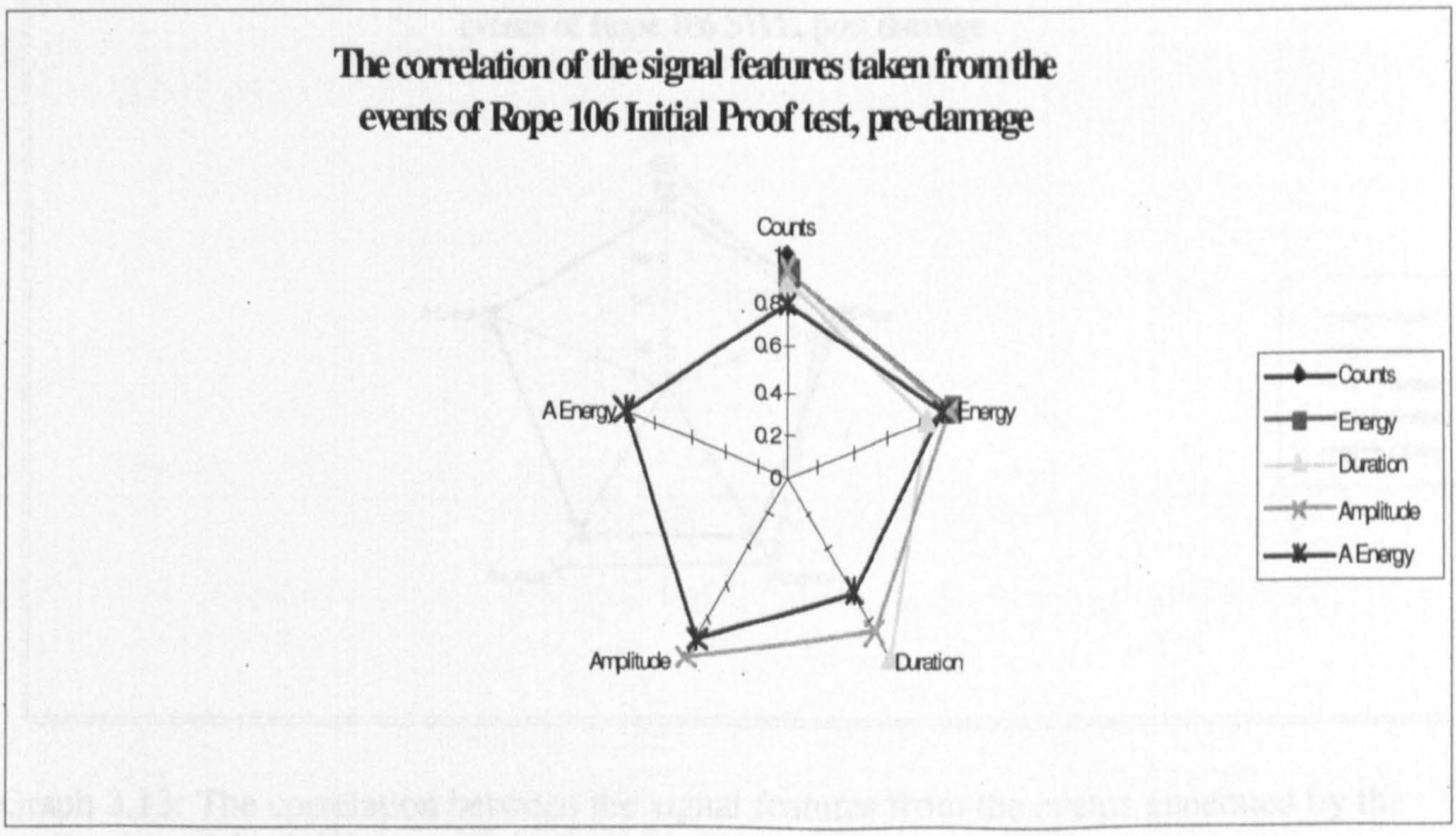

Graph 3.12: The correlation of the signal features taken from the initial proof test for rope 106.

This type of distribution was typical of all initial proof tests with the exception of wire rope 108, which will be discussed latterly. The observable characteristic that should be considered is the relationship between the Amplitude and the Energy (line with crosses) and the relationship between the Duration and Energy (line with solid triangles). The point for observation is on the energy axies. From the population of ropes on the initial

proof test the generalised result was that the Duration repetitively shows a smaller correlation than the Amplitude with Energy.

Considering the results of the events that were generated during the initial SWL application after the damage was induced yields the matrix, table 3.4 and the graph 3.13.

	Counts	*Energy*	*Duration*	*Amplitude*	*A Energy*
Counts	1				
Energy	0.874368	1			
Duration	0.988273	0.892372	1		
Amplitude	0.997342	0.865597	0.974759	1	
A Energy	0.80468	0.989317	0.818795	0.800169	1

Table 3.4: Correlation matrix of the signal features from the events generated by the application of the SWL for rope 106, post damage

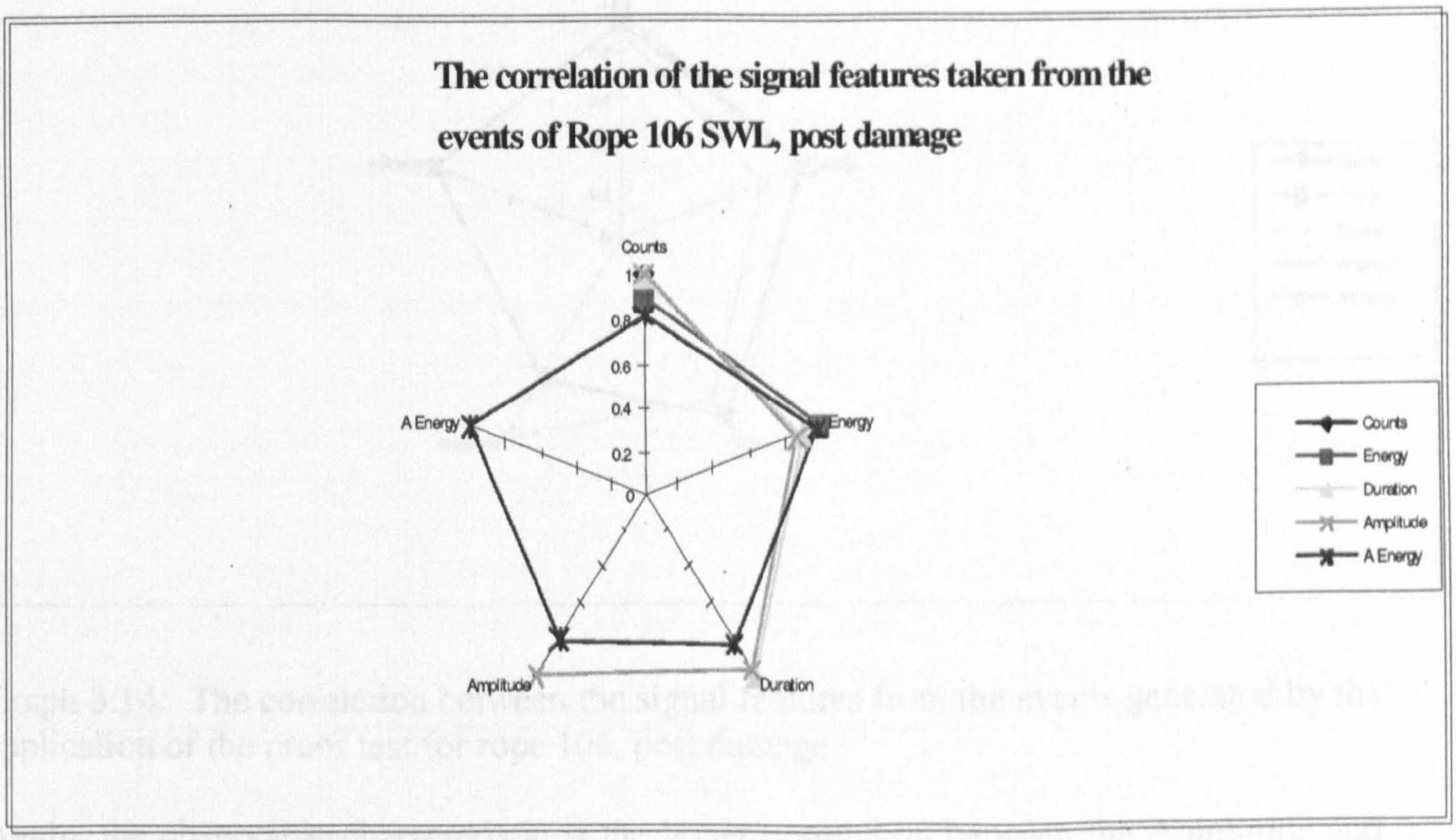

Graph 3.13: The correlation between the signal features from the events generated by the application of the SWL for rope 106, post damage

In this instance the correlation coefficient between the Amplitude is less than the Duration with respect to the energy. The line with crosses line falls within the line with solid triangles illustrates this. This result is typical of all of the SWL applications on all ropes.

Repeating the same procedure for the final proof test gives the matrix and associated radar plot shown by table 3.5 and graph 3.14.

	Counts	*Energy*	*Duration*	*Amplitude*	*A Energy*
Counts	1				
Energy	0.960685	1			
Duration	0.967101	0.940577	1		
Amplitude	0.883248	0.761553	0.801966	1	
A Energy	0.925191	0.9919	0.908141	0.693257	1

Table 3.5: Correlation matrix of the signal features from the events generated by the application of the proof test for rope 106, post damage

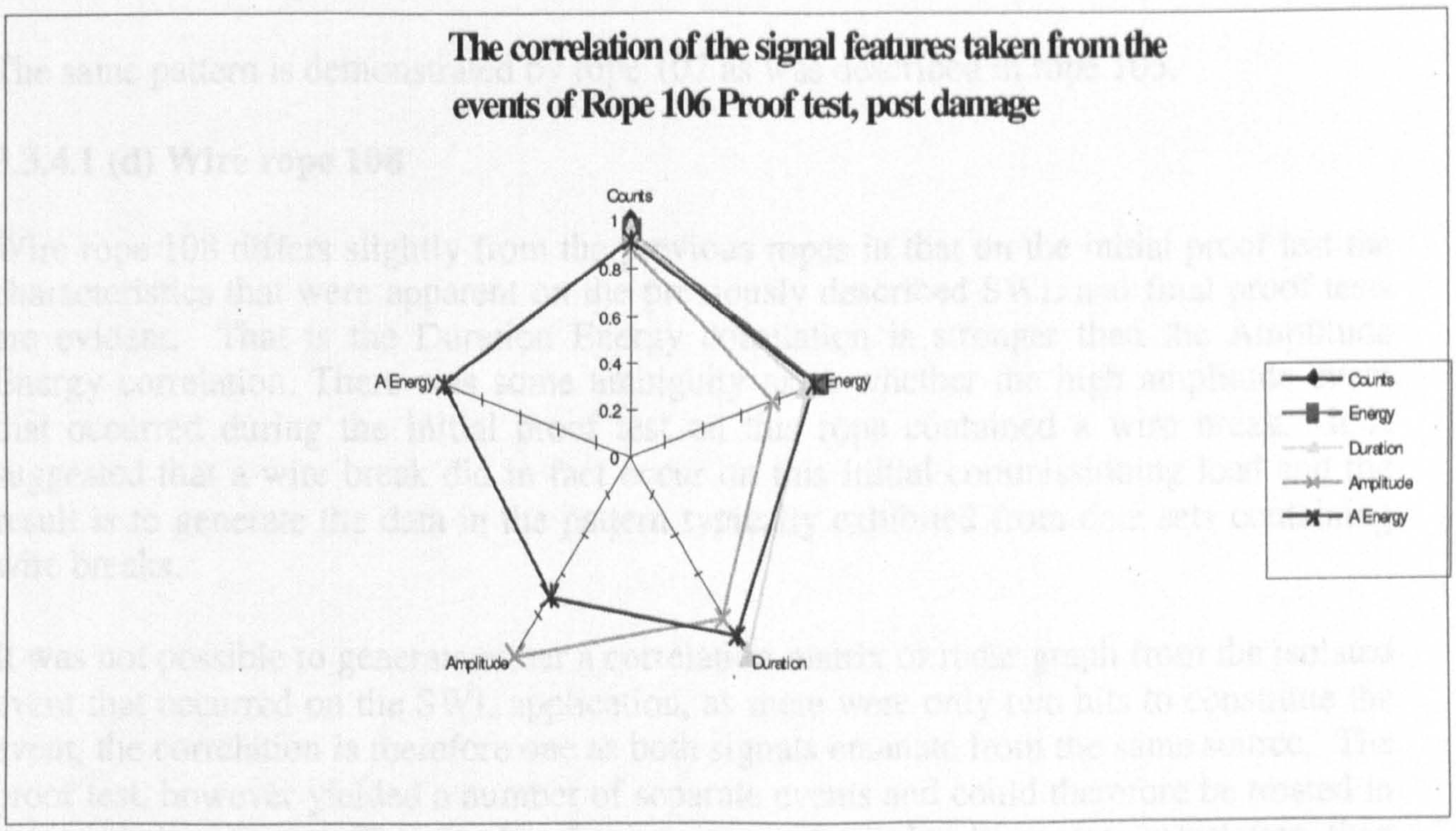

Graph 3.14: The correlation between the signal features from the events generated by the application of the proof test for rope 106, post damage

Again, the observable characteristic is the lesser correlation between the Amplitude and the duration. This generalisation is apparent on all other wire rope final proof tests that generated events during this load application.

3.3.4.1 Summary of results from wire ropes 103,105, 107, 108.

3.3.4.1 (a) Wire rope 103

Wire rope 103 was analysed and only the initial proof test could be used to generate matrices and radar graphs as no events were experienced on either the SWL or the final proof test after the damage was introduced. The initial proof test did generate the generic

result that the Amplitude interrelationship with energy was greater than the duration relationship.

3.3.4.1 (b) Wire rope 105

Rope 105 illustrates a strong reversal of the significance of the parameter correlation coefficients with the amplitude being stronger than the duration on the initial proof test and subsequently during the two load tests after the damage was introduced the duration correlates better with the energy than the amplitude.

3.3.4.1 (c) Wire rope 107

The same pattern is demonstrated by rope 107 as was described in rope 105.

3.3.4.1 (d) Wire rope 108

Wire rope 108 differs slightly from the previous ropes in that on the initial proof test the characteristics that were apparent on the previously described SWL and final proof tests are evident. That is the Duration Energy correlation is stronger than the Amplitude Energy correlation. There was some ambiguity as to whether the high amplitude event that occurred during the initial proof test on this rope contained a wire break. It is suggested that a wire break did in fact occur on this initial commissioning load and the result is to generate the data in the pattern typically exhibited from data sets containing wire breaks.

It was not possible to generate either a correlation matrix or radar graph from the isolated event that occurred on the SWL application, as there were only two hits to constitute the event, the correlation is therefore one as both signals emanate from the same source. The proof test, however yielded a number of separate events and could therefore be treated in the normal manner. The results show a stronger amplitude energy correlation than duration energy, in keeping with all other data sets that are assumed to contain wire failures.

3.3.4.2 Section Summary

From the statistical analysis it is evident that there exists a means of differentiating wire breaks from other sources that may be apparent whilst stressing wire ropes. The best means of achieving a differentiator between wire breaks and other sources is by viewing the interrelationship between the amplitude, energy and duration.

The results for the statistical analysis can be viewed in Appendix III (D)

3.3.5 Classifications using Noesis

The original data files were imported into a specialised Acoustic Emission software package "Noesis" an advanced pattern recognition tool. A unique feature of this package

is that it permits selection of the hits that can be assigned a symbol and a class. Hits have been selected from the initial proof and assigned the symbol "+" and comparison made with the hits generated from the load applications to SWL and the final proof test. The hits generated during the SWL are denoted by solid triangles and solid boxes illustrate the hits generated during the final proof test. Within the graph legend the initial proof test has been abbreviated to "InPr", the SWL remains as "SWL" and the final proof test abbreviated to "FPr".

The approach is demonstrated with rope 106, graph 3.15.

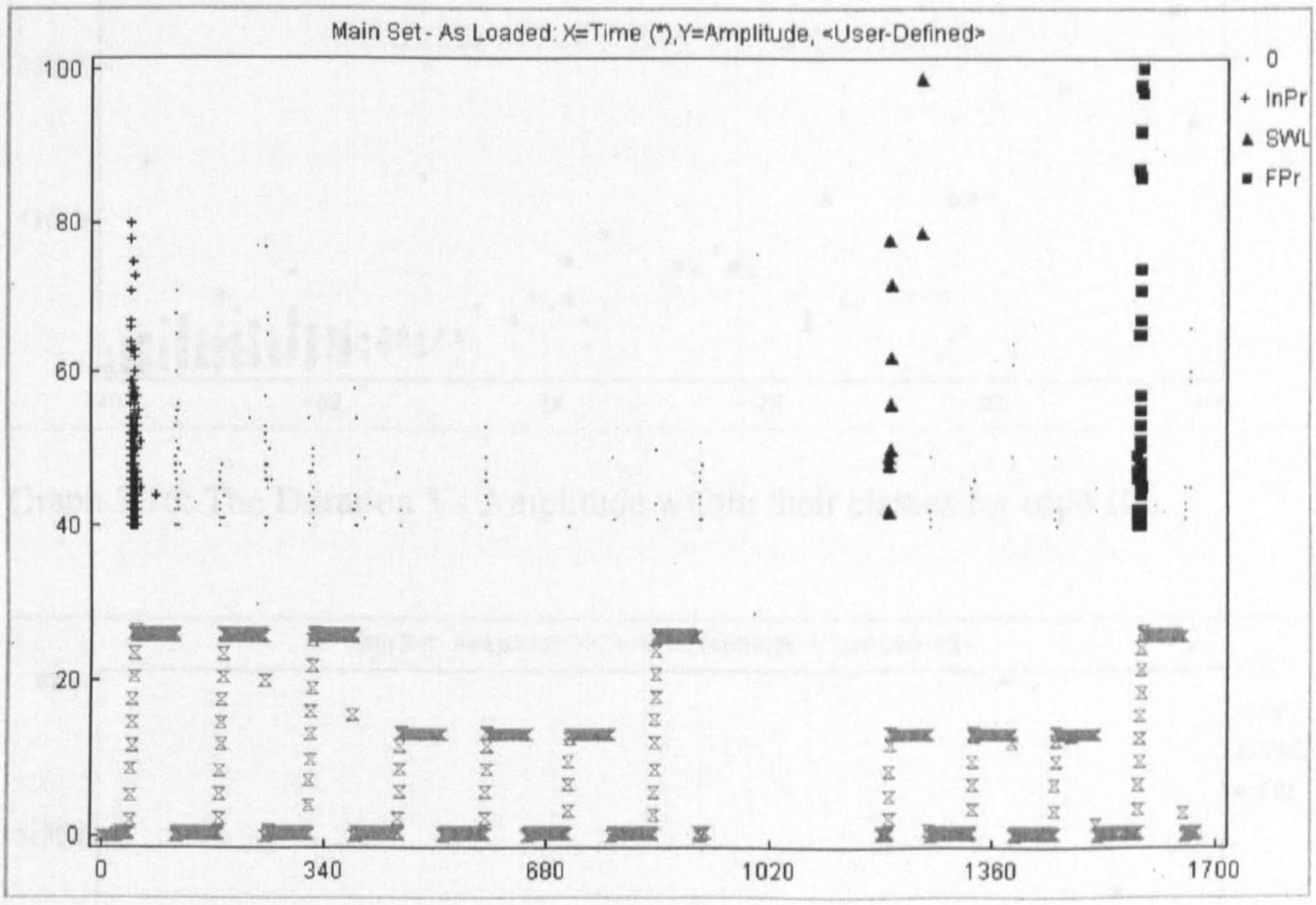

Graph 3.15: The selection of hits and their class representation from rope 106.

Observation of these hits within their classes on cross-plots of the features that were found to be statistically significant is shown in the graphs 3.16-3.18, which are the cross-plots of amplitude and duration, duration and energy, and amplitude and energy, respectively.

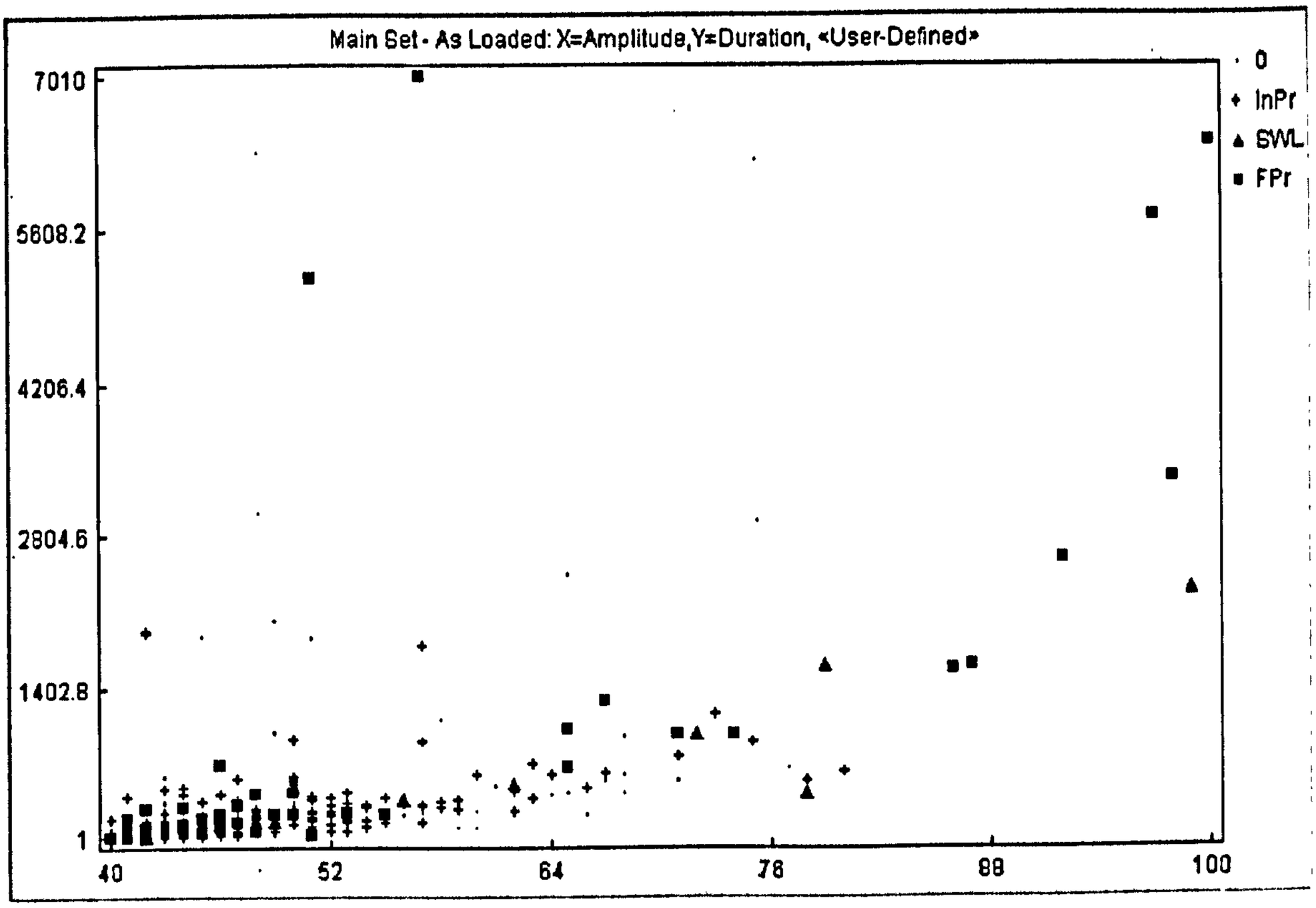

Graph 3.16: The Duration Vs Amplitude within their classes for rope 106

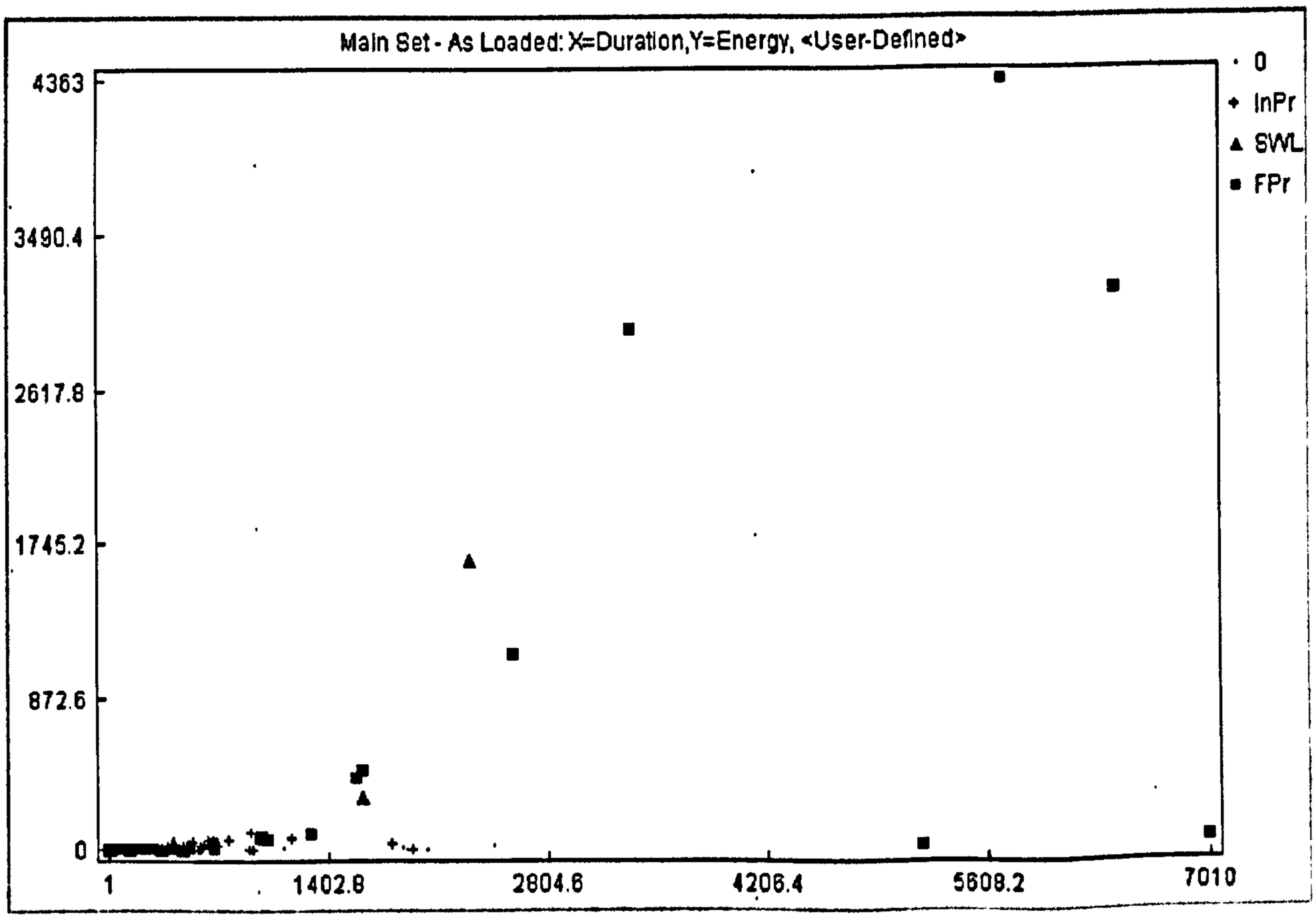

Graph 3.17: The Duration Vs Energy within their classes for rope 106

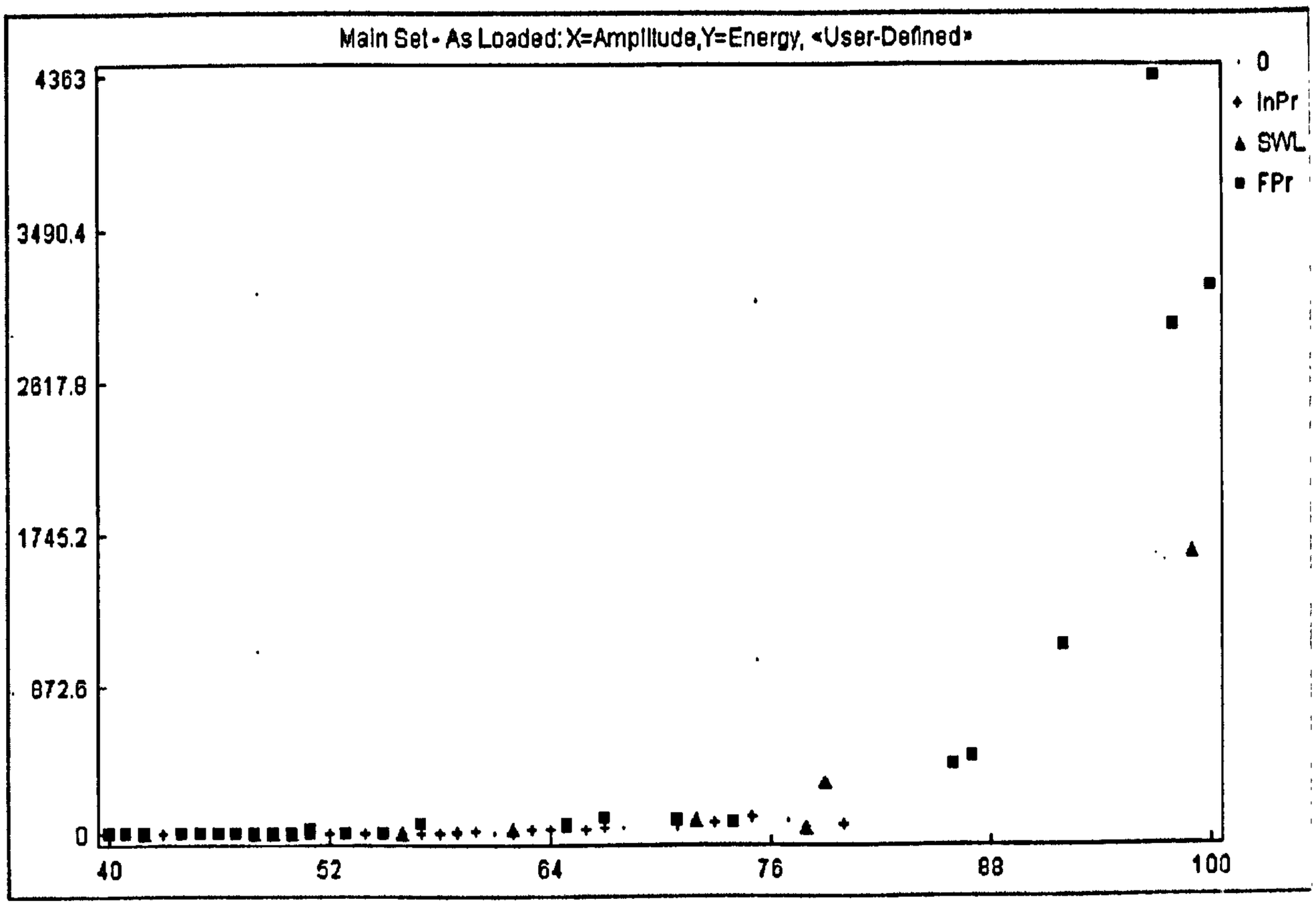

Graph 3.18: Energy Vs Amplitude within their classes for rope 106

3.3.5.1 Section Summary

Although there remains considerable overlap between the classes all the extreme hits belong to either the classes of either the SWL or final proof test, the points where wire breaks are anticipated.

The outputs for the remaining population of ropes are shown in Appendix III (E).

3.3.6 Waveforms from wire breaks

During this process of selection and classification it was observed that almost all of the long duration hits that were not damage related occurred during the falling loads. Equally the facility of the software selection allowed the viewing of the specific waveform that belonged to a specific hit. It is with the evidence generated during this process that a change of methodology was employed. The instruments procedure for measurement uses software configurable settings for the anticipated duration of anticipated hits. If the hit exceeds the software duration setting it will be counted as a new and independent hit. The inverse is also true if a number of discrete mechanical events occur within the specified time period then these hits can overlap and generate a single reportable hit that may comprise of a number of discrete mechanical events.

This concept is illustrated particularly well by interrogating some of the hits experienced on rope 106. During the load hold period of the SWL after the damage was induced there occurred an audible noise that was considered at the time to be a wire break. The fact that it occurred on the load hold suggests that the hits are most likely to be attributable to a wire break as there is least probability of the presence of any other source mechanism. The fact that it additionally source locates in the proximity to the damaged area adds credence to this. When viewing the two waveforms and their Fast Fourier Transforms (FFT) that are generated during this load hold, graphs 3.19-3.20. On the upper graph a circle shows the hit that has been captured. The associated waveform is shown immediately underneath alongside the FFT. This is believed to be the most likely image of a wire break.

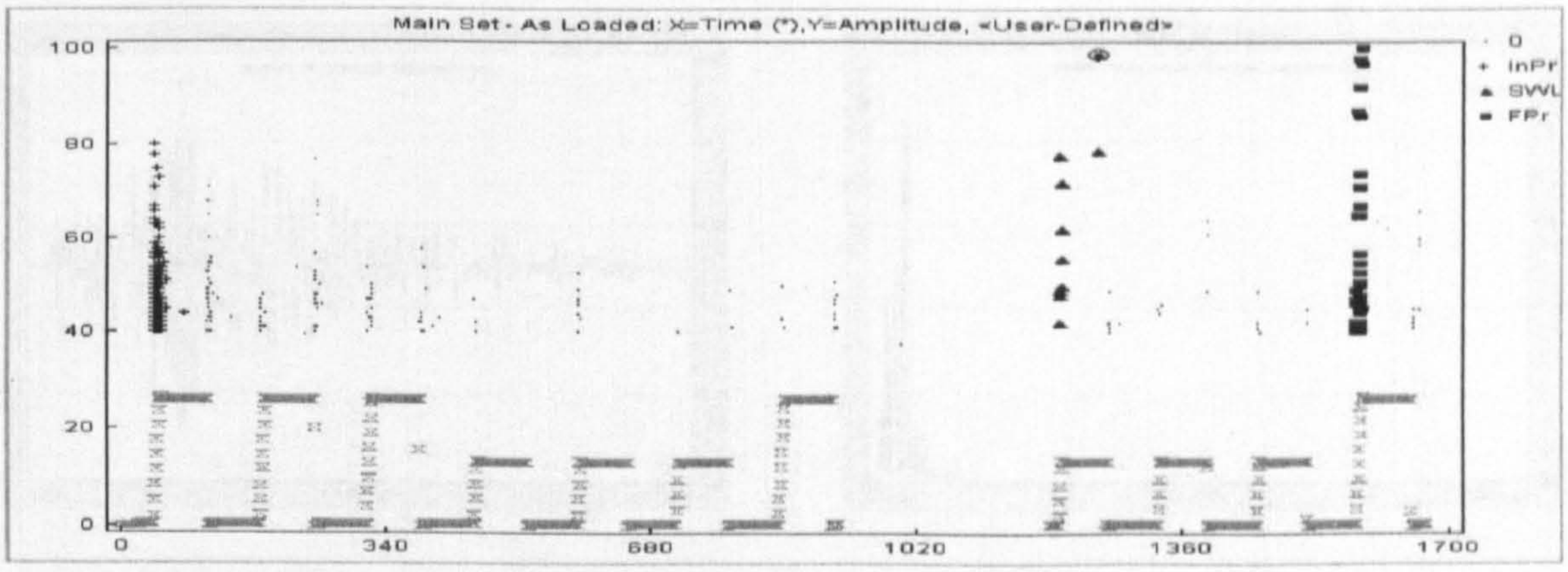

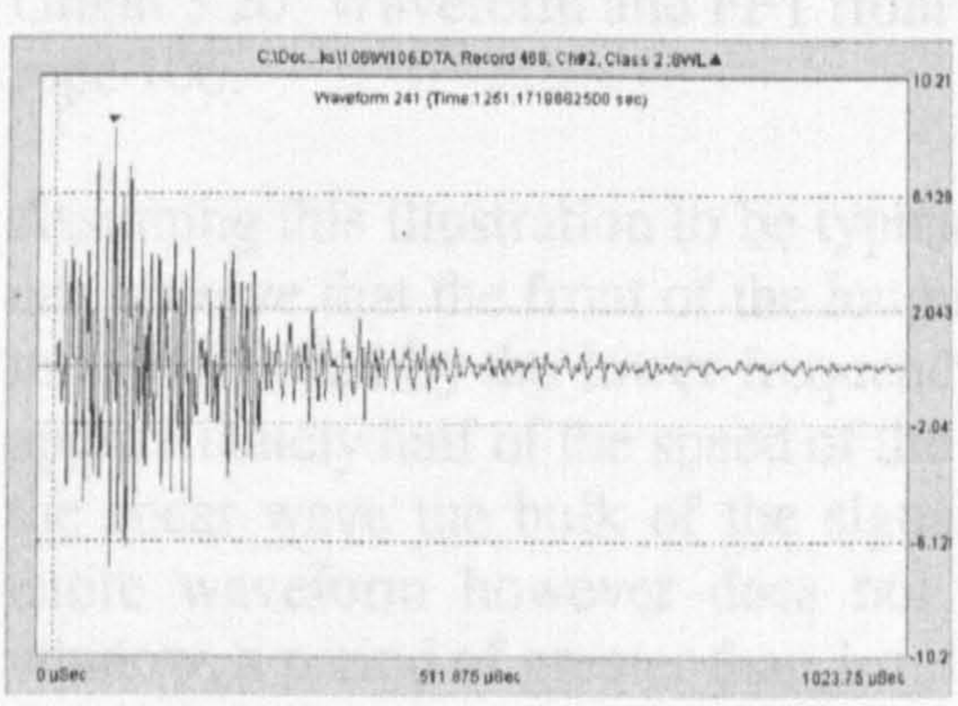

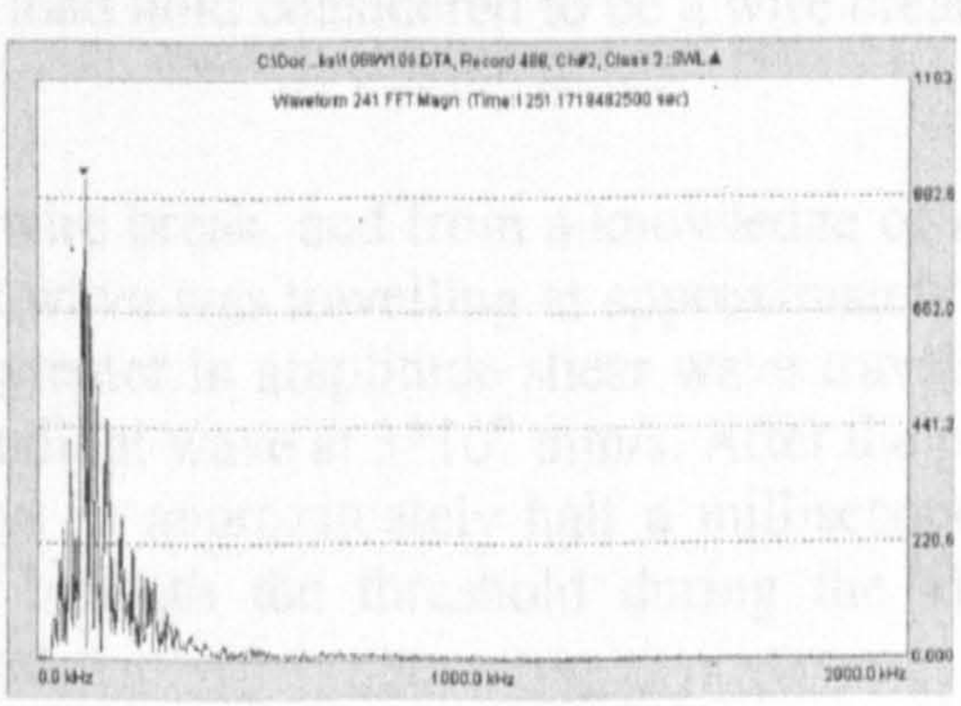

Graph 3.19: Waveform and FFT from hit on load hold considered to be a wire break from rope 106.

The immediately successive hit considered to emanate from the same mechanical event, but a number of microseconds later on the other, more distant channel is shown in graph 3.20

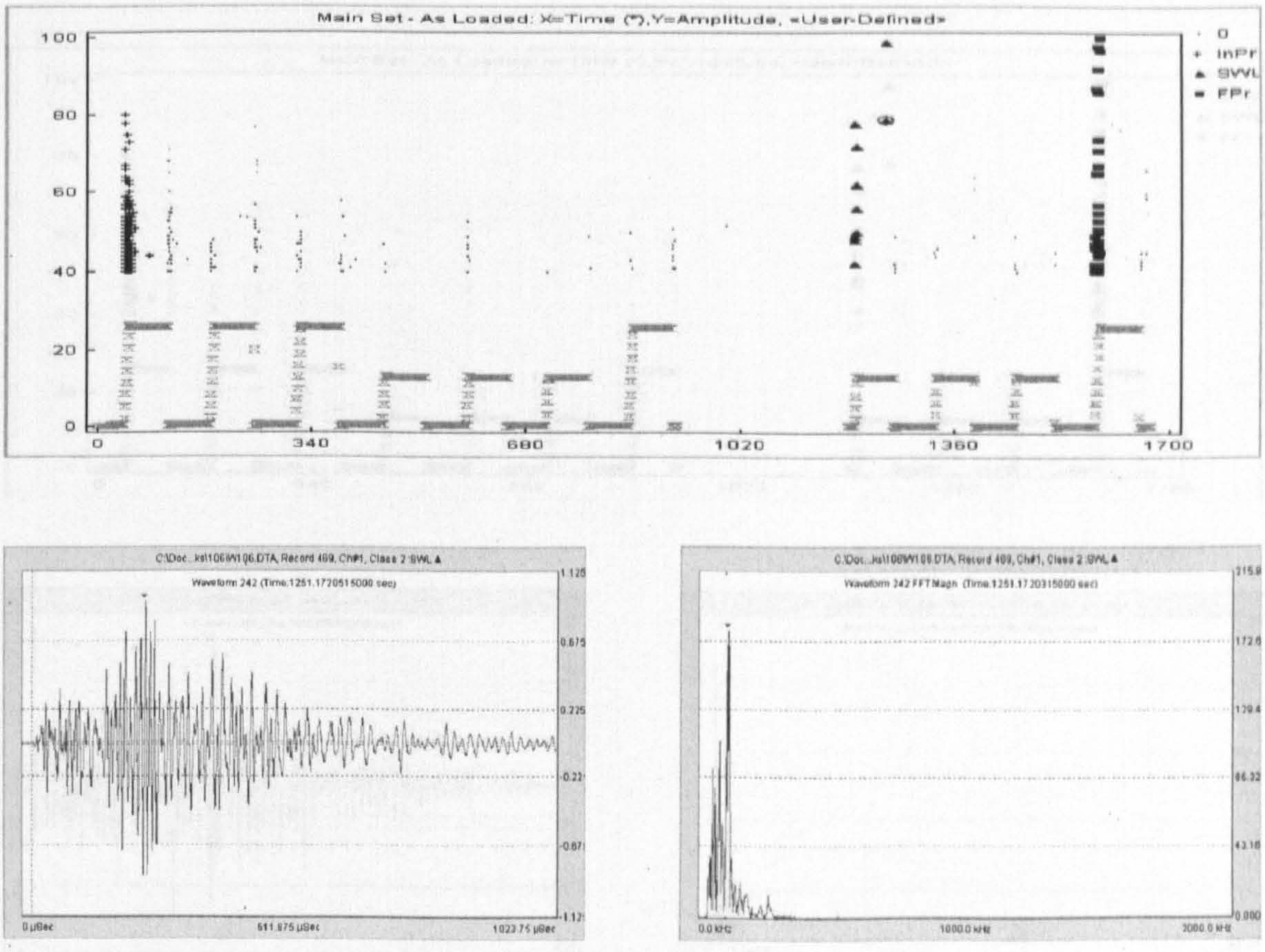

Graph 3.20: Waveform and FFT from hit on load hold considered to be a wire break from rope 106.

Assuming this illustration to be typical of a wire break, and from a knowledge of AE we can observe that the front of the longitudinal wave was travelling at approximately $6*10^6$ mm/s followed by the lower frequency and greater in amplitude shear wave travelling at approximately half of the speed of the longitudinal wave at $3*10^6$ mm/s. After the peak of the shear wave the bulk of the signal decays in approximately half a millisecond. The entire waveform however does not decay beneath the threshold during the viewing window, a period of greater than 1 millisecond.

Comparing the two waveforms seen by each sensor the effects of the attenuation can be observed, the higher frequency components are more evident on channel two, graph 3.19, the channel that is nearest to the source. The higher frequency components decay with increasing distance from the source. (See Appendix II section entitled Attenuation)

Observing the hits generated during the final proof test in the same manner, graphs 3.21-3.22 were obtained.

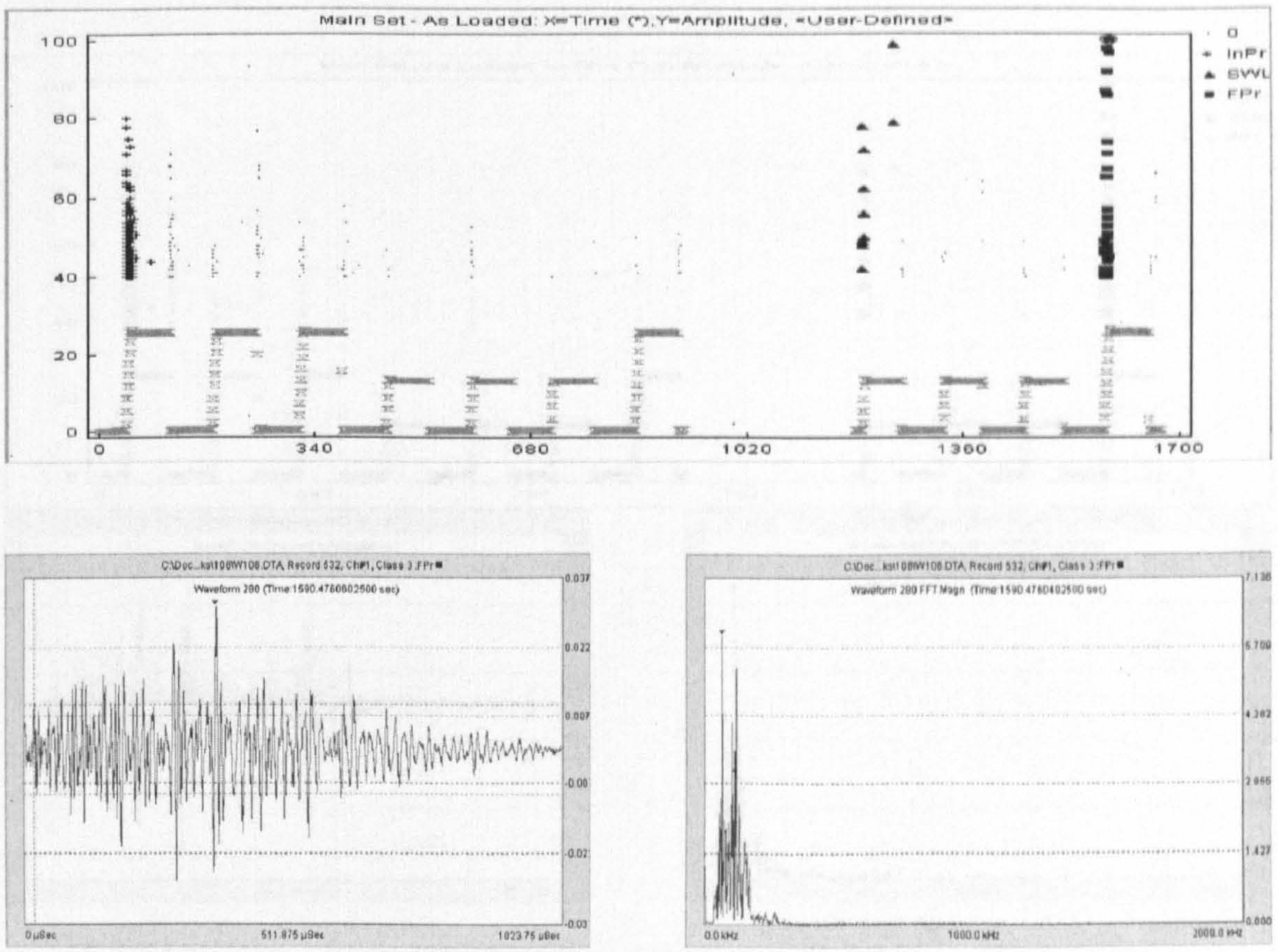

Graph 3.21: Hit selection and waveforms from Final Proof test from rope 106.

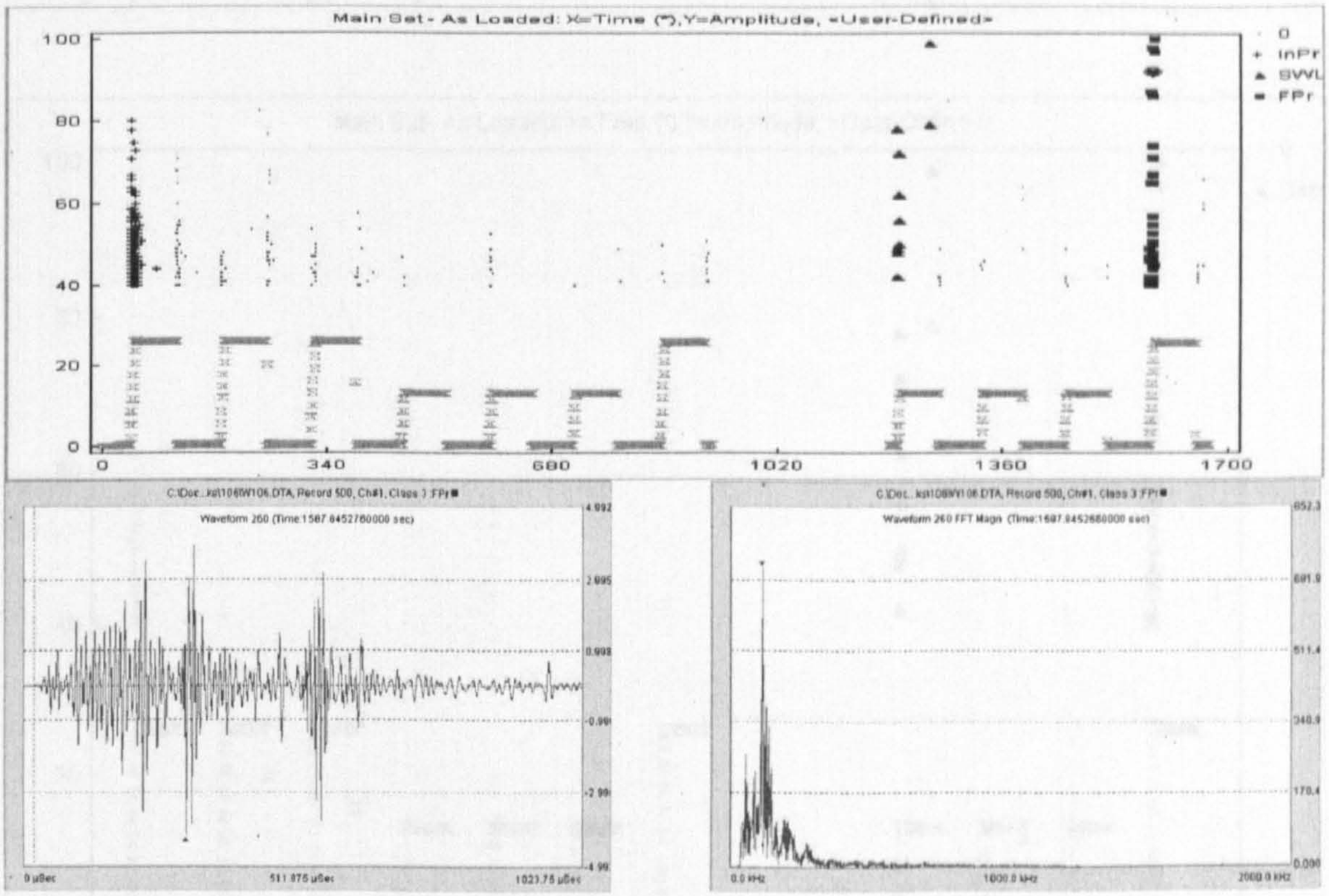

Graph 3.22: Hit selection and waveforms from Final Proof test from rope 106.

Completely different waveform characteristics are evident during the proof test than those that were attained during what was considered to be an isolated wire break. It is almost as if during the millisecond window within which the channel was open, a number of mechanical events have occurred which have superimposed themselves on top of one another. This may be due to a number of wire breaks occurring simultaneously.

3.3.6.1 Section Summary

From these observations the approach of creating discriminator and labelling it as singular wire breaks was abandoned. However the investigation continued in to determining differences between AE associated with damage mechanisms and non damage related AE.

3.3.7. Classifying damage and non damage related AE

It was considered that damage related AE would only be generated on rising loads and all unloading events were deleted from the files. The four classes were merged into two classes, the initial proof test hits was merged with normal AE that occurs on an undamaged rope and both the data from SWL and final proof tests were merged into a single class. In principle, this would provide a means of determining the differences

between hits with damage mechanisms and hits generated from normal wire stressing. The graphs of energy, amplitude and duration were re-graphed.

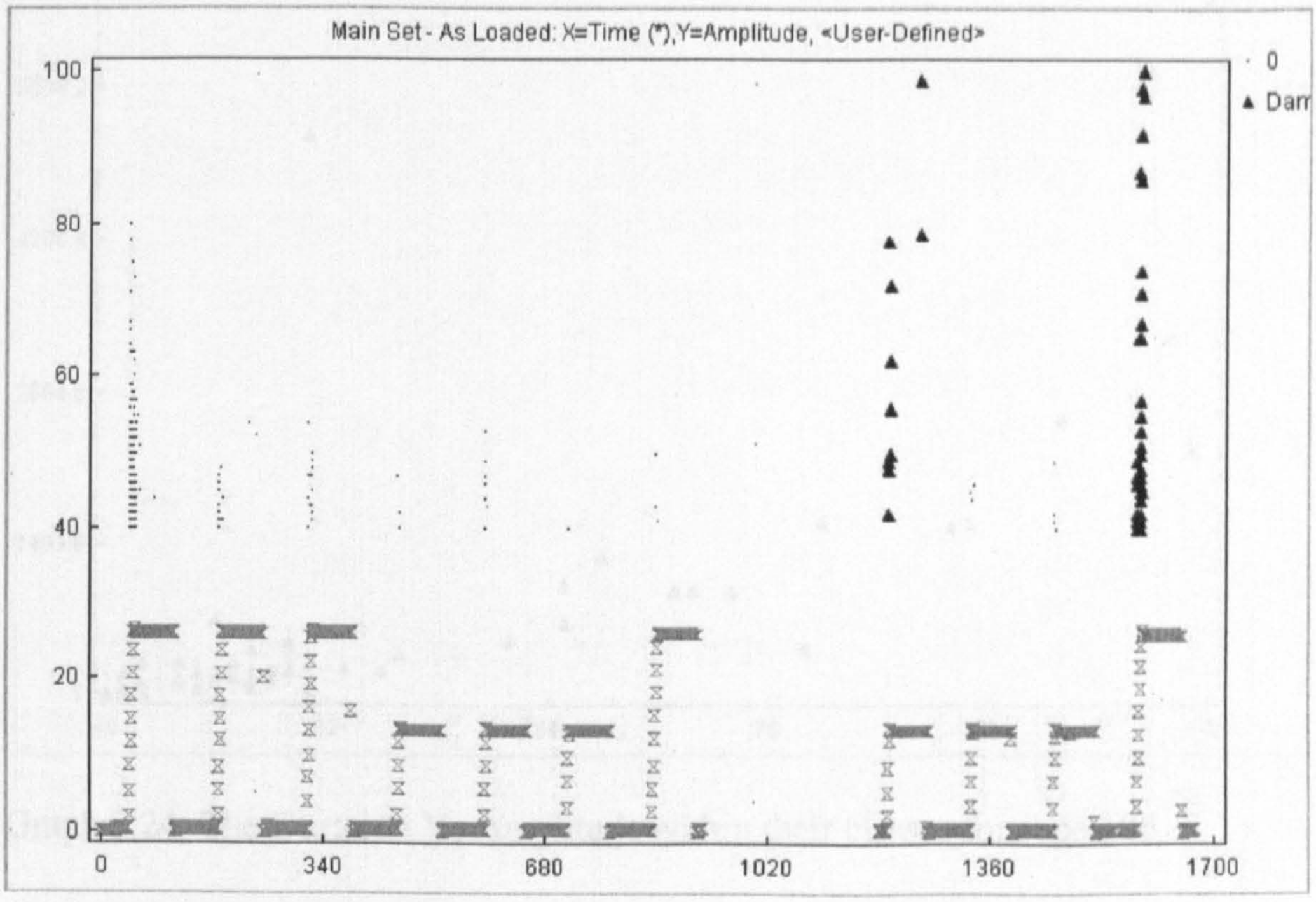

Graph 3.23: Class identification differentiating between damage related and non damage related AE.

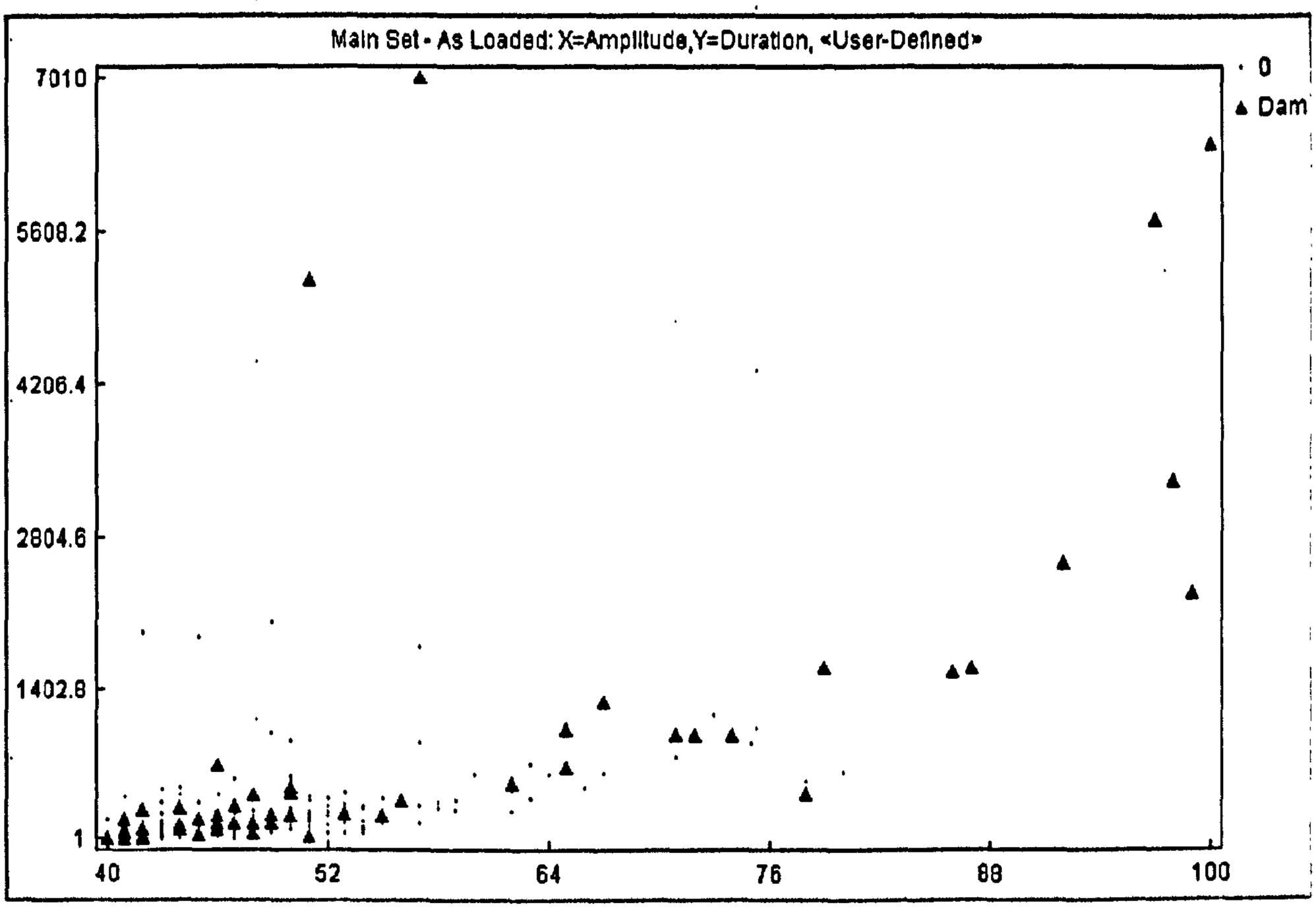

Graph 3.24: The Duration Vs Amplitude within their classes for rope 106

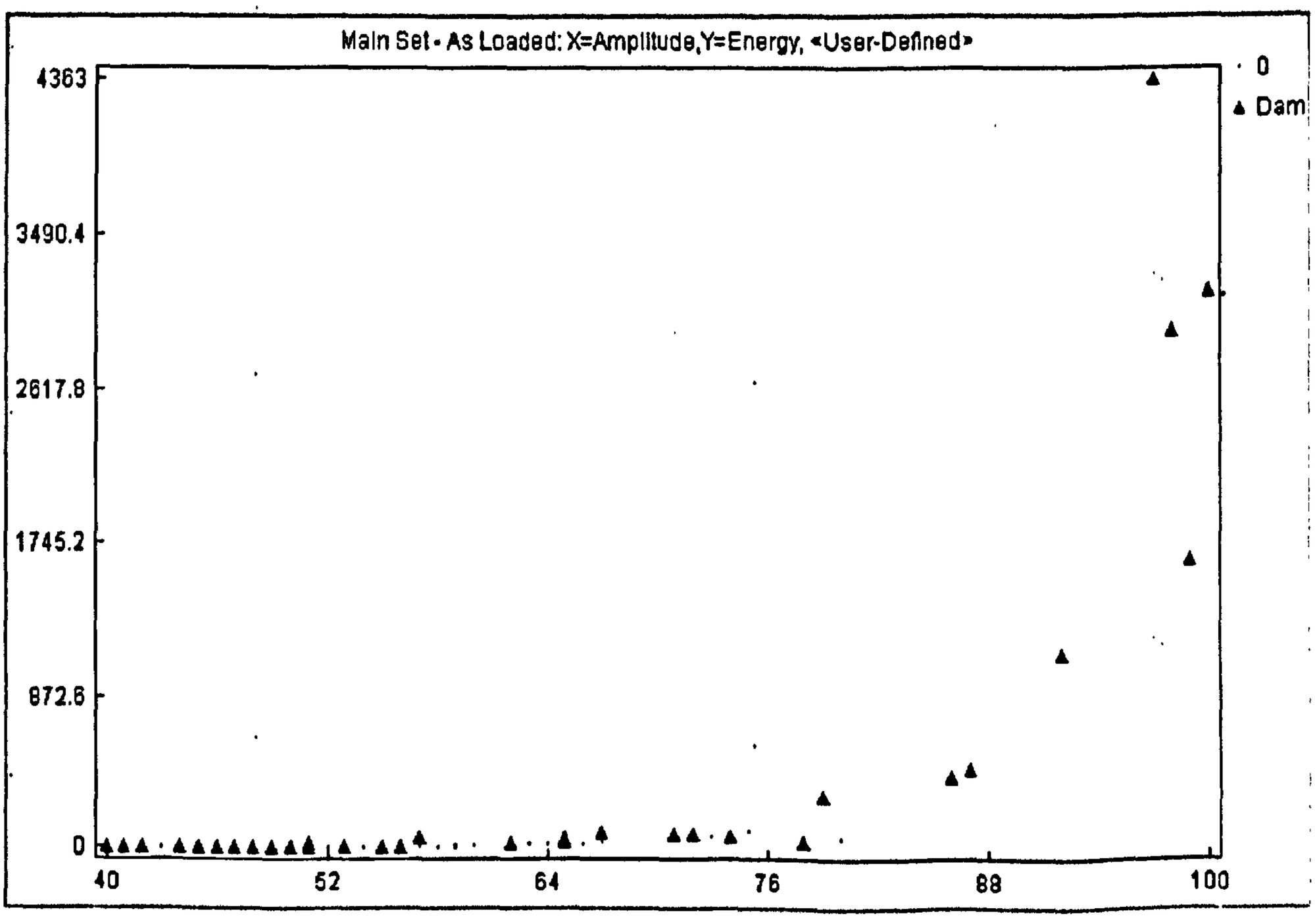

Graph 3.25: Energy Vs Amplitude within their classes for rope 106

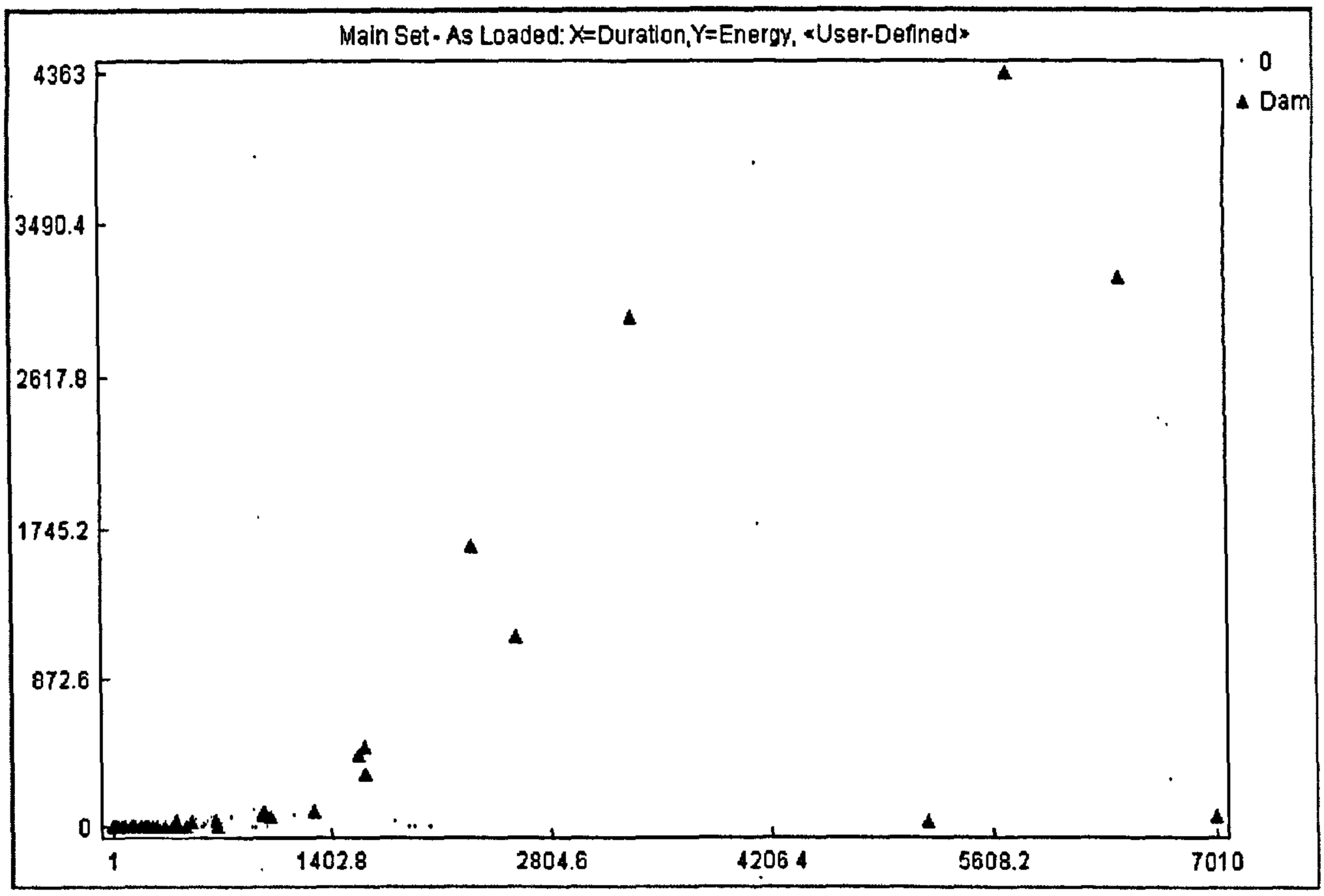

Graph 3.26: Energy Vs Amplitude within their classes for rope 106

From these graphs one can observe that again all the damage related sources provide the largest Amplitudes, Durations and Energies, however the overlap between classes still exists. The information was tabulated from all of the ropes in terms of the maximum values attained from non damage related AE and damage related AE with the intention of determining a generalisation to differentiate between damage and non damage related AE within wire ropes. The results are tabulated in tables 3.6-3.7.

Wire ID	Non Damage Related AE					
	Maximum			Generally < than		
	En	Amp	Dur	En	Amp	Dur
103	105	77	12843	40	70	3000
105	256	92	5642	200	80	4000
106	99	80	2025	70	75	1200
107	60	82	2842	60	75	2200
108	59	74	4902	60	75	2450

Table 3.6: Generalised result of features of hits from non damage related AE the population of ropes

Wire ID	Damage related AE					
	Maximum			Generally > than		
	En	Amp	Dur	En	Amp	Dur
103	3	54	224	-	-	-
105	25256	100	31140	750	80	6600
106	4351	100	7010	300	80	1610
107	23482	100	27996	500	75	3800
108	7741	100	5685	300	80	1280

Table 3.7: Generalised result of features of hits from damage related AE the population of ropes

3.3.7.1 Section Summary

From these results it was decided that the overlap between the durations of damage and non damage related AE could not be used as a means of discriminating. The values of energy and amplitude although still demonstrate overlap between the classes were sufficiently different to permit values of Amplitude values greater than 80 dB and Energy values greater than 300 to be used to differentiate between damage and non damage related AE in wire ropes.

The outputs for the remaining population of ropes are shown in Appendix III (F).

3.4: Fatigue of a wire rope with a seeded fault

A further rope was subjected to constant amplitude fatigue until failure between 30 and 40 kN at a frequency of 1Hz. The rope in the same manner as the previous ropes had a seeded fault in the form of a saw cut introduced to act as a local stress concentration from which damage was anticipated to propagate until failure. The test was conducted over almost four days, although a considerable period of time was spent with the loading inactive. The rope at one point exceeded the pre-determined deformation limits set on the Instron loading device. The loading machine at this point terminated the repetitive loading as this constituted the rope failed. It was not until some time later that this was revealed. On discovery that the loading regime had terminated visual examination of the rope determined the rope remained in tact and so the loading programme was resumed. Approximately nine minutes later the rope parted at the site of the damage. The implication was that the rope had already failed to sustain the load when the test had automatically terminated and the final nine minutes was the loadings required to fracture the remaining wires.

The results of the cumulative energy for the test are shown in graph 3.27.

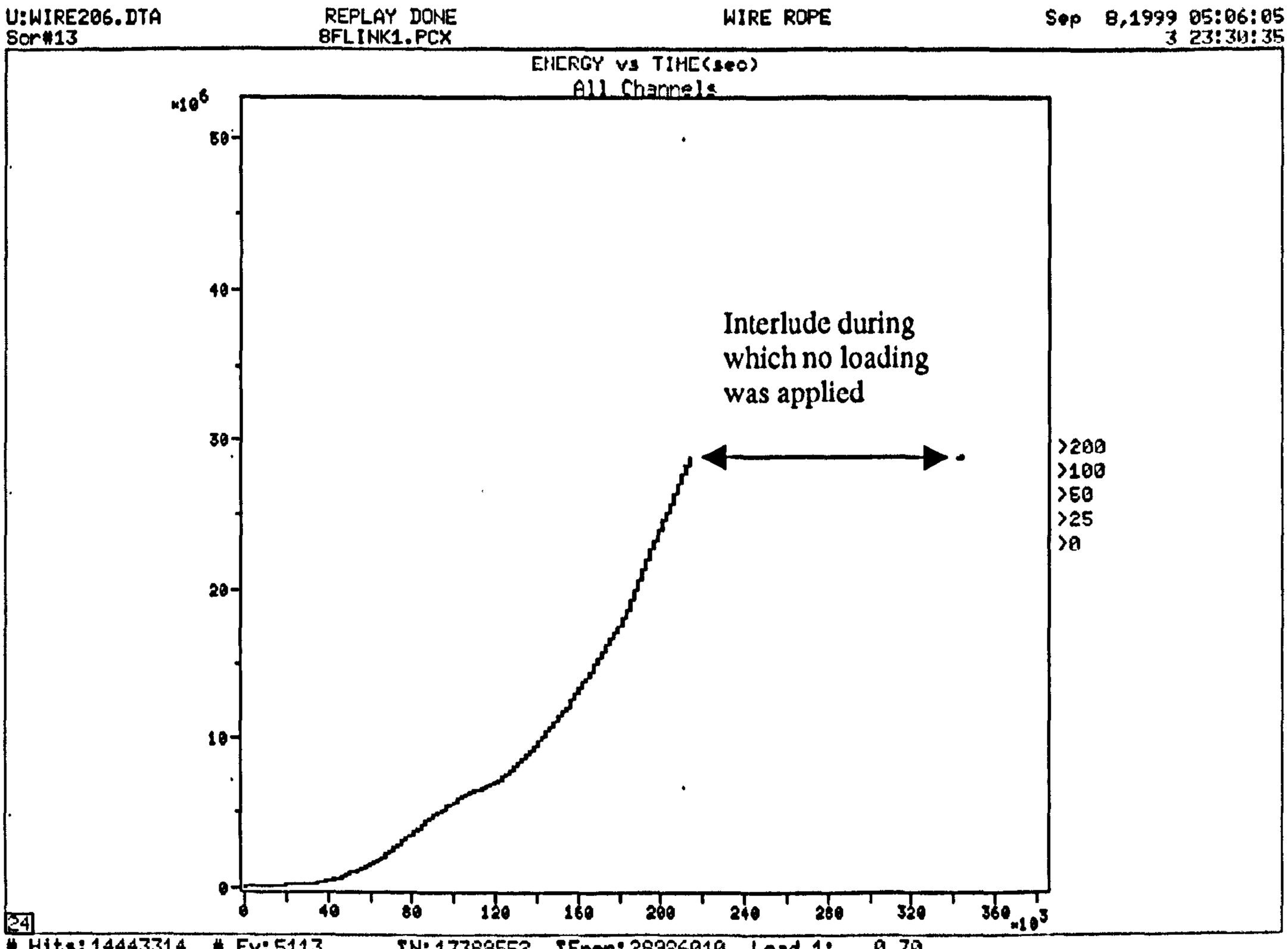

Graph 3.27: Cumulative Energy from a wire rope subjected to fatigue until failure.

A filter was imposed on the raw data to isolate the AE that was attributed to damage from other sources. The filter involved only the inclusion of hits greater than 80dB and 300 energy counts. The cumulative energy of this filtered data is shown in graph 3.28 and the source location of the events in graph 3.29. The effect of the filter is to reduce the volume of data to approximately a tenth of its previous value and the final failure becomes very much more pronounced. The source location results show all the events occurring in a close proximity, which was subsequently found through measurement to be in good agreement with the damage site. Such source located evidence serves to add credence that the imposed filter differentiated between damage and non-damage related AE.

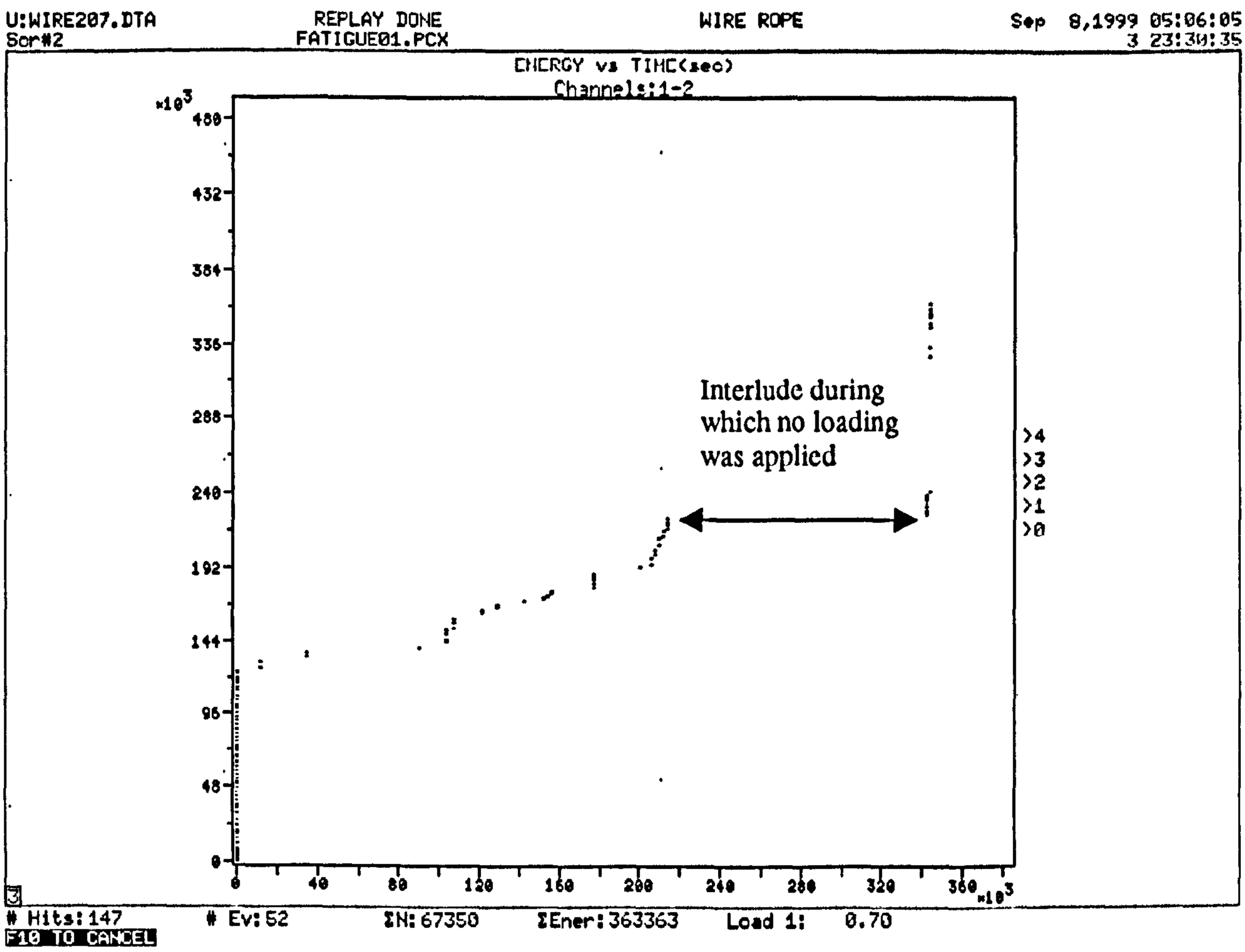

Graph 3.28: Cumulative Energy from a wire rope subjected to fatigue until failure, post filtering.

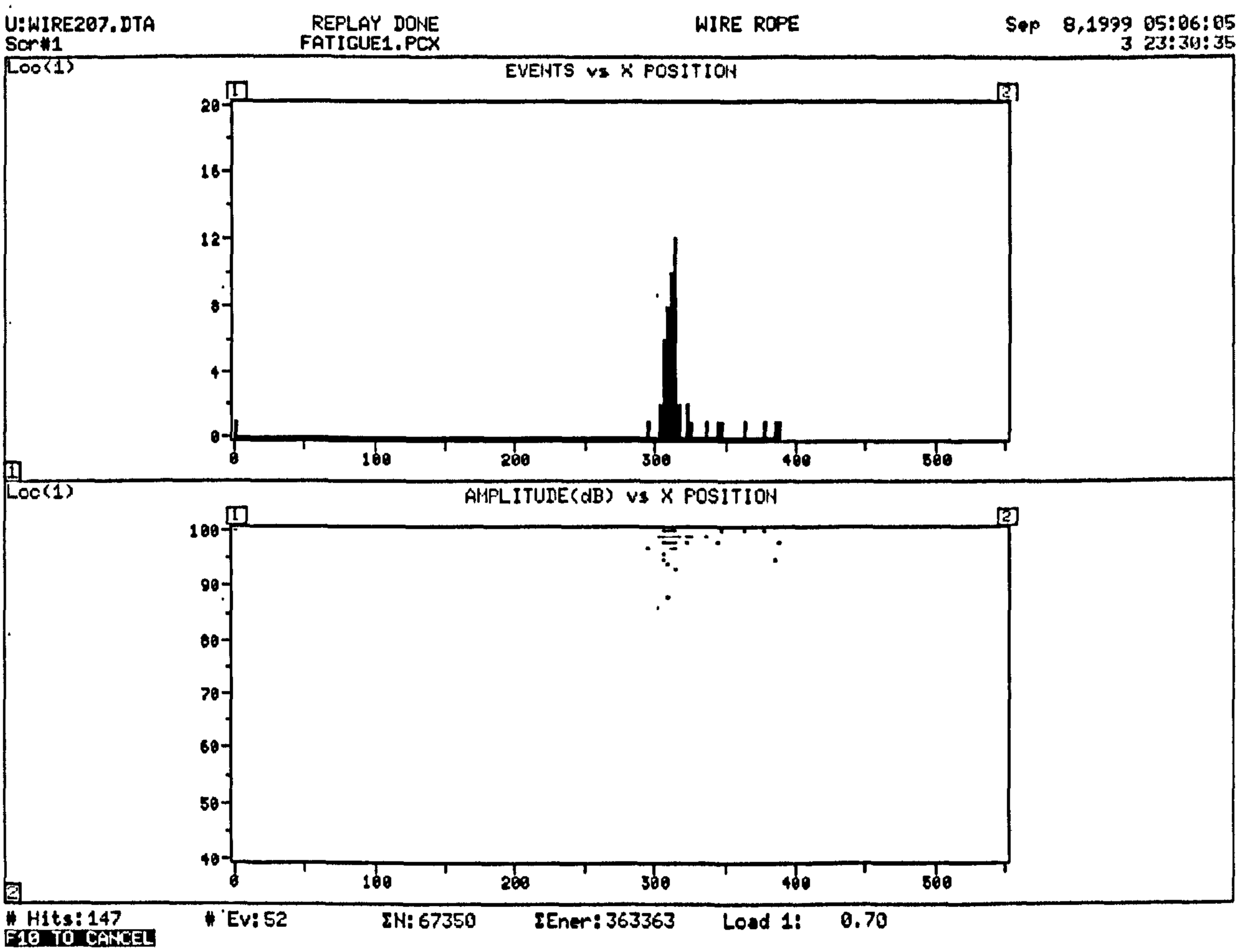

Graph 3.29: The events and the amplitude of the events Energy from a wire rope subjected to fatigue until failure, post filtering.

3.4.1: Discussion of fatigue results

From the data obtained after filtering it can be observed that the increase of AE energy is non-linear. There are clearly defined accelerations in the damage, between 100,000 and 200,000 seconds, during this period the energy increases linearly, but thereafter increases exponentially until failure. It is considered that changes in the rate of change of the cumulative energy are due to acceleration of the physical damage. As the damage progresses less and less residual wires remain intact to support the applied load as a result the rate at which they fail increases.

3.5: Chapter Conclusion

These preliminary results demonstrate the applicability of using Dunegans corollary as a means of defect detection in wire ropes. Both the qualitative and quantitative nature of the AE have been explored and it has been found that the AE can be used as a measure of the condition of a structure whilst subjected to a periodic proof load test. It is therefore not necessary to install instrumentation permanently on a structure in order to determine its condition, but information pertaining to condition can be established by periodic measurement. The subsequent chapter uses a single proof for the purposes of defect detection on in-service structures.

Various analytical techniques were employed to differentiate AE from wire breaks and other sources. Conventional AE analysis determined that there existed an overlap between the sources, which complicated the creation of a discriminator. Statistical analysis illustrated that the signal features that could be best employed for the provision of a wire break classifier were Energy, Amplitude and Duration. Investigation into the waveforms attained from hits considered to be wire breaks identified that the classification of singular wire breaks was unachievable as many wire breaks could be contained within a single hit. Due to the nature of the experiment isolation of breaks could not be attained and the investigation was remoulded to address the discrimination between damage and non damage related AE. It was found that AE greater than 80dB and 300 Marse Energy counts would provide the best differentiator between damage and non damage related AE. The differentiator was employed in a fatigue test on a wire rope.

The events that became evident during the post processing of the fatigue data file with a filter imposed to only include hits of a magnitude greater than 80 dB and 300 energy counts all emanated from a localised region at the damage site indicative that the filter was effective in identifying damage mechanisms in wire ropes.

The results from the fatigue test illustrate the non-linear nature of failure as described within chapter two. Chapter five focuses on this phenomenon as a means of establishing a trendable condition indicator that can be used during the course of a structure's life. The investigation identifies the suitability of using the Dunegan corollary as a means of trending the deteriorative process.

CHAPTER 4: Field trial validation of load testing and acoustic emission as a suitable condition indicator

4.1 Chapter overview

This chapter seeks to substantiate the previously laboratory validated concept in field trials. A number of trials were conducted on differing equipment types, predominately mechanical handling equipment. The chapter is broken down into a number of case studies with objectives, experimental methodology and a discussion regarding the results generated. Most of the acoustic emission testing that is conducted in industrial practices to date has focused on pressurised systems such as pressure vessels and pipe work. The case studies presented here are with the one exception concentrated on equipment that are subjected to mechanical stresses induced by supporting a physical mass. Such stresses are complex and difficult to reproduce. Pressurised systems, however, which endure stresses of a hydrostatic nature are easily replicated.

The chapter initially focuses on demonstration of the Kaiser principle on small load bearing components called pad-eyes, AE operating in the field is demonstrated. Some ten separate tests are reported. The investigation then turns to hybrid pad-eye called a link plate, which is subjected to strain, load and AE measurement whilst load tested up to a proof load. The departure from elastic behaviour is simultaneously measured by both strain gauges and AE. This case study demonstrates the capability of AE to detect localised yielding.

The investigation continues into the suitability of utilising AE in conjunction with periodic proof testing for the condition assessment of cranes. Nine Electrical Overhead Travelling (EOT) cranes are monitored by AE whilst subjected to initial commissioning proof tests. This is succeeded by a pedestal crane boom test. The boom was tested to destruction in order to investigate if AE could identify areas of concern that ultimately manifest themselves as the failure site. From the destruction test results AE evaluative methodologies are used in order to determine the success of AE as not only a qualitative measure of structural integrity, but additionally quantitative.

Ultimately this chapter concludes with a study on a pressure vessel with known fatigue cracks that are subjected to both static and dynamic testing whilst monitoring with AE. The fatigue cracks were sized pre and post the trial using Time of Flight Diffraction (TOFD). During the trial Alternating Current Potential Drop (ACPD) was used to detect any growth that occurred. Such techniques were used to substantiate the claims made by AE that it could detect a propagating defect.

4.2 Pad-eyes

4.2.1 Introduction

The function of a pad-eye is to support load that is applied in either lifting operations or tie down applications. Such items are typically found attached to equipment for the purposes of their transportation. A specific example of where a pad-eye may be found is in a ship's engine room. During servicing of machinery it may be necessary to remove or support heavy cover plates that enclose moving parts in order to attain access to the inner mechanisms. Pad-eyes may be present on the cover plate as well as fixed to the deck head. A chain block or pulley system is employed between the two pad-eyes to lift off and support the weight of the cover plate whilst the inner access is desired.

The purpose of this investigation was to present the results of the proof load testing of pad-eyes whilst monitoring with AE instrumentation on board HMS ARK ROYAL. These particular pad-eyes' function are for Replenishment at Sea (RAS) purposes. Whilst a warship is deployed on station it may take provisions, fuel and stores from a support vessel. This permits the war ship to remain on station for long periods. The RAS operation involves two ships aligning themselves broadside to one another and a wire rope is passed between them. The wire is secured via a shackle to a pad-eye and stores can be passed from one ship to other using a winch. Such an operation is particularly precarious in adverse weather conditions and these pad-eyes can be subjected to highly variable transient loads. The consequence of the failure of such an item can result not only in the loss of the items that are being transported, but also can endanger personnel involved in the operation.

Such items are currently re-qualified and deemed fit for further service by sustaining the application of a proving load of twice its anticipated service load under a test condition. Such a load is applied in differing directions to replicate what might be experienced in-service.

4.2.2 Experimental objectives

The use of the proof test alone allows the validation of the pad-eye's structural performance in what is essentially a binary output. If the pad-eye sustains the applied load then it is deemed fit for continued use and the inability to sustain the applied load constitutes failure. In the instance of gross visible deformation being present after the test the outcome would most probably result in the component being failed. However, for such gross deformation to be present as to be observable, the damage present must be severe and the proximity to ultimate failure close. The judgement of the competent person who might conduct the proving test is highly subjective.

From the previous chapter it was observed that AE used in conjunction with a proof test could discriminate between defective and non-defective wire ropes. Small progressive damage mechanisms that would not constitute a failure during a proof test were detectable. Therefore using AE in conjunction with a proof test would permit an

enhancement to current industrial practices of proof testing. The use of AE with the proof test allows a propagating defect to be recorded and its propagation observed prior to it becoming critical and failing either in-service or during the proof test itself. This would allow a greater knowledge to be attained from the proof test of the equipment's fitness for continued service.

If the AE could forewarn operators during the proof test that a defect was propagating under the applied load then the load could be reduced and examination of the area conducted prior to any continuation of load application. This in itself would be an enhancement in the safety of the industrial practice.

4.2.3 Experimental set up

The tests were conducted in accordance with the test procedures that would be used throughout the life of the aircraft carrier. It is the norm that the procedure of proof testing would be conducted every four years. To accommodate the AE it was necessary to revise the test procedure slightly. Instead of a single load application being applied, two successive proof tests were conducted in order to explore the Felicity Effect. The load test profile can be observed in figure 4.1.

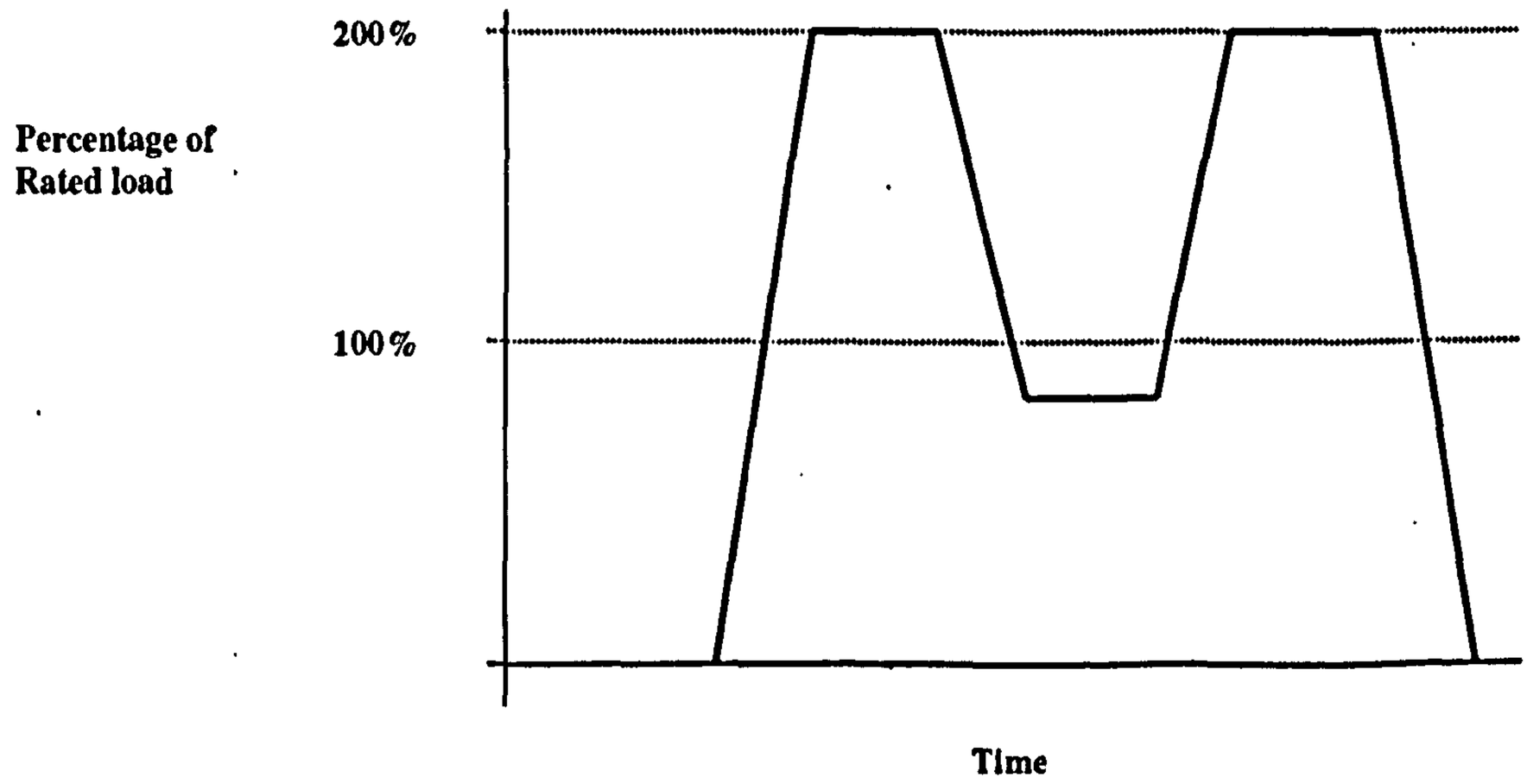

Figure 4.1: The load profile for testing RAS pad-eyes

In terms of proof load testing in conjunction with AE, the following observations are thought to be the most salient for the purposes evaluating of RAS points.

1. If the item under test does not adhere to the Kaiser Effect i.e. has a Felicity Ratio then this will be indicative of a severe structural defect.
2. If the item continues to emit during a period of constant load then this will be symptomatic of continuous degradation at the prescribed load level.

There are two types of RAS points, these are known as a "fixed point" and a "stump mast". The fixed point, as the name suggest is a permanently attached to the ships superstructure. The stump mast is a mast that can be temporally rigged in to the deck and used for RAS operations. Stump masts can be located on both the Fwd and Aft ends of the ship. The test conducted are reported here involve the testing of the one fixed point and two stump masts.

4.2.4 Equipment and settings used

The details for these types of pad-eyes are taken from the "Wood and Clark" manufacturing catalogue for rectangular base pad-eyes suitable for welding. A schematic is shown in figure 4.2. All dimensions given are millimetres with the proof load expressed in metric Tonnes.

Old Pattern No.	Naval Store Cat No.	Wall thk Ring	Hole Diameter	Base Width	Base Length	Base Height	Unit Height	Proof Load
4020		29	57	76	130	18	114	16

Table 4.1: Dimensions of pad-eye

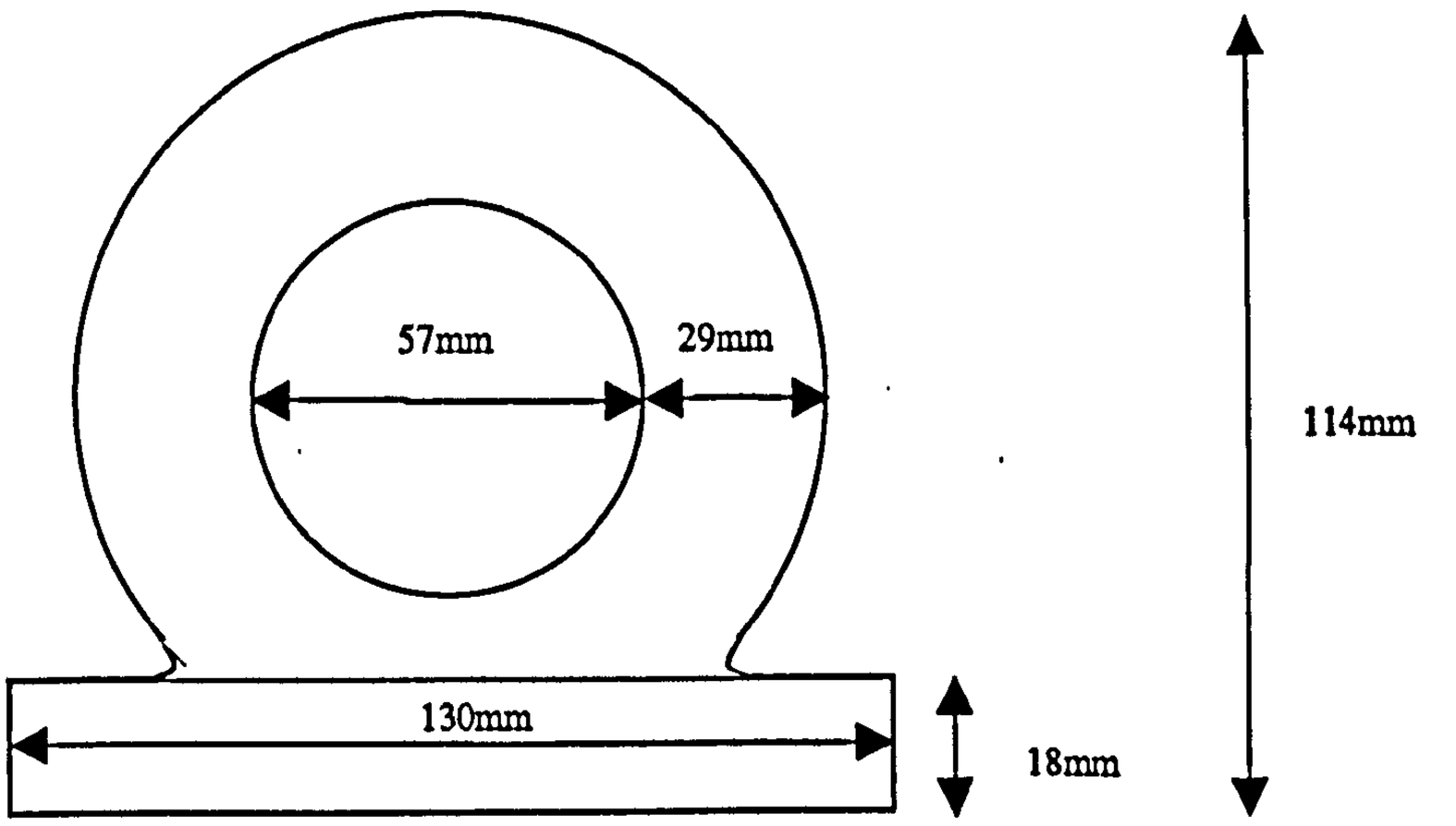

Figure 4.2: Schematic of a pad-eye

The AE equipment was manufactured by Physical Acoustics Corporation, a four channel AEDSP-32/16B with Mistras 2001 software. Only two channels were used for the test. The transducers were Physical Acoustics wide band (WDI) with a frequency range from 0.1 to 1.2 MHz.

The instrument settings were set such that there was a fixed threshold level of 40 dB, a pre-amplifier gain of 40 dB, i.e. x 100, a sampling rate of 4 MHz and a software setting

of a frequency bandpass of 100 kHz – 1.2 MHz. The applied load was also monitored and brought in to the instrument as an additional parametric input. This was achieved by a direct connection into an in line load cell.

The test arrangement is shown in figures 4.3. Figure 4.3 shows the general arrangement using a crane to apply the load by tensioning a wire.

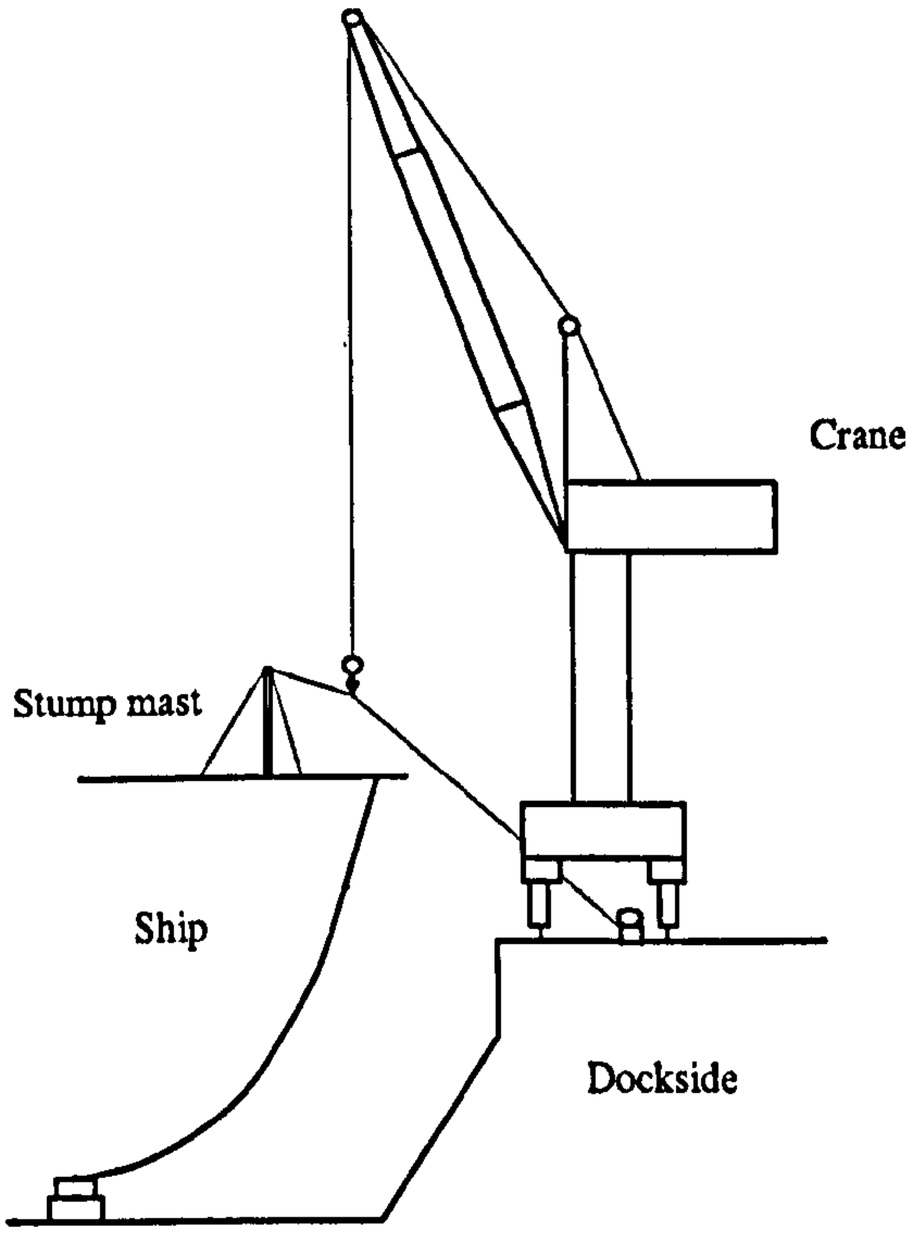

Figure 4.3: Test arrangement

4.2.5 Nomenclature

When testing a fixed point there are a total of four separate tests, whereas on stump masts there are only three. These tests seek to replicate the service conditions by emulating the angles at which the load can be applied. When "RASing" from an aircraft carrier and using a stump mast it is assumed no supply vessel is taller than the carrier and as such it is not necessary to load test in the upwards direction. This scenario does not apply to the fixed point, which is located midships and is therefore lower than the bow and stern of the ship and conceivably could be lower than the supply ship. There are therefore four tests conducted on the fixed point to accommodate the upward direction.

For the purposes of conciseness a nomenclature was established to refer to the different test types. The fixed point pad-eye is tested at 20° to the horizontal in the upwards and downwards directions. These will be denoted as 20°, U and 20°, D, respectively. Equally, these tests are conducted in both the Fwd and Aft directions, again at 20° from

the centre line. This will be referred to as 20°, F and 20°, A. In the case of stump masts a test is also conducted at 0°. So a test might be typically described as 20°, D, 20°, A

The magnitudes for all load tests in this section are 16 Te. Only one of the fixed points tests is described here. The remainder of the tests can be found in Appendix IV (A). The tests are:

Fixed point 20°, U, 20°, A
Fixed point 20°, U, 20°, F
Fixed point 20°, D, 20°, A
Fixed point 20°, D, 20°, F

Fwd Stump Mast 20°, D, 20°, A
Fwd Stump Mast 20°, D, 0°,
Fwd Stump Mast 20°, D, 20°, F

Aft Stump Mast 20°, D, 20°, A
Aft Stump Mast 20°, D, 0°
Aft Stump Mast 20°, D, 20°, F

4.2.6 Results

A display of both the load profiles and associated acoustic activity is shown in graph 4.1. The solid line illustrates the load profile whereas the emission is signified by the dots.

This load test was conducted at 20°, D, 20°, A on the fixed point and can be regarded as typical of the outputs generated from a pad-eye with no indications of an inherent defect.

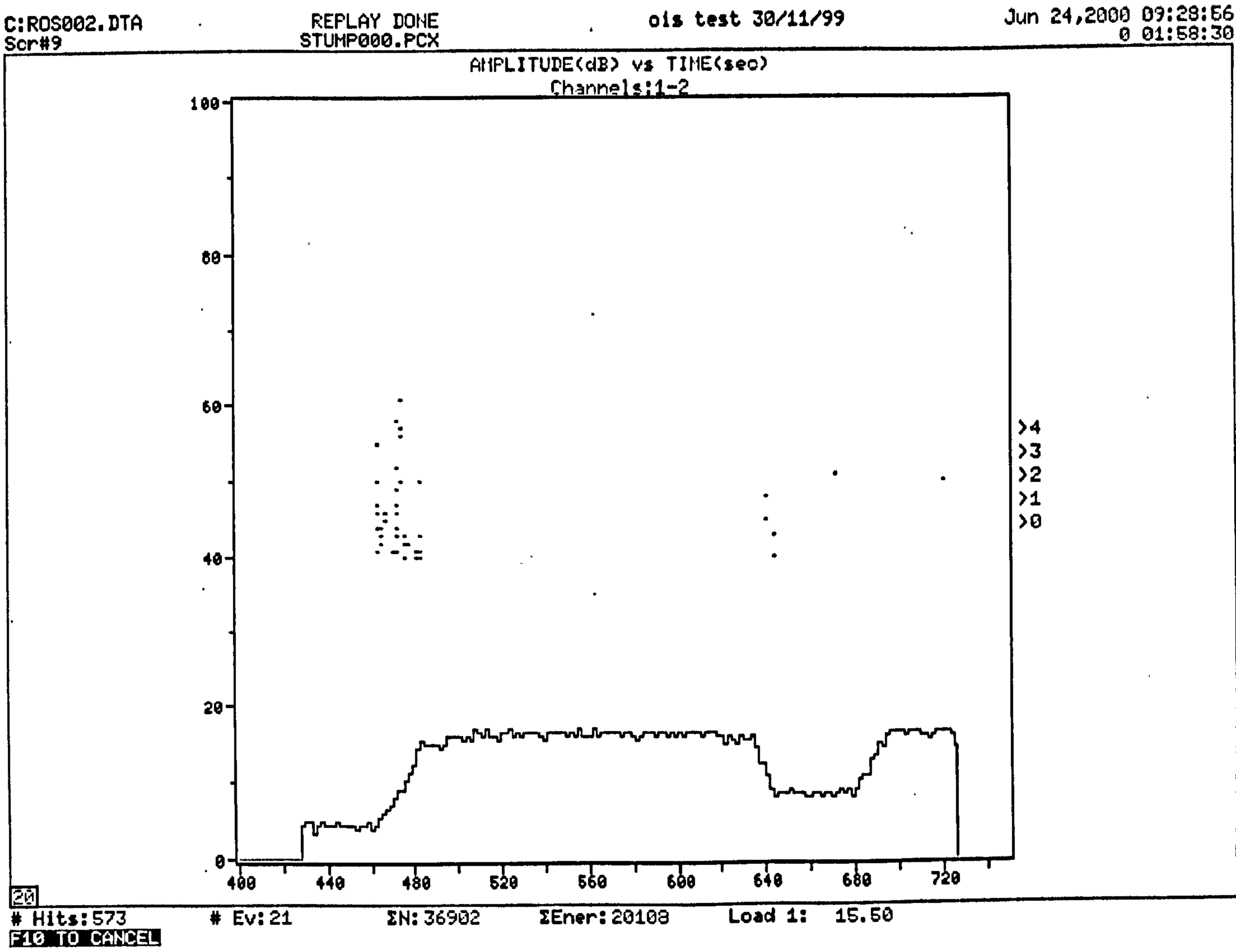

Graph 4.1: Load and Amplitude history for fixed point at 20°, D, 20°, A

Emission is apparent both on the rising load and the falling load. The load reapplication results in no further emission, which is indicative of no stress redistribution due to the excitation of flaws. Whilst there are two emissions on the second load application and hold (at ~680 and 710 seconds) this are not deemed to be significant.

It should be observed that there should be no emission on the initial rising load due to the Kaiser effect as the pad-eye had been previously load tested in this magnitude and direction. However, it is suggested that the Kaiser principle is more appropriate than the Kaiser effect to the testing of this type of equipment. The practicalities of replicating an identical test condition are extremely difficult. It is likely there were minor changes in the test configuration from the manner in which the stress was previously applied.

The Kaiser principle states that if the stress is unprecedented then emission will result. It is considered that stress experienced on this load application was in fact unprecedented; the load application had never before been applied identically in this fashion, but had been applied in a manner broadly similar. The load profile used for this test avoided a

complete unload condition. In the event that the pad-eye had been completely unloaded the tension on the equipment that connects to the pad-eye would have been reduced and the shackle would have slipped around the circumference to a rest position. If the load were then to be reapplied the chances of attaining an identical orientation of the equipment such that at a microscopic level, the structure was being strained in a manner identical to previous load is considered to be unrealistic. Even very small changes in the test condition are thought to contribute to the generation of an unprecedented stress, which in turn will result in emission.

For comprehensive purposes consider an extreme case to exemplify the concept, assume that a certain loading arrangement has given rise to flattened spot on the inner circumference of the pad-eye. Such a situation is likely to have occurred when an overloaded condition causes the local area to deform sufficiently as to exhibit plastic behaviour. Reapplying the same load in notionally the same direction will result in the same flat spot being subjected to the same condition. However the chances of being able to replicate the loading with the equipment seating itself into the same exact shape is impractical, the equipment is more likely to seat itself in a similar position and the result would be a slight reshaping of the flat spot from the load application. For the flat spot to reshape, the local material at the edges of the reformed area must have exceeded the material yield stress and therefore have been subjected to an unprecedented stress and hence generate new emission.

4.2.7 Discussion

This investigation set out to explore the integration of acoustic emission monitoring in conjunction with the current proof load testing practices. This investigation has shown that even under the noisy conditions of a warship under refit it is possible to investigate the structural performance of RAS components under a test condition.

4.2.8 Comments

The items under test covered by this investigation show no indication of lacking structural integrity under a test condition of twice their anticipated operational load. It is apparent that the information pertaining to the structural behaviour is greatly enhanced by the use of AE.

4.3 Link plates

4.3.1 Introduction

There exists a certain hybrid pad-eye called a link plate. Their purpose is to provide an anchorage for aircraft to be tied down on board an aircraft carrier flight deck. Link plates consist of a duplex stainless steel cup casting which encapsulates a forged shackle. Duplex was chosen as the constructional material due to its favourable corrosion resistant properties.

The shackle is hinged at approximately the mid-point and can therefore be folded away and submerged into a bowl whilst not in use. When not in use the shackle remains flush with the casting leaving the deck flat and free from obstructions that may impede operational activities. The design was initiated to replace a cup and cruciform arrangement that had previously proved susceptible to corrosion. With the deck accessible to both precipitation and seawater the previous design had filled with water and degraded sufficiently as to necessitate replacement during refits. It was considered that Duplex would assist in minimising this. Utilising Duplex as the material for manufacture presents problems with fixing. It is difficult to weld the dissimilar material of the duplex to the mild steel decking. The manufacturer overcame this problem by welding a mild steel annulus known as a 'thick adapter ring' to encompass the stainless link plate. This permitted the relatively straightforward weld procedure of the marrying of the two mild steels, the annulus and the deck.

The component is shown in plate 4.1.

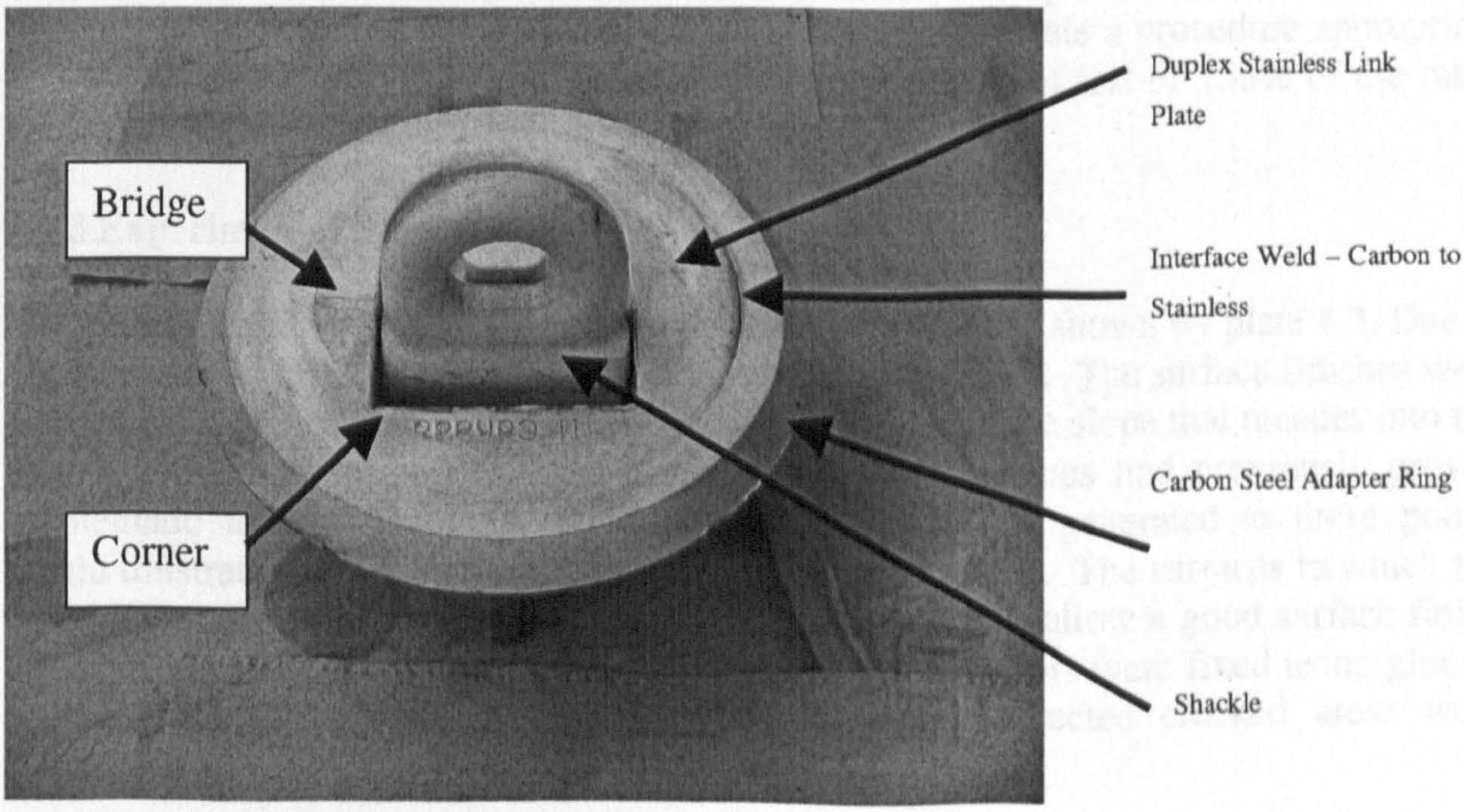

Plate 4.1: Link plate

It was discovered following proof testing link plates of HMS ARK ROYAL that a number of cracks had appeared in the castings. The cracking appeared at the bridges and the corners (illustrated on plate 4.1).

An investigation into the cause and effects of the cracking was commenced which involved a number of organisations. The cracked components were removed from the deck and replaced; the removed components were given to various organisations for testing and analysis. The reason for its inclusion in this work is because both strain measurement and acoustic emission was employed during the proof testing of one of these components. The section explores the characteristics of the AE behaviour with respect to fundamental mechanical behaviours of stress and strain.

4.3.2 Equipment and settings used

The testing was conducted with a Physical Acoustics DiSP-24 channel acquisition unit and R15I sensors.

An HBM spider with Catman software was used to acquire the strain measurement. 45^0 strain gauge rosettes were used so that the principle stresses could be calculated and the angle at which they act.

An Instron testing machine model No 1342 H 1031 applied the load. The applied load was taken into the AE instrument via a direct connection from the load cell.

The SWL and the Proof load loadings, suggested by the manufacturer are 56 kN. It is not the standard procedure for the rated and the test load of a component to both be the same. In consultation with the manufacturer and in seeking to generate a procedure appropriate to AE testing, the manufacturer agreed that to employ a proof test of 150% of the rated load would be acceptable.

4.3.3 Experimental Set up

The strain gauges were mounted on the link plate in the areas shown by plate 4.2. Due to the necessity of affixing strain gauges to a good surface finish. The surface finishes were prepared and the best area to locate gauges B and C was on the slope that recedes into the bowl. The strain gauge positions were chosen as these areas had previously proven problematic through cracking. Measurement of the strains generated at these points would illustrate at what load value the onset of yield occurred. The surfaces to which the strain gauges were to be affixed were cleaned and sanded to allow a good surface finish to which the epoxy could bond. The acoustic emission sensors were fixed using glue in an arrangement to make a square within which all suspected cracked areas were encompassed.

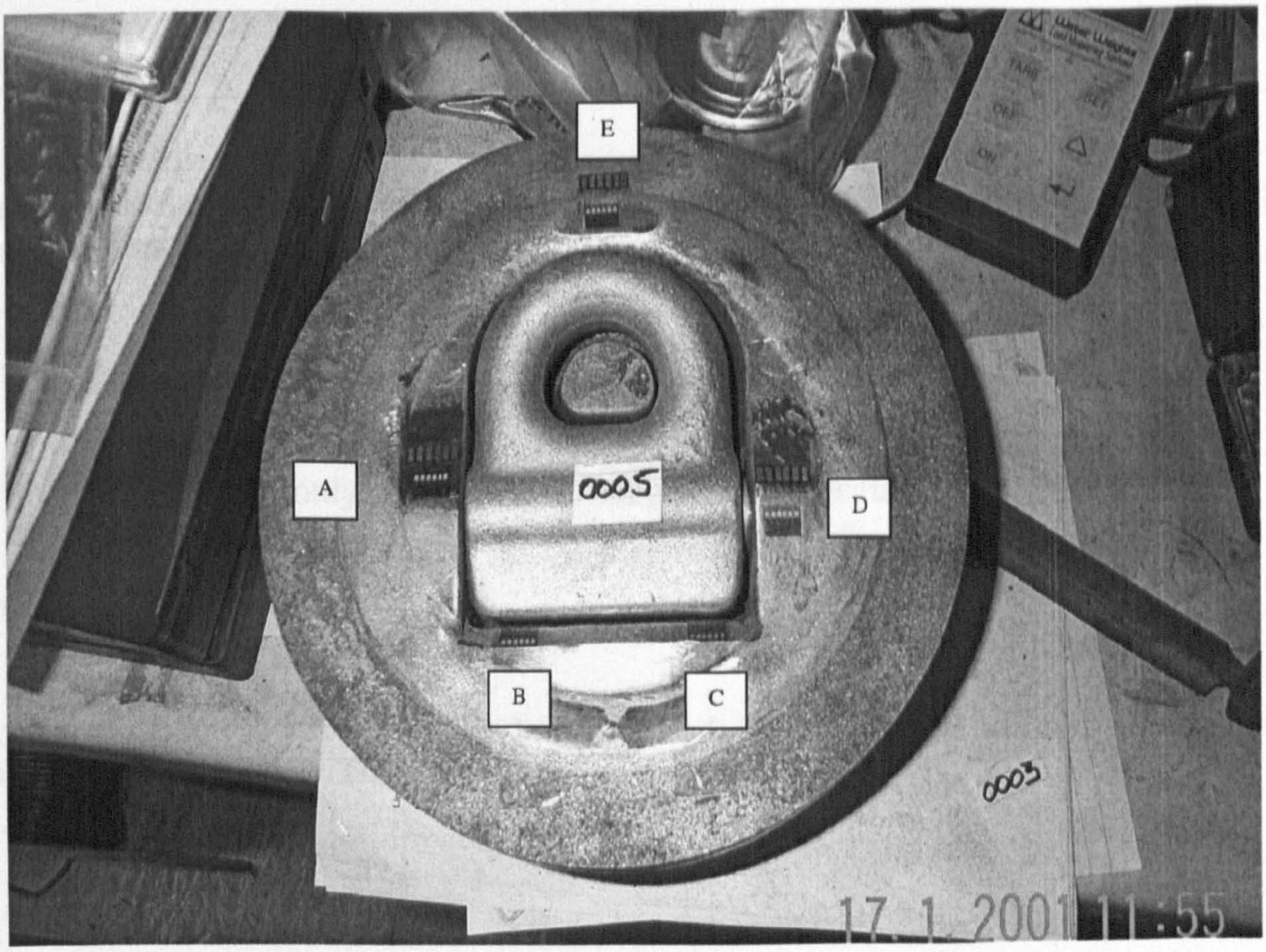

Plate 4.2: Link plate with strain gauges fitted

The instrumented link plate was subjected to incremental load steps of 10 kN up to 56 kN i.e. the service load. Finally, the load was taken up to 84 kN, the equivalent of a 150% proof load condition.

4.3.4 Results

4.3.4.1 Stress Calculations

The format of the 45^0 strain gauge is that there are three legs each labelled A, B and C the measured change in resistance for each leg is measured and is proportional to the change in deformation. The changes in deformation are referenced to changes in strain. These are measured using a Wheatstone bridge. Mohrs circle was used as the means of converting the strain into the respective principle stresses and shear stresses. Mohrs circle is a graphical method of analysis and as such does not lend itself well to computerised solutions, however we can use the proof of the circle to construct equations for a spreadsheet solution.

The calculations used to do this were:

For the centre of the circle (C) the measured strains (ε) are inputted into the equation

$$C = \frac{\varepsilon_A + \varepsilon_C}{2}$$

Having calculated where the centre of the circle lies it is necessary to solve for the angle ϕ as this is an unknown in the equation for the radius (R) of the circle.

$$Tan\ 2\phi = \left(\frac{2\varepsilon_B - \varepsilon_A - \varepsilon_C}{\varepsilon_A - \varepsilon_C} \right)$$

With ϕ calculated the only unknown is R, which can be calculated from the equation.

$$RCos\ \ 2\phi = \varepsilon_A - \left(\frac{\varepsilon_A + \varepsilon_c}{2} \right)$$

To convert strain to stress, Hookes law was used. Where E is the modulus of elasticity and ν is Poissons ratio. The equation is given as:

$$\sigma_1 = \frac{E}{(1 - \upsilon^2)} [\varepsilon_1 + \upsilon\varepsilon_2]$$

Equally;

$$\sigma_2 = \frac{E}{(1 - \upsilon^2)} [\varepsilon_2 + \upsilon\varepsilon_1]$$

This generates all the unknowns to construct the stress circle, the principle stresses are the centre of the circle ± the radius and the magnitude of the principle shear stress is the radius. In terms of the angles the datum reference is with respect to gauge A, and is given as P_1; from stress theory, the principle stress P_2 acts normal to P_1 and the shear stresses act at 45 degrees to both P_1 and P_2.

4.3.4.2 Measured Stresses at Incremental Load Steps

Graph 4.2 illustrates the results of the test. The strain gauge data comes from a rosette that was sited on the left bridge in the vicinity of a visible crack.

Applied Load, the principal stress, and the cumulative AE Energy during incremental steps up to the proof test on Link plate 005

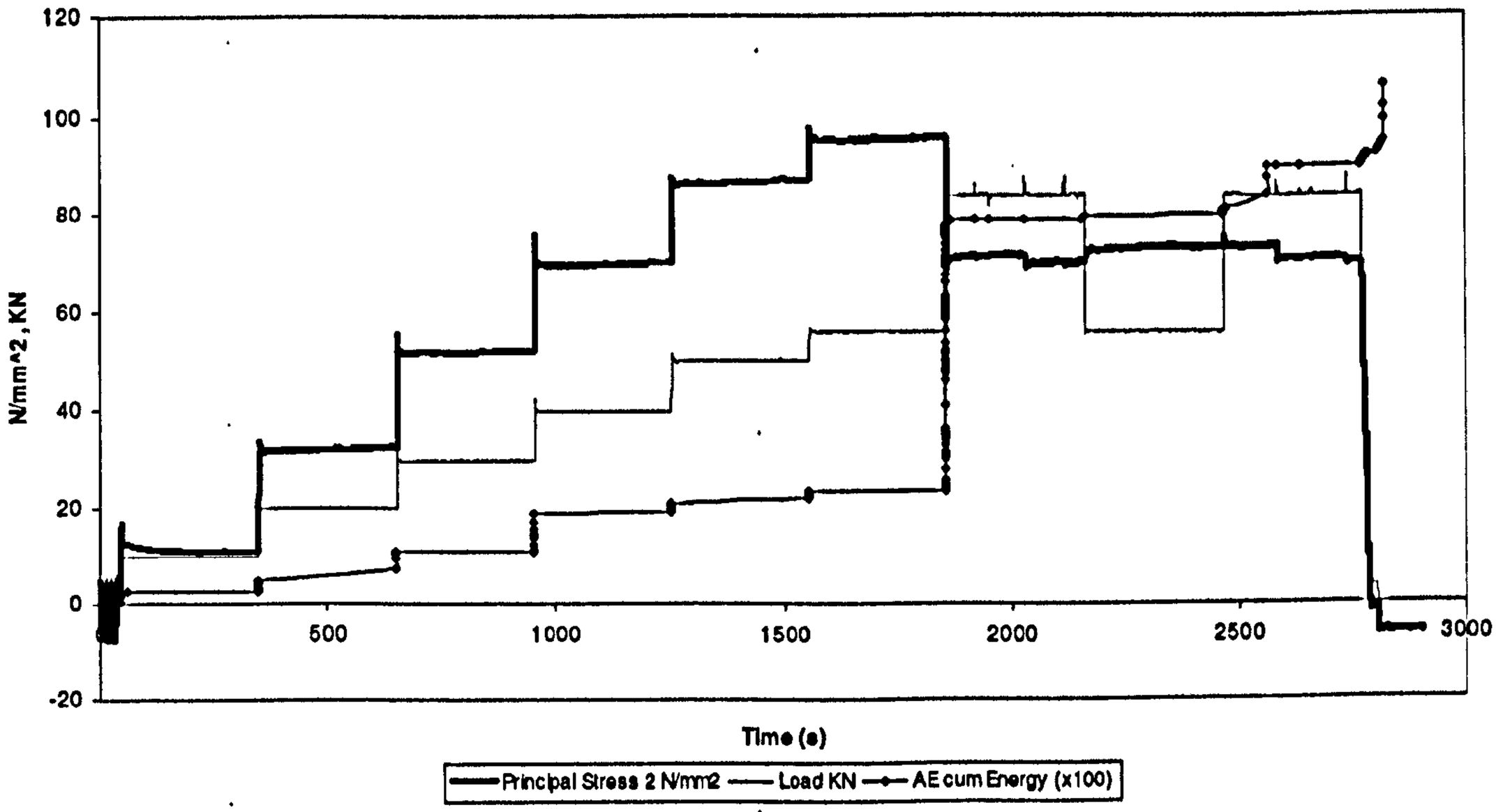

Graph 4.2: The applied load, the principal stress and the cumulative AE Energy during incremental load steps to the proof test.

Only the relevant principal stress (P_2) is shown above for the purposes of clarity. Up to 56 kN, a direct proportionality of increases in load resulting in increases in the applied stress can be observed, which might be reasonably anticipated with elastic behaviour. On the application of load to 84 kN (150% proof test) there is no longer proportionality between load and stress in fact the measured value of stress decreases. This is coincident with a rapid increase of AE energy. On a decrease of load and subsequent reapplication of load back to 84 kN (~2200 seconds) there is no change in stress typifying non-elastic behaviour. The other strain gauges, however showed an increase showing that there was a change in behaviour resulting in a stress redistribution. During the first hold period (~1800-2200 seconds) at 84 kN, the AE activity continues throughout and during the second hold period (~2500-2700 seconds) at 84 kN a jump in acoustic energy is detected. There was no visible change in the crack where this gauge was sited after the test was completed.

4.3.5 Discussion

This particular trial emphasises one of the uses of AE as a means of determining the mechanical behaviour characteristics of materials. The strain gauge is and has been accepted as a means by which the changes in material properties can be examined. The

strain gauge is however limited to the local measurement of the material behaviour that occurs immediately underneath the gauge itself. In this instance the use of AE has been used as a global strain gauge, it has shown the capability of detection of a change in material behaviour from a location remote from the area of interest.

If structural performance is required to be determined then this demonstration has illustrated that AE can detect, the onset of material yield. The nature of most failures of mechanical structures is due to local stress concentrations being subjected to stresses that exceed material yield. AE as a condition indicator shows the promise of being able to detect that. A carefully positioned array of sensors could therefore attain global coverage of an area without necessitating an effective blanketing of strain gauges.

4.4 Cranes

4.4.1 Introduction

This section outlines the approach undertaken to demonstrate the use of AE in conjunction with periodic proof testing on cranes. Two types of cranes are examined, Electrical Overhead Travelling (EOT) and pedestal cranes. These are presented as two separate case studies.

There is limited available information relating to Acoustic Emission inspection of cranes although the US Navy have conducted load testing with AE on crane booms on dockside portal cranes. There additionally exists a strong parallel with the inspection of aerial bucket trucks in that they are both excited by a mechanical load as opposed to hydraulic or a pneumatic stress. In terms of industrial applications limited documented work on the assessment of structures, which have been excited by a mechanical stress exists although there has been considerable laboratory work. There has been substantial focus by the AE community on bucket trucks with a resultant standard.[69] Rogers[94], undertook AE tests on the slew rings bearings of offshore pedestal cranes which are a notoriously difficult components to inspect. There is, however, no documentary evidence to support the condition assessment of crane structures using AE.

4.4.2 EOT cranes

EOT are found in many industrial environments and are often seen spanning the width of the building above the plant. They are generally sited on girders running longitudinally and the crane is free to travel the length of the plant. They have differing functionality within plants. For example in a car production plant where the assembly is moved through the plant on conveyors during manufacture, their only use might be to lift defective or obsolete manufacturing machines out of the production area and to replace the new or renovated machine back in place. Their service duty is therefore minimal. In other instances their function maybe process critical, for instance within a steel works, the product is moved through the manufacturing process almost exclusively by overhead cranes and in such a case their duty cycle is almost continuous.

The EOT cranes that are investigated in this section are mounted on the hanger deck of aircraft carriers, their purpose to move heavy items such as engines and gearboxes around the hanger deck in support of maintenance activities. The three British aircraft carriers HMS ARK ROYAL, HMS INVINCIBLE and HMS ILLUSTRIOUS all have EOT cranes on their hanger decks.

The three aircraft carriers were all recently refitted and part of the work package involved the replacement of the EOT cranes. In total, nine of these types of cranes were tested: four onboard, ARK ROYAL and three on INVINCIBLE and two on ILLUSTRIOUS. All were subjected to a post installation commissioning proof load test, during which the

cranes performance was monitored by both AE and traditional deflection tests. The load was fully applied, sustained for five minutes and partially removed and then reapplied to the same value with a view to exploring the Felicity effect.

4.4.2 (a) Experimental objectives

The programme of research reported here aimed to assist the competent person with the provision of information pertaining to the integrity of the item whilst under test. Again similarly to the pad-eye investigation if the information that was provided by the load test were enhanced by the simultaneous measurement of acoustic emission then it would provide a more reliable empirical means of condition assessment than proof testing alone.

In terms of proof load testing in conjunction with AE, the following are thought to be the most salient for the purposes of crane testing.

1. If the item under test does not adhere to the Kaiser Effect i.e. has a Felicity Ratio then this will be indicative of a severe structural defect.
2. If the item continues to emit during a sustained constant load then this will be symptomatic of continuous degradation at the prescribed load level.

4.4.2 (b) Equipment and settings used

A Physical Acoustics 24 Channel DISP system was used with 8 of the available 24 channels used with 150 kHz resonant sensors.

The load was taken into the instrument as a supplementary input achieved by a direct connection into a load cell.

4.4.2(c) Experimental Set up

For EOT cranes an arrangement as shown by a plan view in figure 4.5 was used. Plate 4.3 illustrates one EOT crane onboard HMS ARK ROYAL. The boom sections of the cranes were monitored with eight acoustic emission sensors during a static load test. Each boom was treated as a separate linear array for location purposes. The test procedure involved the load being applied up to 6Te, held for five minutes, reduced to 3Te, and then reapplied to the maximum of 6Te and held for a further minute.

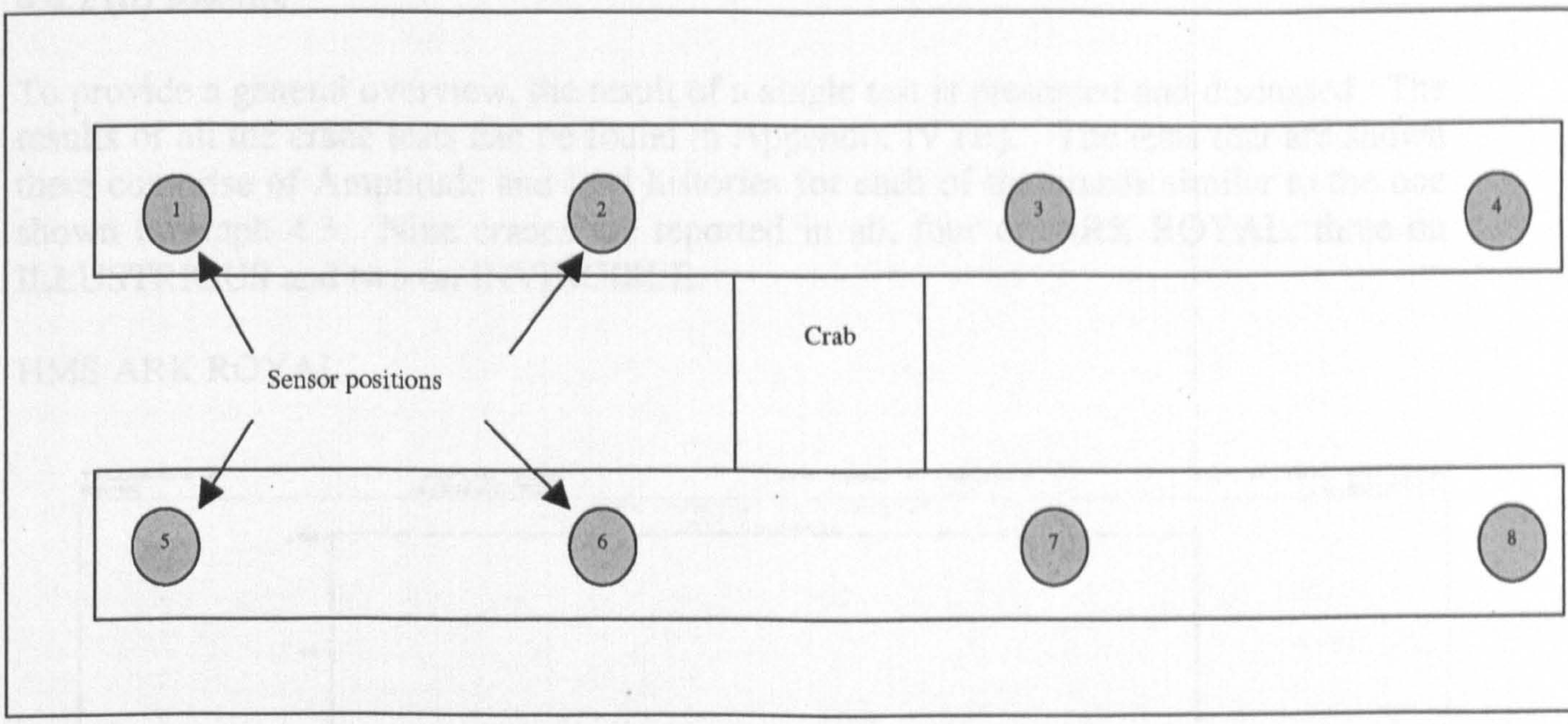

Figure 4.4: Sensor Set up on EOT cranes

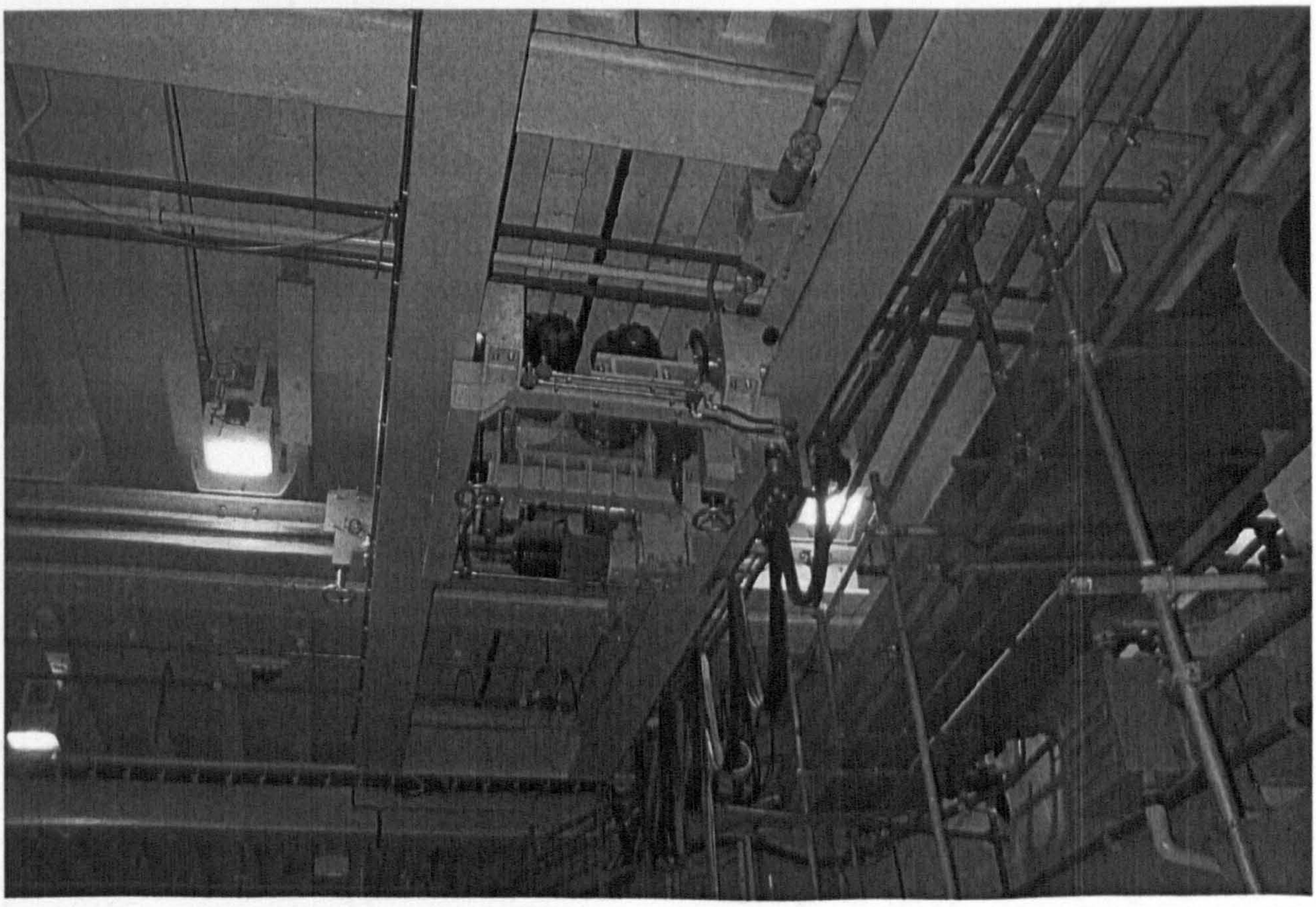

Plate 4.3: EOT Crane on HMS ARK ROYAL's hanger deck.

4.4.2 (d) Results

To provide a general overview, the result of a single test is presented and discussed. The results of all the crane tests can be found in Appendix IV (B). The tests that are shown there comprise of Amplitude and load histories for each of the cranes similar to the one shown in graph 4.3. Nine cranes are reported in all, four on ARK ROYAL, three on ILLUSTRIOUS and two on INVINCIBLE.

HMS ARK ROYAL

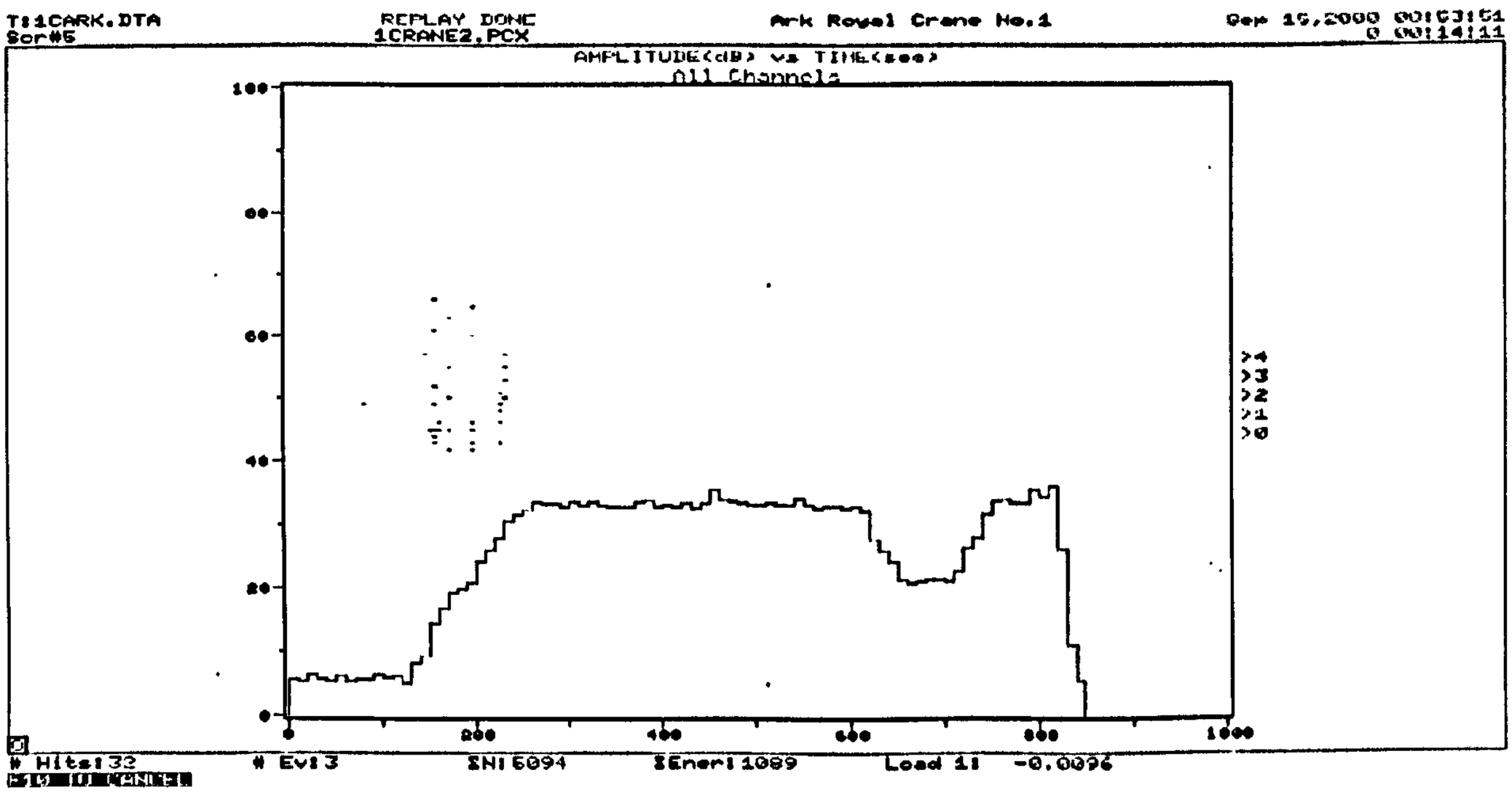

Graph 4.3: Amplitude and load history for HMS ARK ROYAL Crane No. 1

Graph 4.3 illustrates a typical result for one of the ship board tests. The solid line is the voltage proportional to the applied load, the dots denote the accompanying emission. The load has been mulitiplied so that it can be viewed on an amplitude graph. The values are not absolute as the true magnitudes of the applied load are 6 and 3 Te. It is evident that on the initial increasing load there are accompanying emissions although the density and total energy is small. There is no activity on the load hold period nor on the unloading and subsequent reapplication of load.

When load testing mechanical handling equipment it is especially important to only partially remove the applied load before the subsequent reapplication. The nature of stresses excited in a pressurised system are hydrostatic in nature and act uniformly. However with mechanical load the stresses have a directional component and the likelihood is that if the load was completely removed an identical stress could not be reapplied. This is significant because if the stress is unprecedented it would give rise to a breakdown of the Kaiser effect i.e. a Felicity effect leading to the conclusion of a false indication.

It is unknown whether the booms had undergone a factory acceptance test prior to their installation. This could be one of the reasons that the total energy content for the whole test is so low. The energy content can be viewed as numerical values in the lower portion of the graph and is shown as " ΣEner: 1089". Much of the stored energy could have been allieviated by such a test had it been conducted. In all tests it was found that the energy was very low. It is also feasible to speculate that due to nature of application of the cranes on a warship the fact that they are designed with very high factors of safety means that the applied static load could have produced minimal excitation to the structure and hence generated little activity.

The Kaiser principle as opposed to the Kaisier effect could again be relevent. Assuming a factory acceptance test had been conducted, stress redistributions and structural stabilisation would have occurred and in accordance with theory no emission would be generated during the application of a further load test. During the fitting and final assembly, however, minor changes in the orientation can affect the load path and hence the stress applied is unprecedented.

The source located events, of which there were few in all cases, generally emanate in the centre of the boom section. This seems logical in that it at this point of maximum bending occurs. The two linear arrays representative of each boom are shown in graph 4.4, which is taken from one of the INVINCIBLE crane tests. All deflection measurements yeided no permanent set in the structures.

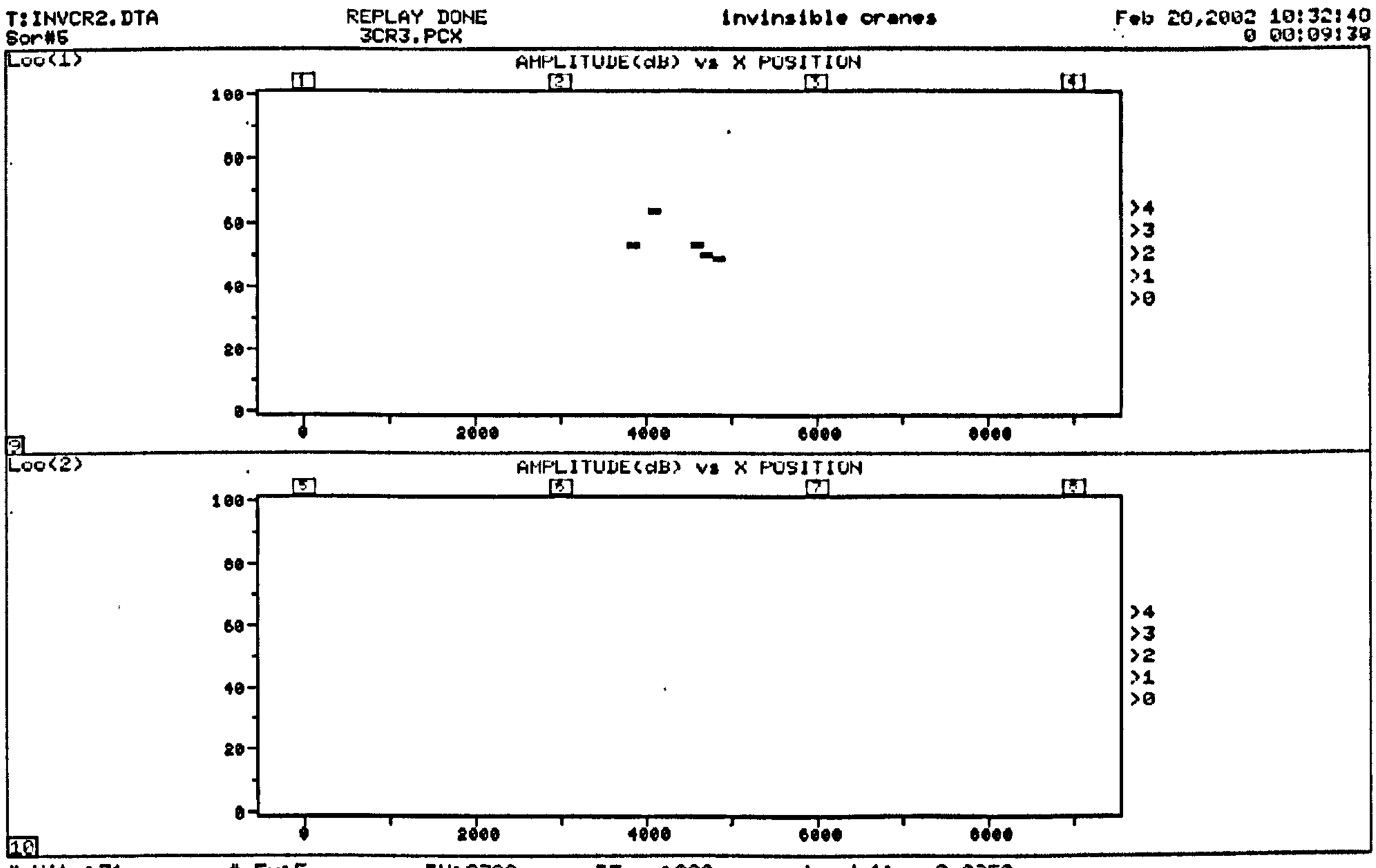

Graph 4.4: Location of data on HMS INVINCIBLE crane No.2

4.4.2 (e) Conclusion

With respect to the acoustic activity that was considered to be important it can be concluded that because there was no activity on the load hold the structure is experiencing no instability at a load greater than the generally applied service load. Further as there is no Felicity effect, the structure is fit for purpose as it generates no indications of structurally significant flaws under a 200% load test condition.

This section has shown that acoustic emission is applicable to EOT crane booms, but in order to be effective it must address all the structural failure modes that might be experienced in service. For instance, only the stimulus of maximum bending was explored i.e. when the crab was at the midpoint. In order to generate a test procedure it would be necessary to explore the point at which the maximum shear stresses are excited i.e. when the crab is loaded at either extremity of the boom.

4.4.3 Pedestal cranes

4.4.3 (a) Introduction

The second type of crane that was investigated was a Pedestal crane. Pedestal cranes are often found on docksides and are generally used for the movement of goods between ships and shore. They are also frequently found on offshore platforms where their function is again the movement of goods. These cranes are distinctive in their appearance in that the boom section is generally not solid, but comprises of a lattice arrangement that provides a good strength to weight ratio. In this investigation the test was conducted on a crane boom section with induced defects and loaded to destruction. Post test analysis investigated the severity of the indications found during a load test using some established methods of AE evaluation.

4.4.3 (b) Experimental objectives

The intention of the tests was to demonstrate the capability of the AE to highlight and identify sites in advance of the ultimate failure. Specifically to identify with what factor of safety a defect becomes active, which could therefore alert the competent person of its presence, prior to the site resulting in failure. Such an investigation could provide the evidence that AE as a technique could be used qualitatively to assess structural integrity of crane booms and identify what levels of forewarning of failure can be given.

In conducting a destructive test differing means of evaluating the severity of the flaw were explored. Post test, the data was analysed in order to determine an evaluation criterion. This analysis sought to examine that if AE was merely a qualitative assessment or could be used to quantify the defect severity. Four separate methods of evaluation were explored as a means of ascertaining the defect severity. The evaluative techniques were applied to each load increment. The methods applied were the Felicity Ratio, Persistence, the β value and Intensity Analysis. Software was designed to automate these calculations. Such AE evaluation criteria have been used successfully in the past a means of determining the significance of the defect and correlated to threat to the integrity of the structure in predominately pressurised systems.

4.4.3 (c) Equipment and settings used

A Physical Acoustics 24 Channel DISP system was used with 8 of the available 24 channels used with 150 kHz resonant sensors.

The load was taken into the instrument as a supplementary input achieved by a direct connection into a pressure transducer.

4.4.3 (d) Experimental set up

The results presented are of a destruction test that was conducted on a section of tubular lattice crane boom that had been previously retired from service. The section was

subjected to induced damage that would act as stress raisers and would propagate under the incremental applied load. The nature of the load application was a three point bending arrangement chosen to replicate the service conditions of bending that a crane boom would experience, in-service.

The sensors were deployed at the corners of the section. Each cord was treated as a separate linear arrangement for location purposes. The load was applied in increments of 2.5 Te to a maximum of 10 Te. Fixing the ends of the boom and applying a hydraulic jack to the centre of the section achieved the bending. Notches were introduced in the lattice cord connections. The hydraulic pressure in the pipe between the pump and the jack was measured to give a parametric input into the instrument proportional to the applied load.

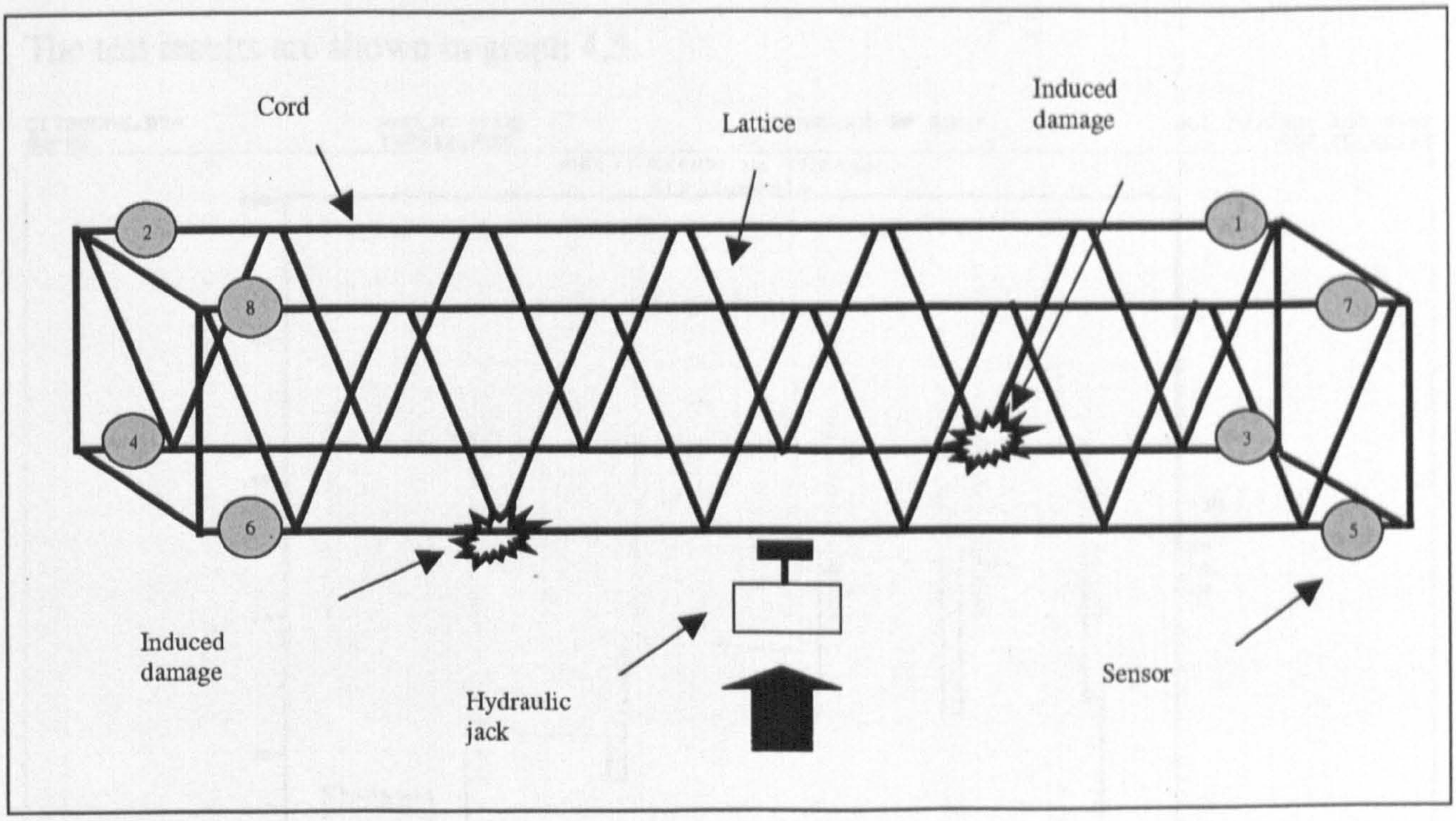

Figure 4.5: Sensor set up and bend test arrangement

4.4.3 (e) Results

The test results are shown in graph 4.5.

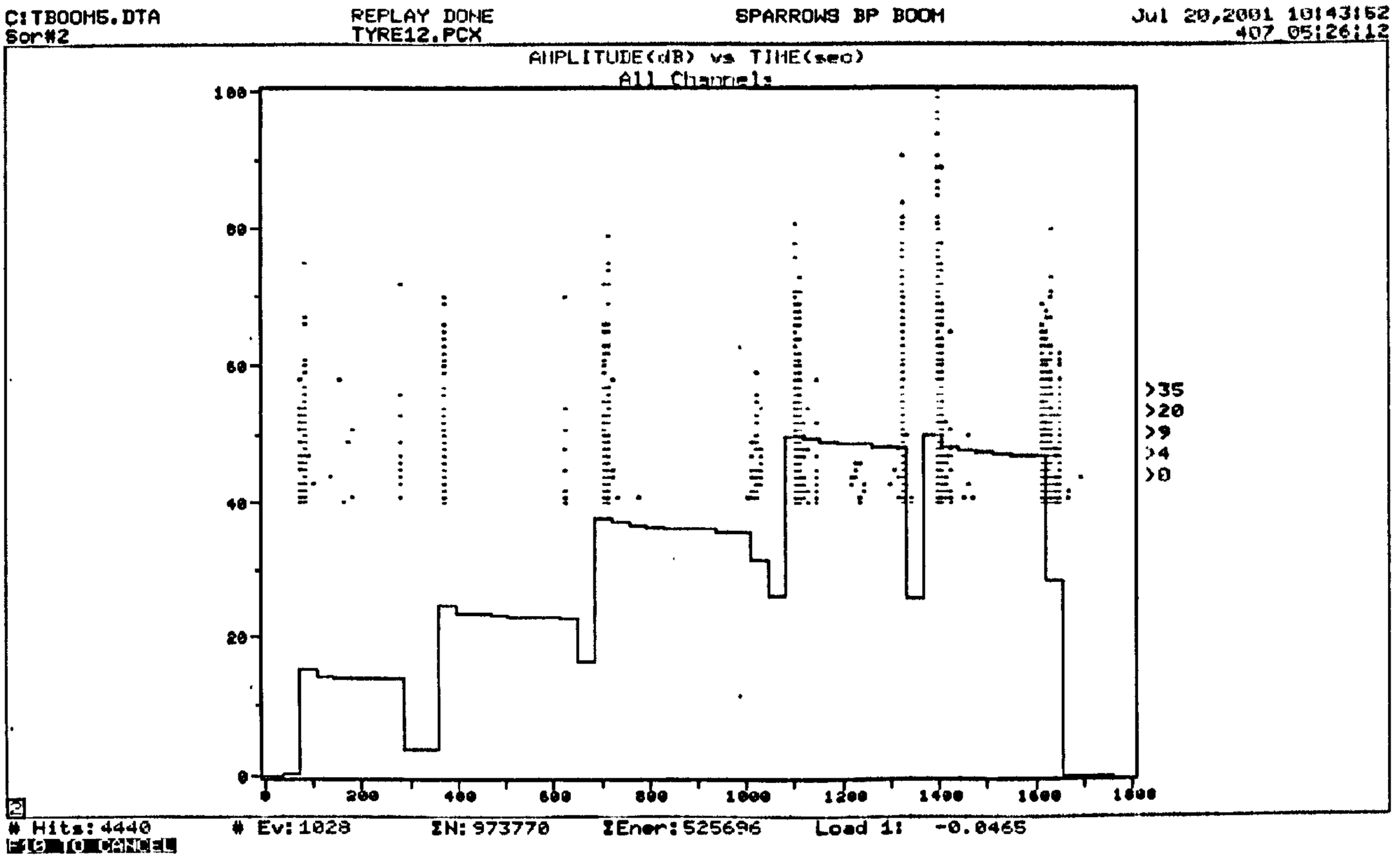

Graph 4.5: Amplitude and load history on crane boom section destruction test

Even the very first application of load shows a 75 dB hit indicative of a large mechanical source event. With increasing load there is a corresponding increase in activity and amplitude as might be anticipated. Following each load increment, the load was reduced prior to reapplying it to the next maximum level. This loading permitted the exploration of the Felicity Ratio.

Inspection after the destruction test showed one of the lattices was visibly buckled. The damage can be viewed in plate 4.4. The buckled lattice was located at one of the points where damage had been introduced. Damage was introduced at two separate sites and although there was pronounced activity from the other site there was no visual evidence of propagation at either physical location after the test.

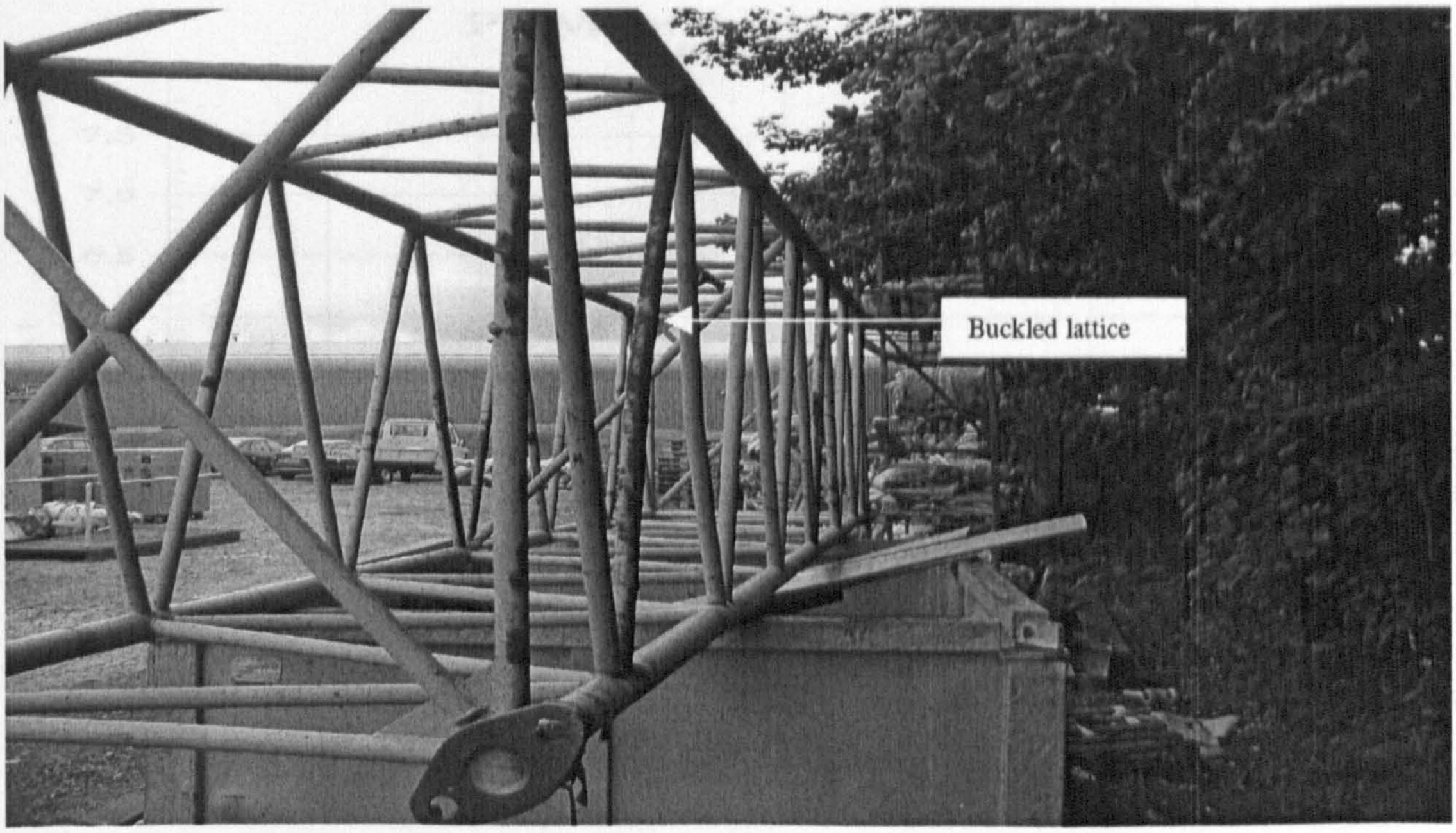

Plate 4.4: Buckled lattice

Post-test data evaluation investigated the most effective means by which the defect could be graded for its severity. Evaluation criteria were applied at each increment of load to identify which best illustrated an indicator of increasing defect severity.

The results of the evaluation criteria are illustrated in graphs 4.6 - 4.9. Only the results generated from the 7.5 Te load step are illustrated here. The results for all of the load increments can be found in Appendix Section IV (C). A summary of those results is tabulated in table 4.1, which illustrates the effectiveness of each evaluation method as a means of reliably identifying the severity of the defect at each load step.

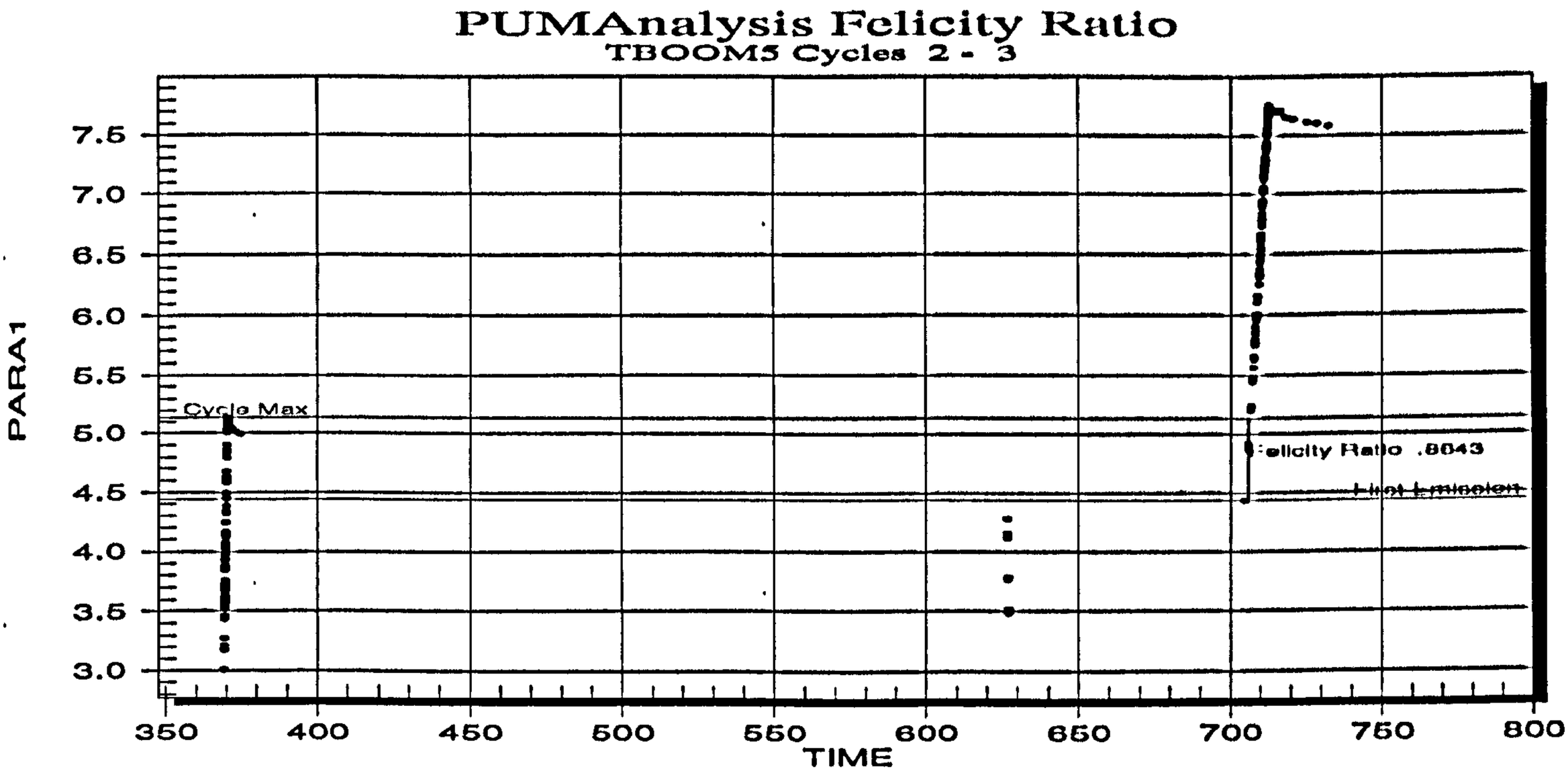

Graph 4.6: Software computation of Felicity Ratio at 7.5 Te

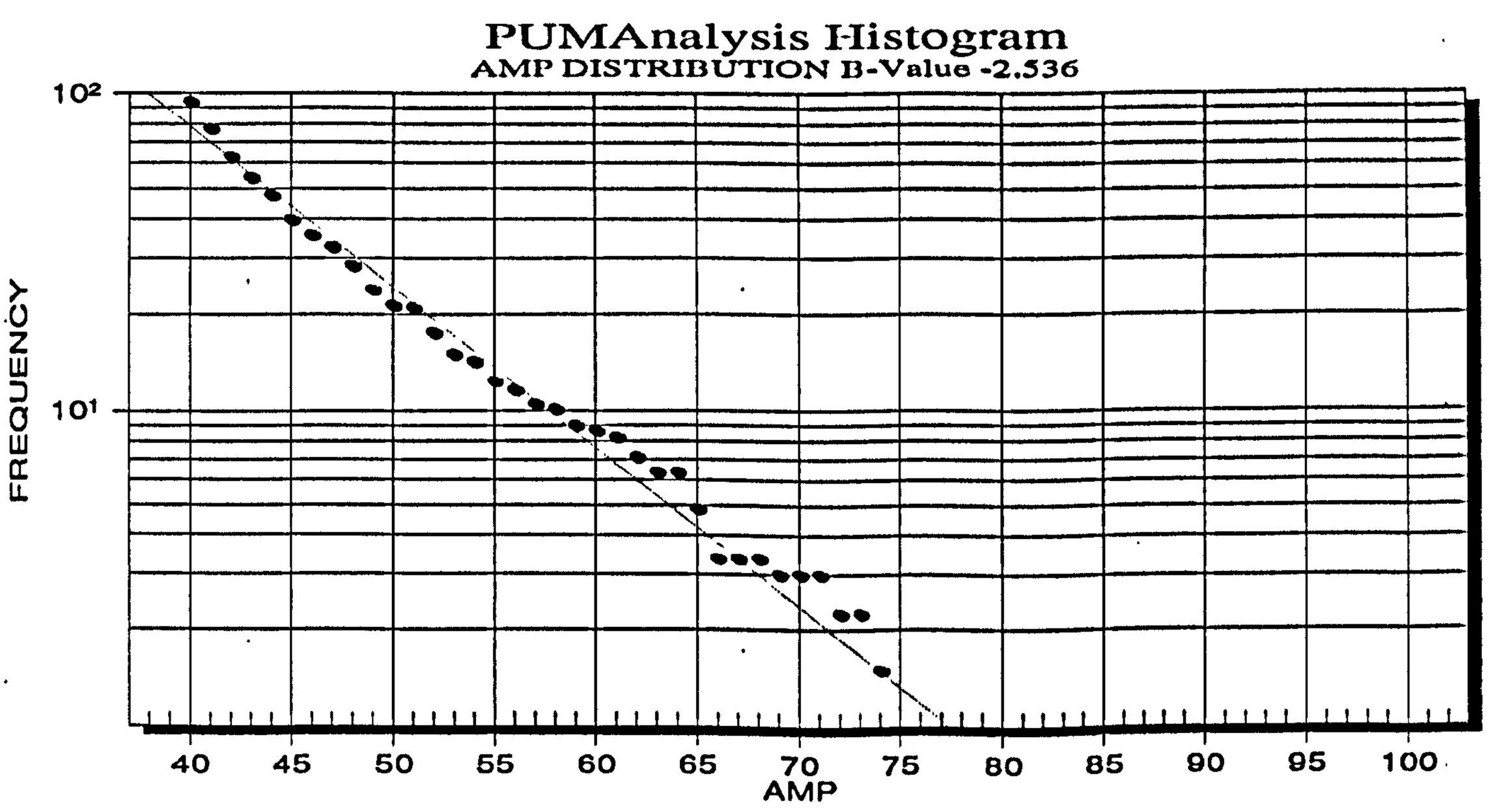

Graph 4.7: Software computation of β value at 7.5 Te

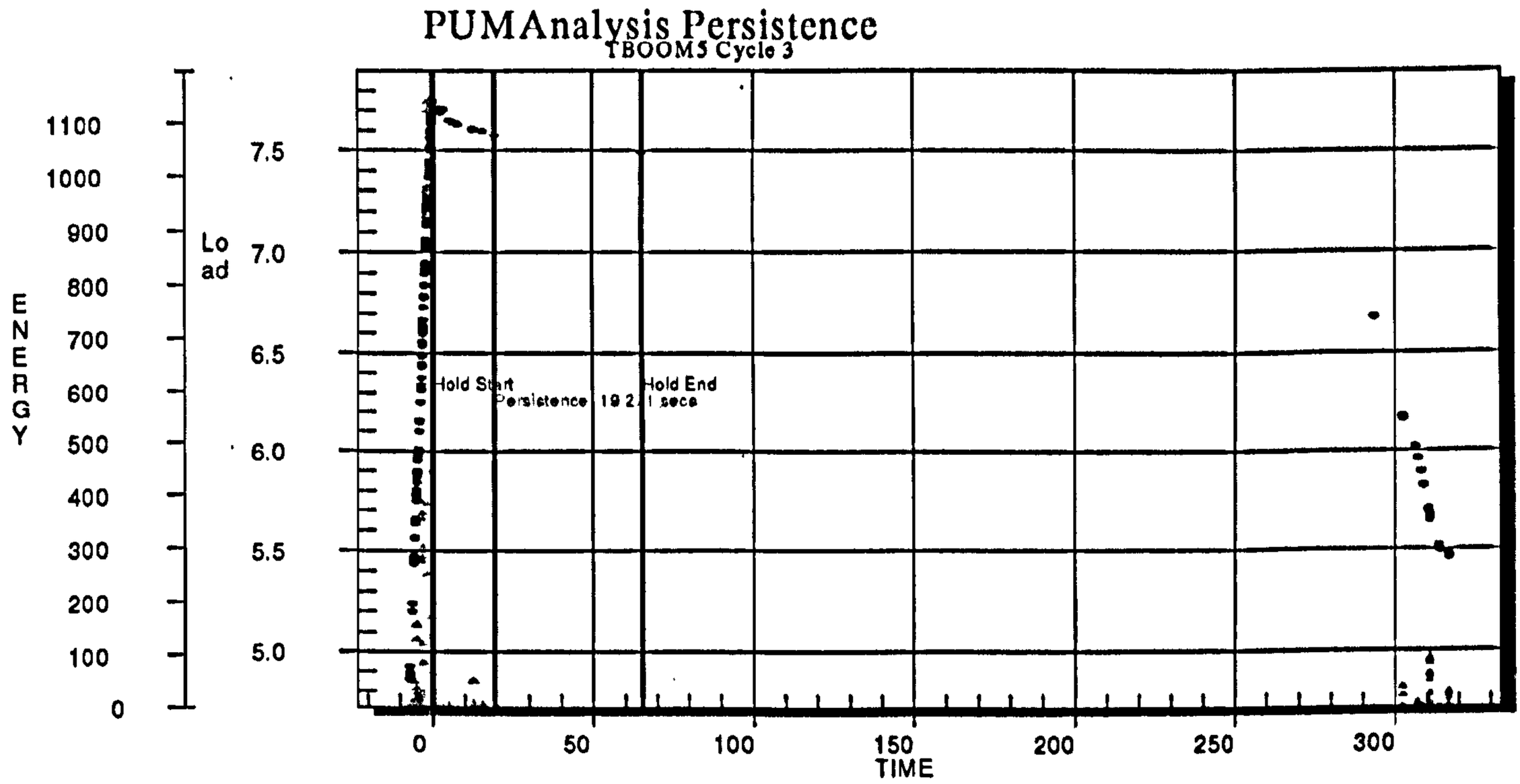

Graph 4.8: Software computation of Persistence at 7.5 Te

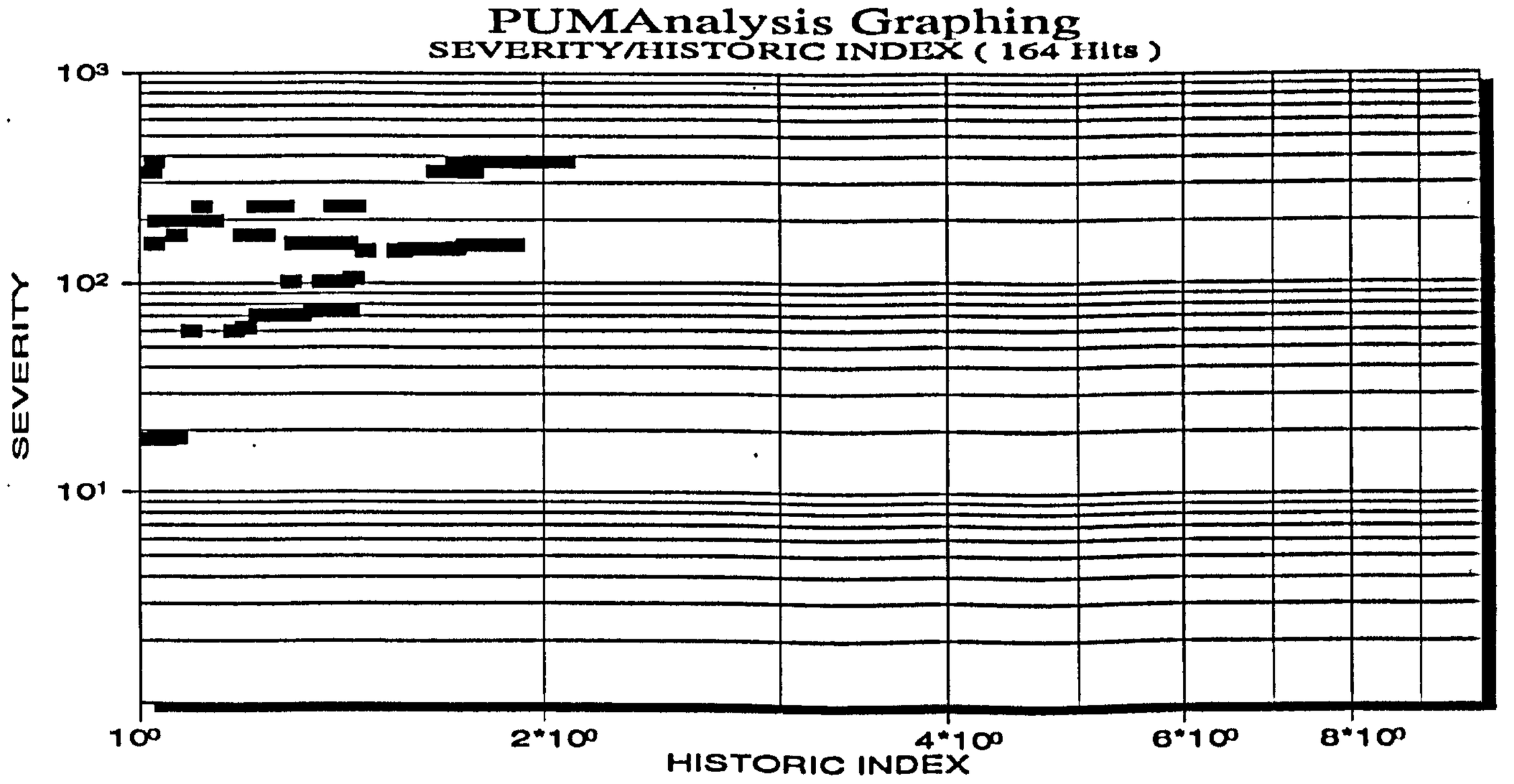

Graph 4.9: Software computation of Intensity Analysis at 7.5 Te

	2.5 Te	5 Te	7.5 Te	10 Te
Felicity Ratio	0.93	0.86	0.97	0.57
Persistence	81.76	4.05	19.27	39.41
β value	-3.13	-2.98	-2.54	-3.43
Intensity Ch. 6	C	C	D	E

Table 4.2: Outputs of Evaluation Criterions at each stepped Load increment

All evaluation show largely that they could be used as a means of trending or assessing the severity of degradation, but all with the exception of the intensity analysis have an anomaly at one of the load increments. The Felicity Ratio at the 7.5 Te load level shows 0.97 when in theory it should have reduced to less than 0.86. Persistence shows a progressive rate of degradation at the upper levels of loading, but took a long period to stabilise on the initial load application. The β values approaches zero with increasing loading as might be anticipated, but at the peak load reverts back to the most negative number experienced during the test. Intensity analysis is the only evaluation criterion that demonstrated a sequential trend towards failure. It was additionally found to be repeatable on other channels of interest, suggesting that this would be the most effective means of assessing defect severity.

4.4.3 (f) Conclusion

One objective of this investigation was to observe the load level at which evidence of the failure site would become apparent. This would illustrate what factor of safety could be given by an AE indication. Some events were source located at the initial load level at the site of failure, but it is important to realise that the structure did not fail and therefore the factors of safety are greater than four.

It has been successfully shown that the conjunction of periodic proof testing and AE would enhance the quality of the information of crane boom integrity. This is true of both a qualitative assessment where it is required to merely identify the presence of an integrity threatening flaw, but this work has also illustrated that quantitative assessment of the defect severity is also possible. Of the four differing evaluation criterions explored the intensity analysis method performed most effectively, although all methods of evaluation showed some ability to trend a defect's increasing severity.

4.5 Under water vehicle

4.5.1 Introduction

The final case study investigates the use of acoustic emission, Alternating Current Potential Drop, and Time of Flight Diffraction for the assessment of structural integrity of underwater vehicles. This work was undertaken with a view to employing a permanently installed condition monitoring instrument on board the hull of remotely operated underwater vehicle. (ROV)

The trial was designed to exercise the structure in the manner of its normal operation whilst monitoring AE. A model of a typical vehicle hull with previously induced integrity threatening defects was subjected to static and dynamic tests with a view to growing the defects and observing the AE associated with that growth.

Three complementary technologies were used during the trials: Acoustic Emission (AE), Alternating Current Potential Drop (ACPD) and Time Of Flight Diffraction (ToFD). Both ACPD and ToFD provide a means by which a crack's dimensions can be physically measured. ACPD measures the drop in potential difference across the crack faces hence can ascertain the crack depth and TOFD is a hybrid ultrasonic technique. Using these three technologies in conjunction permits the AE to be used as a screening technique that can identify sites of particular interest and the subsequent use of ACPD and TOFD allows defect sizing, which can then be used for modelling and evaluative purposes.

This section will present the results and data analysis of these tests, illustrating the detection of fatigue crack growth at two sites and the confirmation of the detected sites by all three techniques.

The tests were conducted on a model that was identical to the material and fabrication processes used during the fabrication of a ROV. The model was subjected to both static and dynamic tests whilst the structural performance was assessed by AE.

4.5.2 Experimental objectives

The intention of the programme was to grow inherent fatigue cracks in the model and to confirm that the detected AE activity could be verified by physical measurement using other techniques. The AE and ACPD were measured continuously and TOFD was measured pre and post the test.

4.5.3 Experimental set up

Trials were conducted in a simulation chamber, figure 4.6, where the model was subjected to both static and dynamic tests whilst the structural performance was assessed. The static test replicated an evolution to maximum anticipated depth pressure whilst the dynamic tests replicated seventy excursions to the maximum depth and return to surface dives with an equivalent straining rate as might be experienced in service. During

previous material property trials on the model, fatigue cracks had both been initiated and propagated. The applied loadings were selected to enable crack growth.

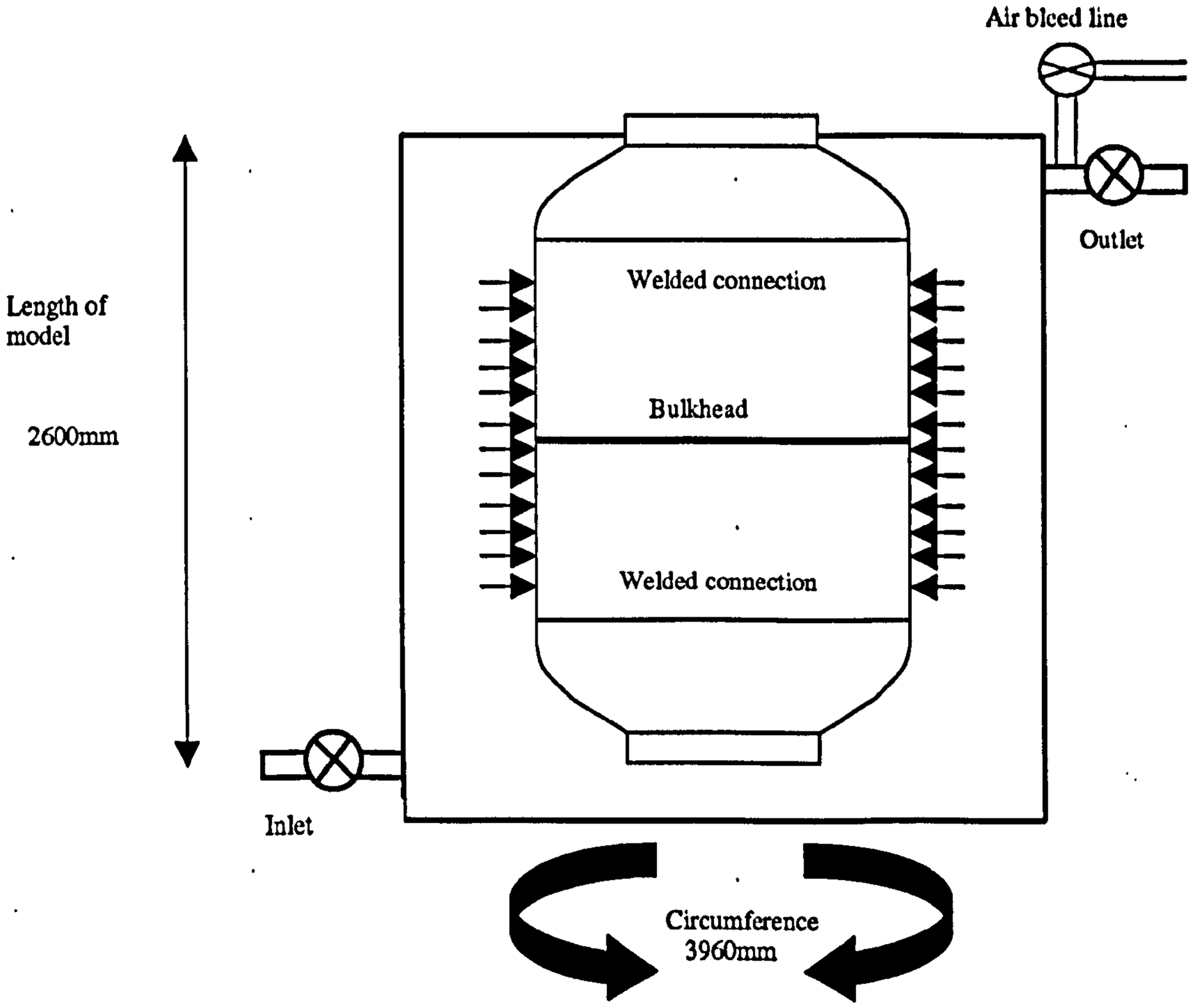

Figure 4.6: Physical test set up

Figure 4.6 illustrates the general configuration of the model whilst situated within the pressure rig. Internally the model is at atmospheric pressure and the excitation pressure is applied to the outside of the vessel. The sites of known fatigue cracks were around the upper circumference of the bulkhead. There were five in total. The crack sites were located at the change in direction where the cylinder is welded to the bulkhead, the bulkhead being representative of one of the frames that are located within the hull.

Crack behaviour

This particular configuration gives rise to a crack behaviour that gapes whilst in an unloaded state and closes at the peak excitations of the applied pressure. In terms of the hulls behaviour whilst at the greatest depth there is the least chance of leakage. The growth is most likely to occur on a depressurisation cycle whilst the crack faces are subjected to a tension-tension condition. Figure 4.7 explains this.

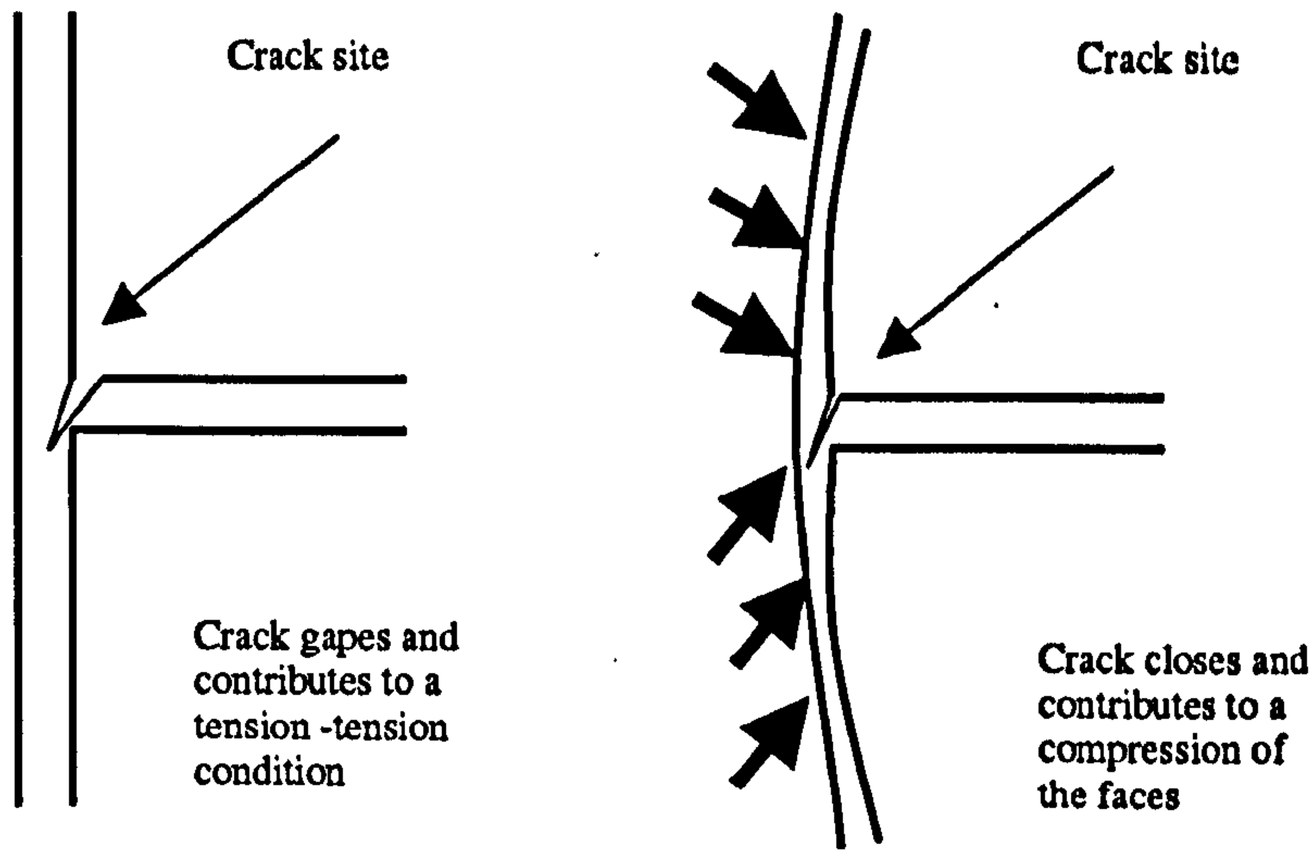

Figure 4.7: Anticipated crack behaviour

Sensor set up

Sensors were deployed in four arrays circumferentially around the vessel. Purposefully the two outer arrays were placed out with the dome welded connections to ensure that detectability was achieved through the welded connections. Each array was stepped by 45° at vertical intervals, giving an offset that lent itself to the creation a planar area segregated into triangles. This assists in one of the notable functions of AE, its ability to source locate by triangulating the source. Both figures 4.9 and 4.10 assist in the explanation of the sensor set up.

The ACPD probes were placed astride of the cracks, which as previously described were located circumferentially around the upper part of the bulkhead.

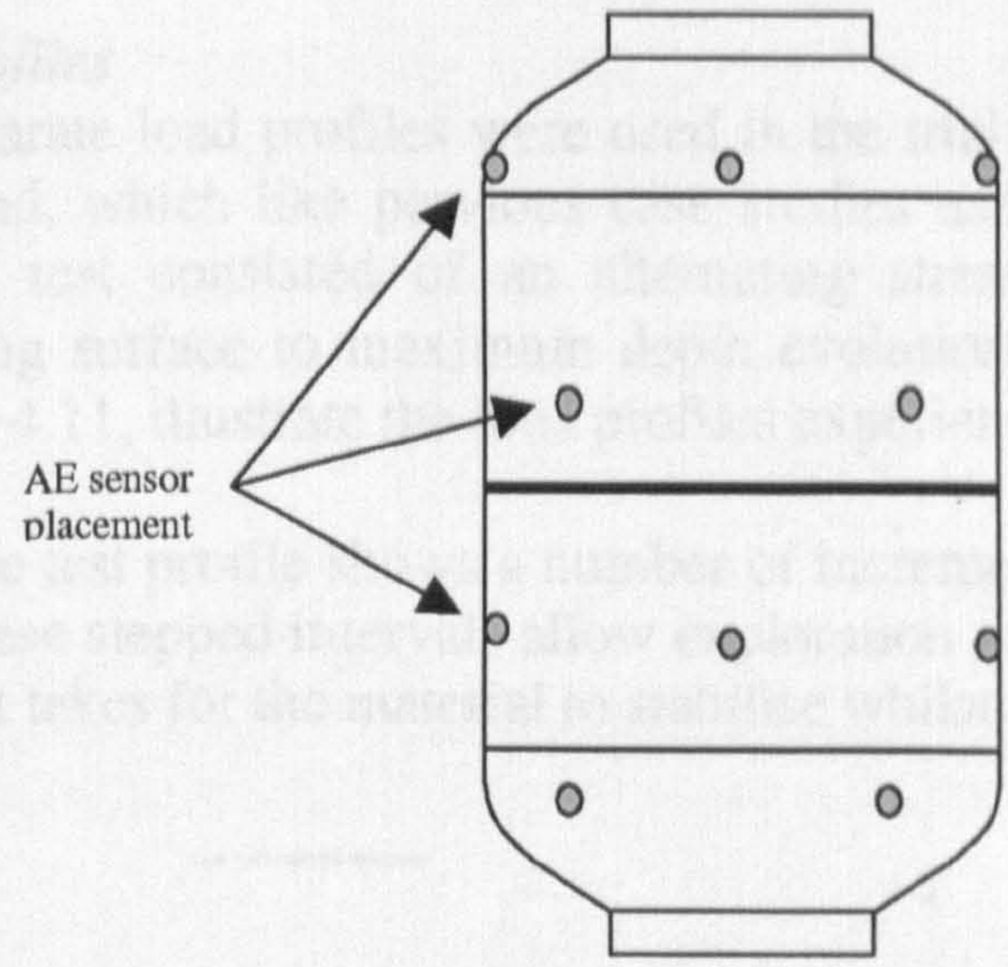

Figure 4.8: Sensor placement

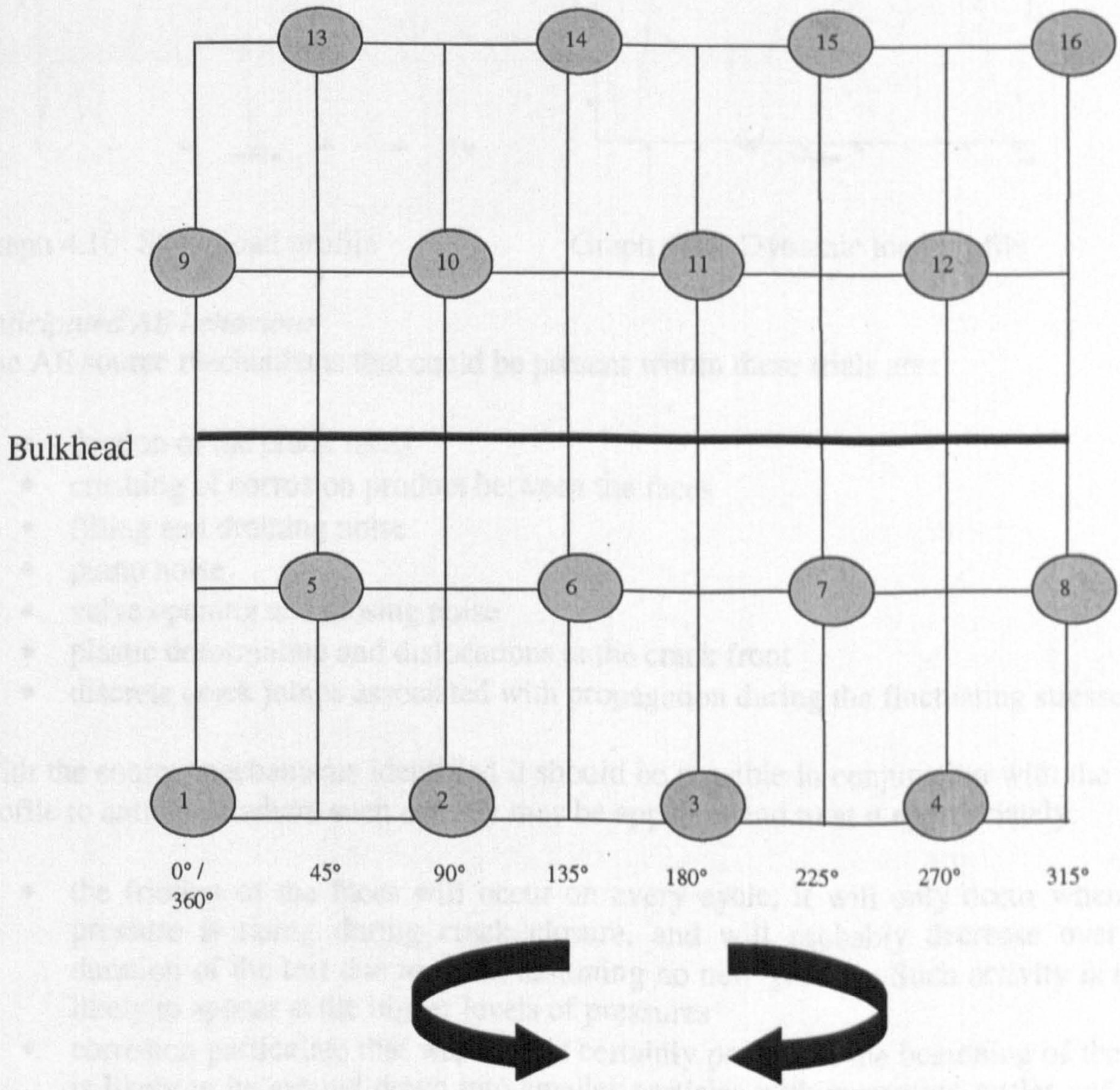

Figure 4.9: Sensor set up

Load profiles

Two separate load profiles were used in the trial. Initially the model was subjected to a static load, which like pervious case studies uses increments up to the maximum. The dynamic test consisted of an alternating stress cycle of constant amplitude fatigue replicating surface to maximum depth evolutions. The two subsequent graphs, graphs 4.10 and 4.11, illustrate the load profiles experienced by the model.

The static test profile shows a number of incremental rises up to the peak pressure of 145 Bar. These stepped intervals allow exploration of both the Felicity effect and the amount of time it takes for the material to stabilise whilst subjected to a sustained constant load.

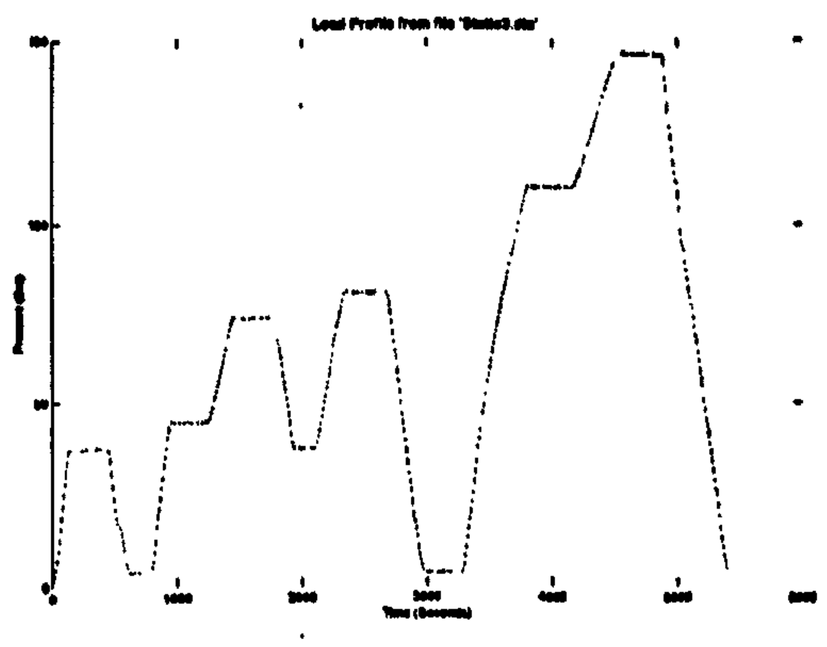

Graph 4.10: Static load profile

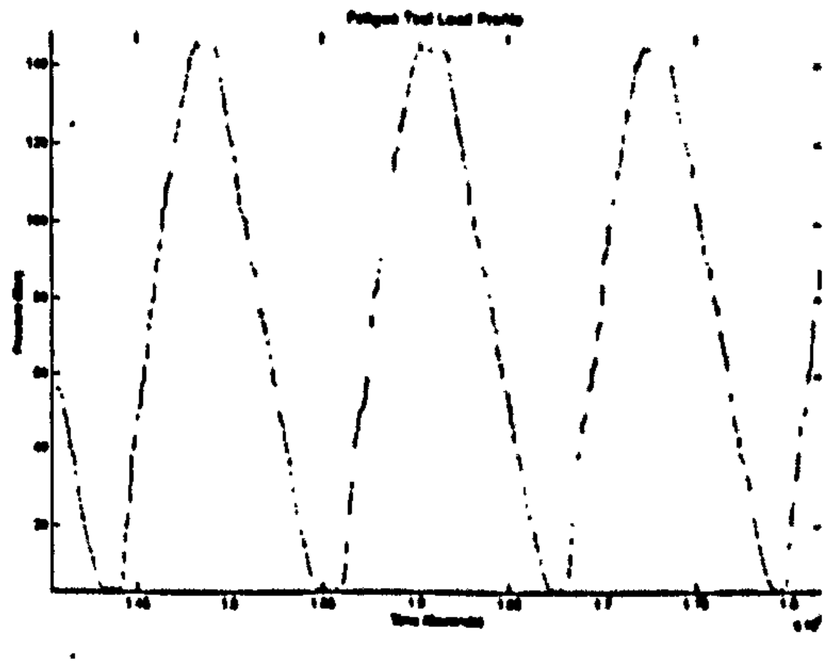

Graph 4.11: Dynamic load profile

Anticipated AE behaviour

The AE source mechanisms that could be present within these trials are:

- friction of the crack faces
- crushing of corrosion product between the faces
- filling and draining noise
- pump noise
- valve opening and closing noise
- plastic deformation and dislocations at the crack front
- discrete crack jumps associated with propagation during the fluctuating stresses.

With the source mechanisms identified it should be possible in conjunction with the load profile to anticipate where such activity may be apparent and treat it appropriately:

- the friction of the faces will occur on every cycle; it will only occur when the pressure is rising during crack closure, and will probably decrease over the duration of the test due to wear, assuming no new growth. Such activity is most likely to appear at the higher levels of pressures
- corrosion particulate that was almost certainly present at the beginning of the test is likely to be ground down into smaller particles with increasing cycles and that

will also occur only on the rising pressure cycle i.e. closure. Again, this is likely to decrease with increasing cycles, due to the particles becoming finer

- fill and drain noise will appear on the rising and falling load respectively and can be considered constant
- pump noise, will appear on the rising load and is likely to be constant
- the valve operations are likely to not only be of a constant magnitude, but are likely to occur at the point at directional changes of the load, predominately on the falling pressure as the valve has to be opened manually to control the rate of the depressurisation
- plastic deformation and dislocations are only likely to occur in the event of new growth, this is most likely to occur on the falling pressure cycle, particularly at the base of the cycle where the maximum tensile stresses are experienced at the crack
- discrete crack jumps are likely to occur during the crack gaping at peak excitation i.e. during the falling load and particularly at the base of the cycle

From these assumptions we can conclude that the regions of the cycle that are of most interest are during falling pressure particularly the zero load condition, because it is at this point that the crack experiences its maximum stress condition.

4.5.4 Results

4.5.4 (a) Static test

The results of the full static test are presented below in graph 4.12.

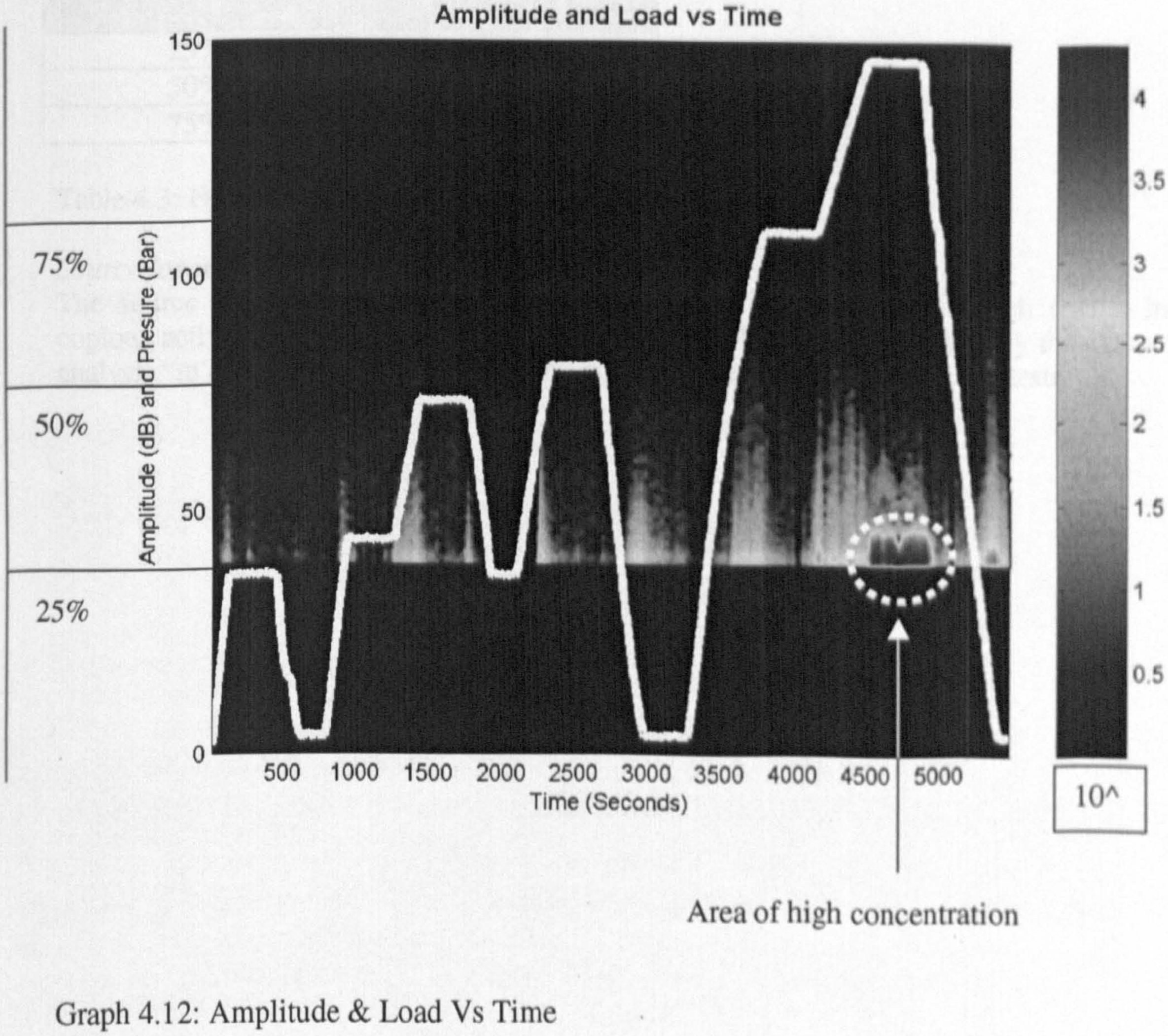

Graph 4.12: Amplitude & Load Vs Time

The applied pressure is shown in graph 4.12 as a white line with marked percentages of the full load condition. The AE is denoted by contour intensity plot. The legend is logarithmic and depicts the quantity of hits that occur at the amplitude value per unit time. Focussing on the high density of AE depicted by the dotted circle at the peak load, there are an extremely high number of hits of low amplitude coincident with the maximum pressure. This can be explained as leakage, the identification of the leakage will be explained in a subsequent section. Firstly, we will examine the materially related AE.

Conventional AE analysis focuses much of its attention on the presence or absence of emission i.e. the Kaiser and Felicity effect. Each percentage step is designed to examine the onset of AE. In the following cases it is clear that there is a defect, however at the uppermost load step the Felicity ratio reduces contrary to anticipated behaviour. Table 4.3 details the Felicity Ratio values.

Load step	Felicity Ratio
25%	0.77
50%	0.78
75%	0.07

Table 4.3: Felicity ratios for load steps

Source location

The source location was masked by the leak during the static test, which results in copious activity on the right hand side of the vessel. The sources marked by the cluster analysis "m & o", graph 4.13, become more pronounced during the dynamic tests.

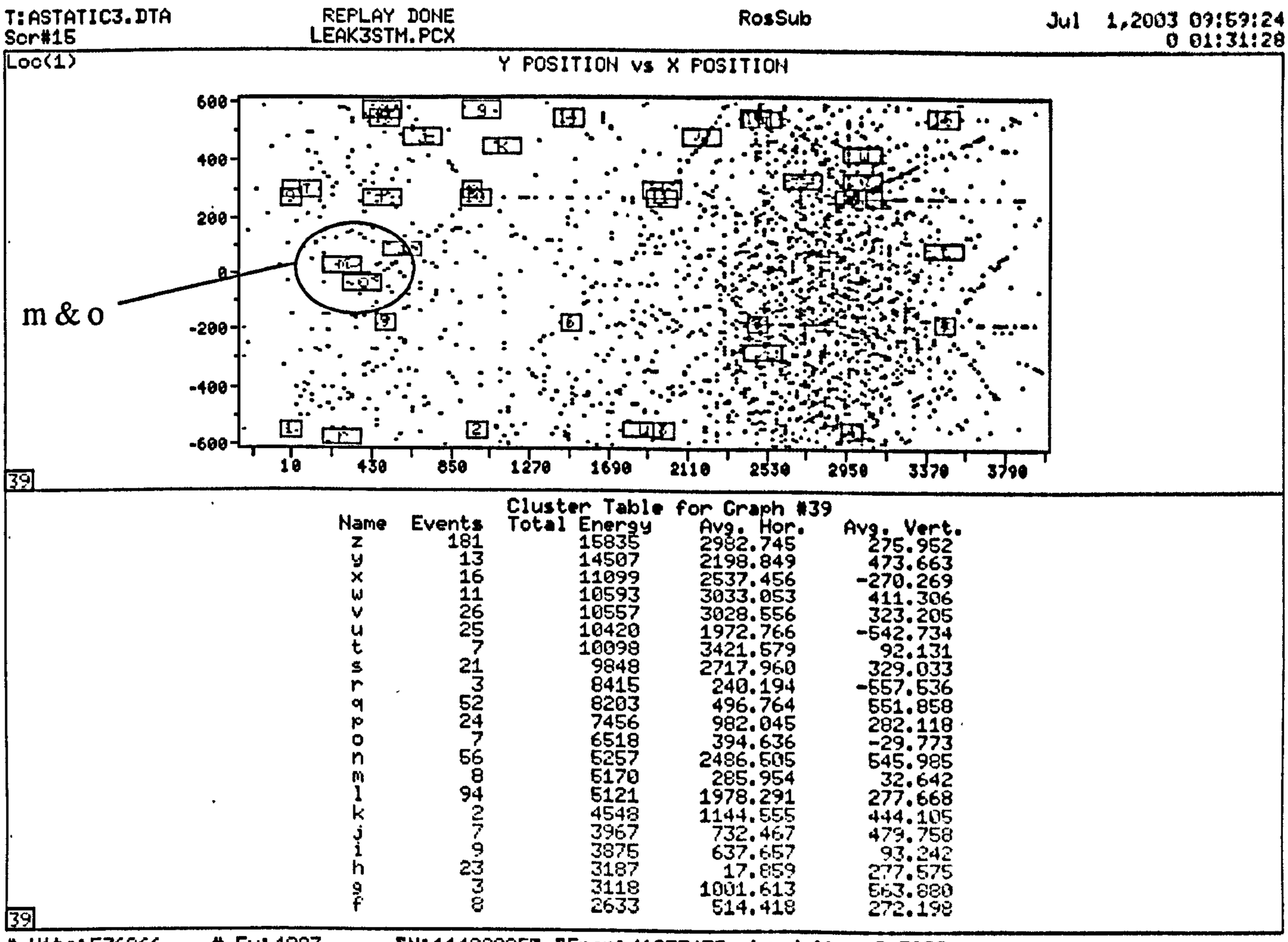

Graph 4.13: Source location for the static test

Identification of leak

During the static test, at the peak pressure, there occurred copious quantities of AE. The arrival of large quantities of AE is more often than not attributable to either imminent failure or leakage during pressure testing. During the set up for the dynamic test a small seepage was observed on the top hatch of the model. With further investigation it was found that a threaded fitting in the upper part of the rig had stripped and had been the cause of leakage.

Graph 4.14 illustrates the difference in the pattern of AE generated from different source mechanisms. The leakage occurred at the top of the maximum pressure cycle. The three lower graphs show the entire AE history depicted on three counts versus amplitude graphs. The dashed vertical lines on the upper load profile graph divide the test into three equi-spaced time intervals and the three counts versus amplitude graphs display the activity within such periods. The materially generated AE is observable in the first two graphs, which appears as lighter concentrations at the base of the graphs. The third graph

shows two very distinctive vertical lines, suggesting reasonably low amplitude hits with a high number of counts. Chapter two discussed in the case of interpretation of data from rail road tank cars, leakage can be characterised by this particular pattern of the low amplitude hits with a high number of counts. The inclusion of this section in this work has been to illustrate that AE can be used as a means to differentiate between different source mechanisms.

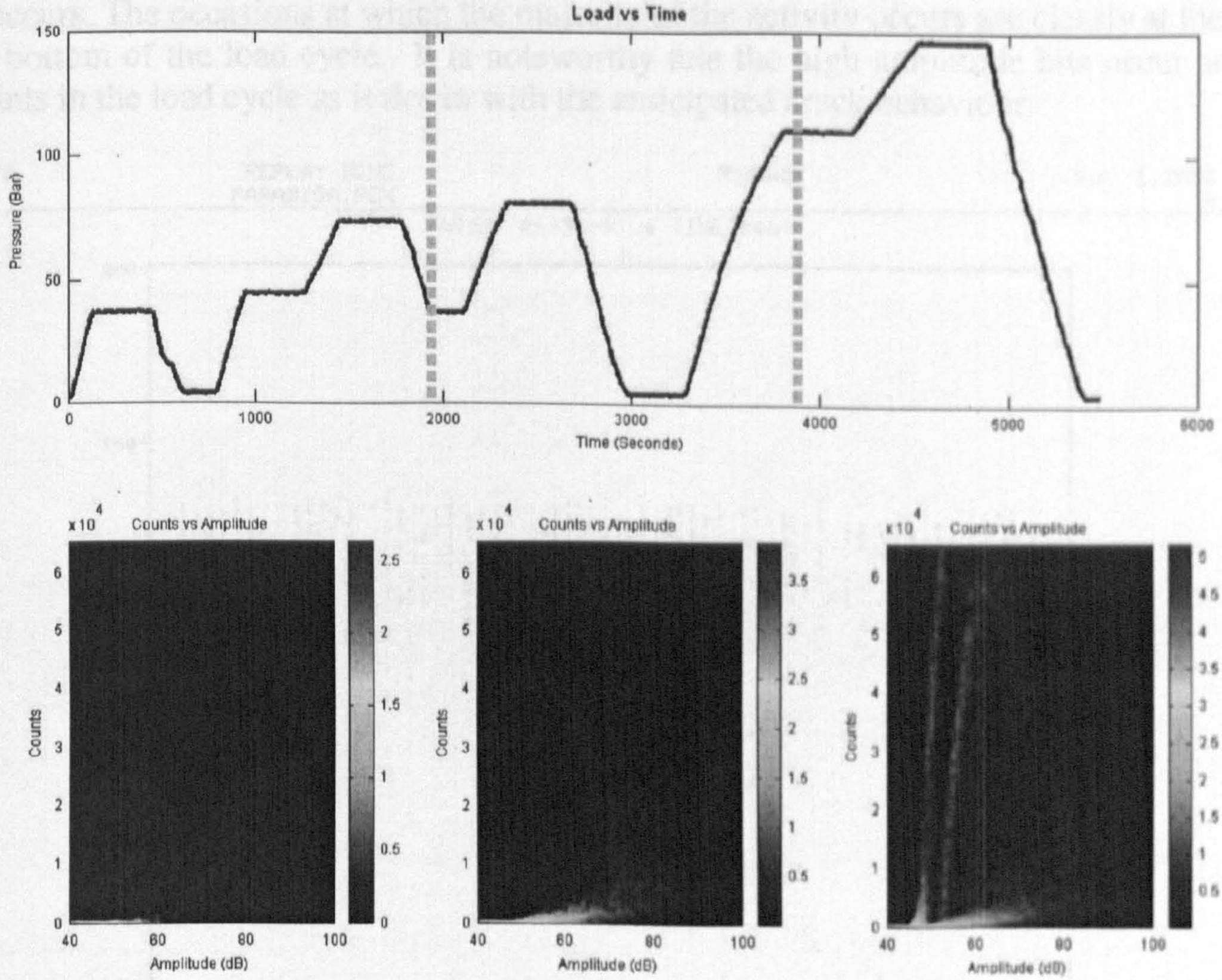

Graph 4.14: The difference in AE generated by a leak

4.5.4 (b) Dynamic test

Each pressurisation cycle took approximately 17 minutes during the dynamic test. The volume of the data capture proved almost unmanageable and the results presented here are representative of the filtered data of only hits that exceed Amplitudes of 80 dB.

Examining a special type of load graph, graph 4.15 that plots a load point only when an AE hit occurs. The occasions at which the majority of the activity occurs are clearly at the top and bottom of the load cycle. It is noteworthy that the high amplitude hits occur at such points in the load cycle as it ties in with the anticipated crack behaviour.

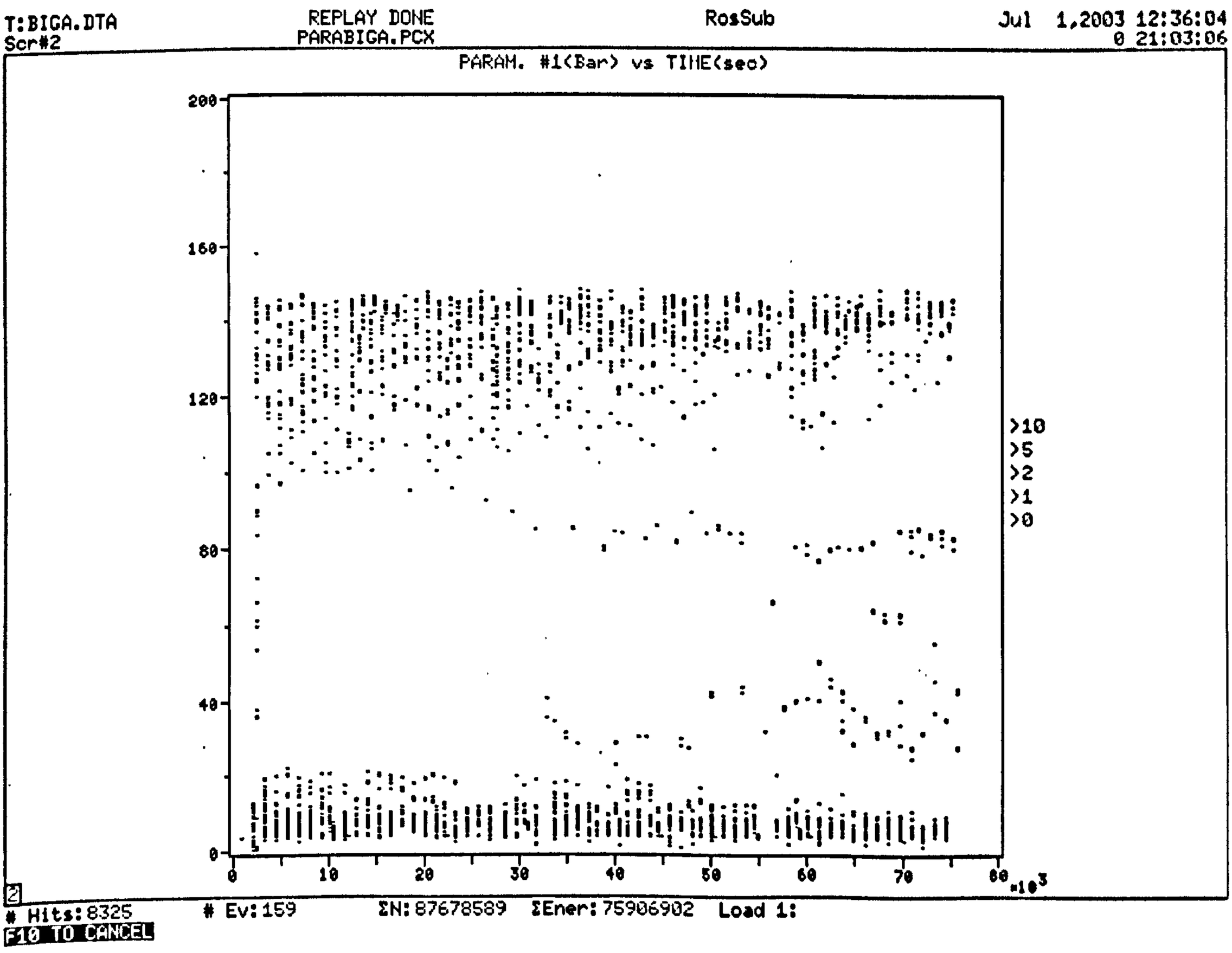

Graph 4.15: Hit occurrence load graph

Examining a few cycles in detail illustrates more specifically the behaviour we might anticipate, graph 4.16. The high amplitude hits appear at the tops and bottoms of the cycles, highlighted by the asterisks superimposed on the load profile which is shown as a solid line.

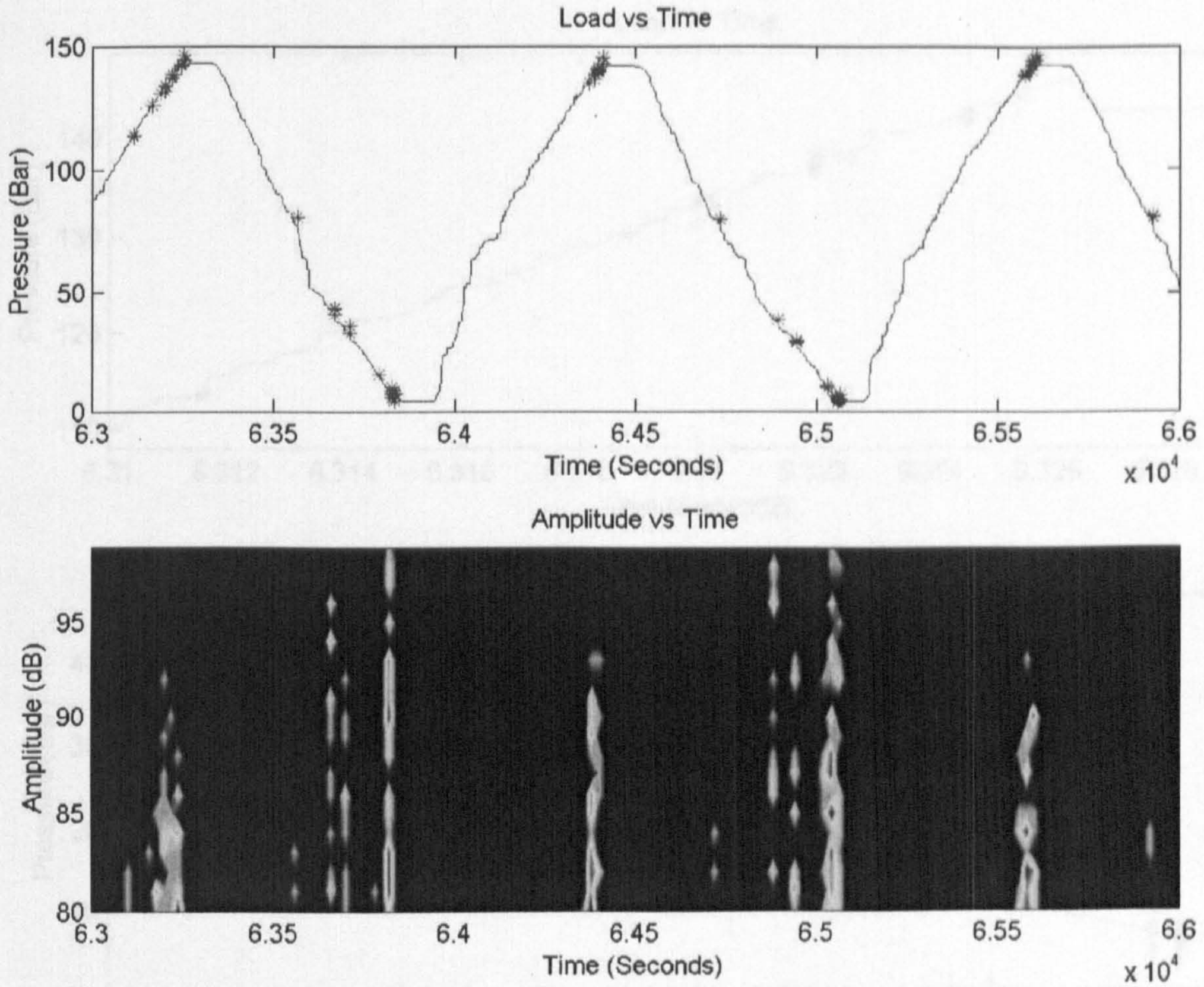

Graph 4.16: Load profile with hits superimposed and the Amplitude intensity

The Amplitude at the top of the cycle is considerably less than the Amplitudes at the base of the cycle. This ties in with anticipated crack behaviour. The coincidence of the hits at the exact points of the change in direction of the load cycle might make one suspicious as to the source mechanism, perhaps all of the hits are associated with the solenoid valve motion. This was further investigated by focussing in further at the very local point of the change in direction of the load cycle. The results of this are shown in graph 4.17.

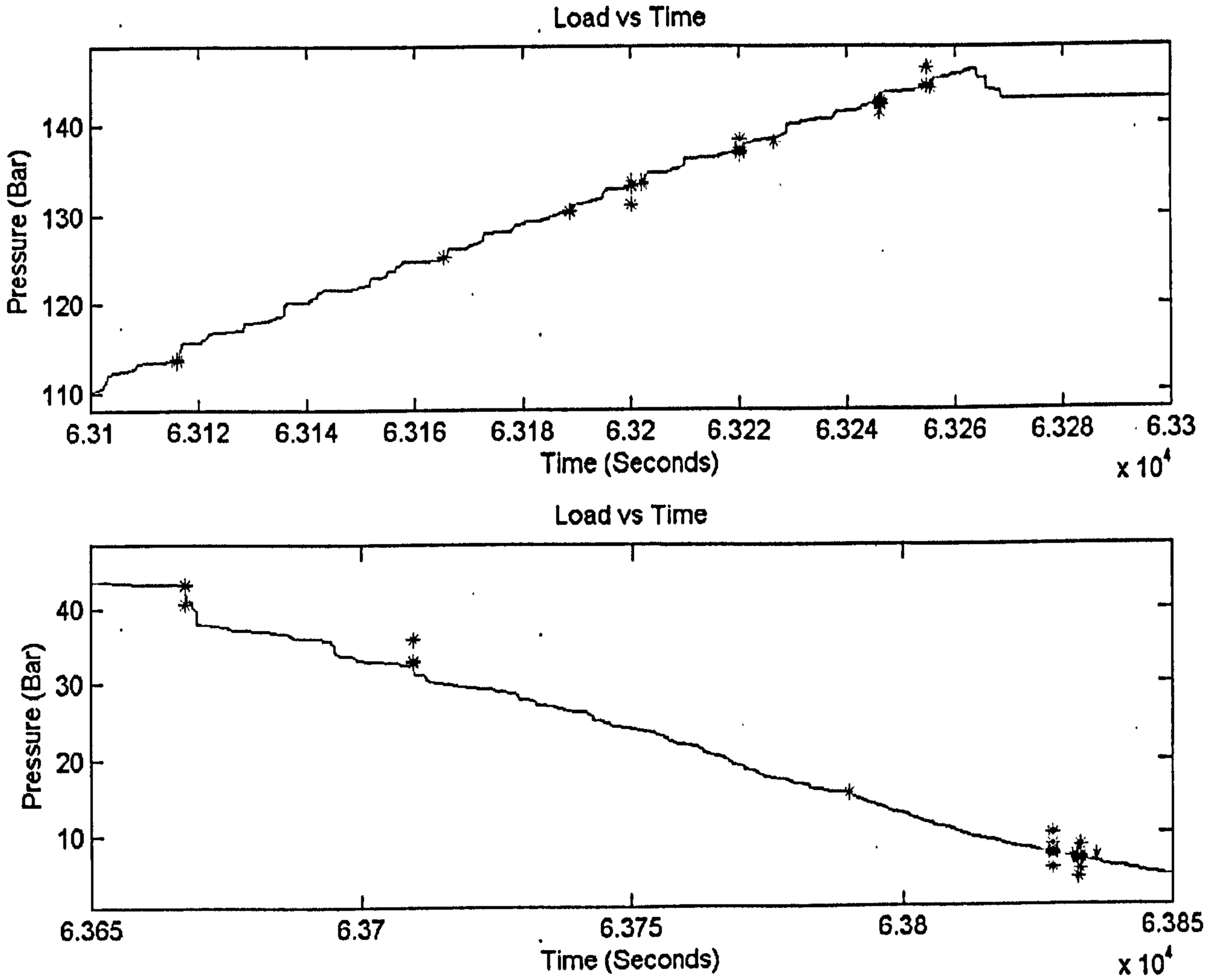

Graph 4.17: Load profiles at the changes in pressure over 200 second period

These graphs show the change in direction of the load profile over a 200 second period, the hits are generated throughout the period as opposed to at a single instance, thereby negating the hits being associated with a noise such as the solenoid valve. This was investigated and the mechanical operations of the valves are such that during the pressurisation sequence the valve is closed, but during the depressuriation the rate is controlled manually and as such may give rise to periodic noise.

Viewing the location plot for all of the filtered high amplitude hits, the result is shown in graph 4.18.

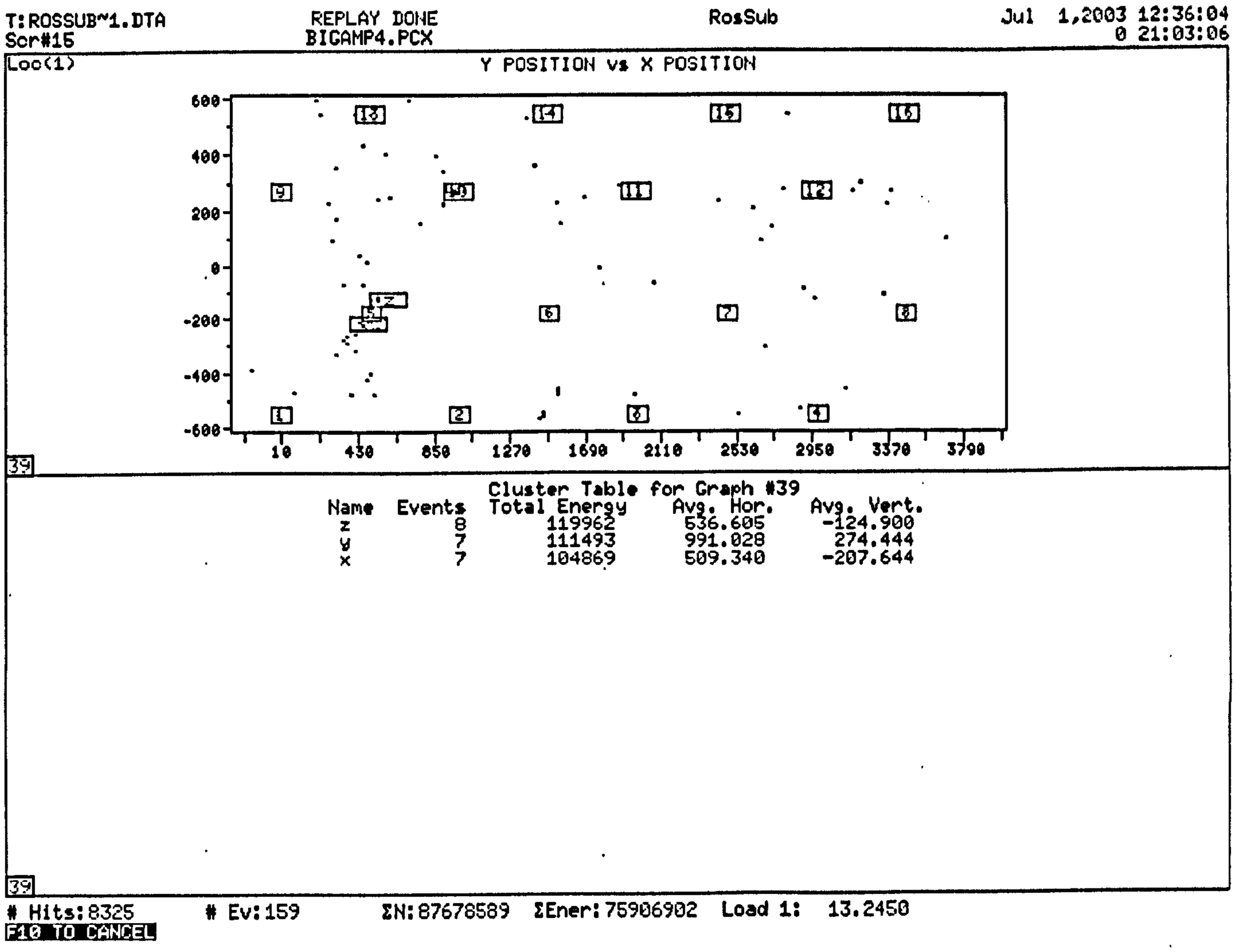

Graph 4.18: Location graph for the high amplitude hits with cluster analysis

There are three specific sites that have been identified by cluster analysis as regions that have an area less than 5% of the surface area covered by the sensors and as having energy of greater than 100,000 and amplitudes greater than 80dB. Two of which are in close proximity to sensor number 5, which is below the bulkhead and at approximately 45^0 around the circumference. The third cluster is beside sensor 10, which is above the bulkhead at approximately 90^0. The bulkhead in the location graph was used as the reference and is located as zero on the Y-axis, so in the both instances of site determination the indications are shown either higher or lower than the crack's physical position.

4.5.4 (c) Results of the ACPD and TOFD

ACPD Results

Prior to the trial, the model was subjected to non-destructive examination to confirm the status of five possible sites of fatigue cracking. During previous fatigue testing semi-

elliptical notches had been machined into the pressure hull along the weld toe at five locations and fatigue cracks had been grown from these notches under the applied loading. To determine if crack propagation was occurring during the fatigue test phase of the trial, crack monitoring in the form of 'on-line' ACPD was installed across the centre of each notch. The measured depth (crack and notch) and surface length of the notches pre and post the trial is given in table 4.4.

Monitoring site from crown posn.	10 Degrees	90 Degrees	164 Degrees	225 Degrees	270 Degrees
Surface notch length	117mm	134mm	95mm	105mm	95mm
Baseline ultrasonic ToFD and corrected ACPD crack depth	15.5mm	17.9mm	10.7mm	13.6mm	13.6mm
ACPD indicated amount of crack closure	2.1mm	1.3mm	0.3mm	2.1mm	0.7mm
Final ACPD crack depth	16.4mm	18.5mm	10.8mm	13.6mm	13.5mm
Indicated crack growth	0.9mm	0.6mm	0	0	0

Table 4.4: Indicated Growth

During the fatigue cycling ACPD readings from each potential crack site were recorded at the top and bottom ends of each cycle. This data was normalised and corrected to the ultrasonic ToFD measurements at the beginning of the trial. The ACPD crack depth measurement is based on the ratio of the potential dropped over a known, crack free, length of the steel (referred to as V_0) and the potential dropped over a known length of the steel containing the crack (referred to as V_1). The correction takes into account errors in the ACPD measurement due to the presence of the machined notch, which increases the length that 'V_1' is measured over by an unknown amount. An increasing 'V_1' measurement during the fatigue cycling indicates crack growth. The recorded trends in the measured 'V_1' values are shown in graph 4.19, while the normalised and corrected ACPD crack depth measurements are given in table 4.3. These indicate the following:

- at the beginning of the fatigue cycling crack closure (measurement recorded at 145bar) is evident and amounts for up to 2.1mm (Table 4.3). This progressively decreases as the fatigue cycling progresses, as shown by the increasing trend in the 'V_1' measurement of all monitoring sites in graph 4.19;
- crack growth (measurement recorded at 3bar) is evident in the increasing trend in the 'V_1' measurement from the monitoring sites at 10 and 90 degrees from the crown. The other three sites show no growth;
- the indicated crack growth at 10 and 90 degrees is 0.9 and 0.6mm respectively.

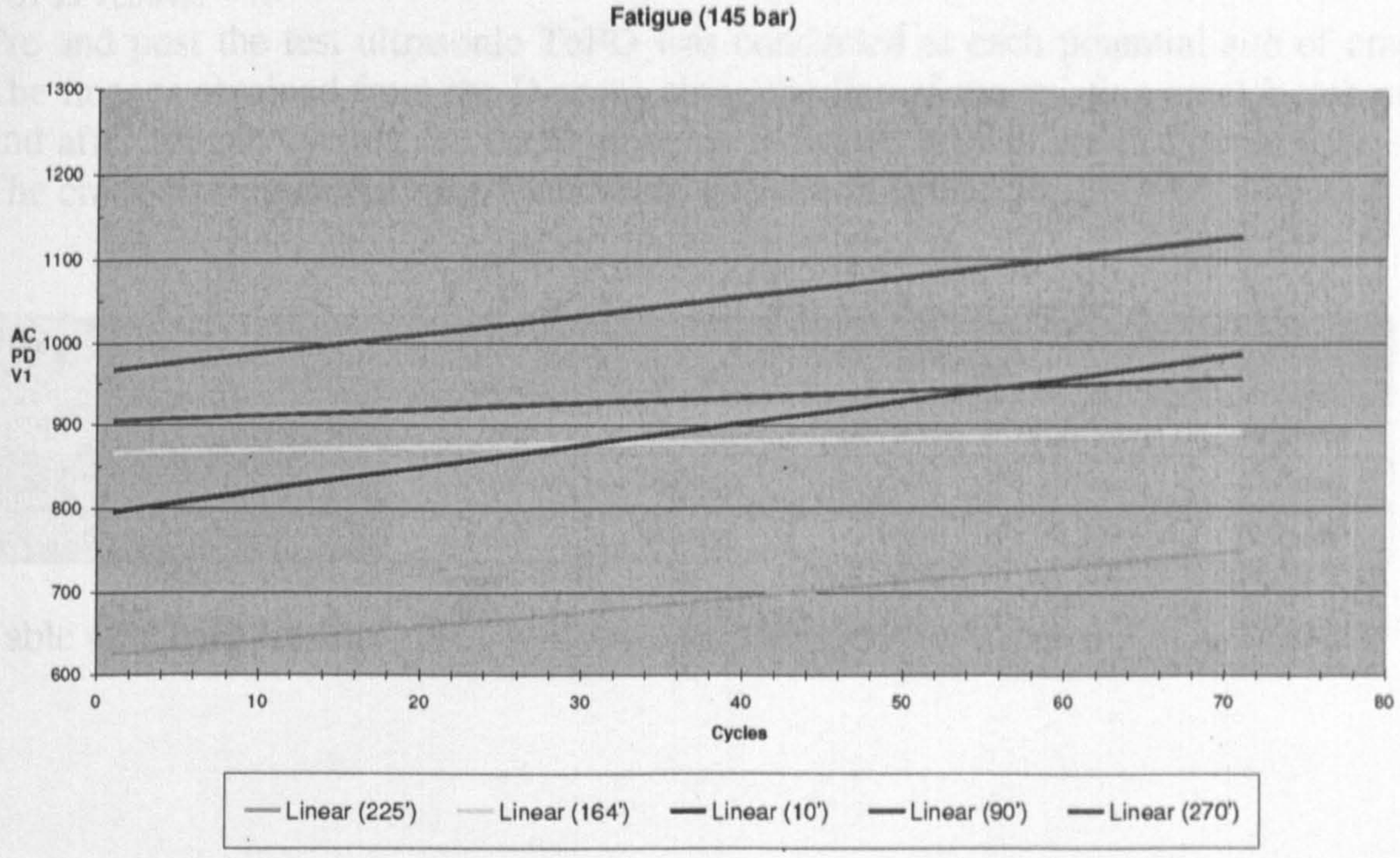

Graph 4.19: ACPD indications acquired during crack closure

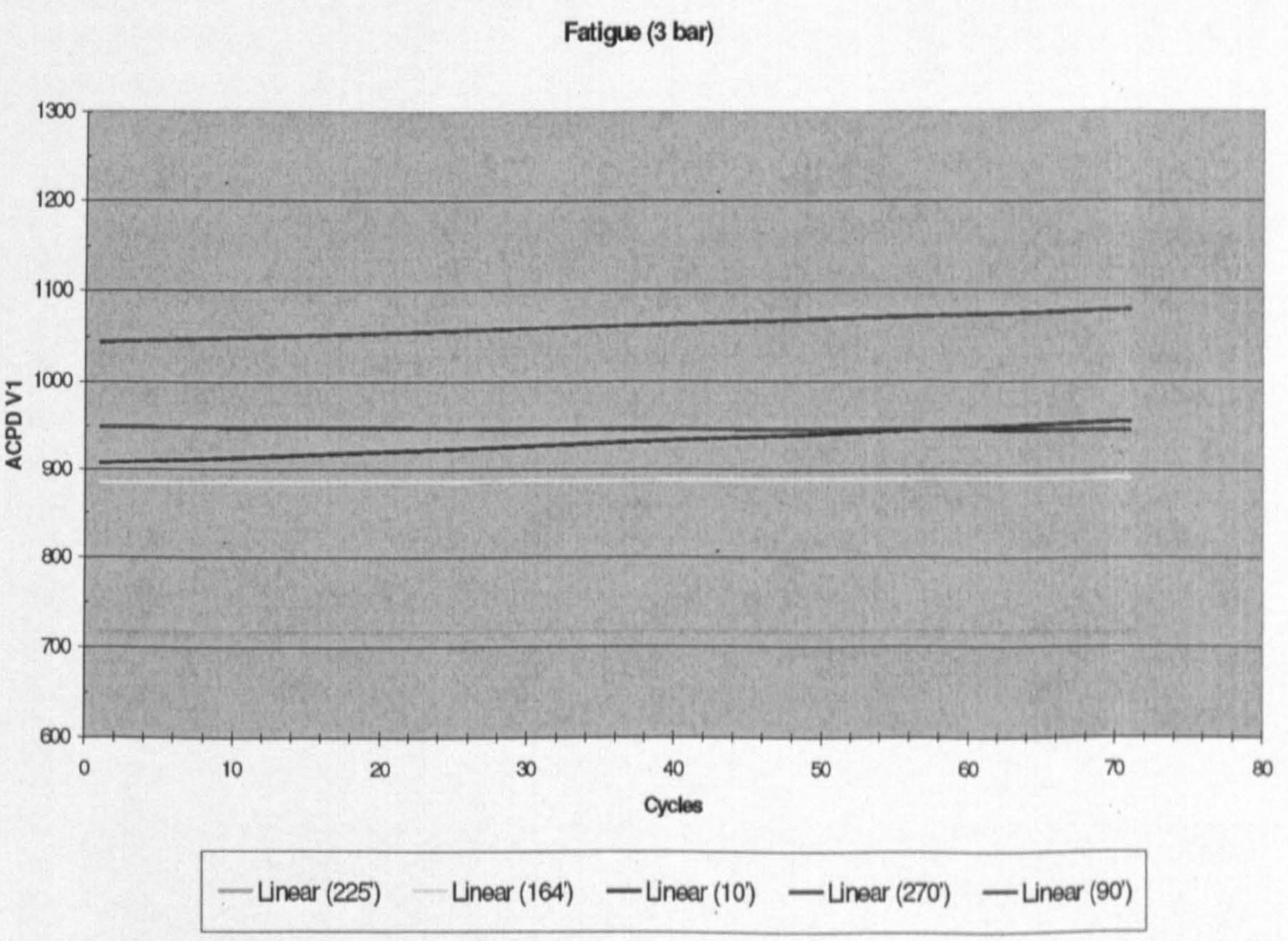

Graph 4.20: ACPD indication acquired during crack growth

ToFD results

Pre and post the test ultrasonic ToFD was conducted at each potential site of cracking. The images obtained from the D-scans along the line of the existing crack/notch prior to and after fatigue cycling are the cracks that indicated growth are in figures 4.21 – 4.22. The crack size measured from these scans is given in table 4.5.

Monitoring site from crown posn.	10 Degrees	90 Degrees	164 Degrees	225 Degrees	270 Degrees
Baseline ultrasonic ToFD	15.5mm	17.9mm	10.7mm	13.6mm	13.6mm
Final ultrasonic ToFD	16.1mm	18.4mm	10.6mm	13.5mm	13.8mm
Indicated crack growth	0.6mm	0.5mm	-0.1mm	-0.1mm	0.2mm

Table 4.5: ToFD results

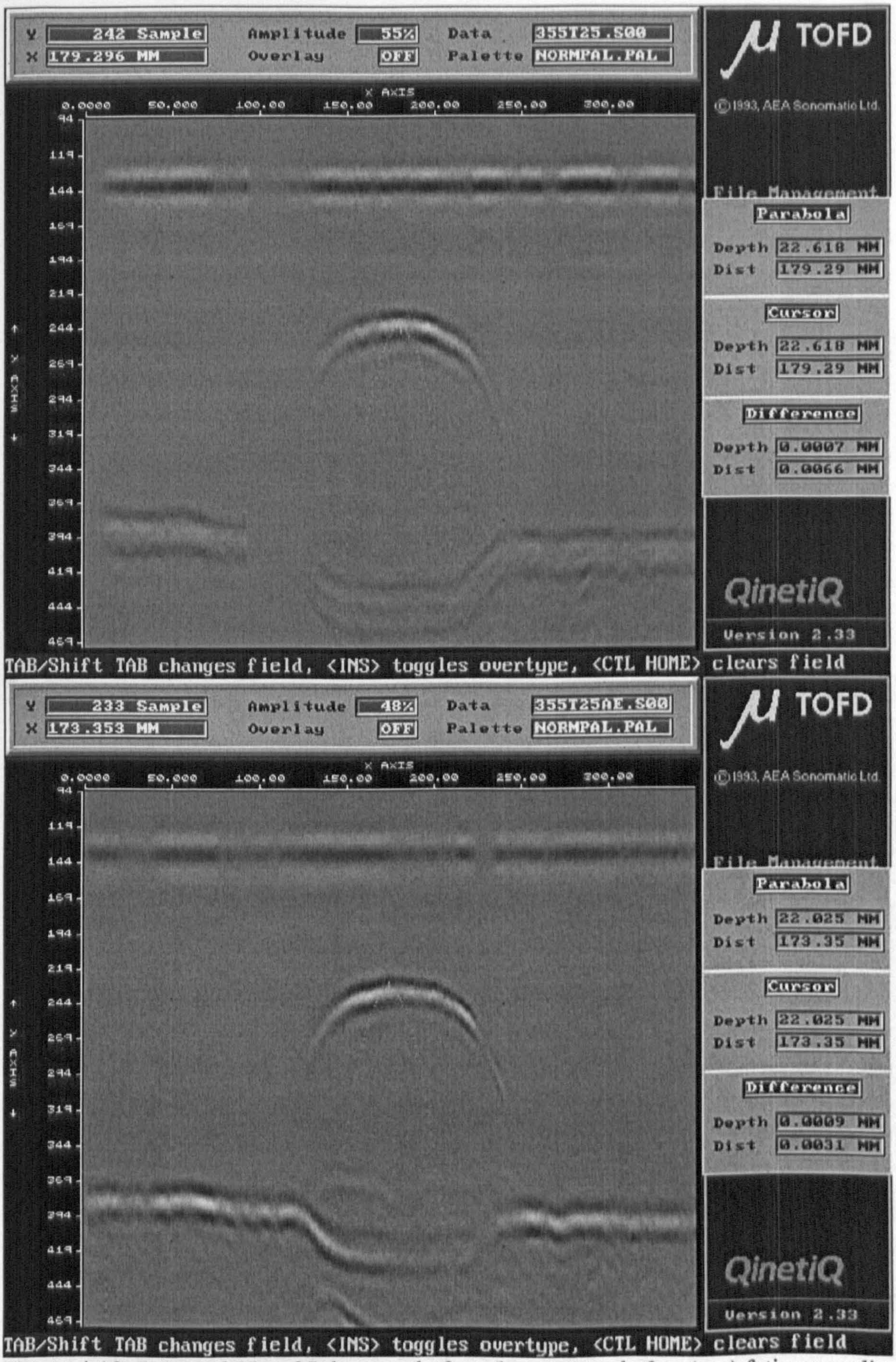

Figure 4.10: D-scan 355 to 25 degrees, before (bottom) and after (top) fatigue cycling

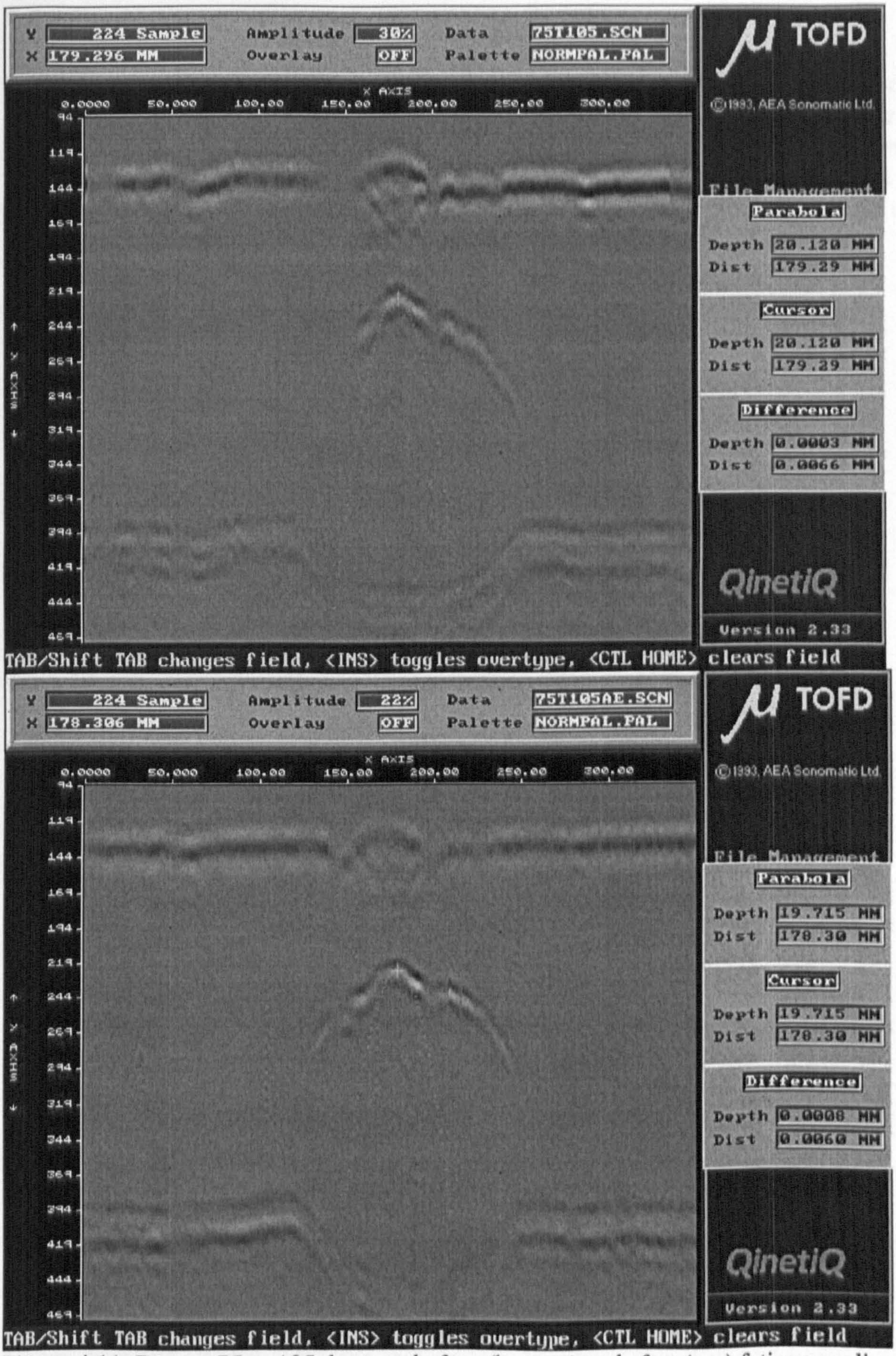

Figure 4.11: D-scan 75 to 105 degrees, before (bottom) and after (top) fatigue cycling

4.5.5 Conclusion

It is considered that the trials have yielded successful results in the detection of activity from the crack behaviours as the anticipated crack behaviour correlated well with the AE. When the data was rigorously filtered, meaningful information that could be used to identify the presence of cracks was obtained. When the AE is viewed in conjunction with ACPD results and the measurements attained with the ToFD it is clear that all three techniques have concluded that crack growth occurred at the sites of 10^0 and 90^0.

4.6 Chapter conclusion

Five case studies of AE operating in field trials as a means of defect detection have been described. These case studies have demonstrated that the use of AE in conjunction with a periodic proof test can be used as a means of defect detection within mechanical structures.

The use of AE in conjunction with periodic proof testing was illustrated in the cases of ten tests conducted on pad-eyes and nine overhead travelling cranes. It was apparent that the use of the Kaiser principle as opposed to the more traditional Kaiser effect might be more appropriate to the testing of equipment that endure stresses imposed by the sustaining a mechanical load. The reasons suggested for this is the difficulty in replicating an identical stress distribution in this type of testing arrangement.

The case study that focused on the hybrid pad-eye, the link plate demonstrated the use of AE as a means of detecting localised yielding in mechanical structures. This was substantiated by the simultaneous measurement of strain during incremental load increases to a proof load.

In the instance of the destruction test on the crane boom section it was observed with increases in applied load there was a corresponding increase in the acoustic activity at the sites of induced defects. The sites that ultimately constituted a "failure" were active at a quarter of the ultimate failure load, demonstrating indications could be given with a factor of safety of four. Further analysis of data, post test and exploration of previously utilised AE evaluative techniques illustrated that AE showed the promise of not only being qualitative but also quantitative. Of the four evaluative techniques tested, intensity analysis proved to generate the most applicable means of ascertaining defect severity in this particular application.

The final case study used three NDT techniques. Correlation was achieved between the active sites identified by AE with two other complimentary methods of measurement.

CHAPTER 5: Laboratory trials to investigate the feasibility of a through life trendable condition indicator

5.1 Chapter Introduction

The evidence described to this point to date supports that AE used in conjunction with periodical proof testing can identify flaws within a mechanical structure that will ultimately lead to failure. However it remains to investigate the robustness of the technique throughout the life of a mechanical structure. The objective of this part of the investigation is to identify if periodical measurement of AE taken during the course of the life will repetitively generate information pertaining to detection of the flaws. Additionally, the AE as a measure of the severity of the flaw as it initiates and propagates to failure is explored. It was considered that to produce empirical data from the field would take a great many years as typically a proof test is only applied incrementally at a frequency of multiple years. Therefore accelerated life tests were conducted to explore the feasibility of being able to forewarn of mechanical failure.

Specimens were subjected to three point bending constant amplitude fatigue until failure. Nominally identical specimens were subjected to the same fatigue loading, but their lifetimes were punctuated with proof tests. For different specimen sets the magnitude of the proof tests was 110% and 120% of the maximum constant amplitude load. Whilst the primary objective of the examination of the robustness of AE as a through life condition indicator, it was considered that the accelerated life tests could additionally yield important information about the merits of proof testing, specifically whether proof testing is detrimental to fatigue lives or conversely enhances lifetime.

5.2 Experimental objectives

1. To determine if the AE on the proof tests alone could establish a trend that relates the condition of the structure.
2. To investigate the reliability of fitting a power law for the provision of a reliable condition indicator from the information generated during proof tests.
3. To verify the results visually using a scanning electron microscopy.
4. To determine the effect of proof testing on the life of a mechanical structure and determine the minimum frequency with which it might be applied.

5.3 Experimental set up

5.3.1 Materials

Three material types were used during the investigation. The materials were chosen as they are representative of structural steels used for fabrication of mechanical structures. These materials were selected due to their diverse range of mechanical and chemical properties. The materials, their generalised usage and their mechanical and chemical properties are shown in tables 5.1 – 5.3:

BS 970 (1955)	BS 970 (1991)	Useage [95]
EN8	080M40	A medium tensile steel for general engineering
EN1A	230M07	Free-cutting steel for fast machining and long tool life
EN3B	080A15	General engineering, machinable and weldable.

Table 5.1: Materials and their usages

BS 970 (1955)	BS 970 (1991)	C (%)	Mn (%)
EN8	080M40	0.4	0.8
EN1A	230M07	0.15	1.1
EN3B	080A15	0.15	0.8

Table 5.2: Chemical composition

BS 970 (1955)	BS 970 (1991)	UTS (MPa)	Yield stress (MPa)	Elongation (%)
EN8	080M40	510	245	17
EN1A	230M07	360	215	21
EN3B	080A15	380	205	25

Table 5.3: Mechanical properties

Although EN1A is not a constructional steel it was chosen because it exhibited a ductility (% elongation) that split the two other chosen constructional steels, EN8 and EN3B.

Destruction tests on specimens that were to be used in the trials were conducted in bending, as the compressive loadings required to fail a specimen are larger than the equivalent tensile loading. This permitted a suitable fatigue loading to be deduced.

5.3.2 Loading configuration

For both the destruction and fatigue tests, notched specimens were subjected to three point bending in the arrangement depicted by figure 5.1. The specimens were cut to length from ½ inch bar.

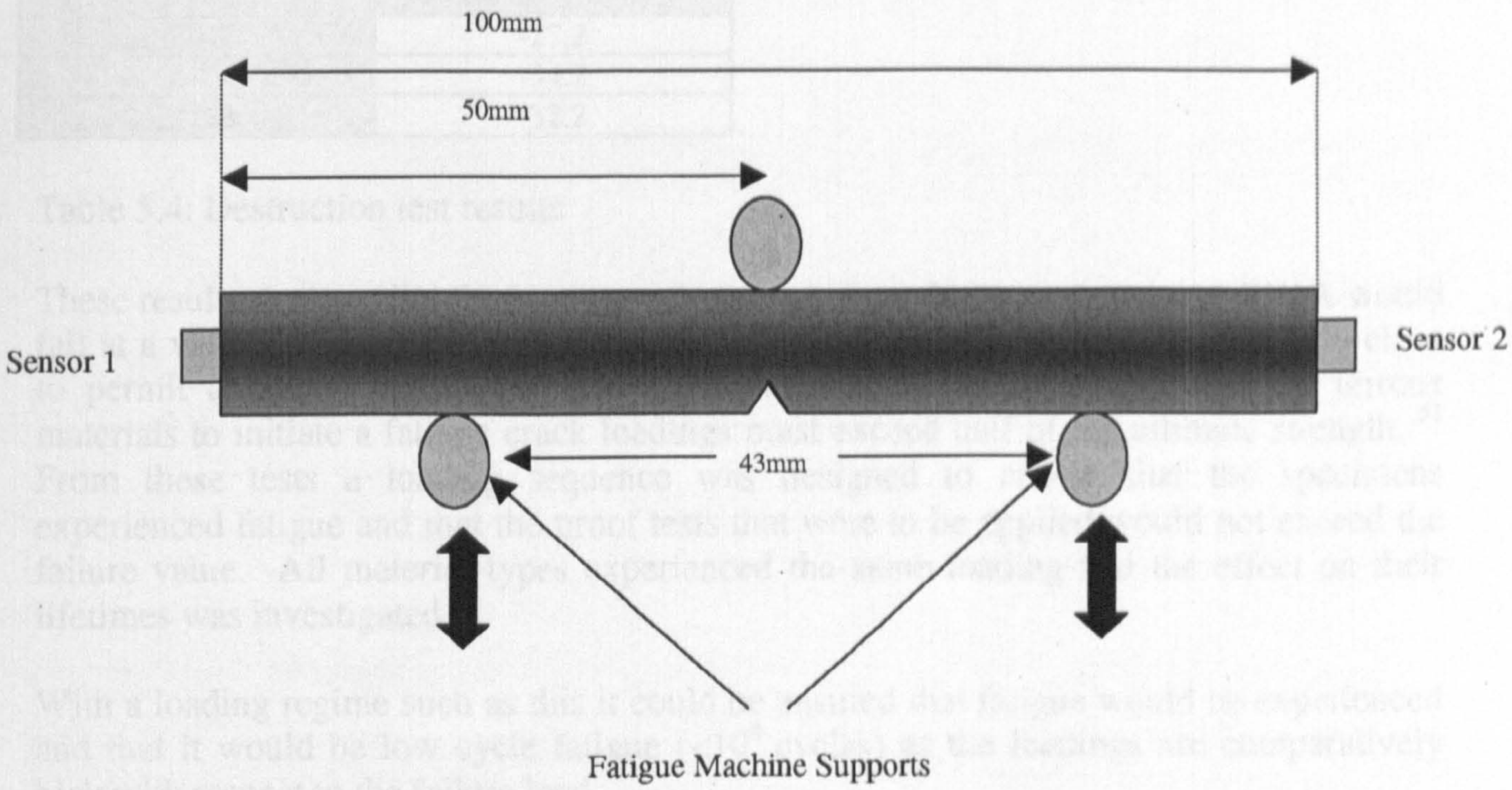

Figure 5.1: Loading configuration

5.3.3 Notch

The notch was introduced to act as a site of stress concentration from which a crack would initiate. The notch was introduced using a 45° cutting disc to a depth of 2mm. Introducing a flaw depth of 2mm reduced the materials cross section to 10.7mm. The support bearings were therefore set 43mm apart to give a 4:1 distance ratio between the support bearings and the specimen height from the top of the notch.

5.3.4 Compressive Destruction tests

A specimen from each material type was subjected to a compressive three point bend destruction test with a constant deflection rate of 0.001mm/second.

The results of these are shown in table 5.4.

Sample	Load at Destruction (kN)
EN8	-27.2
EN1A	-34.2
EN3B	-32.2

Table 5.4: Destruction test results

These results deviate slightly from the anticipated, it might be expected that EN1A would fail at a value between EN8 and EN3B, however these results were all sufficiently close to permit a fatigue loading regime to be designed. It is considered that for ferrous materials to initiate a fatigue crack loadings must exceed half of the ultimate strength. [51] From these tests a loading sequence was designed to ensure that the specimens experienced fatigue and that the proof tests that were to be applied would not exceed the failure value. All material types experienced the same loading and the effect on their lifetimes was investigated.

With a loading regime such as this it could be ensured that fatigue would be experienced and that it would be low cycle fatigue ($<10^4$ cycles) as the loadings are comparatively high with respect to the failure load.

5.3.5 Fatigue

The materials were subjected to three types of fatigue; constant amplitude, and constant amplitude punctuated every 500 cycles with periodic proof tests of 110% and 120%.

5.3.5.1 Constant amplitude fatigue

In the first case the fatigue was a constant amplitude sinusoid with a mean level at –12 kN with amplitude of 6 kN and at a frequency of 1Hz. The fatigue profile is shown in figure 5.3. Purposefully the load did not fluctuate through the zero point. This ensured that the notch was maintained in a constant tension condition enabling crack growth.

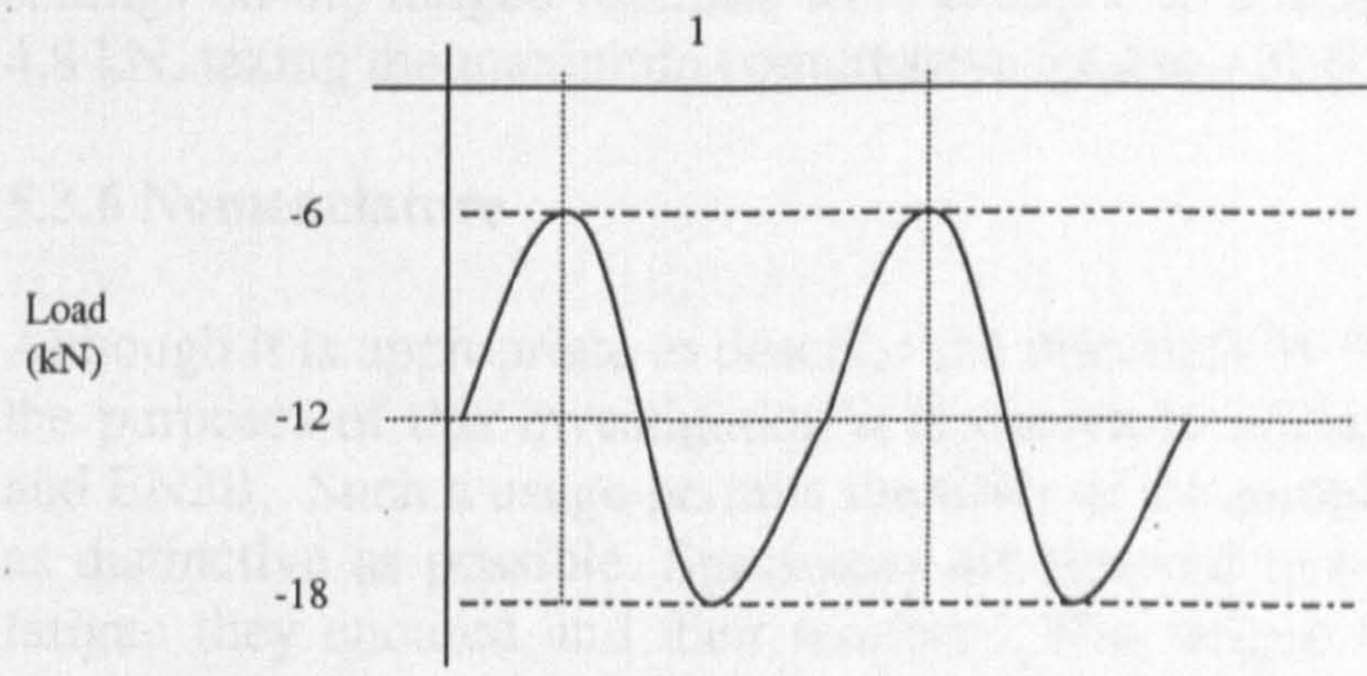

Figure 5.2: Cyclic fatigue load profile

5.3.5.2 Cyclic fatigue with 110 % periodical proof tests

The next set of specimens were subjected to the same fatigue regime, but with periodical proof tests interjected after every 500 cycles through out their lives. The proof tests involved two consecutive load applications to 110% of the maximum compressive fatigue load. On achieving the load, it was sustained for a period of half a second before being reduced and subsequently reapplied to the same value. The settings on the fatigue machine were changed for the proof tests to a mean of –15.9 kN with amplitude of 3.9 kN. The proof tests were conducted using a square wave. AE is proportional to the straining rate [62] and it was considered that the use of a square wave that applies the load more rapidly than a sinusoid would benefit the information that could be generated from the proof tests. A typical proof test is shown in figure 5.4.

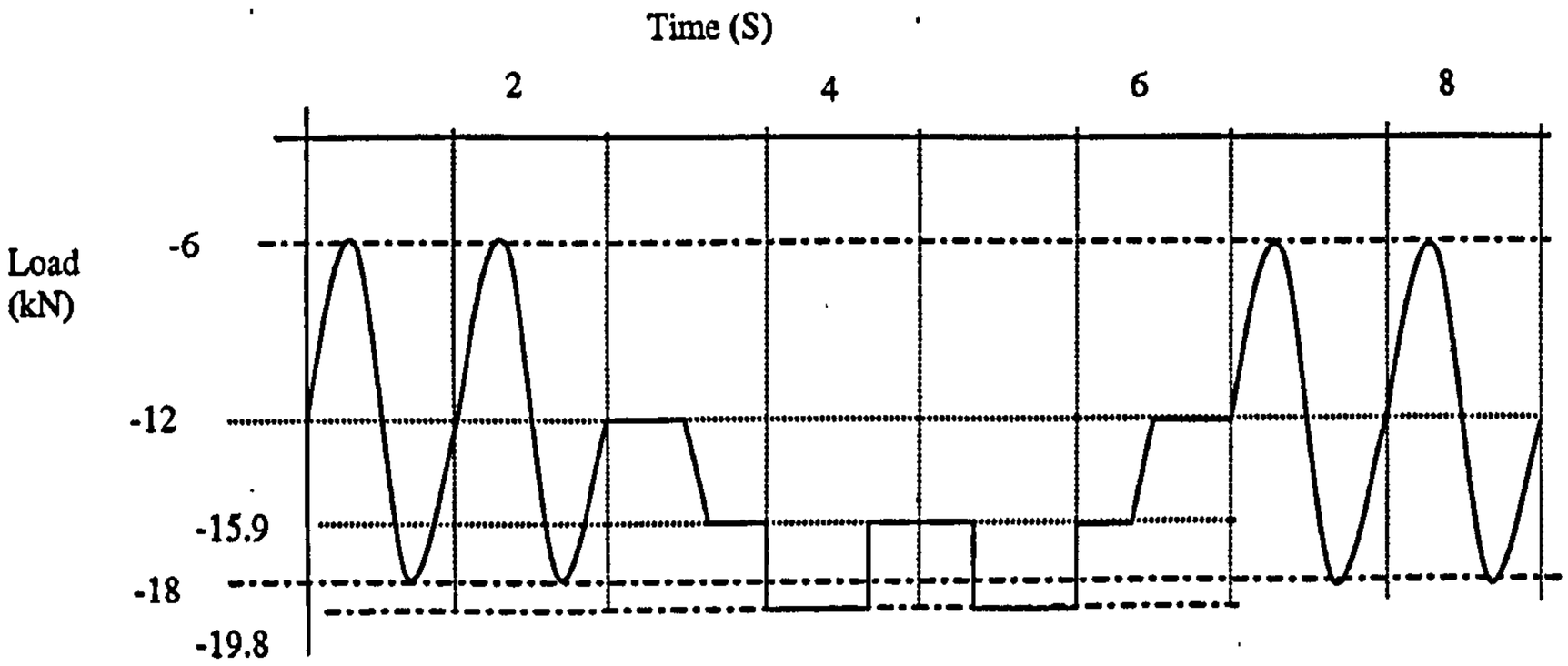

Figure 5.3: Fatigue load profile with 110% proof tests

5.3.5.3 Cyclic fatigue with 120 % periodical proof tests

The 120% proof tests were conducted in the same manner as the 110% proof tests, but the settings on the fatigue machine were changed to a mean of –16.8 kN with amplitude of 4.8 kN, taking the maximum compressive load to –21.6 kN.

5.3.6 Nomenclature

Although it is appropriate to describe the materials by their BS 970 1991 designation, for the purposes of this investigation it is chosen to utilise their 1955 titles of EN8, EN1A and EN3B. Such a usage permits the titles of the sample numbers to be kept as brief and as distinctive as possible. Specimens are referred to by their material type, the type of fatigue they endured and their number. The fatigue types are named CF for constant amplitude fatigue, P11 and P12 for 110 and 120 % proof tests, respectively. So, typically, a specimen will be referred to as: EN8 P11 03

For the purposes of describing maximum and minimum points on the load cycles, the maximum will always be discussed with reference to the stress condition, so whilst –21.6 kN is the minimum load, and –6kN the maximum, the stresses at the crack are at their highest at –21.6kN. Therefore –21.6kN is described as the maximum.

5.3.7 Crack behaviour

With reference to chapter 2, the crack can be expected to blunten at the maximum stress condition and will close during the unloading phase. The proof test will generate the highest stress condition and consequently the greatest AE. The AE at the maximum stress condition will be attributable to yielding, the formation of the plastic zone ahead of the notch, and to discrete crack jumps. The anticipated crack behaviour is shown in figure 5.5.

In chapter 2 it was discussed that mechanical engineering uses a power law to describe the rate of crack growth. The use of a power law indicates that the magnitude of the crack extension will increase nonlinearly with increased crack length. Because the AE is a component of the energy released during such a process the investigation will determine the suitability of using such an approach for trending the degradation. The power law relationship will be investigated only on data attained during the proof tests that is applied incrementally though out the life. As a means of verifying the results a Scanning Electron Microscope was used to visually examine the fracture surface. Increasing increments between striations would confirm the anticipated behaviours.

Maximum load

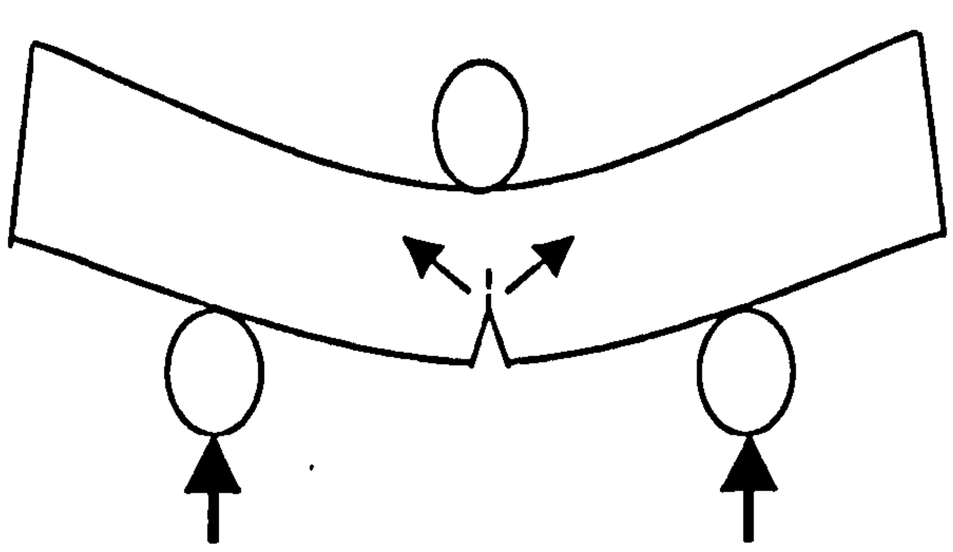

At the peak stresses the crack will gape and the crack is likely to grow, particularly on the proof tests

Minimum load

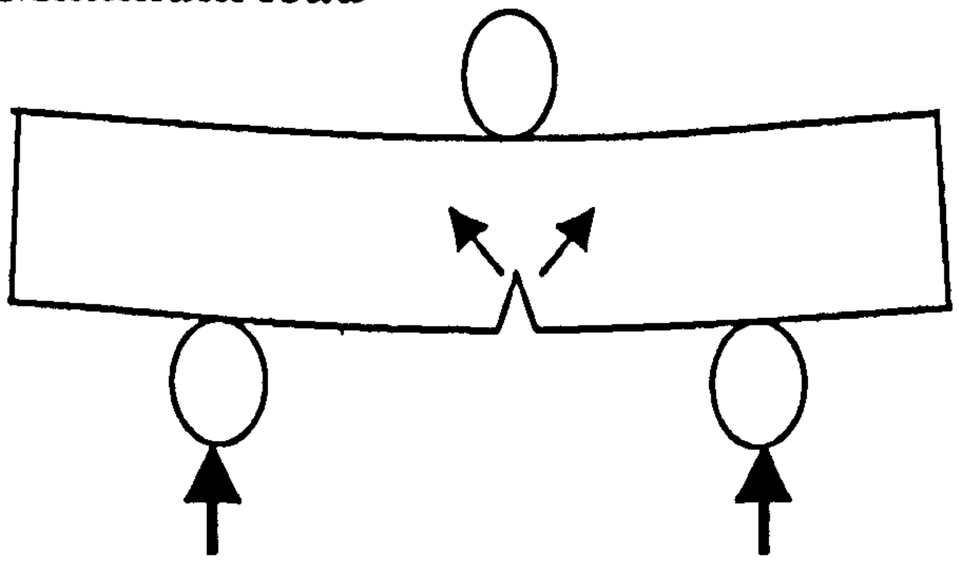

At the minimum load the crack will never fully close as it is subjected to a constant tension, but the load is sufficiently low (<50 % $_{uts}$) as to not cause growth.

Figure 5.4: Crack behaviour at maximum and minimum loads

5.3.8 Instrument settings

The microscope was a Leo Scanning Electron Microscope, Model Number S430.

The testing was conducted with a Physical Acoustics Mistras 2 channel acquisition unit using both Wideband (WDI) and Resonant 150 kHz (R15I) sensors with integral preamplifiers. An Instron testing machine model, Number 1342 H 1031, applied the load. The applied load was taken into the AE instrument via a direct connection from the load cell.

In the instances where the wideband sensors were used the instruments threshold was set to only acquire hits greater than 32dB whereas with the resonant sensors it was set at 40dB. The presence of noise with the resonant sensors prevented the settings being retained at the same values. Additionally a front-end filter was set on the instrument to only include hits with counts greater than 5.

The hit definition times and hit lockout times were set after some initial pencil lead break tests on the specimens. Iterations of these times permitted the instrument to be optimised to source locate a single event and two hits from the simulated source. As the specimens were small this proved difficult to achieve as the sound wave reflected off the boundaries and frequently gave rise to more than two hits.

Each test was preceded by an initial verification of the instruments performance. Three lead breaks were conducted at the notch site and the events viewed on screen on an amplitude scale. Confirmation of three events in the proximity of 100dB at the mid point on a source location plot constituted the instrument fit to conduct the monitoring. Such a practice proved erroneous, ultimately. The effect on the results and the countermeasures employed will be discussed.

5.3.9 Data analysis employed

Initially, the data was filtered to include only the events that were source located on the specimen. Such an approach was taken to exclude any noise that may be apparent during the trails and the use of events increases the confidence that the AE is materially related. Such a procedure proved flawed as it had the effect of filtering out the AE that occurred at the maximum loads, this became apparent with data files, which used the resonant sensors. An example is shown in graph 5.1, which is taken from EN8 P12 01. The graph illustrates the load value at the instance when the instrument records a hit. Such graphs are referred to as hit driven data. There exists a clear definition of where the majority of the activity occurs, at –18 kN. When this is compared with a file that has been filtered to include only the source located events, graph 5.2, it can be observed that much of the activity particularly at the high stress condition has been omitted.

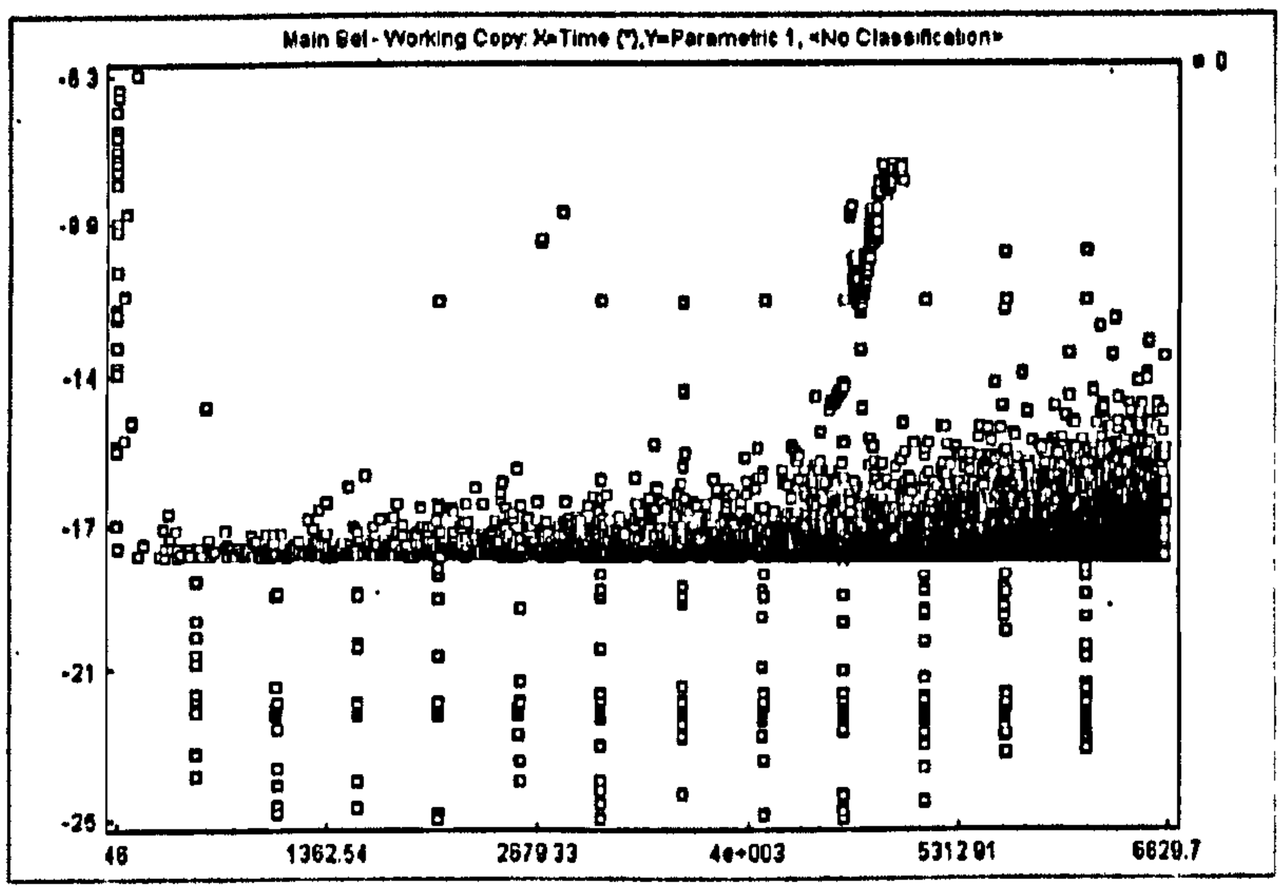

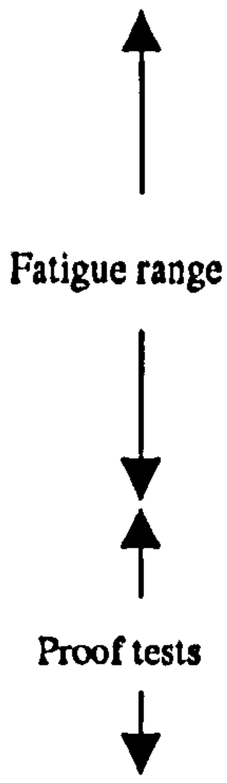

Graph 5.1: Hit driven data from EN8 P12 01 – pre filtering

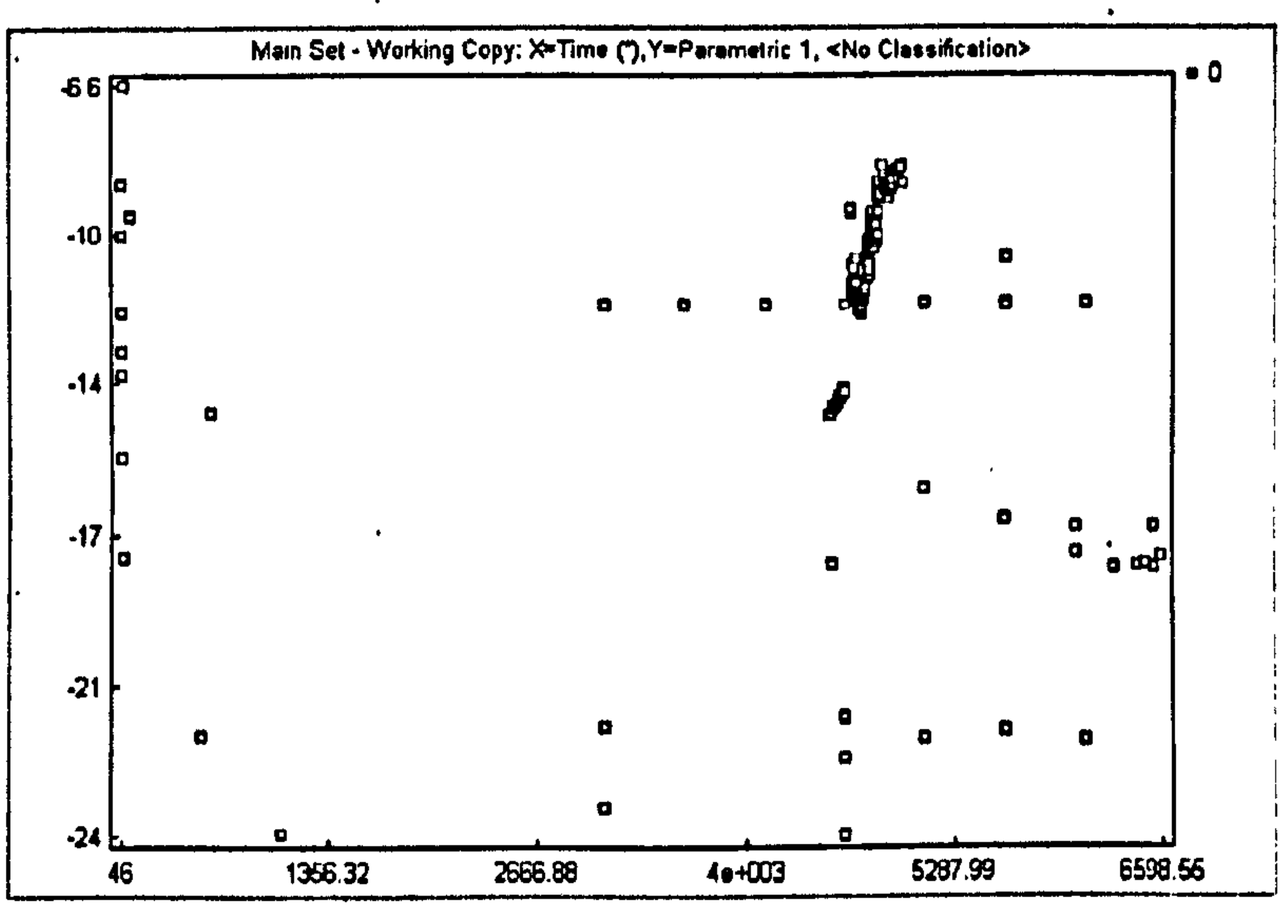

Graph 5.2: Hit driven data from EN8 P12 01 – post filtering

The reason this occurs is because the hits that are coincident with the peak stresses are reasonably small in amplitude and fail to register at both sensors to constitute an event. On closer examination it was found that in some cases the differential of the sensitivities between the two sensors was considerable. The lead breaks conducted at the beginning of the test may have registered as a 100dB event on the source location plot, but that may have been due to channel 1 reporting 100, but channel 2 only reporting 70dB. The instrument still reports the event as a 100dB. Such a differential reduces the sensitivity of the instrument and the consequently the number of reportable events is reduced. Comparison of the two counts amplitude cross-plots generated by the process of event filtering and otherwise are shown in graphs 5.3 and 5.4, and the reason for an event filter omitting the AE at higher loads becomes more discernable.

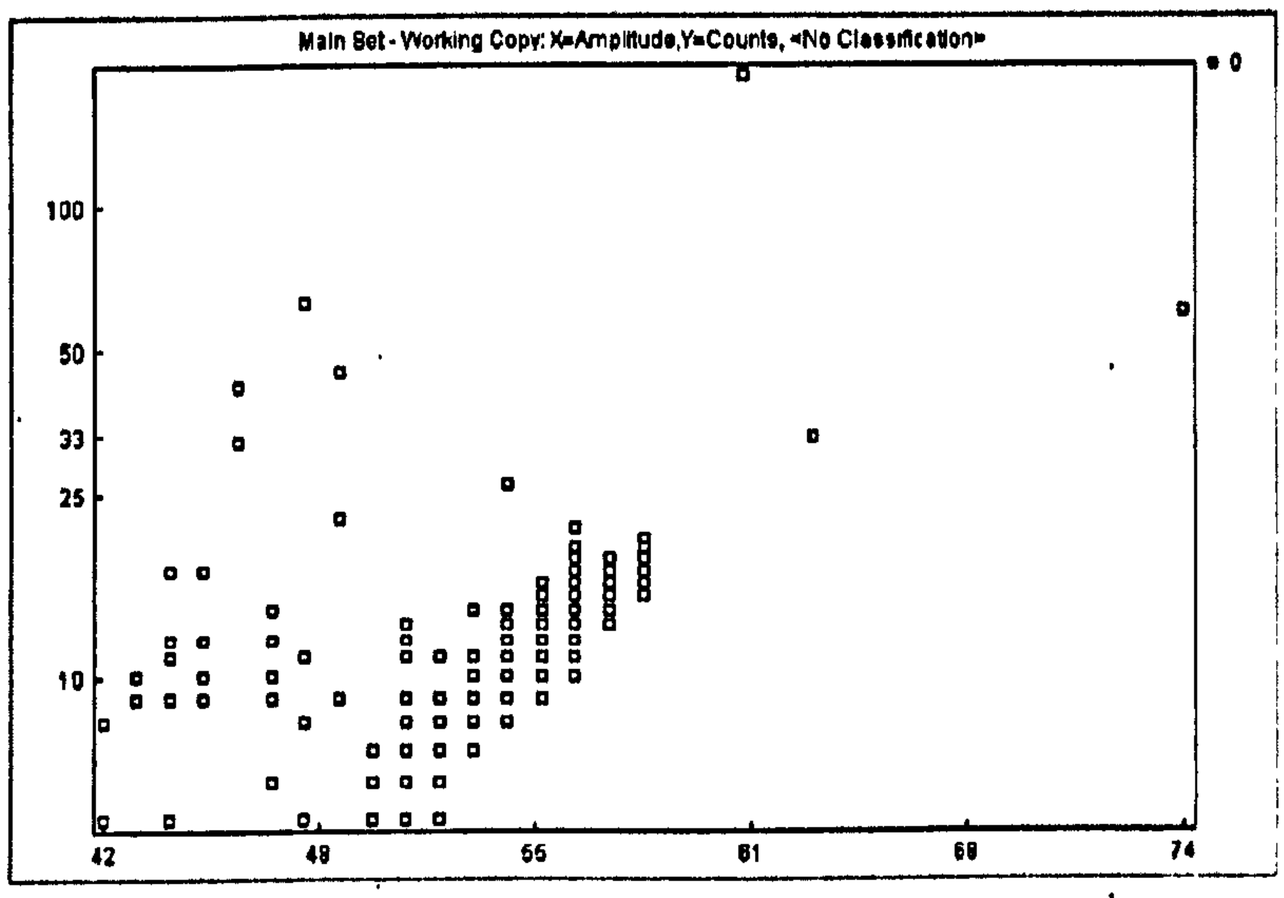

Graph 5.3: Counts Amplitude distribution from EN8 P12 01 – post filtering

Within the event-filtered distribution, graph 5.3, there are few hits within the 42 – 48dB range, in graph 5.4, however there are two distinctive patterns. The second pattern is predominantly within the 40-50dB range. The differential between the sensors means that the smaller amplitude hits are omitted if event filtering is conducted, as the hits are slight enough as to not exceed the threshold of the least sensitive sensor.

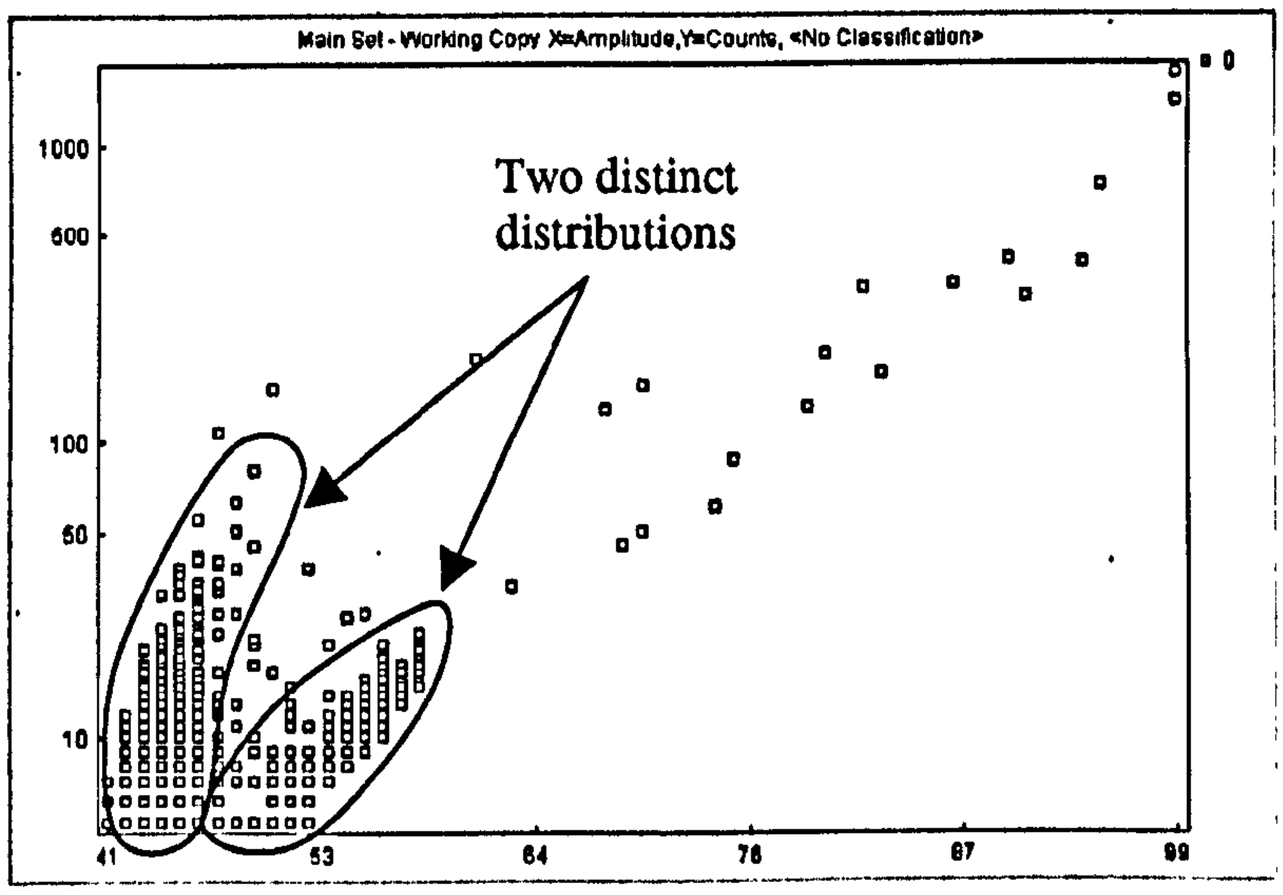

Graph 5.4: Counts Amplitude distribution from EN8 P12 01 – post filtering

Closer investigation into these distributions determined that the two patterns could be attributable to different source mechanisms. The lower amplitude banding was produced by material degradation at the peak stresses whereas the other banding is considered to emanate from the crack face fretting. Graph 5.5 shows the hit driven data, which are depicted as squares on the graph as well the time driven data (data generated from sampling the load at 4Hz). The time driven data is shown as crosses. When observing the data over just four seconds the resolution is such that it can be observed at what point in the load cycle the hits occur. The hits that occur at the maximum (~ -18 kN) arise during

the rising load whilst the hits at lower levels (~ -10 kN) occur during falling loads. A dotted line has been superimposed to aid visualisation.

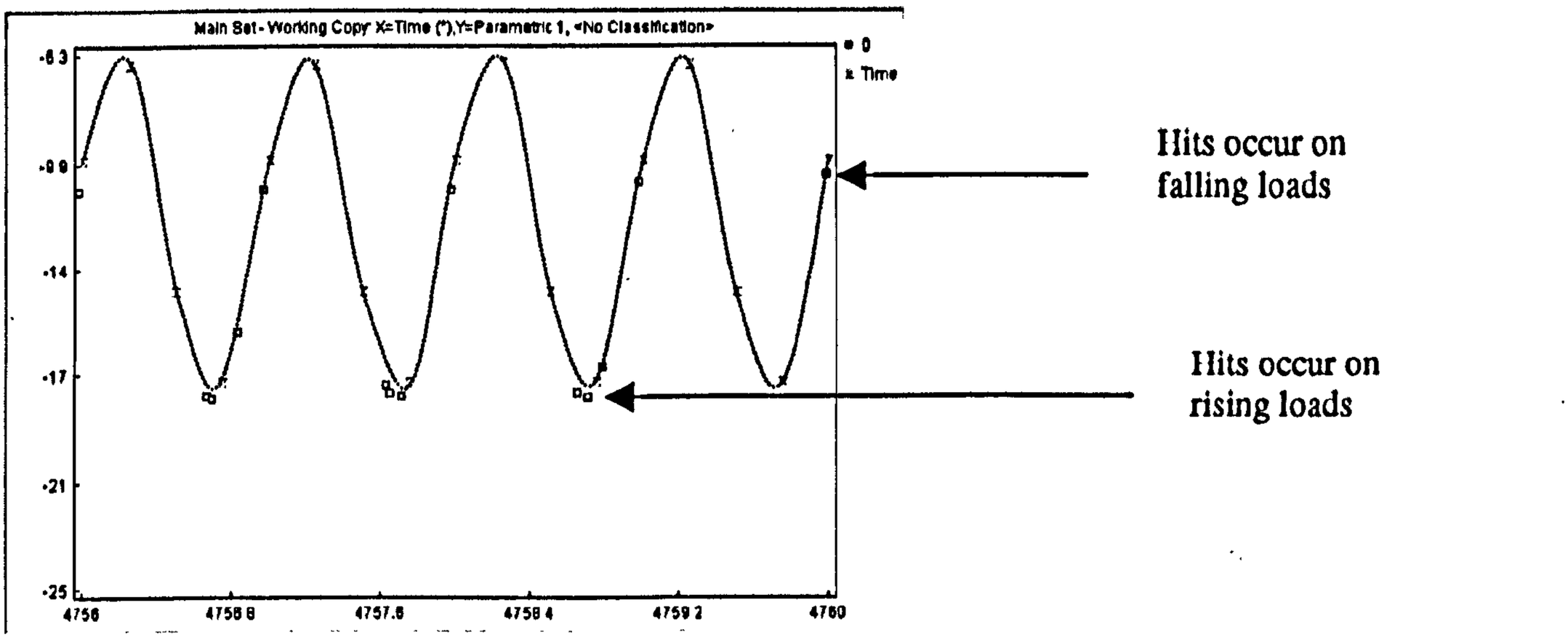

Graph 5.5: Counts Amplitude distribution from EN8 P12 01 – post filtering

Returning to the Hit driven data, the four-second time period selected for graph 5.5 was selected to expose the characteristics of the unique cluster that is evident during the period between 4600 and 5000 seconds in graph 5.6. It is considered that because the hits occur during the falling load these hits are most probably generated by a frictional source from the crack faces fretting. Perhaps during a preceding period the crack may have changed direction slightly and during closure the faces contact and generate AE. In all data files the occurrence of such clusters were evident, most frequently, these appear close to end of life. Such an observation is in agreement with the findings of Morton [89] who also applied a power law to AE fatigue data.

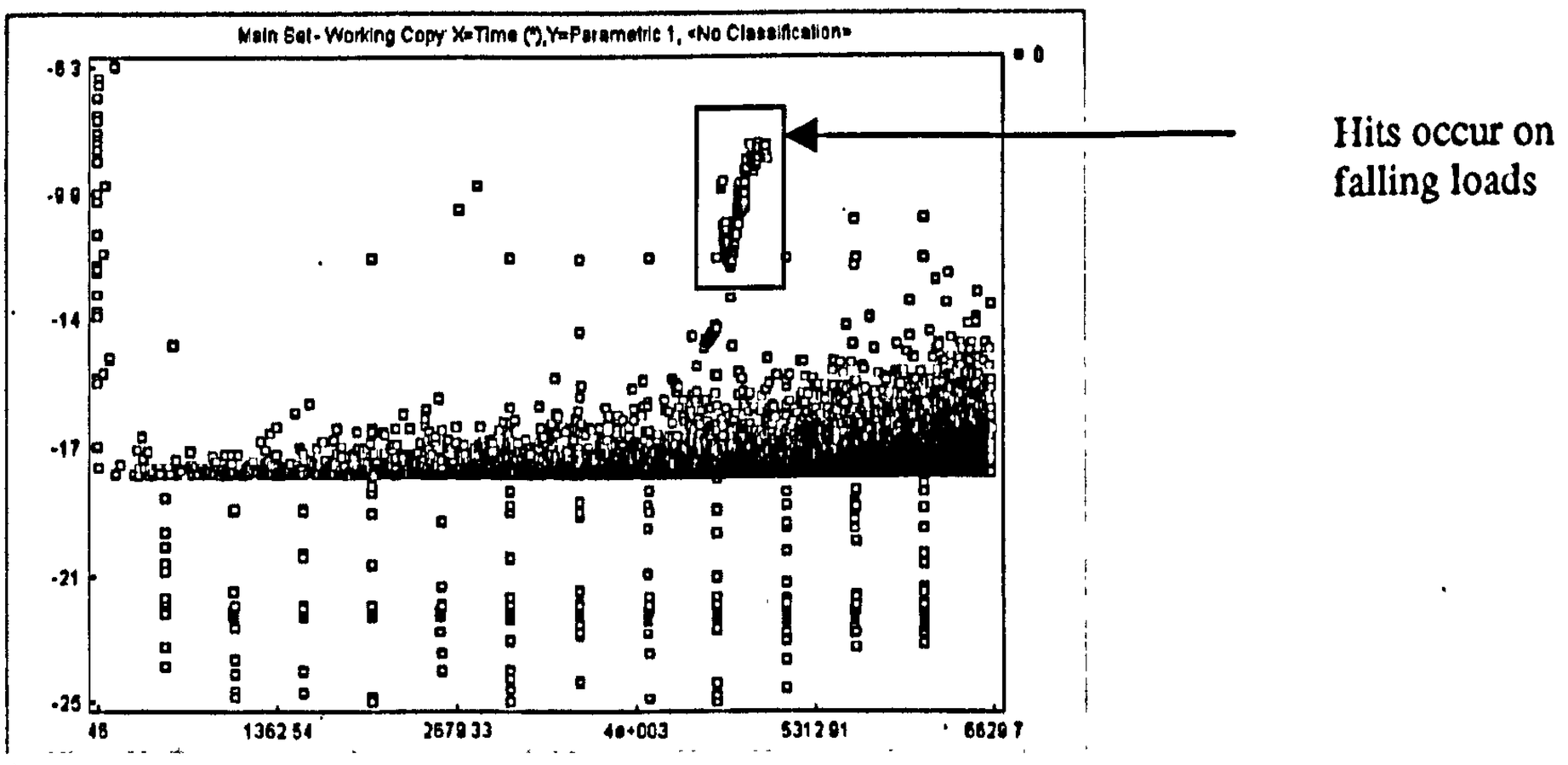

Graph 5.6: Hit driven data illustrating the hits on falling loads

The frictional sources generated by crack face fretting are not particularly interesting for the purposes of this investigation, they serve as a useful means for defect detection in that

they give rise to comparably high amplitude hits that can be source located. The frictional source generated by the faces fretting is a consequence of the presence of a defect, but is not useful for trending the degradation. Plate 5.1 shows how the direction of the crack can change during the fatigue life. The crack initiation site can also be seen, as well as the plastic zone in front of the crack tip.

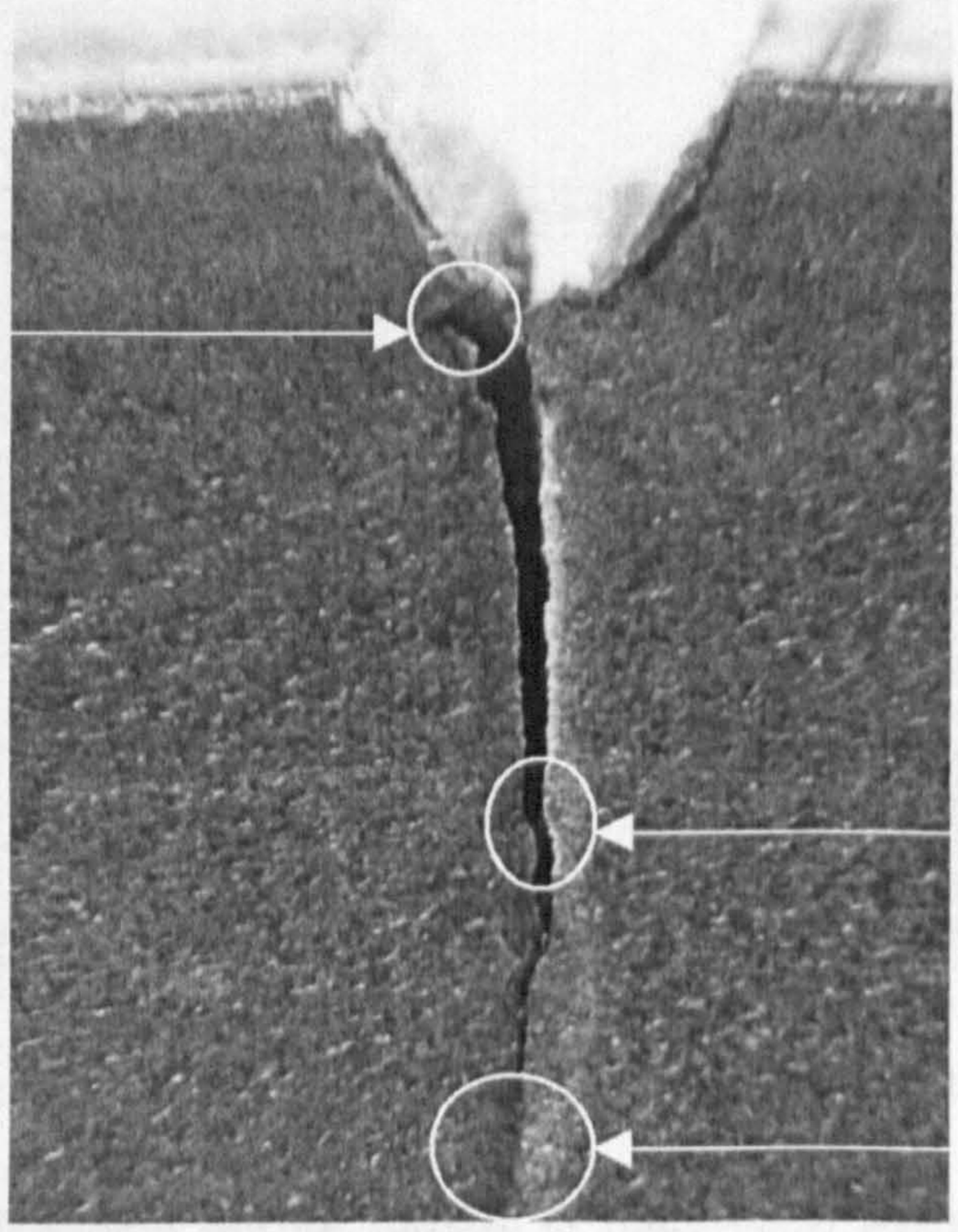

Plate 5.1: An example of crack growth

For the continuation of this work the smaller amplitude hits that are generated at the maximum loads are the most relevant as these are associated with the progressive degradation. For this reason the data files were filtered to only include the hits that occurred on the most energetic channel. The channel that reported the highest energy from the pencil lead breaks was chosen.

With the data reduced to only a single channel, the hits generated from the initial instrument verification process were filtered out, as indeed was the final failure. This ensured that residual data was attributable to material deterioration, enabling the investigation to focus on the trendable nature. For the purposes of demonstration, EN8 CF 01 is illustrated through the process.

The emission that occurs during the final failure is huge in comparison to the hits that are generated during the course of the lifetime. On all history plots the final failure data essentially masks all the lesser hits. The high energy hits can be viewed on the energy

plot in graph 5.7, these are shown on a logarithmic scale. These energetic hits were not considered to be relevant to this investigation for two reasons. If during industrial practices an in-service failure occurs whilst monitoring the structure with AE, then the condition monitoring strategy has failed to serve any purpose. Secondly, the hits generated during the failure are due to unstable crack propagation and additionally may be contaminated with other AE source mechanisms such as motion of the specimen or sensors becoming detached. Hence, on all specimens the final cycle during which the failure occurs has been filtered out of the data for subsequent analysis.

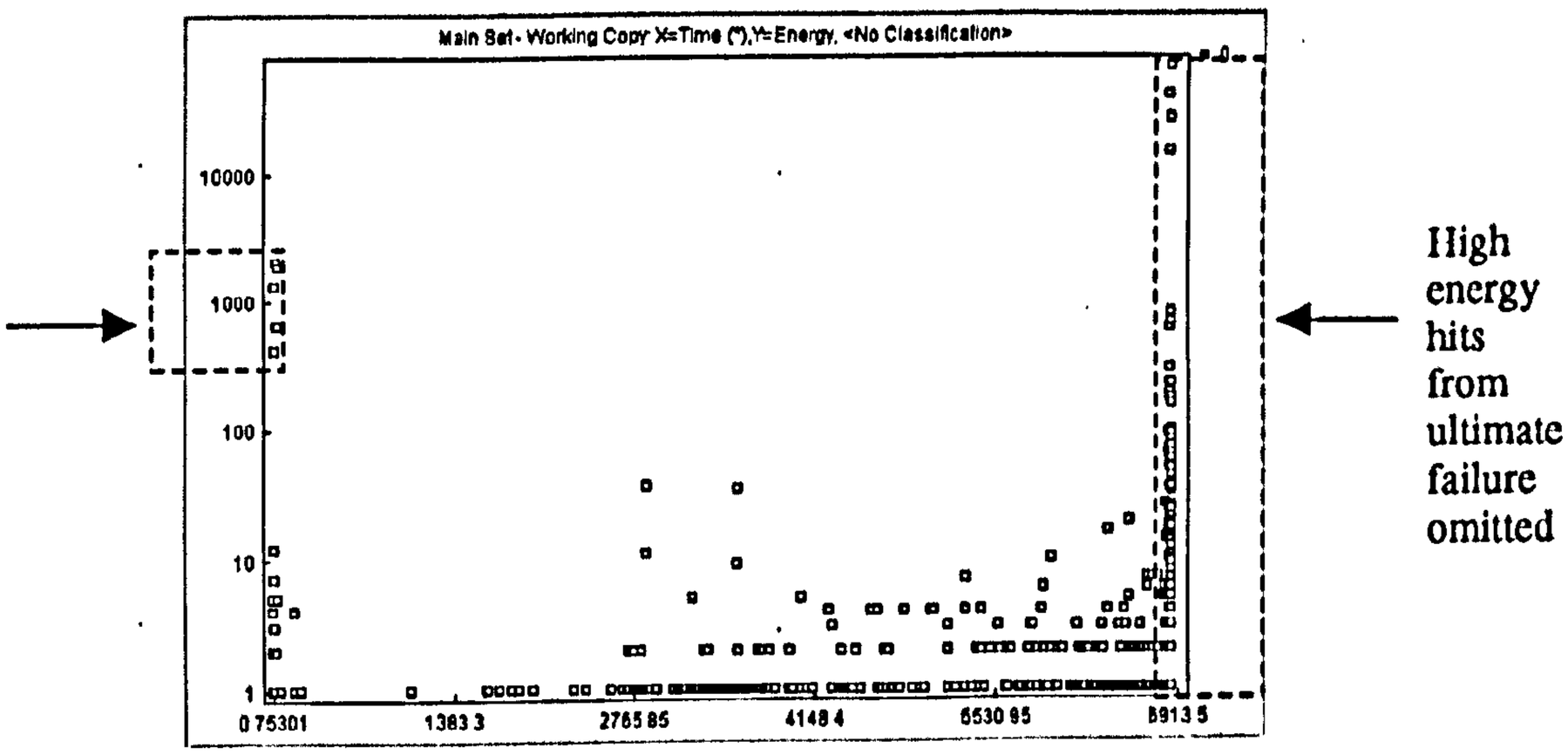

Graph 5.7: Filtering the initial instrument verification and the final fracture

The fracture surface generated during fatigue is featureless surface and can be seen in plate 5.2, which portrays a failed specimen in section. The view given is one side of the crack. The fatigue surface is created by the slow progression of crack jumps until the remaining strength of the material is insufficient to sustain the load and the specimen fails in fast fracture. The fracture surface created during the fast fracture is distinctly different from the fatigue surface.

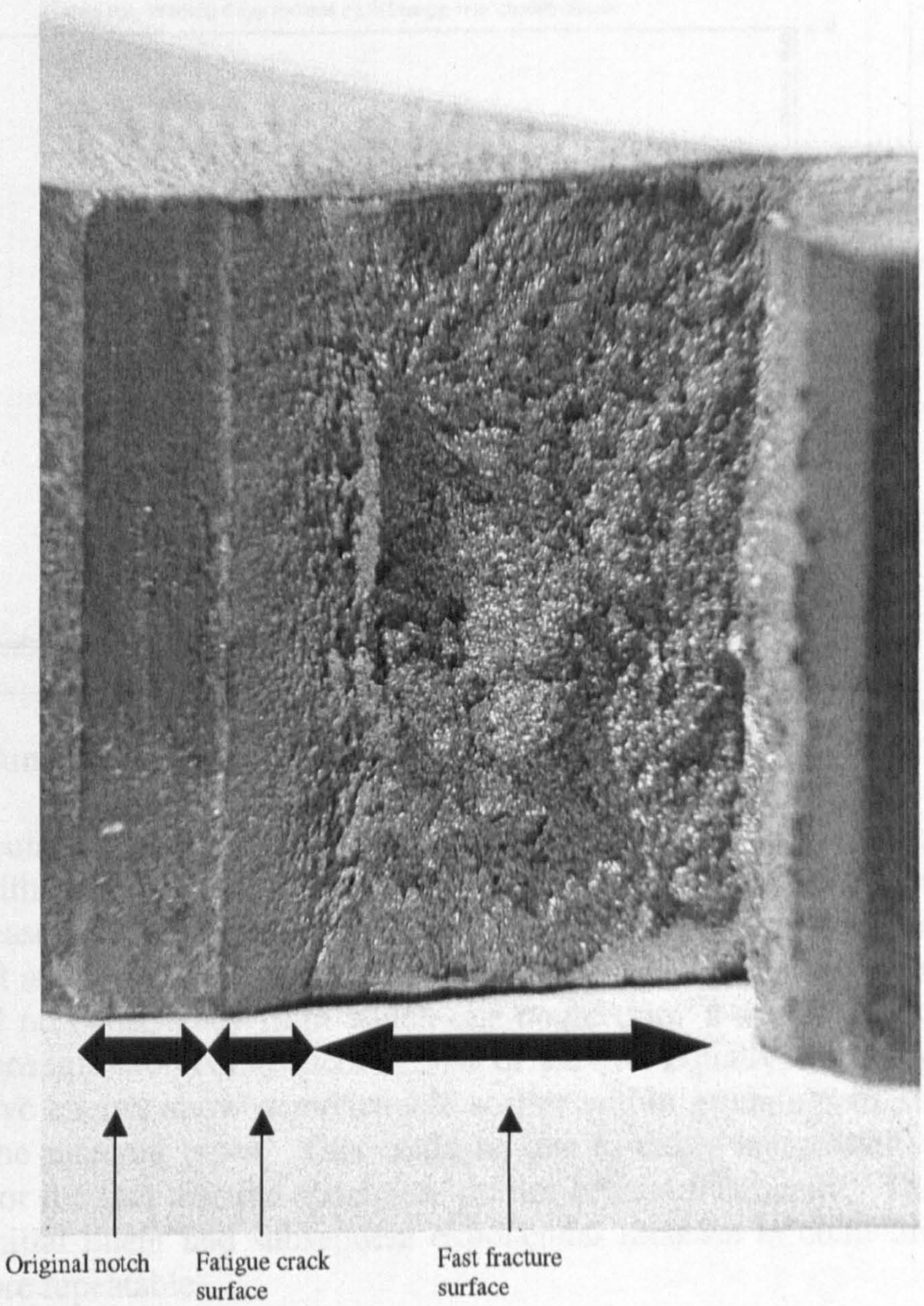

Plate 5.2: An example of the different phases of the fracture process

The removal of the final failure from the data ensures the activity that remains is associated with only the fatigue crack surface. For all tests, after the final failure and initial lead breaks had been omitted, a cumulative energy plot was created. Graph 5.8 is typical of a result set and is from EN8 CF 01. In almost all cases such a distribution was evident. There exists the onset of emission, which is frequently followed by a gradual linear increase in the cumulative energy that subsequently becomes near vertical as proximity to failure approaches. Such a distribution supports the prospect that a power law will generate a good fit.

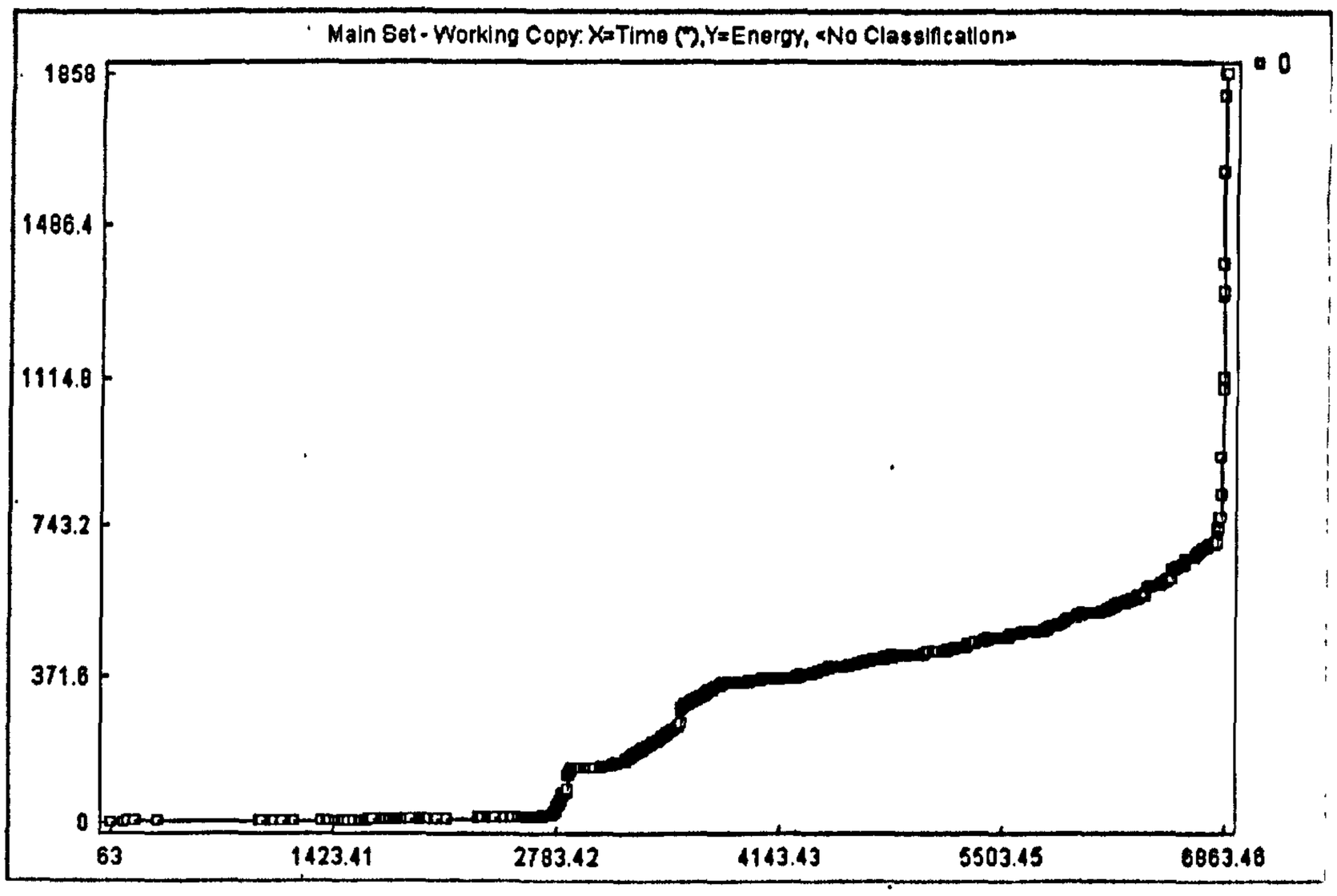

Graph 5.8: Cumulative energy from EN8 CF 01

In this particular case there exists a clear demarcation point, which is considered to be associated with crack initiation at approximately 2780 seconds. Some specimens showed a linear increase from almost the start of life whilst others like this example have a clearly defined point at which significant emission commences. Even within the material groups there existed no consistency from which one could draw a conclusion such as for this loading pattern initiation commences at 30% of the life. Equally, the numerical values of the cumulative energy show demonstrable scatter within groupings of similar materials and across the material types. This could be due to either inconsistency in the sensor sensitivities or the fact that the specimens do not behave identically. The shapes of the curves, an initial linear and subsequent exponential increase in cumulative energy are, however, more repeatable.

The results for each specimen can be viewed in Appendix V. In cases where the specimens were subjected to either a 110% or 120% proof tests, the cumulative energy generated from the proof tests in isolation is also shown. This allows comparison with the cumulative energy curve for the test in its entirety. The degree of correlation can be discerned visually. The AE generated from the proof tests was separated by imposing a filter on the hit driven data, all hits that were generated at a load values within the range – 18.1 kN to the maximum (-22 kN for 120% proof tests) were discriminated from other hits. A power law was subsequently fitted to the data to identify the suitability of using a Paris type relationship to trend the degradation..

5.4 Results

Discussion of results will initially segregate the specimen sets into material groupings and the fatigue type they experienced. This is succeeded by an investigation into the forewarning generated by the proof tests and an investigation into the trendable nature of energy released from the proof tests. Finally in the results section, the images of SEM are discussed.

5.4.1 Cyclic fatigue

Three specimens of each material type were each subjected to the fatigue regime until failure. The number of cycles to failure and the calculated average lifetimes of the three specimens, within their material grouping are shown in table 5.5.

Material	Specimen No.	No. Cycles to failure	Average Lifetimes for cyclic fatigue
EN8	CF 01	6805	6903
	CF 02	6341	
	CF 03	7341	
	CF 04	7125	
EN1A	CF 01	13017	11750
	CF 02	9800	
	CF 03	12432	
EN3B	CF 01	18988	20372
	CF 02	20140	
	CF 03	20998	

Table 5.5: Lifetimes from cyclic fatigue

Reasonable repeatability is shown in the lifetimes for each material type and there exists a significant difference between the lives experienced by the different materials.

The nature of failure differs slightly for each material type. EN 8 tended to fail in a curved manner, and the crack frequently changed direction during the course of life. The fracture surface displayed pronounced 45^0 shear lips. EN 1A exhibits crack behaviour that acts almost vertically before it ultimately tears, EN3B acts initially vertically, but the final failure tends to be at 45^0 to the propagating crack. EN3B also best demonstrated a visible plastic zone in front of the tip. EN3B is the most ductile of materials investigated. Plates 5.3 – 5.4, are of EN8 CF 01, EN1A CF 01 and EN3B CF 01 respectively. Such plates are typical of what is found for each specimen set in the Appendix V section. In addition, the plates in the Appendix permit visualisation of each side of the specimen and each fracture surface.

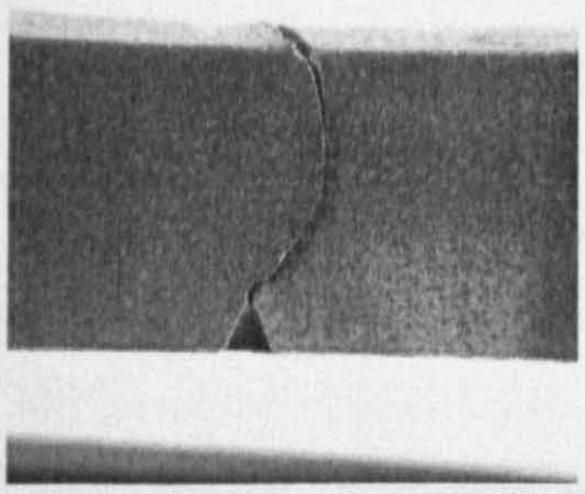

Plate 5.3: EN8 CF 01

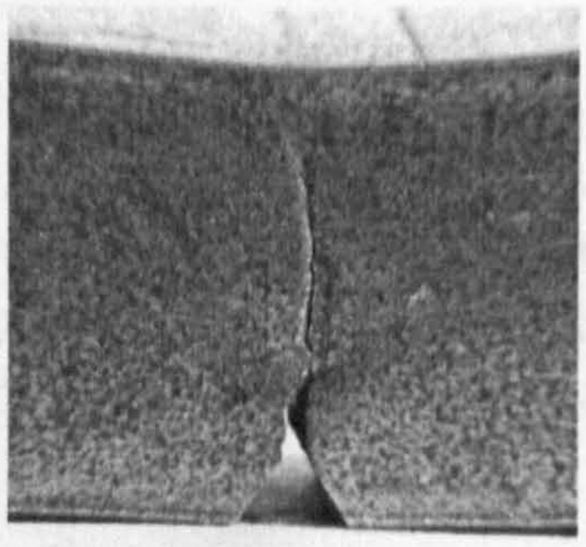

Plate 5.4: EN1A CF 01

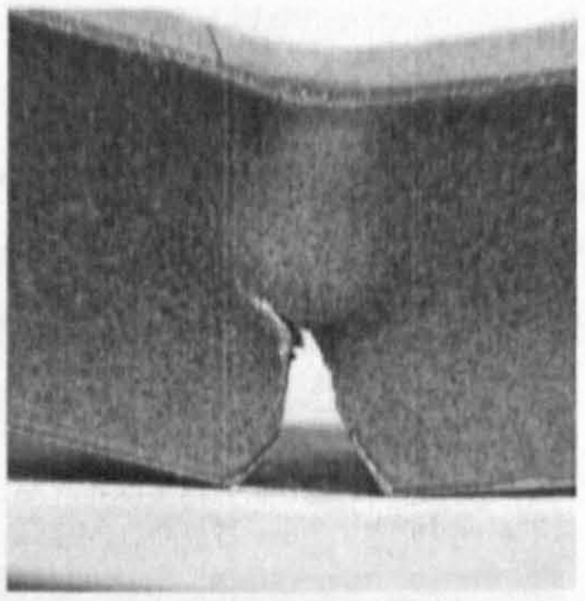

Plate 5.5: EN3B CF 01

In all of the above tests wideband sensors were used. The AE that was generated during the fatigue are shown two formats. One example is shown to explain the methodology; again, EN8 CF 01 is chosen to demonstrate the results.

EN8 CF 01- 6806 cycles

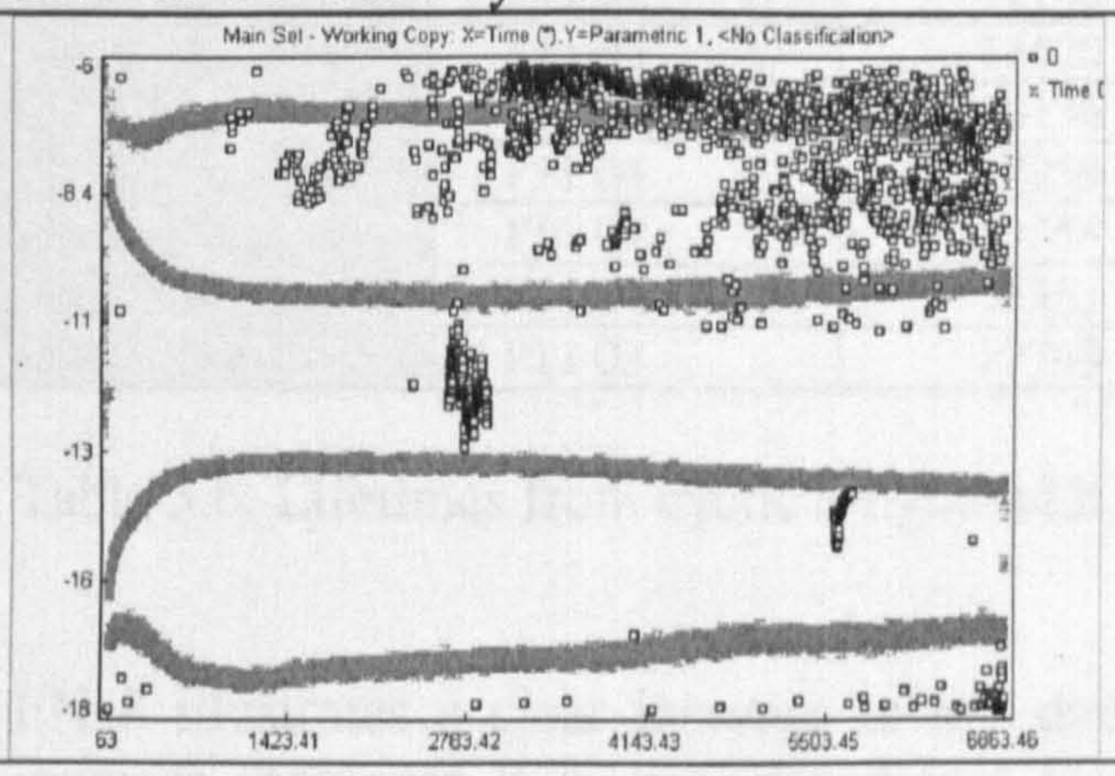

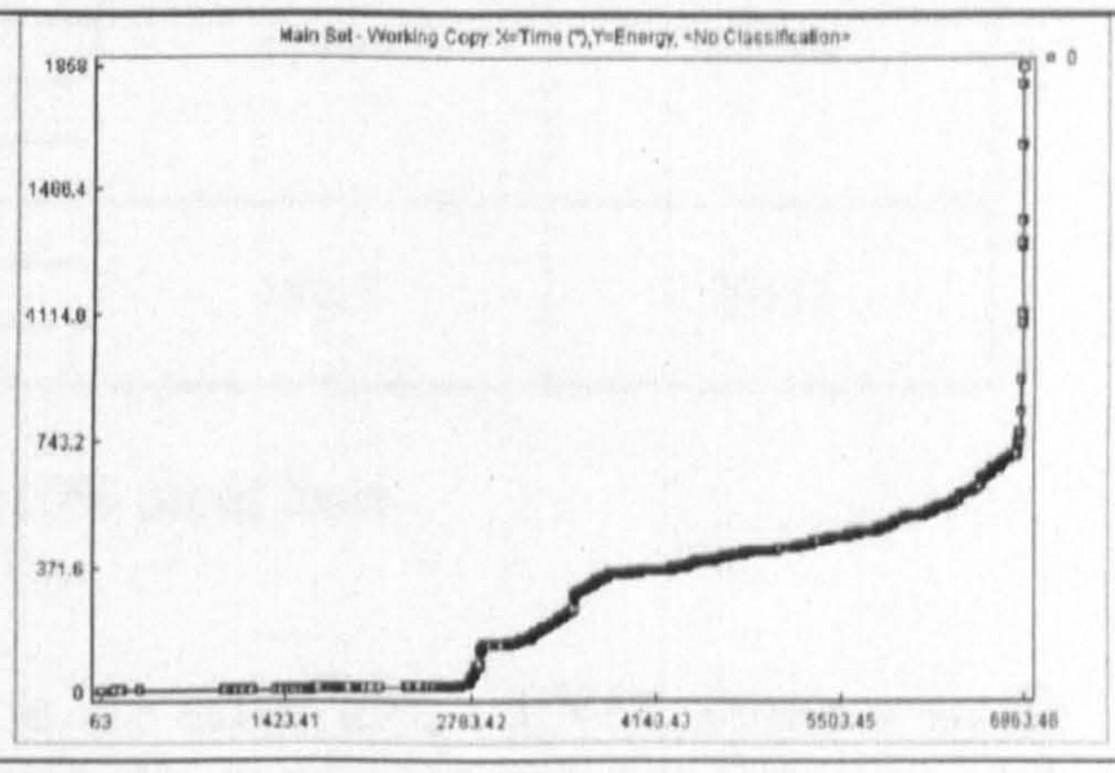

Graph 5.9: Hit driven and Time Driven data and Cumulative energy plot for EN8 CF 01

The left hand graph of 5.9 illustrates the time and hit driven data. In this case and generally in cases that used the wide band sensors the activity is concentrated at the base of the load cycle with few hits at the maximum load. Note the discrete clusters of activity that have been previously been shown to emanate from friction. The wideband sensors proved to be not as effective as the resonant sensors for detection of the low amplitude hits generated at the peak stress and attributable to the progression of damage.

The right hand graph illustrates the cumulative energy, which has already been described in conjunction with graph 5.8. The onset of emission at 2780 seconds is considered to correspond to initiation of a crack at the notch site and the emission thereafter to stable crack propagation and the fretting. Whilst it is considered that these emissions are associated with initiation, no visual evidence was attained during the trials. It was not until very much later in the tests that a crack could be viewed gaping at the peak stress.

5.4.2 Cyclic fatigue with 110 % proof tests

Table 5.6 depicts the lifetimes for each material, which experienced the cyclic fatigue regime, but after every 500 cycles was subjected to two consecutive proof tests of 110% of the maximum cyclical value. For comparative purposes the final column shows the average lifetimes of the specimens that only experienced constant amplitude fatigue.

Material	Specimen No.	No. Cycles to failure	Average Lifetimes for cyclic fatigue with 110% proof tests	Average Lifetimes for cyclic fatigue
EN8	P11 01	9119	8341	6903
	P11 02	9120		
	P11 03	8106		
	P11 04	7599		
	P11 05	7763		
EN1A	P11 01	11148	11966	11750
	P11 02	13620		
	P11 03	10136		
	P11 04	12959		
EN3B	P11 01	19353	19157	20372
	P11 02	18355		
	P11 03	19763		

Table 5.6: Lifetimes from cyclic fatigue with 110% proof tests

EN 8 illustrates a clear increase in life due to the proof tests. EN1A shows a small increase, however it is considered that because the population set that made up the average for the cyclic fatigue comprised of only three samples of which one value was comparatively low in relation to others (9800; in comparison to 13017 & 12432) this information maybe slightly skewed. More probably, like the results from EN 3B, the lifetimes are slightly shortened, or remain unchanged.

The nature of the visually observable failure differs slightly from the failures observed in the simple constant amplitude fatigue case. In almost all instances the failure occurred on the application of one of the proof tests. The cracks created during fatigue with proof tests have the appearance of being ragged with more frequent changes in direction. This is considered to be due to difference in the nature of the applied stress during the proof tests. The crack must react more rapidly to the applied square wave. This may cause trans-granular as opposed to inter-granular cracking. Plates 5.6 – 5.8 are selected to show some of the more pronounced changes in direction of the 110 % group. It is appreciated that views shown here are of the specimen having completely failed and as such the view has not only the fracture surface associated with the fatigue, but additionally the final fast fracture. All of the specimens shown failed during a proof test so if these dramatic changes in direction are observable on this macroscopic view of the damage it can be interpolated that the same changes in direction are present on the smaller fatigue surface.

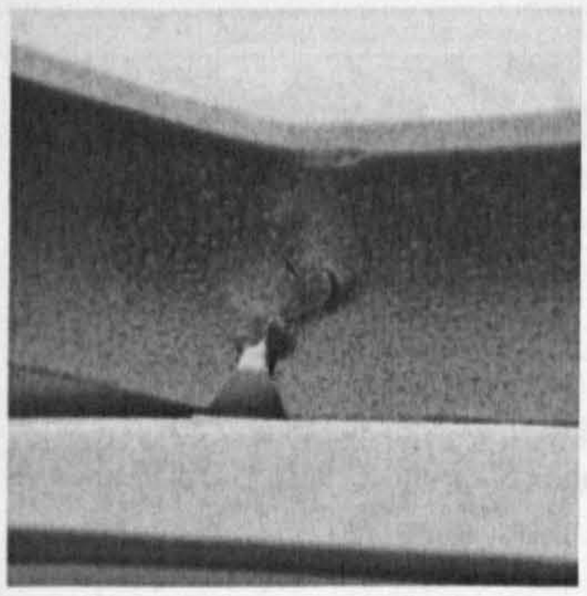

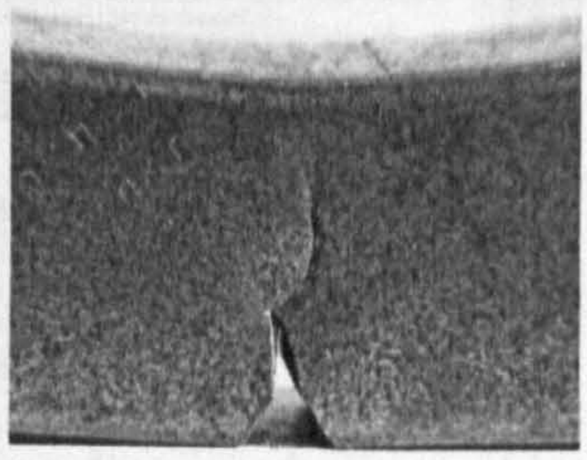

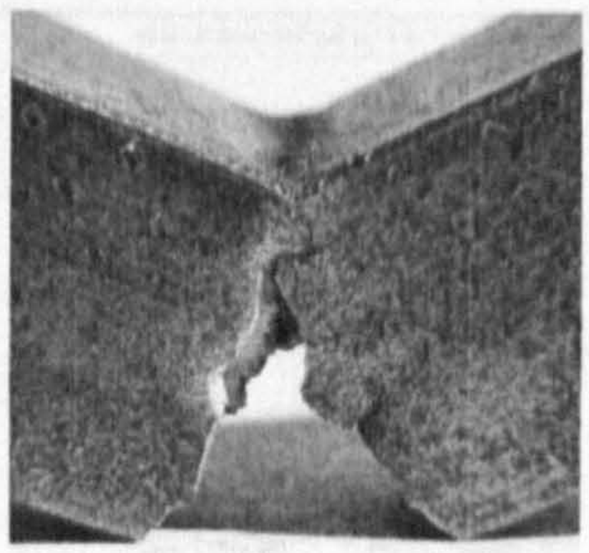

Plate 5.6: EN8 P11 011 Plate 5.7: EN1A P11 011 Plate 5.8: EN3B P11 012

The AE results from the 110% proof tests and their purported success at providing a trendable condition indicator can be described as mixed. Factors that affected the relative success are the ductility of the material and the comparative sensitivities of the sensors. These factors will be discussed in depth in the chapter section entitled "Investigation into the trendable nature of the AE from proof tests". At this point, however, a description of how the data was treated is given by way of an example and EN8 P11 01 is chosen to demonstrate the approach. The results shown for each specimen in the Appendix V are given as a suite of graphs, the significance of each graph is discussed here.

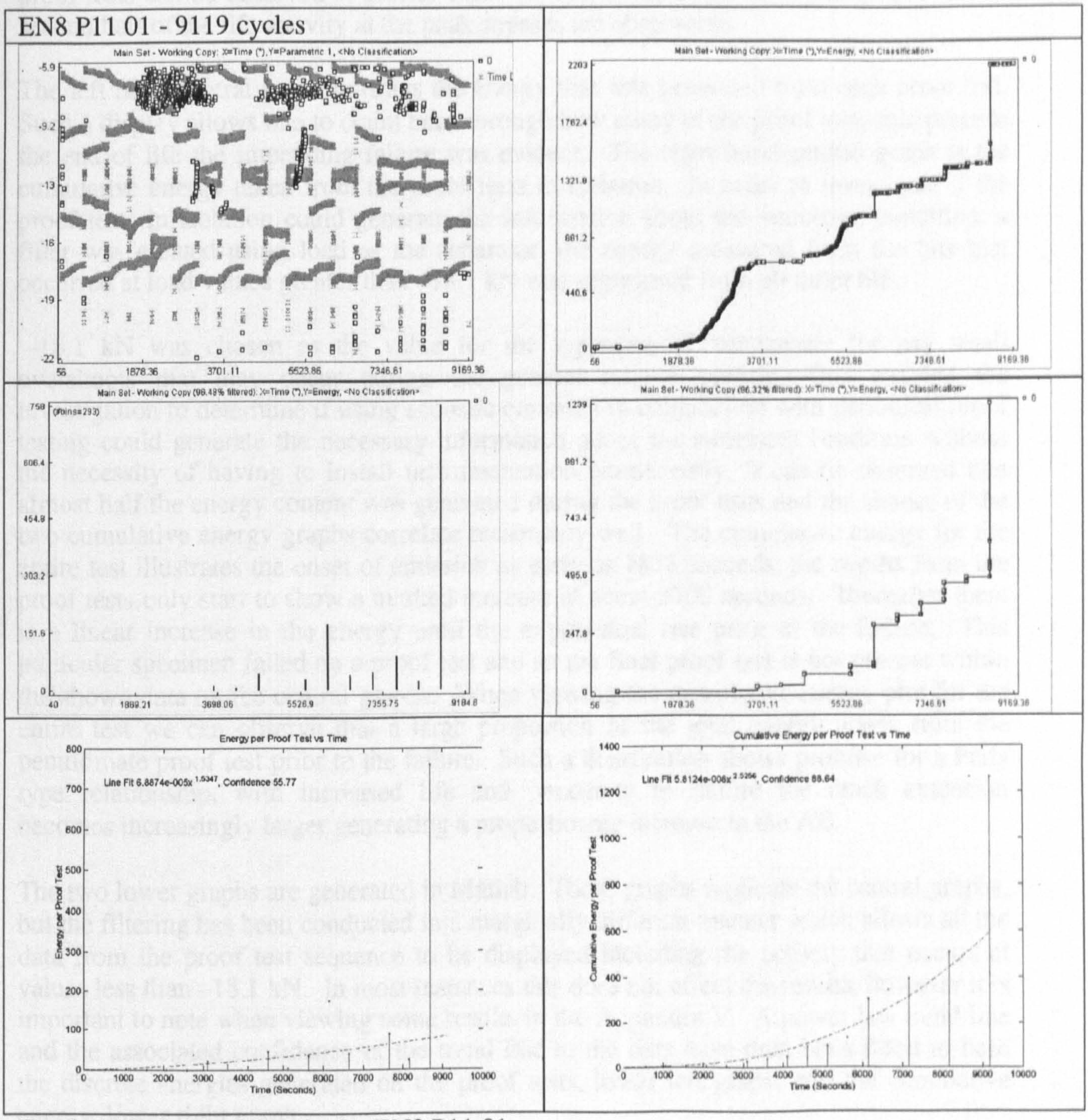

Graph 5.10: Suite of Graphs for EN8 P11 01

In the same fashion as the constant amplitude fatigue, the two uppermost graphs are the hit and time driven data and cumulative energy for the entire test. Again, on the load graph there are distinctive clusters at different load values, predominately at the base of the load cycle. The cumulative energy graph shows activity commencing at 1878 seconds, which increases and plateaus coincident in time with the clusters as illustrated in the upper left hand graph. In the final third of the life the activity increases in a stepped fashion, these steps emanate from the hits generated during the proof tests. The periodic

proof tests can be observed at greater than –19 kN, in the upper left hand graph. In the second half of the life activity at the peak stresses are observable.

The left hand central graph portrays the energy that was generated from each proof test. Such a display allows one to count back through how many of the proof tests that precede the end of life the impending failure was evident. The right hand central graph is the cumulative energy taken from the proof tests in isolation. In order to investigate if the proof tests in isolation could generate the information about the structures condition, a filter was created using load as the separator, the energy measured from the hits that occurred at load values greater than –18.1 kN was segregated from all other hits.

–18.1 kN was chosen as the value for the separator to compensate for any small overshoots that may occur during the general fatigue cycling. This enabled the investigation to determine if using acoustic emission in conjunction with periodical proof testing could generate the necessary information about the structures condition without the necessity of having to install instrumentation permanently. It can be observed that almost half the energy content was generated during the proof tests and the shapes of the two cumulative energy graphs correlate reasonably well. The cumulative energy for the entire test illustrates the onset of emission as early as 1878 seconds; the results from the proof tests only start to show a marked increase at about 3700 seconds. Thereafter there is a linear increase in the energy until the exponential rise prior to the failure. This particular specimen failed on a proof test and so the final proof test is not present within the shown data on the central graphs. When viewing the cumulative energy plot for the entire test we can observe that a large proportion of the total energy arises from the penultimate proof test prior to the failure. Such a distribution shows promise for a Paris type relationship, with increased life and proximity to failure the crack extension becomes increasingly larger generating a proportionate increase in the AE.

The two lower graphs are generated in Matlab. These graphs replicate the central graphs, but the filtering has been conducted in a marginally different manner which allows all the data from the proof test sequence to be displayed including the activity that occurs at values less than –18.1 kN. In most instances this does not affect the results, however it is important to note when viewing some results in the Appendix V. A power law trend line and the associated confidence of the trend line to the data have then been fitted to both the discrete energies generated on the proof tests, lower left graph, and the cumulative energy, lower right graph.

Such a result was typical of all specimens although the energy proportions between the proof tests in isolation and the cumulative energy for the tests entirety varied considerably. In some instances the proportion of total energy generated on the proof tests was very low. In general, it can be concluded that the information generated from the proof tests correlates well with emission generated through out the tests. (See Appendix V)

5.4.3 Cyclic fatigue with 120 % proof tests

Table 5.7 depicts the lifetimes for each material, which experienced the cyclic fatigue regime, but after every 500 cycles was subjected to two consecutive proof tests of 120% of the maximum cyclical value. For comparative purposes the final columns shows the average lifetimes of the specimens that experienced cyclical fatigue and cyclical fatigue with 110% proof tests. The average values of the number of cycles to failure for each type of fatigue are additionally shown graphically in graph 5.11.

Material	Specimen No.	No. Cycles to failure	Average Lifetimes for cyclic fatigue with 120% proof tests	Average Lifetimes for cyclic fatigue with 110% proof tests	Average Lifetimes for cyclic fatigue
EN8	P12 01	6584	6585	8341	6903
	P12 02	7092			
	P12 03	6079			
EN1A	P12 01	9541	9732	11966	11750
	P12 02	8613			
	P12 03	9625			
	P12 04	11148			
EN3B	P12 01	12669	13682	19157	20372
	P12 02	12669			
	P12 03	15709			

Table 5.7: Lifetimes from cyclic fatigue with 120% proof tests

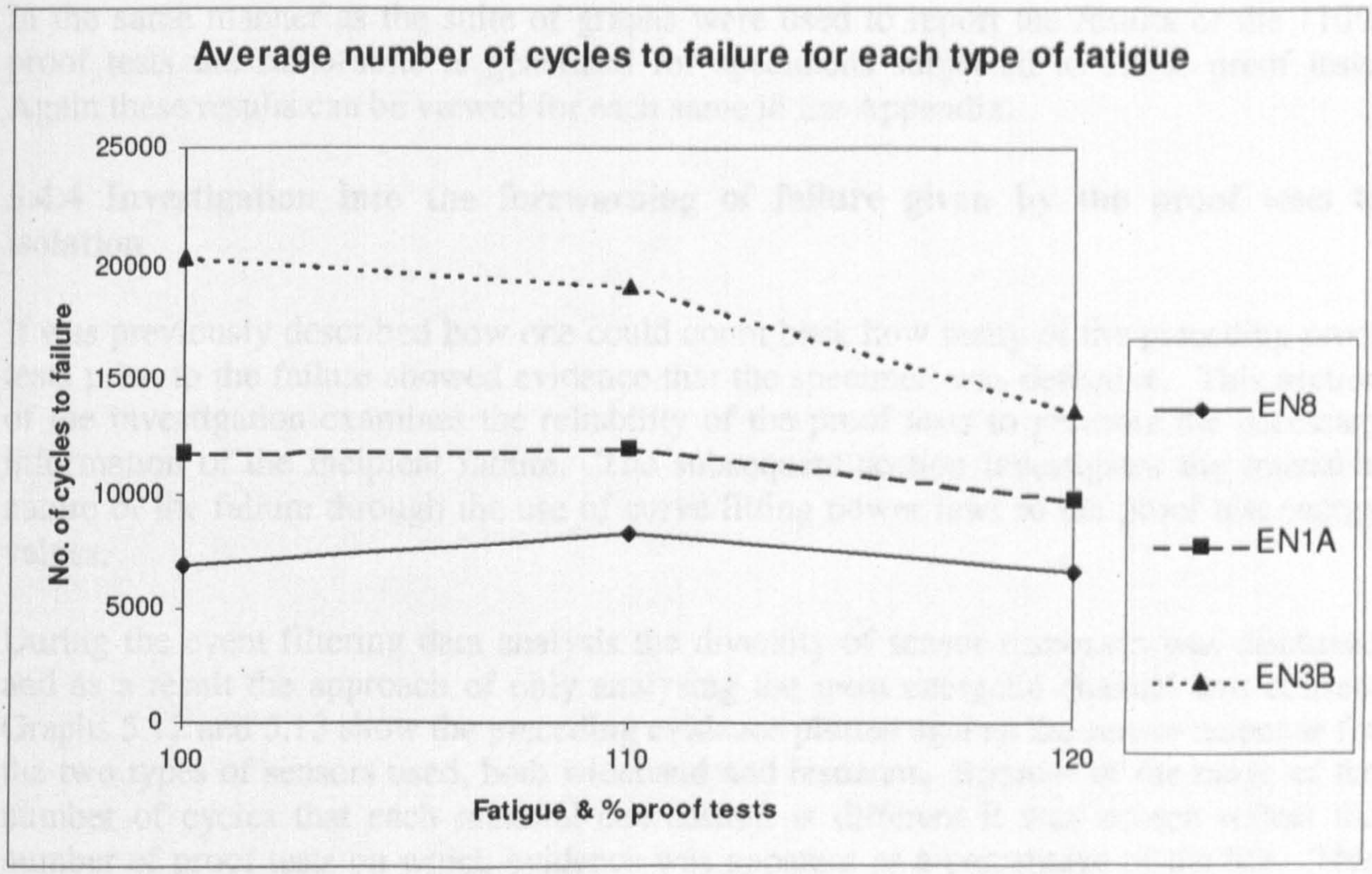

Graph 5.11: The average number of cycles to failure for each material for each fatigue type.

From these results, the effect of proof testing is shown to be detrimental to the longevity of the specimen; EN8 with 110% proof tests proves the exception. The magnitude of the proof test additionally has an effect, the greater the magnitude the more pronounced the effect on the life times.

The nature of the observable failure of specimens subjected to 120% proof tests is similar to those described in the 110% proof test grouping. The nature of the failure is ragged. Again for the three materials plates 5.9-5.11 are selected to demonstrate the irregular shapes of the failure.

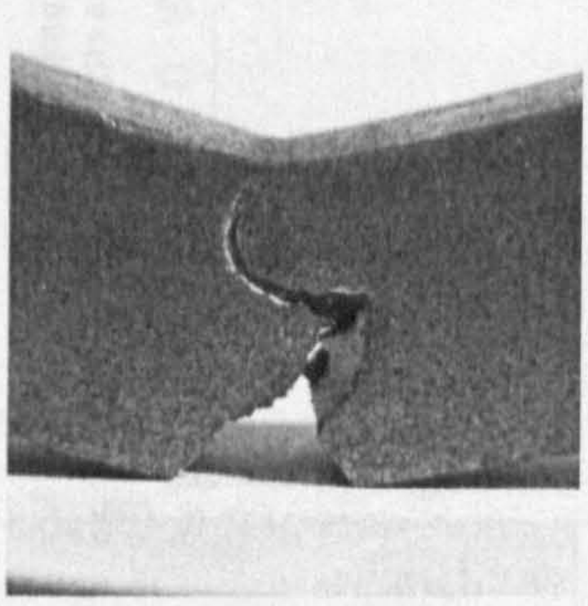

Plate 5.9: EN8 P12 02

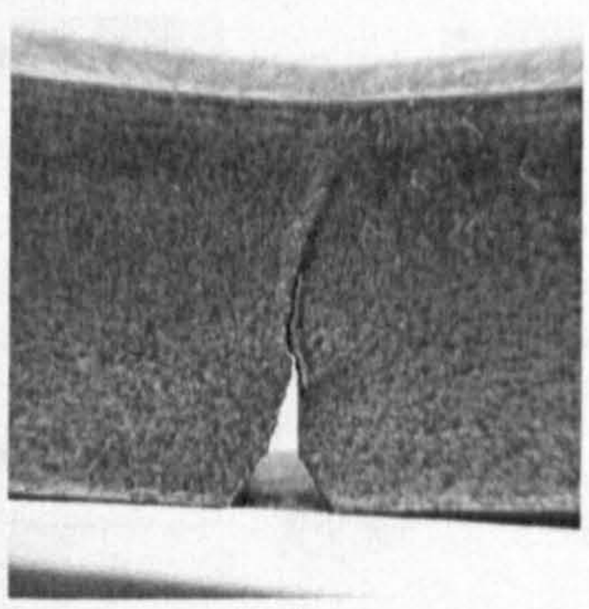

Plate 5.10: EN 1A P12 04

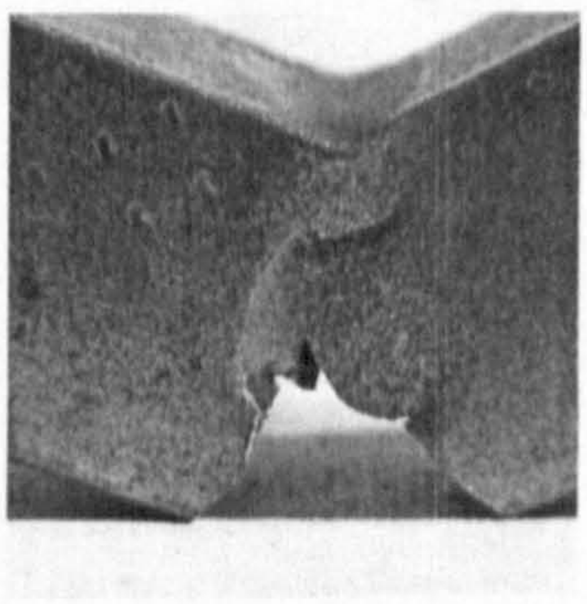

Plate 5.11: EN 3B P12 03

In the same manner as the suite of graphs were used to report the results of the 110% proof tests the same suite is generated for specimens subjected to 120% proof tests. Again these results can be viewed for each same in the Appendix.

5.4.4 Investigation into the forewarning of failure given by the proof tests in isolation

It was previously described how one could count back how many of the preceding proof tests prior to the failure showed evidence that the specimen was defective. This section of the investigation examines the reliability of the proof tests to generate the necessary information of the incipient failure. The subsequent section investigates the trendable nature of the failure through the use of curve fitting power laws to the proof test energy values.

During the event filtering data analysis the diversity of sensor responses was discussed and as a result the approach of only analysing the most energetic channel was chosen. Graphs 5.12 and 5.13 show the preceding evidence plotted against the sensor response for the two types of sensors used, both wideband and resonant. Because of the range of the number of cycles that each material can sustain is different it was chosen reflect the number of proof tests on which evidence was apparent as a percentage of the life. This ensured that EN3B, which may have reported evidence on twenty of the preceding proof tests prior to failure could be directly compared with EN8, which may have only reported evidence on eleven of its proof tests. In addition, the energy reported by the sensor for the three pencil lead breaks acquired during the instrument verification process were summed, averaged, and then within the sensor type grouping, normalised.

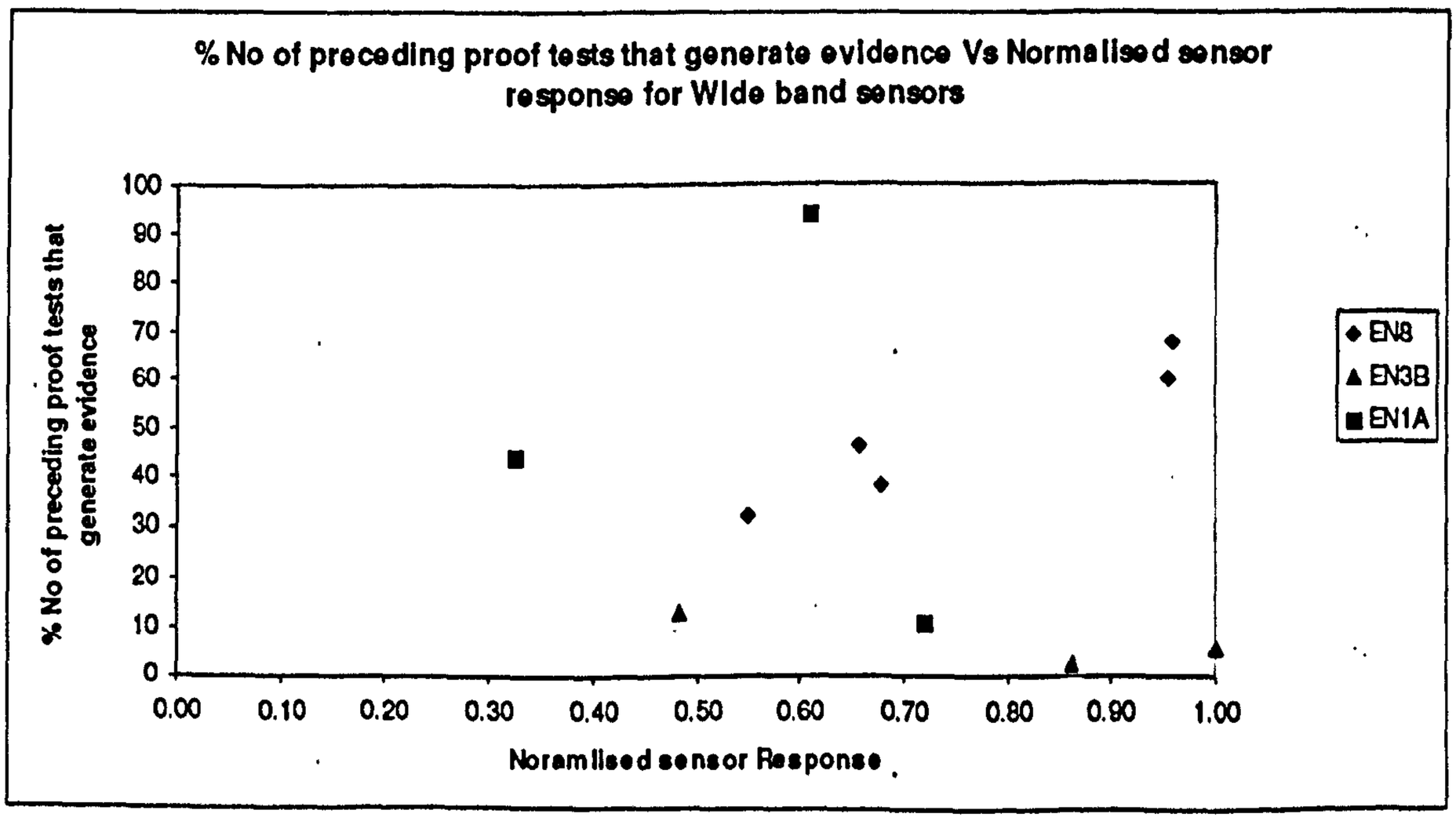

Graph 5.12: The degree of evidence generated by the normalised wideband sensors

The results of the normalisation illustrate that very little prior evidence is gained from the most ductile material EN3B, generally less than 10%. EN8 show diminishing evidence with decreasing sensor sensitivity. EN1A has an inexplicable result, in that the highest normalised sensor response generated the least evidence.

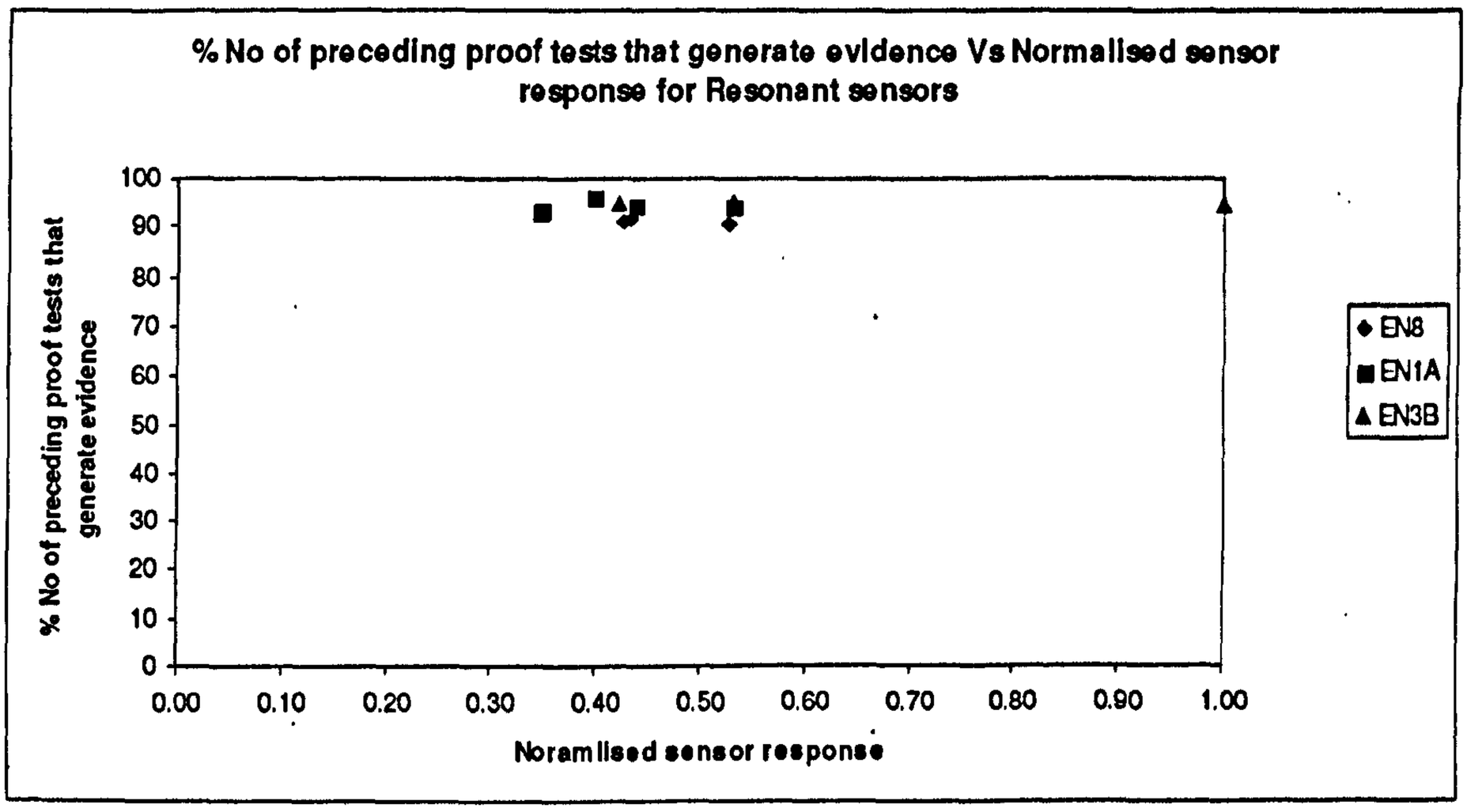

Graph 5.13: The degree of evidence generated by the normalised resonant sensors

When the results of the wideband sensors are compared with results generated using resonant sensors the percentage prior evidence given by the wide band sensors is comparably low, the results from the resonant sensors give in excess of 90% prior warning for all material types.

From these results the importance of the correct choice of sensor for effective detection of the degradation process is demonstrated. It is clear that the wide band sensors do not exhibit the effective frequency response to best achieve detection of the localised yielding and crack extension that occurs at the peak stress levels. The effect was most prominent in the ductile material, EN 3B, which only managed to show effective detection of the degradation at approximately 10% of the residual life.

5.4.5 Investigation into the trendable nature of the AE from proof tests

To all specimens that were subjected to proof tests a power law curve fit was applied and the confidence of the line fit to the data was calculated. Tables 5.8 – 5.10 illustrate the equations for each specimen with each material type groupings and the associated confidence. The confidence was generated using the statistical method of least squares. The constant and the exponent, to eight significant figures, have been extracted as separate columns in the table for ease of use. Both the confidence and the evidence generated from the number of preceding proof tests were then used to determine which

specimens would go for further analysis using a Scanning Electron Microscope. It was considered that the use of the microscope would assist in verifying the results and perhaps provide an explanation for any anomalous behaviour. The confidence is a measure of the effectiveness of the Paris type relationship. A high level confidence is indicative that the nature of failure is non-linear which becomes increasingly severe towards end of life.

Specimen No.	Power Law Equation	Confidence	Constant	Exponent
EN8 P11 01	6.8874e-005x^ 1.5347	0.56	0.00006887	1.53470600
EN8 P11 02	4.2098e-006x^ 1.8899	0.50	0.00000421	1.88991900
EN8 P11 03	2.0109e-006x^ 2.0398	0.66	0.00000201	2.03975500
EN8 P11 04	4.4035e-003x^ 0.9948	0.10	0.00440346	0.99483910
EN8 P11 05	7.2362e-001x^ 0.4650	0.02	0.72361550	0.46499610
EN8 P12 01	4.2689e-003x^ 1.4273	0.58	0.00426892	1.42734800
EN8 P12 02	1.2289e+000x^ 0.7162	0.49	1.22887500	0.71615780
EN8 P12 03	2.4143e-003x^ 1.5050	0.41	0.00241429	1.50499700

Table 5.8: Power laws for EN8

Specimen No.	Power Law Equation	Confidence	Constant	Exponent
EN1A P11 01	2.4967e-001x^ 0.5990	0.27	0.24967440	0.59902210
EN1A P11 02	3.0334e+000x^ 0.0236	0.00	3.03336600	0.02363801
EN1A P11 03	6.9964e+004x^ -0.9643	0.28	69964.07000000	-0.96433670
EN1A P11 04	5.3443e-001x^ 0.5302	0.39	0.53442770	0.53023300
EN1A P12 01	2.2951e-004x^ 1.6026	0.93	0.00022951	1.60265000
EN1A P12 02	2.5818e+003x^ -0.4634	0.28	2581.76800000	-0.46344540
EN1A P12 03	1.5653e+005x^ -0.9103	0.48	156532.10000000	-0.91025590
EN1A P12 04	1.4368e+000x^ 0.6402	0.79	1.43675200	0.64020000

Table 5.9: Power laws for EN1A

Specimen No.	Power Law Equation	Confidence	Constant	Exponent
EN3B P11 01	1.5229e-005x^ 1.3932	0.30	0.00001523	1.39324300
EN3B P11 02	1.5558e+000x^ 0.1012	0.00	1.55582400	0.10118150
EN3B P11 03	1.1838e+003x^ -0.3719	0.06	1183.81000000	-0.37185340
EN3B P12 01	8.1566e+002x^ -0.4287	0.27	815.65920000	-0.42872900
EN3B P12 02	7.5909e-002x^ 1.0128	0.88	0.07590919	1.01284900
EN3B P12 03	4.7348e+001x^ 0.2084	0.44	47.34834000	0.20836240

Table 5.10: Power laws for EN3B

The confidences expressed as a function of one are not particularly high. It is also apparent that there are some negative exponents, with correspondingly large constants. Viewing the graphs associated with these negative exponents, it is evident that there

occurred a proof test with a large energy content at some instance in the life which exceeded the penultimate proof test energy value. In such instances the power law fit yields an asymptote as opposed to the anticipated exponential increase. To enable further investigation the confidence, the exponent, the number of preceding proof tests that generated evidence as well as the normalised sensor response were graphed for each specimen. The constant was not plotted as the same information is contained within the exponent and therefore it would provide no further benefit. The evidence previously expressed as a percentage of the life was expressed as a function of one to permit a comparable scale. Such graphs permit all salient factors on a single display and the relative success can be observed for each sample. This served to determine which specimens should go on for further investigation with SEM. From each material type three specimens were selected for SEM, generally the best and worst confidences were selected supplemented by a further sample of which gave rise to inexplicable AE behaviour

The graphs for each material type are shown in graphs 5.14 - 5.16.

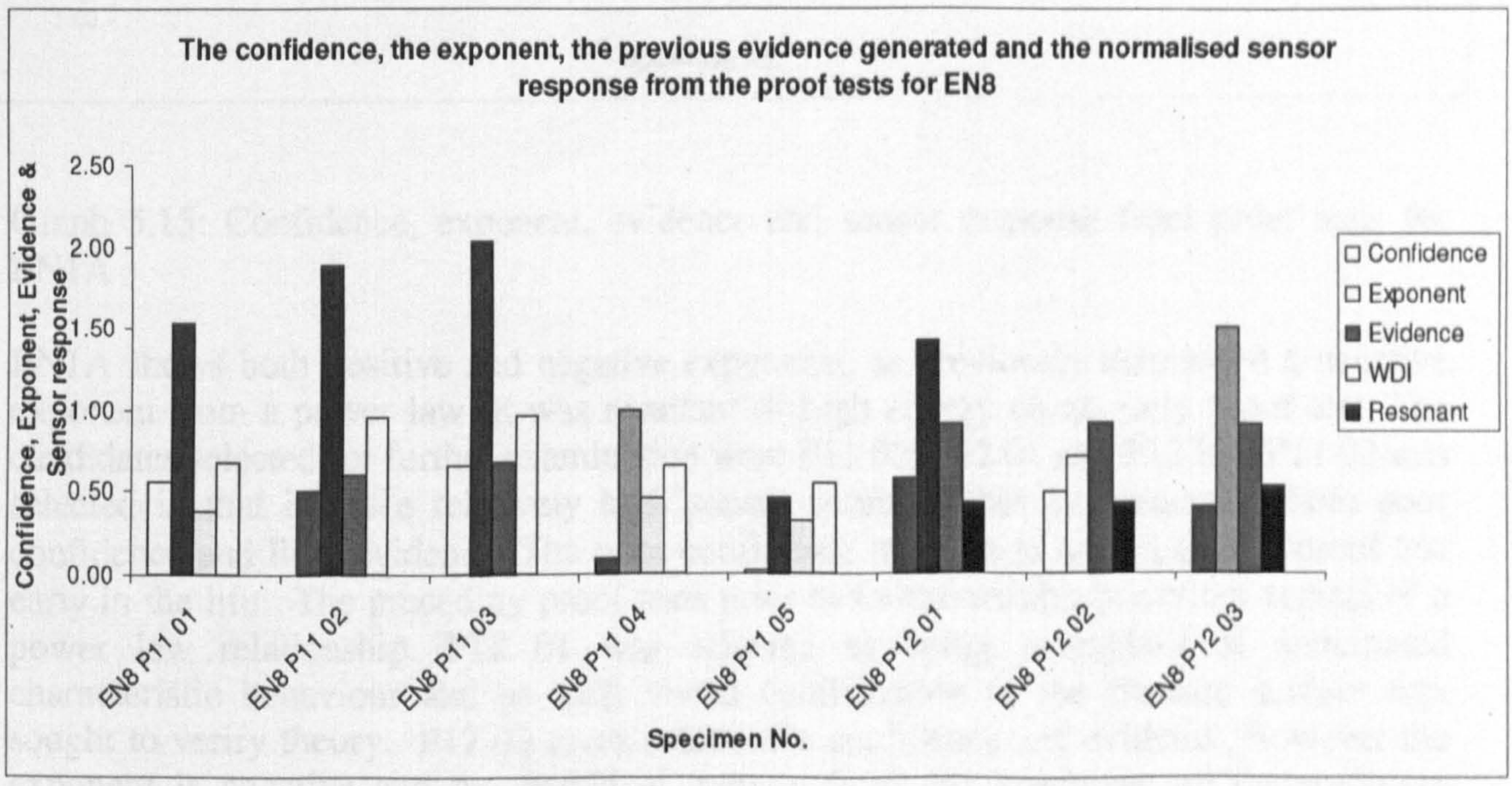

Graph 5.14: Confidence, exponent, evidence and sensor response from proof tests for EN8

Separate shadings depict the two sensor types to avoid drawing a direct correlation between them. Viewing initially the wideband sensors, P11 01-05, both the confidence of the line fit to the power law relationship and the evidence increase with increasing sensitivity. Once the sensitivity diminishes beneath a certain level the confidence falls off sharply. P11-03 gives the largest degree of both confidence and evidence and as such was selected to go for further investigation using the SEM. P11 04 shows a poor confidence, but acceptable evidence, examination of the graph illustrates the confidence is poor due to large energy on the fourth preceding proof test prior to failure. The SEM might detect an anomaly and explain such a cause. P11 05 gave both poorest confidence

and evidence and as an extremity of the data was additionally selected for further investigation.

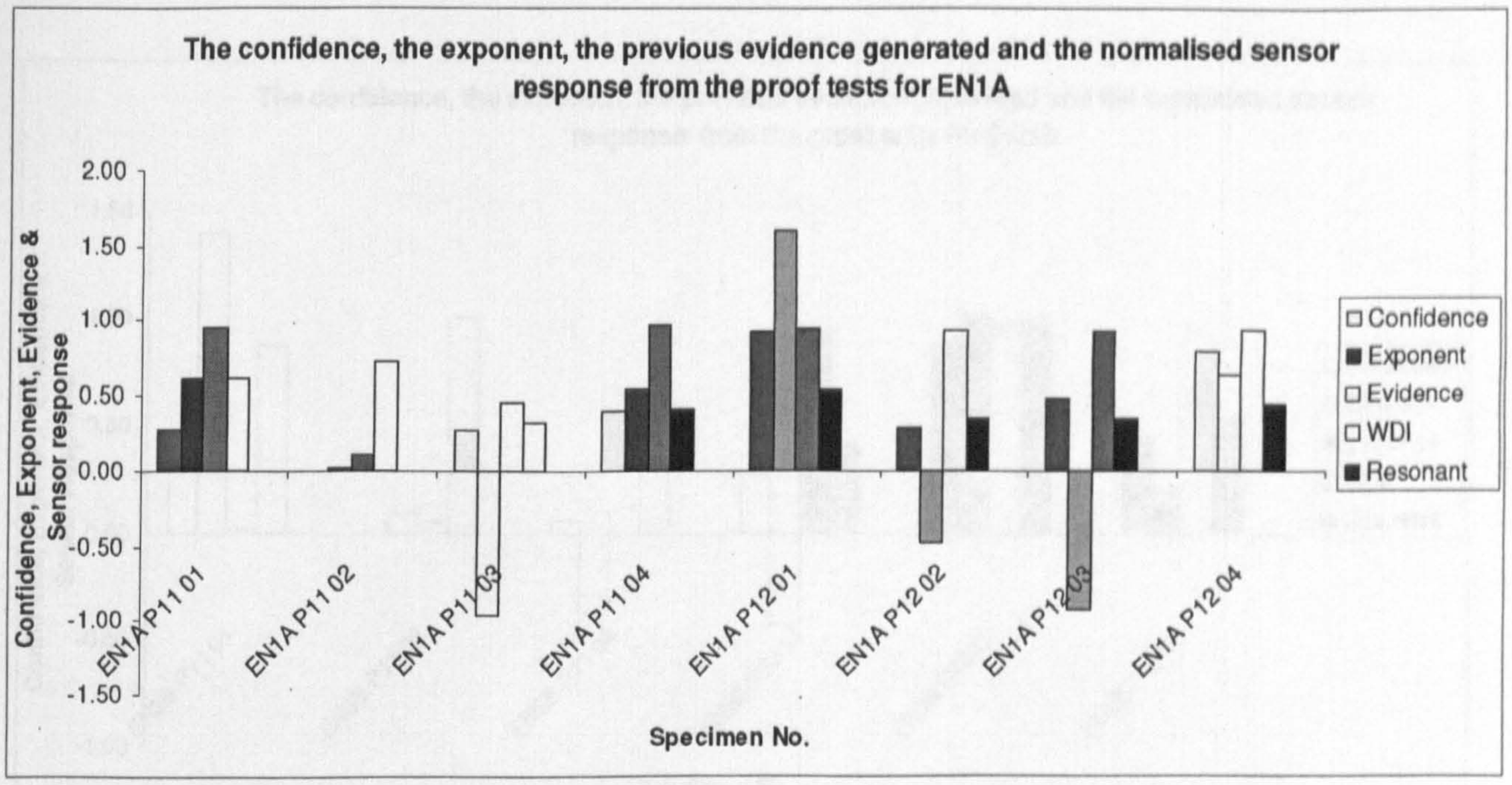

Graph 5.15: Confidence, exponent, evidence and sensor response from proof tests for EN1A

EN1A shows both positive and negative exponents, as previously mentioned a negative exponent from a power law fit was resultant of high energy on an early proof test. The candidates selected for further examination were P11 02, P12 01 and P12 03. P11 02 was selected in that it has a relatively high sensor response, but yet generated both poor confidence and little evidence. The poor confidence was due to a high energy proof test early in the life. The preceding proof tests prior to failure exhibit behaviour typical of a power law relationship. P12 01 was selected as being exemplary of anticipated characteristic behaviour and as such visual confirmation of the fracture surface was sought to verify theory. P12 03 gives reasonable confidence and evidence, however the exponent is negative and the graphical outputs from this specimen are extraordinary showing prolific activity at the beginning of life, which stabilises mid life before exhibiting failure characteristics that are considered normal.

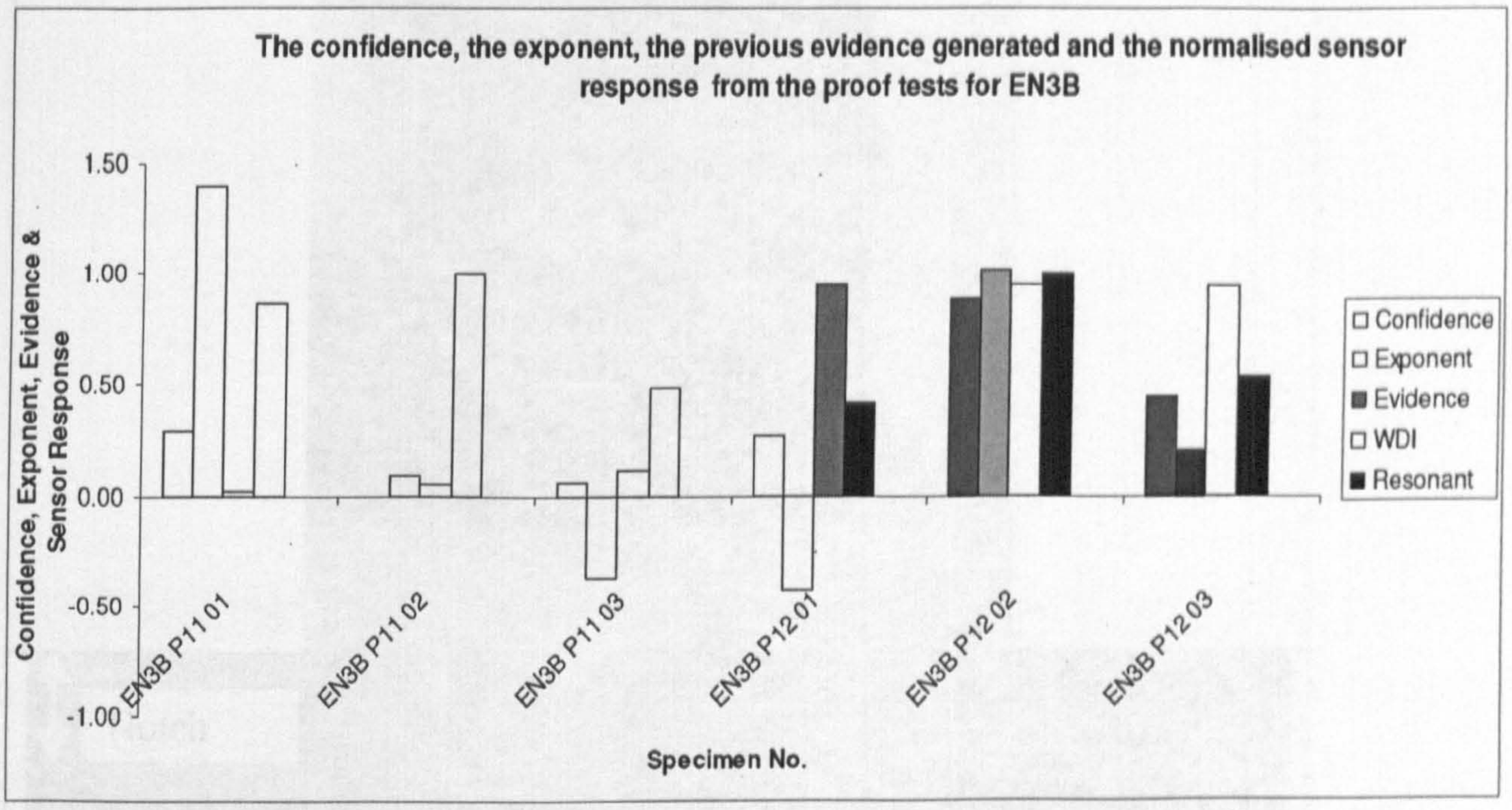

Graph 5.16: Confidence, exponent, evidence and sensor response from proof tests for EN3B

Again, negative exponents are observable in this material grouping. P11 02 was selected for further analysis on the basis that it generated very little evidence and a poor confidence although the sensitivity was high. P11 03 was selected due to the presence of a negative exponent and observation of its proof test graph shows the large mid-life energy event, which upset the power law fit. SEM may determine a local anomaly that would expose the reason. P12 02 was selected as having exemplary behaviour.

5.4.6 Scanning Electron Microscopy (SEM) results

Prior to discussing the results of the SEM a description of the methodology applied to each specimen is given. EN3B P12 02 is used as the example. Only the fatigue surface was examined as the AE generated was considered to emanate from only within such a region. Each side of the crack surface was examined at a magnification of 50. A white circle on the plate of the specimens fracture surface encapsulates the approximate area of the SEM image. The images shown here and within the Appendix section have had their size altered during formatting and therefore the images are not scaled to a 50x magnification. Such a magnification proved effective at creating a view of the depth of the fatigue surface. Obviously the higher the magnification used the smaller the visible area that can be examined at one time. Plates 5.12-5.14 demonstrate the approach.

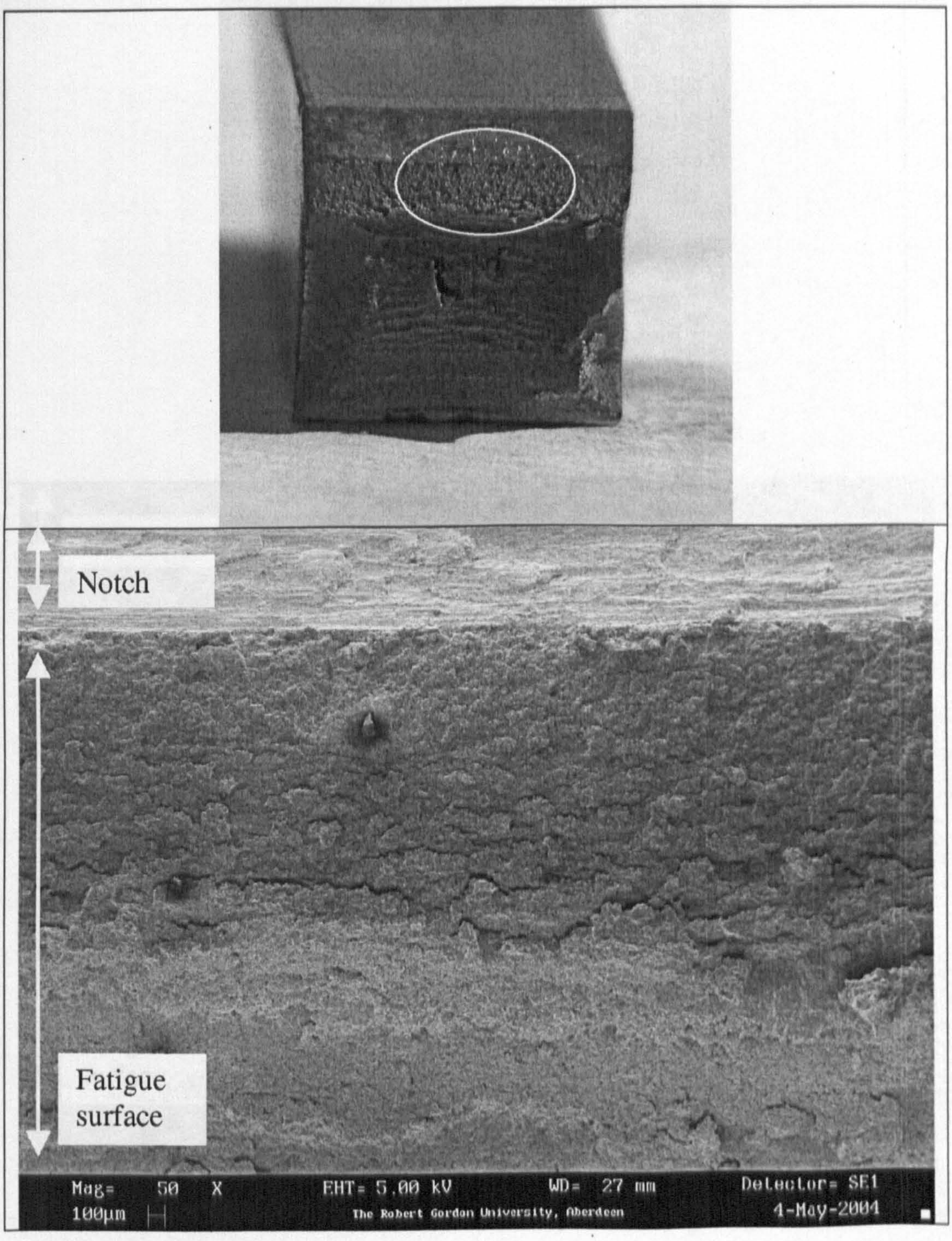

Plates 5.12: The fracture surface of one side of the specimen and the SEM image of the local fatigue surface

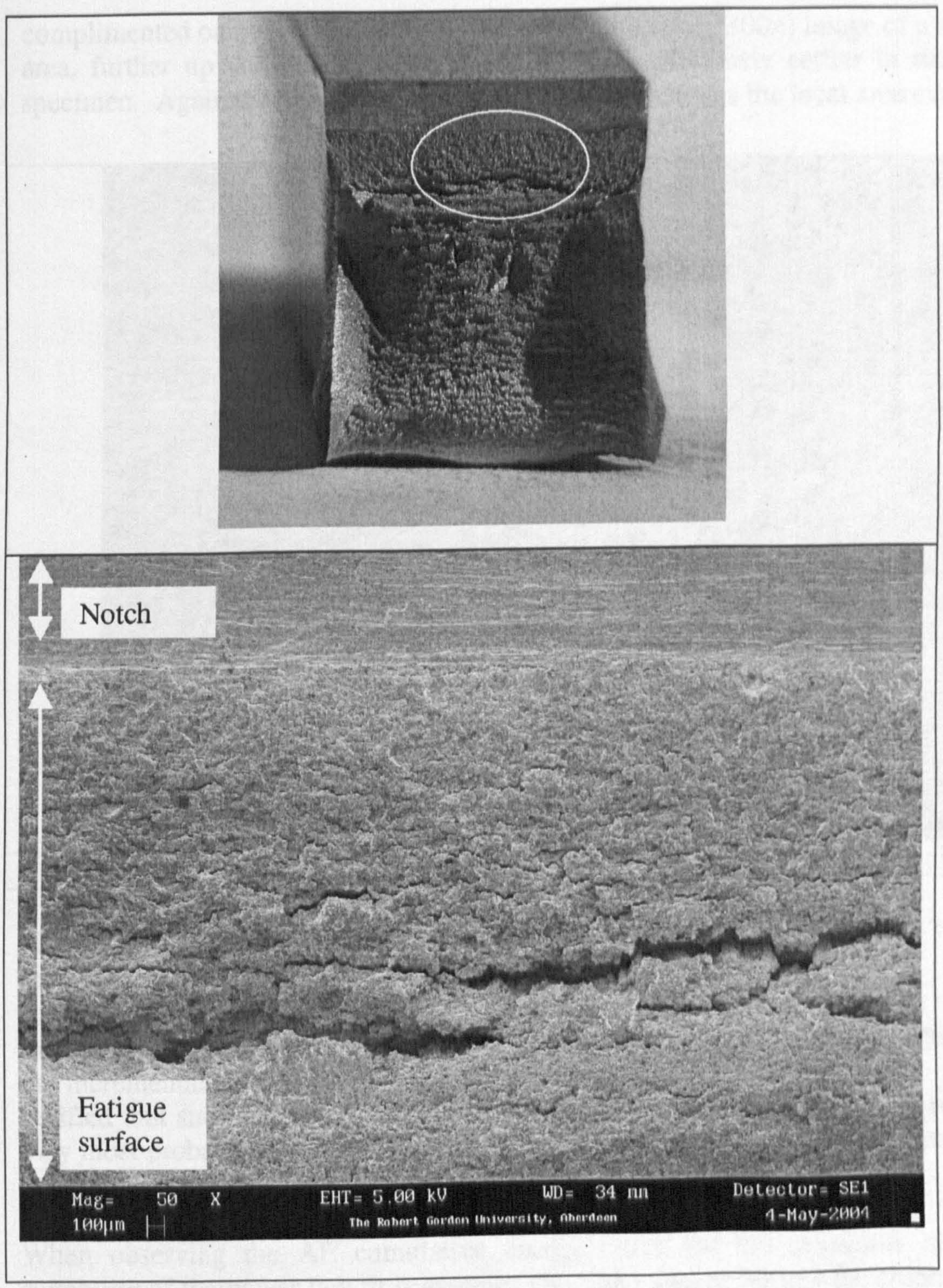

Plates 5.13: The fracture surface of the other side of the specimen and the SEM image of the local fatigue surface

In both SEM images, particularly the second, plate 5.13, lateral cracks can be observed across the depth of the fracture surface. These lateral cracks increase in their severity with increasing depth through the fatigue surface. Additionally the distance between these lateral cracks increases with increasing depth. A SEM split image was created, which on the left side has a 50x magnification showing the full fatigue surface depth and is

complimented on the right side by a greater magnification (300x) image of a smaller local area, further up and closer to the notch, which is obviously earlier in the life of the specimen. Again a white circle, on the left image, illustrates the local area examined.

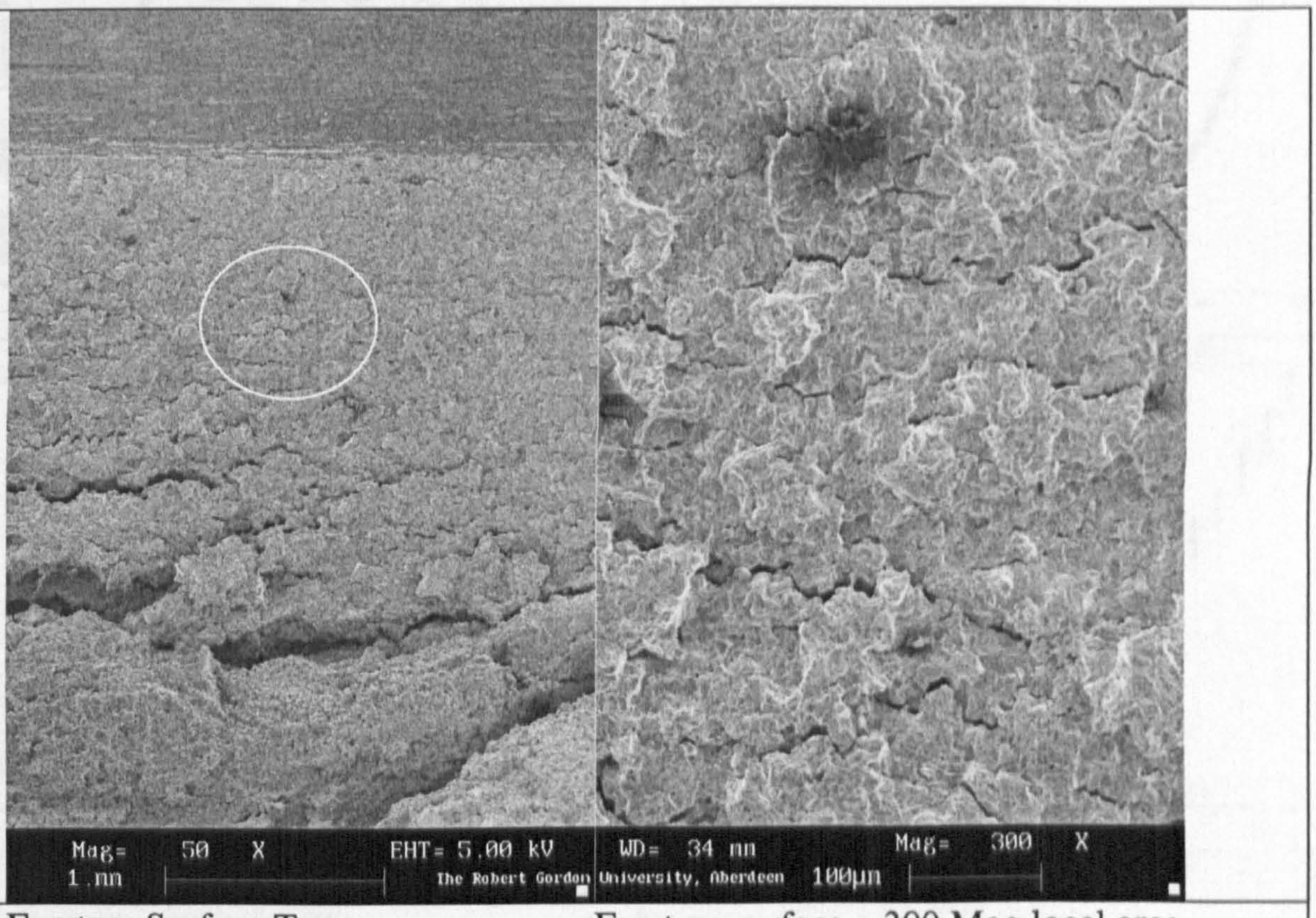

Fracture Surface Top | Fracture surface – 300 Mag local area

Plates 5.14: The fracture surface of one side of the specimen and the SEM image of the local fatigue surface

Lateral cracks are observable in the right image. These lateral cracks are considered to be the incremental extensions of the crack as it progresses during the fatigue. It cannot be verified that such extensions occurred during the proof tests although it is surmised that they most probably did as almost invariably the specimen failed during a proof test. This substantiates at least some extension occurs during the proof tests.

When observing the AE cumulative energy curve for this particular specimen the suitability of the power law fit is evident. The SEM images portray the crack extension is non linear, that is with increasing crack depth the extensions increase disproportionately. The confidence of the line fit for this particular specimen is good.

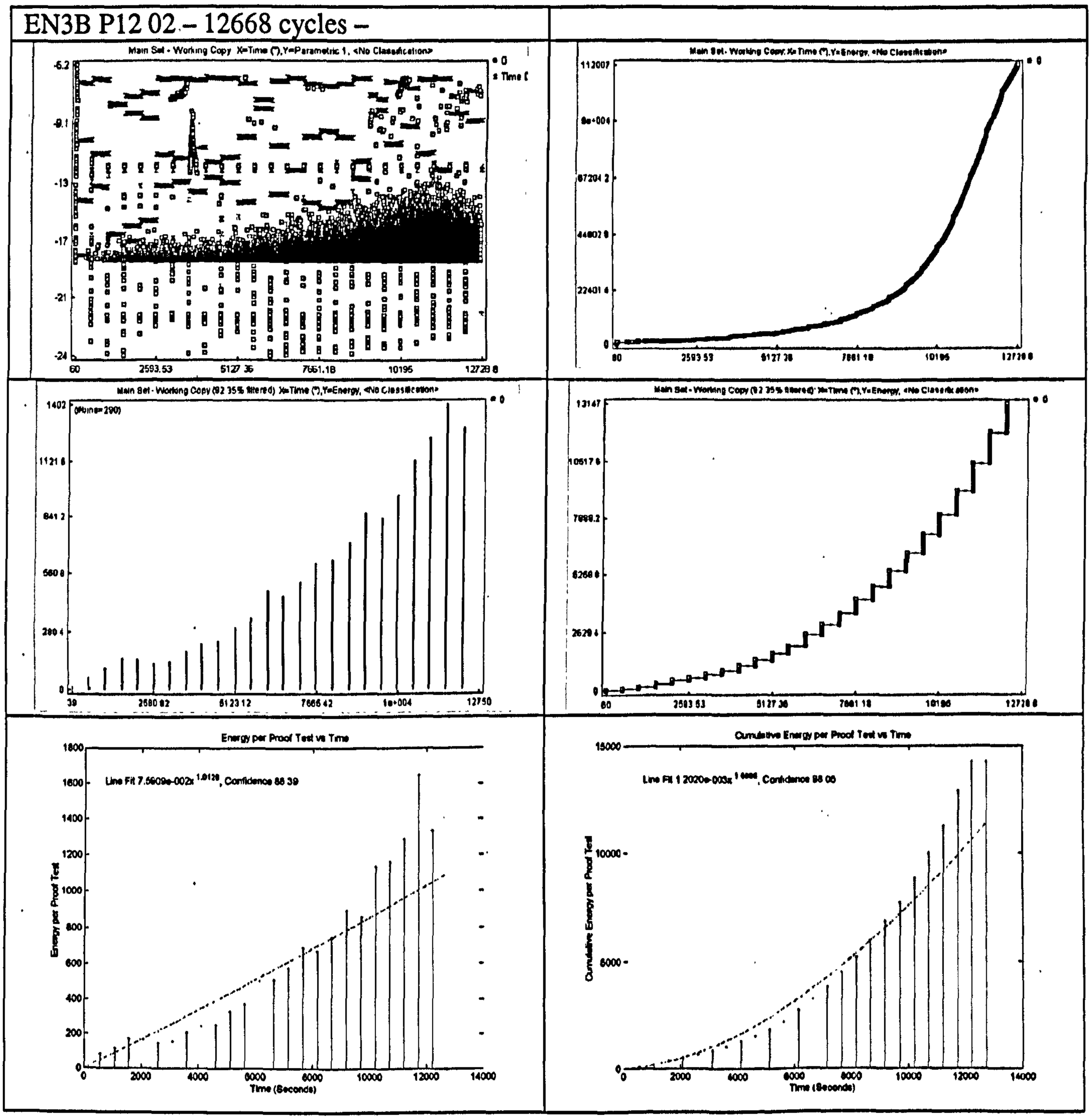

Graph 5.17: The AE results for EN3B P12 02

There follows a discussion of the results for each SEM. The SEM results for each specimen can be viewed in Appendix V alongside their associated suite of graphs.

Initially observable from the SEM results is the differences in the nature of the failure for each material type. The specimens selected from EN8 material group did not exhibit any appreciable lateral cracking. EN1A shows lateral lines of cracking as it progresses, which increase in their distance apart as the proximity to failure approaches. The same is

true of EN3B, the cracking is more pronounced most especially at the end of life where cracks are visible as quite considerable cavities.

EN8

EN8 P11 03
This specimen was selected for SEM as it illustrated anticipated behaviour and visual evidence was sought for confirmation. The fracture surfaces are unremarkable; there are the appearances of some small micro cracks that do not adjoin. The visual evidence that was sought to verify the anticipated behaviour was not substantiated in this specimen.

EN8 P11 04
There exists an energy burst that is not in keeping with anticipated behaviour in that the highest energy from the proof tests appears on the fourth preceding proof test prior to the failure. From the SEM, prior to the final failure there exists a quite considerable lateral crack that may be associated with the large inexplicable energy event that occurs at two thirds of the life.

EN8 P11 05
This specimen was selected for SEM because the evidence appears quite late in the life of the specimen and there exists a high energy proof test that appears early in the life which consequently upsets the curve fit. Obviously whilst conducting the SEM procedure indications for inexplicable activity was sought. Within EN8 P11 05 there was evidence on the high magnification of a crack high up on the fatigue surface and therefore early in life. The generation of such a crack may be associated with the early high energy proof test. Having conducted the SEM the reason suggested for the lateness of the evidence given in this sample is due to the insensitivity of the instrument for this test. This test was conducted with wide band sensors which have been previously shown to be not as effective as the resonant sensors and as such the evidence appears later in life as the energy released during the degradation becomes significant enough as to become detectable.

The notable feature of the SEM results for this material is the fairly limited amount of lateral cracking in comparison with the other materials.

EN1A

EN1A P12 01
Confirmation of anticipated behaviour was sought. The lateral cracks appear more pronounced with increasing depth within the fracture surface and equally the distance between them increases. Such an observation serves to confirm the applicability of a fitting a power law to proof test data.

EN1A P11 02
EN1A was selected for SEM as the evidence arrives late in life, although it does trend well. This is considered to be due to the comparative sensor response, which in this instance is 0.6 of the wideband sensor grouping and like the previously described EN8 P11 05, it is considered that there was insufficient energy in the formulation of the cracks to excite the sensor at these lower sensitivities. The lateral cracks increase in both severity and distance between them with increasing life.

EN1A P12 03
This specimen in the first part of the life generated extraordinary AE behaviour and visual evidence was sought for explanation. The SEM found a crack at the notch site that grew in transverse to the notch as opposed to in the direction of the induced stress concentration. Because this feature was found at the top of the fatigue surface it is considered that this was the source of the extraordinary AE behaviour.

EN3B

EN3B P12 02
Anticipated behaviour was exhibited by this specimen and as such it was subjected to SEM to attain visual confirmation of the results. The fracture surfaces exhibit pronounced lateral cracks that increase in severity at the base of the fracture surface. Equally the lateral cracks show an increase in the distance between them at these lower levels of the fatigue surface. Such an illustration serves well to substantiate the claim of fitting a power law for the trending of the degradation. Even on the high magnification of the surface close to the notch exhibits such characteristic.

EN3B P11 02
EN3B P11 02 exhibited evidence very late in life in fact evidence was only gleaned on the final proof test. The lateral cracks on the fracture surface, in comparison with the others within this material group, do not seem as pronounced as its companions. This could explain that the degeneration might not be as energetic to be detectable. The sensor was the best performing within the wideband sensor group and as such should have ensured such degradation would have been detectable. The SEM, high magnification exposes the increasing distance between lateral cracks with increasing proximity to the final fracture surface.

EN3B P11 03
Again this specimen was chosen due to its unanticipated and uncharacteristic AE behaviour. The largest energy event did not appear on the penultimate proof test but appeared approximately mid life, thereafter it did not appear to trend particularly well. Again, the value of the normalised sensor response was comparatively low. No evidence was found of any notable feature that may indicate a reason for the activity at the point of the mid life. The lateral cracks that are evident with SEM, again, show an increasing distance between them towards end of life.

5.5 Chapter Discussion and conclusions

One of the most observable features of this trial is the quietness of the defect growth. With the sensor in close proximity to the source, the progressive degenerative sources of the material have been reasonably difficult to detect. Initial detectability was determined through the use of a Hsu Neilsen lead break methodology. In almost all of the previously reported cases the average energy content of such sources were found to approximate 1000 energy counts. The sources of the degradation proved to be a fraction of such a value. It would be difficult to recommend this as an implemental industrial practise if it had not been previously reported that laboratory based specimens were notoriously quiet. The practise of AE as an NDT method used in the field benefits from environmental embrittlement of defects, as well as crack face friction and emissive corrosive and non-metallic substances captured within the defect during the fabrication process. [77]

This investigation has shown in all circumstances at least one of the preceding proof tests prior to the failure generated evidence of the structural condition. It was found that the amount of evidence given by the proof tests was a function of the sensor type and the comparable sensitivities between different tests. The use of resonant sensors generated the best evidence and the proof tests could forewarn of the defective condition on all specimens tested from almost the beginning of life on the materials tested. The wideband sensors failed to detect the deterioration with such notice and in the case of the most ductile material EN3B, the ability to forewarn of the failure was limited to the final 10 % of remaining useful life. The information generated from the proof tests in isolation can be used as a measure of the structural condition. The trendable nature of the evidence is obviously affected by the amount of evidence generated. A trend cannot be established from a single proof test prior to the failure. Where resonant sensors were used and considerable evidence generated throughout the life it was found that the information could be used as trendable condition indicator.

The confidence of the line fit was used as a measure of the success of fitting a power law relationship to the discrete energies released during sequential proof tests conducted during the life. In cases of high sensitivities with resonant sensors high confidence illustrated the suitability of the approach. In some instances a rogue energy proof test occurred in an uncharacteristic manner that affected the confidence. The origin of such uncharacteristic behaviours was investigated and through the use of the SEM a probable cause was identified in some circumstances. The SEM also verified that with increasing proximity to failure the distance between lateral cracks increased, as did their severity. Such an observation permits the conclusion of that the approach of fitting a power law to the discrete energies from sequential proof tests is an appropriate method.

Although no analysis or discussion was given to the cumulative curves created by summing the energies from the proof tests, such curves naturally take the shape of a power law and as such generate very much better confidences than fits to the discrete energies. They also minimise the effects of any anomalous behaviour as in no instance will they become produce the result of an asymptote.

It was found during these trials that proof testing was detrimental to the longevity of the specimens; no evidence was generated to support the claims of enhanced durability through the effects of load interactions. Some reasons as to why this might be the case include the fact the crack was never fully unloaded and therefore plastically induced crack closure effects were never permitted to act and the use of the square wave to apply the proof tests may additionally have had a derogatory effect.

In conclusion the effect of the proof test to facilitate the use of AE as a through life condition indicator is a compromise between having the available information to assess structural integrity and asset longevity. The frequency and magnitude of the proof tests should be limited to have the least detriment on the structure. The frequency and magnitude possible constitute a study in their own right.

CHAPTER 6: Conclusions and recommendations for further work

Chapter 1 framed the context in which the title and therefore the investigation was set. The objectives stated that load testing legislation was moving away from statutory testing on a regular basis and the onus of responsibility had shifted to the owner of the structure/equipment to ensure it's fitness for purpose and capability for safe operation. LOLER, dictates that it is a matter for the competent person to determine the necessity and nature of any load test. This work embarked upon enhancing the information that can be attained from a load test to enable informed decisions on asset safety.

The current industrial practices of maintenance were examined and Reliability Centred Maintenance was identified as the state of the art of industrial practices. RCM prioritises maintenance to the areas that are most likely to be problematic and ensures that the correct types of inspection and testing are matched to the established modes of failure. The available methods of inspection and testing which the competent person could draw upon were reviewed as well as failure modes for both metallic and composite structures. It was identified that for the fulfilment of a condition monitoring strategy for the assessment of mechanical structures a technique that was passive was favoured over techniques that involved active scrutiny of the structure using a point-by-point interrogation. Such a chosen approach could operate in conjunction with the load test and assist the competent person in empirically proving a structure.

Ultimately, in chapter 1 a decision matrix was formulated to address which particular inspection strategy was most appropriate for the successful identification of factors that contribute to a loss of strength in mechanical structures. Factors that were considered important were that the technique must be already accepted commercially as implementation would be otherwise difficult. It should have the proven ability to detect as many of the failure modes as possible, both in composite and metal materials. The technique should be capable of monitoring the structure in its entirety and should not have any adverse effect on the structure's future performance. It should therefore be non intrusive. The technique must exhibit the potential to detect information pertaining to the dynamic nature of failure and address the structures performance under its loaded condition. This was considered important, as it would permit discrimination between benign and malignant flaws. The information should lend itself to being stored as a permanent record and given the current environment data storage should be electronic. Non-subjective expert interpretation of outputs from the monitoring strategy was considered desirable to facilitate technology transfer. Finally, the technique itself should not present any health, safety or environmental issues.

Four techniques were found to be appropriate for condition monitoring mechanical structures, strain gauging, acoustic emission, thermography and shearography. Neither thermography nor shearography have existing standards to assist with their commercial acceptability and implementation. Strain gauging had the deficiency that the gauge detects the localised strain beneath its gauge length and the nature of failure of

mechanical structures is initiated from highly localised stress concentrations that propagate and ultimately contribute to catastrophic failure. The likelihood of being able to ensure that the gauge length lies over the local stress concentration was considered unlikely and as such the approach would fail to detect the mechanisms that ultimately contribute to failure.

A decision was reached that acoustic emission used in conjunction with periodic proof testing merited further investigation. The coupling of AE monitoring with the established industrial practice of proof testing may provide previously unavailable data to monitor structural integrity and provide the basis upon which a structure can be re-qualified for future service.

Chapter two examined more deeply the nature of failure of engineering materials. A conclusion was reached that structural engineering constructions have for the most part been fabricated from metal. The historic dependence on metal for the fabrication of engineering structures implies metal structures are closer to approaching the end of their design lives and would more readily benefit from any development in condition monitoring. The prevalent failure modes for such structures were identified as being corrosion, creep and fatigue. Fatigue was found to contribute to 90% of all structural failures and as such became the focus of the investigation latterly. A common theme of the failure modes, corrosion, creep and fatigue was that the nature of the deterioration was a progressive degradation of a localised area.

The sources of AE were examined and it was found that the sources of the elastic waves were attributable to the degradation processes that occur in engineering materials. Within the literature AE demonstrated a capability to detect the progressive deterioration of localised areas. The AE is a proportion of energy released during such deterioration. It was discussed that AE had the ability of AE to locate the origin of such sources. In principle, this permits AE to be used as a screening technique for the identification of structurally significant flaws, which can subsequently be investigated by complimentary techniques.

The phenomenon of the Kaiser effect was described and how under the maximum stress condition of a proof test has been used as a means of periodic re-qualification of structures. It was described how the AE is not only qualitative, but also quantitative as the amount of AE generated during the proof test is a measure of the damage severity. This could provide an enhancement to the AE being used simply as a screening tool.

The practices of load testing were examined and conflicting evidence presented on the perceived benefits. In some circumstances it appears that load testing may arrest crack growth and contribute to an increase in material durability.

A variety of evaluative techniques were discussed, a commonality of some of evaluative methods was the recognition the non-linear nature of the AE to determine the significance of defects. It was apparent that the deterioration of mechanical structures, particularly fatigue crack growth is a non-linear process to which engineering conducts the procedure

of fitting a power law to model crack behaviour. The use of the power law implies that with increasing crack length, the crack extensions that occur on subsequent load applications increase. It was postulated that as the AE energy is a component of the energy released during the deterioration the fitting of a power law to AE data might be appropriate for trending the degradation process of mechanical structures. If the power law could be applied to data that was acquired only periodically throughout the life of the structure it may be appropriate for the generation of a trendable conditional indicator. This would give the competent person a supplementary tool and when used in conjunction with a periodic proof test provides better information on the structural condition, without the necessity of permanently installed instrumentation.

The chapter concludes with the formulation of a programme of experimentation that sought to verify the applicability of the approach both in laboratory and field trials. Evidence was sought that AE generated during proof testing was symptomatic of a structural integrity threat. The investigation was focussed on determining if the AE was merely qualitative and as such would only permit its implementation as a screening technique or alternatively if quantitative assessment could be made.

Chapter three proved the qualitative and quantitative nature of AE during proof tests conducted on wire ropes with seeded faults in a laboratory environment. A series of wire ropes were subjected to a loading pattern that simulated normal operational conditions. The objective of this investigation was to demonstrate the methodology that could be used for the non-destructive evaluation of wire ropes, an example of lifting equipment to which LOLER is applicable. The tests sought to replicate the life of a typical rope. Initially, the rope was commissioned with the application of a pre-stressing proof load, prior to the rope going into service. The rope was then put into normal service during which the operator utilised the rope at the predetermined SWL for a specific usage period. Damage was introduced mid way through the life and thereafter it was assumed that the operator would continue to use the rope without any awareness of the inherent defect. A periodic proof test inspection took place in conjunction with Acoustic Emission monitoring and the condition of the rope determined from the AE.

The test results showed the concept could provide a means by which wire ropes could be non-destructively tested. The proof load when considered in isolation will prove a structure as it demonstrates that the structure has all inherent flaws less than the critical size. If critical flaws were present the excitation of the proof test would cause the rope to fail. When AE was used in conjunction with the industrial practice of the application of a proving load, flaws that did not necessarily result in the parting of the rope could be identified and their location established. Such flaws could then be subjected to further investigation. This investigation substantiated a qualitative assessment was given through the use of AE. This provides a significant enhancement to industrial practices. Defects that were not sufficiently large as to cause the failure of the rope during proof testing could be identified sooner and a decision on whether they were safe for continued use determined.

A near perfect correlation between the acoustic energy generated during the proof test and the amount of introduced damage was established, and it can be stated that for increasing damage severity there was a corresponding increase in the energy content of the emission. Evidence that AE was not only qualitative, but was also quantitative was achieved.

Chapter four took the study to applying the approach on structures in the field. A series of five case studies explore the use of AE on a variety of differing mechanical structures, mostly lifting equipment. The case studies were conducted on pad-eyes, link-plates, cranes, both Electrical Overhead Travelling and pedestal cranes and finally, an underwater vehicle pressure hull.

The chapter initially focuses on demonstration of the Kaiser principle on small load bearing components called pad-eyes, AE operating in the field is demonstrated. Emission was apparent both on the rising load and the falling load during all tests. A load reapplication resulted in no further emission, indicative that there was no stress redistribution due to the excitation of flaws. Whilst there were a few emissions on the load reapplication on some components these were not deemed to be significant.

It was observed there should not be any emission on the initial rising load due to the Kaiser Effect as the pad-eye has been previously load tested in this magnitude and direction. However, it is suggested that the Kaiser principle more than the Kaiser effect is more appropriate to the testing of this type of equipment. The practicalities of replicating an identical test condition are extremely difficult. It is likely there were minor changes from the previous test configuration in the manner in which the stress was applied previously.

The Kaiser principle states that if the stress is unprecedented then emission will result. It is considered that stress experienced on this load application was in fact unprecedented; the load application had never before been applied in this unique fashion, but had been applied in a manner broadly similar.

The items under test covered by this investigation show no indication of lacking structural integrity under a test condition of twice their anticipated operational load. It was apparent that the information pertaining to the structural behaviour is greatly enhanced by the use of AE.

Link plates are a hybrid pad-eye. The component was subjected to strain, load and AE measurement whilst load tested up to a proof load. The departure from elastic behaviour was simultaneously measured by both strain gauges and AE. The strain was resolved into principal stresses using Mohrs Circle. The onset of plasticity was observed with the strain gauge and a coincidence with bursts of AE. The strain gauge was discussed to be limited to the local measurement of the material behaviour immediately beneath the gauge and in this instance the use of AE was used in effect as a global strain gauge. It showed the capability of detection of a change in material behaviour from a location remote from the

area of interest. This case study demonstrates the capability of AE to detect localised yielding.

The investigation continued into the suitability of utilising AE in conjunction with periodic proof testing for the condition assessment of cranes. Nine Electrical Overhead Travelling (EOT) cranes were monitored by AE whilst subjected to initial commissioning proof tests. In all instances the anticipated behaviour of the Kaiser effect was observed demonstrating the use of AE to give a fitness for purpose assessment for equipment of this type. There is no previous documentary evidence that AE has been used for the assessment of cranes.

This is succeeded by a pedestal crane boom test. The boom was tested to destruction in order to investigate if AE could identify areas of concern that ultimately manifest themselves as the failure site. Post test analysis of the destruction test results appraised some of the AE evaluative methodologies determine the success of AE as not only a qualitative measure of structural integrity, but additionally quantitative. Four separate methods of evaluation were explored as a means of ascertaining the defect severity. The load test to destruction was applied in incremental steps with hold periods at each interval.

The evaluative techniques were applied at each load increment. The methods applied were the Felicity Ratio, Persistence, the β value and Intensity Analysis. Inspection after the destruction test showed one of the lattices was visibly buckled. All evaluation methods showed that they could be used as a means of trending or assessing the severity of degradation, but all with the exception of the intensity analysis exhibited an anomalous result at one of the load increments.

Ultimately chapter four concludes with a study on a pressure vessel with known fatigue cracks that were subjected to both static and dynamic testing whilst monitoring with AE. The fatigue cracks were sized pre and post the trial using Time of Flight Diffraction (TOFD). During the trial Alternating Current Potential Drop (ACPD) was used to detect any growth as it occurred. Such techniques were used to substantiate claims AE could detect a propagating defect.

The trial was designed to exercise the structure in the manner of its normal operations whilst monitoring AE.

The static test replicated an evolution to maximum anticipated depth pressure whilst the dynamic tests replicated 70 repetitive excursions to the maximum depth and return to surface dives with an equivalent straining rate experienced in service. During previous material property trials, fatigue cracks had been both initiated and propagated. The applied loadings were selected to enable crack growth.

During the static test, at the peak pressure, there suddenly occurred copious quantities of AE. The arrival of copious quantities of AE is more often than not attributable to either imminent failure or leakage during pressure testing. During the set up for the dynamic

test, which succeeded the static test a small seepage was observed on the top hatch pressure hull. With further investigation it was found that a threaded fitting in the upper part of the rig had stripped and had been the cause of leakage. The literature has often characterised leakage by a particular pattern. The inclusion of this in this work was to illustrate that AE can be used as a means to differentiate between different source mechanisms.

High amplitude hits were found to occur at top and bottom of the load cycle which tied in with the anticipated crack behaviour. The ACPD showed indicated crack growth at two sites of 0.6 and 0.5mm. The trials yielded successful results in the detection of activity from the crack behaviours, in that the anticipated crack behaviour correlated well with the AE. When the data was rigorously filtered, meaningful information used to identify the presence of cracks was obtained. When the AE is viewed in conjunction with ACPD results and the measurements attained with the ToFD it was clear that all three techniques concluded that crack growth occurred at two sites.

The case studies demonstrated that the use of AE in conjunction with a periodic proof test can be used as a means of defect detection on in-service mechanical structures. The evidence generated to this point supported the claim that AE in conjunction with periodical proof testing can identify flaws within a mechanical structure that will ultimately lead to failure, both in the laboratory and field trials.

However, it remained to investigate the robustness of the technique through the life of a mechanical structure, and as such the investigation returned to the laboratory. The objective to identify if periodical measurement of AE taken during the course of the life of the structure would repetitively generate information pertaining to the identification of the flaw as well as the severity of the flaw as it initiates and propagates through to failure. It was considered that to produce empirical data from the field would take a great many years as typically a proof test is only applied at given intervals.

Accelerated life tests were conducted to explore the feasibility of being able to forewarn of mechanical failure. It was felt that the accelerated life tests could additionally yield important information about the relative merits of proof testing.

Three material types were used during the investigation. The materials were chosen, as they were representative of structural steels used for fabrication of mechanical structures. Notched specimens were subjected to three point bending fatigue. All material types experienced the same fatigue regime and the effect on their lifetimes was investigated. The materials were subjected to three types of fatigue, sinusoidal constant amplitude fatigue, and sinusoidal constant amplitude fatigue punctuated every 500 cycles with periodic proof tests of 110% and 120%. The proof tests involved two consecutive load applications to 110% or 120% of the maximum compressive fatigue load with a square wave.

A power law was fitted to the data acquired during the proof tests. The use of a power law was considered appropriate due to the previously identified non-linear nature of

material failure. Because the AE is a component of the energy released during such progressive failure the investigation sought to determine the suitability of using such an approach for trending the degradation as a new means of condition assessment throughout the life of mechanical structures. As a means of verifying the results a Scanning Electron Microscope was used to visually examine the fracture surface. It was considered that increasing increments between striations on the fracture surface would demonstrate that with increasing crack severity the crack extensions would increase non-linearly.

During the data analysis it became apparent that two sources of AE were present. Closer investigation into these sources revealed a low amplitude banding was produced by material degradation at the peak stresses whereas the series of higher amplitude hits emanated from the crack face fretting. In some specimens the sensor response was sufficiently low as to fail to detect the deterioration, however in all data files the occurrence of the friction generated by the fretting was evident. Most frequently this source appeared close to end of life. These frictional sources served as a useful means for defect detection in that they give rise to comparably high amplitude hits, but were not useful for trending the degradation as they were a consequence of defect presence and not the deterioration mechanism.

In almost all cases a cumulative energy plot was created the shape of which was a gradual linear increase in the cumulative energy that subsequently becomes near vertical as proximity to failure approaches. Such a distribution supported the prospect that the fitting of a power law would generate a good fit.

The cracks created during fatigue with proof tests differed from the cracks created during the constant amplitude sinusoidal fatigue, they had the appearance of being more ragged with frequent changes in direction. This is considered to be due to difference in the nature of the applied stress during the proof tests. The crack must react more rapidly to the applied square wave, which was how the proof tests were applied.

From the results, the effect of proof testing was shown to be detrimental to the longevity of the specimen, however the most brittle material subjected to 110% proof tests proved exceptional to such a generalisation. The magnitude of the proof test was additionally found to influence the lifetimes, the greater the magnitude of the proof test the greater the reduction in the lifetimes.

Two parameters were used to assess the success of the trials, evidence and confidence. Evidence investigates how many of the proof tests that precede the end of life had hits that forewarn of the impending failure. Evidence is a qualitative measure of the effectiveness of AE in conjunction with Proof testing. It was found that the amount of evidence given by the proof tests was a function of the sensor type and the comparable sensitivities between different tests. The use of resonant sensors generated the best evidence and the proof tests could forewarn of the defective condition on all specimens tested from almost the beginning of life on the materials tested. The wideband sensors failed to detect the deterioration with such notice and in the case of the most ductile

material EN3B, the ability to forewarn of the failure was limited to the final 10 % of remaining useful life. The information generated from the proof tests in isolation can be used as a qualitative measure of the structural condition.

The confidence of the line fit was used as a measure of the success of fitting a power law relationship to the discrete energies released during sequential proof tests conducted during the life. In cases of high sensitivities with resonant sensors a high confidence illustrated the suitability of the approach. In some instances a rogue energy proof test occurred in an uncharacteristic manner that effected the line fit and therefore the confidence. The origin of such uncharacteristic behaviours was investigated and through the use of the SEM and a probable cause was identified in some circumstances. The SEM additionally verified that with increasing proximity to failure the distance between lateral cracks increased, as did their severity. Such an observation permits the conclusion of that the approach of fitting a power law to the discrete energies from sequential proof tests is an appropriate method of attaining a trendable condition indicator.

In conclusion the effect of the proof test to facilitate the use of AE as a through life condition indicator is a compromise between having the available information to assess structural integrity and asset longevity. The frequency and magnitude of the proof tests should be limited to have the least detriment on the structure. The frequency and magnitude possible constitute a study in their own right. Researchers investigating load interaction effects may benefit for the use of AE in that it will give an insight in to the material performance that was previously unavailable to them. A systematic study into differing material types, geometries and load test procedures could ultimately determine the optimal frequency and magnitude of proof tests that could be applied to mechanical structures to enhance longevity. Coupling enhanced longevity with a method of periodic condition assessment would ultimately provide a better comprehension of the behaviour and limit the risk of in-service structural failures.

Discussion regarding the nature of failure of engineering materials suggested that all failure modes could be non-linear and the use of a power law to trend the nature of failure may have more far reaching implications than merely the fatigue crack growth examined within this study.

REFERENCES

1. LOLER, "The Lifting Operations and Lifting Equipment Regulations" SI 1998/2307, 1998; Crown Copyright
2. The Shipbuilding (Lifting Appliances, etc, Forms) order 1961, SI 1960/431, 1960 Crown Copyright
3. The Construction (Lifting Operations) Regulations 1961, SI 1961/1581, 1961 Crown Copyright
4. The Offshore Installations (Operational safety, Health and Welfare) Regulations, SI 1976/1019, 1976 Crown Copyright
5. The Offices, Shops and Railway Premises (Hoists and Lifts) Regulations, SI 1968/849, 1968 Crown Copyright
6. The Lifting Plant and Equipment (Records of Tests and Examinations etc) Regulations SI 1992/195, 1992 Crown Copyright
7. Courney, S; "Condition monitoring – why it sometimes goes wrong" Insight Vol 43, No8, August 2001, pp 510 - 512
8. Moubray J; "RCM II, Reliability-centred Maintenance", Oxford, Butterworth, ISBN 0 7506 0230 9, 1992
9. Pheasy W, "The role Reliability-centred maintenance in the Defence industry" Training course, The Hatton, London, 2002
10. Allen T; "U.S Navy Analysis of submarine maintenance data and the development of age and reliability profiles" Fleet maintenance symposium, San Diego, USA, 2001
11. Duthie J.C; Robertson M.I; Clayton A.M; & Lidbury, D.P.G; "Risk-based approaches to ageing maintenance management" Nuclear Engineering and Design. No.184, pp 27-38, 1998
12. Croes K; Manca J; De Ceuninick W; De Schepper L; & Molenberghs G; "The time of guessing your failure distribution time is over" MicroElectronics Reliability Vol.38, pp 1187-1191, 1998
13. Iddings, F.A; "NDT: What, Where ,Why and When" 1997 http://www.asnt.org/techinfo/basics/oct97basics/oct97basics.htm
14. Witherall C.E; "Mechanical failure avoidance, Strategies and Techniques" ISBN 0-07-071170-4. McGraw Hill, 1997
15. Iddings, F.A; "Visual Inspection" http://www.asnt.org/techinfo/basics/oct97basics/oct97basics.htm
16. Lovejoy, D.J; "Penetrant testing – Part 1: The penetrant method in outline." Insight. Vol.41, No 5, pp 310-311, May 1999
17. Lovejoy, D.J; "Penetrant testing – Part 6: Potential sensitivities and limitations" Insight. Vol.41, No 10, pp 658-659, Oct 1999
18. Orton B.R; Copaul M; & Velez-Ospina C.E; "The potential use of infrared thermography to detect aircraft pressurisation leaks" Insight. Vol.41, No 3, pp 164-165, Mar 1999
19. Teletherm infrared, Image gallery 1998 http://homepage.eircom.net/%7Ethermalvision/page7.html
20. Gregory R; "Production inspection of Aerospace composites using laser shearography" Insight. Vol.44, No 4, pp 220-223, April 2002

21. Jones J; & Tyrer J; "An introduction to laser speckle strain imaging as a quantitative tool for structural NDT and lifetime prediction." Insight. Vol.45, No 4, pp 272-275, April 2003
22. Gregory, R; "Composite repair inspection using laser shearography" Insight. Vol.45, No 3, pp 183-185, March 2003
23. Hands. G; Dec 2003 http//www.hands-ltd.demon.co.uk/mag.htm
24. Chapman, R. "Magnetic NDE methods for pipeline inspection: a study of interacting defects" Insight. Vol.44, No 2, pp 74-78, Feb 2002
25. BINDT Yearbook 2004, ISSN 0952 2395. 2004
26. Stalenhoef J.H.J; & De Raad J.A; "MFL and PEC tools for plant inspection" Insight. Vol.42, No 2, pp 74-77, Feb 2000
27. Sophian A; Tian G.Y; Taylor D & Rudlin J; "Electromagnetic and eddy current NDT: a review" Insight. Vol.43, No 5, pp 302-305, May 2001
28. Hands. G; Dec 2003 http//www.hands-ltd. Demon.co.uk/mag.htm
29. Zhou J; Chen K; & Dover W.D; "Uniform ac field measurement in anisotropic bar and alternating current potential difference stress measurement" Institute of Physics, Journal of Physics D: Applied Physics, pp 1600-1604, 1999
30. Marques F.C.R; Martins M.V.M; & Topp, D.A; "Experiences in the use of ACFM for offshore platform inspection in Brazil" Insight. Vol.43, No 6, pp 394-398, June 2001
31. Halmshaw R; "Radiographic methods - Part 4 Standards for radiography" Insight. Vol.42, No 2, pp 103-105, Feb 2000
32. Burch S.F; "X ray computerised tomography for quantitative measurement of density variations in materials" Insight. Vol.43, No 1, pp 29-31, Jan 2001
33. Bach P; "Mobile neutron radiography systems and applications" Insight. Vol.42, No 4, pp 258-261, April 2000
34. Georgiou G.A; & Wooldridge A.B; "The basic principles, capabilities and limitations of ultrasonic NDT" Insight. Vol.43, No 3, pp 188-192, March 2001
35. Huang M; Jiang L; Liaw P.K; Brooks, C.R; Seely R. & Klarstrom L; "Using Acoustic Emission in fatigue and fracture materials research" Jom, Vol 50, No 11.
36. Cupo J.V; "Strain indicators with brittle coatings" Technical report – Westinghouse Electric Corp, Atomic power division, 1955
37. Chen T.; Chen T.F "Whole field digital measurement of isochromatics and isoclinics in photoelastic coatings" optics and lasers in Engineering 31, pp 325-338, 1999
38. Hoffmann K; "An introduction to measurements using strain gauges" Hottinger Baldwin Messtechnik GmbH, 1989
39. Prevey, P.S; "X-ray diffraction residual stress techniques" Metals handbook, American Society for Metals, pp 380-392, 1986
40. Young P.R & Collins D.S; "10 years of AE/MS Research at the URL (1987 –1997)" Ontario Hydro No: 06819-REP – 01200-0045- R00 http://www.live.ac.uk/seismic/pubs/19710yr.html
41. Waterweights "promotional literature"
42. Miller R; & McIntire P; "Non destructive testing handbook 2nd Ed Vol 5, Acoustic Emission" ISBN 0-931403-02-2, 1987

43. Callister W.D; "Materials Science and Engineering; An Introduction" Fourth edition Wiley and sons, ISBN 0-471-13459-7, pp 179, 1997
44. E 1067-85 Standard Practice for Acoustic Emission Examination of Fiberglass Reinforced Plastic Resin (FRP) Tanks/Vessels; 1985
45. Article 11, 'Acoustic Emission Examination of Fiber-Reinforced Plastic Vessels' Subsection A, Section V. Boiler and Pressure Vessel Code, 1983
46. Cole P.T; "The capabilities and limitations of NDT Part 7 Acoustic Emission" ISBN 0 903 132 08 7, 1988
47. Gere and Timoshenko "Mechanics of Materials" Third edition, Chapman and Hall, ISBN 0-412-36880-3, 1991
48. Varkoly L; "Fatigue crack tip closure" Zeszyty Naukowe politechni Opolskiej Nr kol 269, 2001
49. Harris; B & Bunsell A.R " Structural and properties of engineering materials" Longman, ISBN 0-582-44001-7 pbk, pp 239, 1977
50. Gordon J.E "Structures or why things dón't fall down" Clays ltd, St Ives plc. pp 64, 1978
51. Formby, C.L; "Desirability of proof testing reactor pressure vessels periodically" International Journal of Pressure vessels and Piping, Vol 19, Issue 1, pp 45-68, 1985
52. Shoup G.J; Tipton S.M; Sorem J.R; "The effect of proof testing on the fatigue behaviour of stud link chain" International journal of Fatigue, Vol 14, Issue 1, pp35-40, 1992
53. Dewicke D.S; Poe C.C; Newman J.C; & Harris C.E; "Evaluation of pressure proof test concept for thin sheet 2024-T3" Theoretical and Applied Fracture Mechanics, Vol 14, Issue 2, Pp 106 – 116, Nov 1990
54. Skorupa M; Schijve J; Skorupa A; & Machiewicz T; "Fatigue crack growth in a structural steel under single and multiple periodic overload cycles" Fatigue and Fracture of engineering materials and structures Vol 22, pp 879-887, 1999
55. Skorupa M; "Load interaction effects during fatigue crack growth under variable amplitude loading – a literature review. Part II; qualitative interpretation." Fatigue and fracture of engineering materials and structures Vol 22 Issue 10 pp 905, 1999
56. ASTM E610 –82 "Standard definitions of terms relating to Acoustic Emission"
57. Mathews J.R & Hay D.R; "Acoustic Emission Evaluation" Non destructive testing monographs and Tracks, Vol 2, 1981
58. Drouillard T. F; "A history of Acoustic Emission" Journal of Acoustic Emission Vol 14 No 1, 1996
59. Weavers M; "Fundamentals in Acoustic emission"; 22nd European conference on Acoustic Emission testing, Aberdeen, 1996
60. Physical Acoustics "Promotional literature"
61. Brown E.R. Reuben R.L & Steel J.A "Some approximate measurements of acoustic emission energy associated with dislocation motion". EWGAE 2000 24th European Conference on Acoustic Emission Testing
62. Heiple C.R & Carpenter S.H; "Acoustic Emission produced by deformation of metals and Alloys – A review : Part 1" Journal of Acoustic Emission Vol 6 No 3 pp177 –204
63. Vemvakousis A; Samoilis G; & Prassianakis A; "Microscopic origins of Acoustic emission" Insight Vol 44, No 1 Jan 2002

64. Heiple C.R & Carpenter S.H; "Acoustic Emission produced by deformation of metals and Alloys – A review: Part II" Journal of Acoustic Emission Vol 6 No 4 pp 215-237
65. Pollack A.A; "Acoustic emission Inspection" Metals Handbook" Ninth Ed, Vol 17, pp 278 –294,1989
66. Drouillard T. F; "A history of Acoustic Emission" Journal of Acoustic Emission, Vol 14 No 1, 1996
67. Pollock A.A "personal communication" 2001
68. Article 12, Subsection A, Section V, Boiler and Pressure Vessel Code "Acoustic Emission Examination of Metallic Vessels During Pressure Testing" December 1988 Addendum
69. ASTM E1930-97 "Standard test method for the examination of seamless, gas filled, pressure vessels using Acoustic Emission" 1997
70. ASTM F 914 "Test method for Acoustic Emission for Insulated Aerial Personnel Devices."
71. ASTM 569-82 Acoustic Emission Monitoring of structures during controlled stimulation, 1982
72. Fowler T.J; & Scarpellini R.S; "Acoustic Emission of FRP Equipment – I" Chemical Engineering, Oct 1980
73. SNT-TC-1A "Level II Course notebook" 2001
74. Fowler T.J; Blessing J.A; Conlisk P.J; & Swanson T.L; "The MONPAC System" Journal of Acoustic Emission, Vol 8, No3, pp 1-8, 1989
75. Association of American Railroads "Procedure for Acoustic Emission Evaluation of Tank cars and IM1010 Tanks" Issue 7, 1999
76. Pollock A.A; "Acoustic Emission Amplitude Distributions" International advances in Non destructive testing, Vol 7, pp215 –239, 1981
77. Pollack A.A; "Personal Communication" 1999
78. Leaird, J.D; "Acoustic Emission Training Guide – How to ensure an accurate and valid Acoustic Emission test" ISBN 1-890545-00-7, 1997
79. Morton T.M; Harrigton R.M; & Bjeletich J.G; "Acoustic emissions of fatigue crack growth" Engineering fracture mechanics Vol 5, Issue 3, pp 691-692, 1973
80. Harris D.O; & Dunegan H.L; "Continuous monitoring of fatigue crack growth by Acoustic emission techniques" Experimental Mechanics, Vol 14, No 2, pp 71-81, 1974
81. Roberts T.M; & Talebzabeh M; "Fatigue life prediction based on crack propagation and acoustic emission count rates" Journal of constructional steel research 59, pp 679 –694, 2003
82. Harris; D.O & Dunegan; H.L "Acoustic Emission Testing of Wire Rope" Materials Evaluation, Vol 15. pp. 79 –82, 1974
83. Pollock; A.A; Personal Communication. 1999
84. Casey; N.F & Taylor; J.L " Acoustic Emission of Steel Wire Ropes" Wire Industry. Vol. 51, No.601, pp. 79 –82, 1984
85. Casey; N.F & Taylor; J.L " Evaluation of Wire Ropes by AE techniques" British Journal of NDT. Vol. 27, No.6, pp. 351 – 356, 1985
86. Casey; N.F, Wedlake; D, Taylor; J.L & Holford; K.M. "Acoustic detection of Wire Rope Failure" Wire Industry. Vol. 52, No.617, pp. 307 –309, 1985

87. Casey; N.F, Taylor; J.L & Holford; K.M. "Wire Break detection during Tensile Fatigue Testing of 40mm wire Rope". The British Journal of NDT, Vol. 30, No.5, pp. 338 –341, 1985
88. Casey; N.F, White; H & Taylor J.L "Frequency Analysis of the signals generated by the failure of constituent wires of a wire rope" NDT International. Vol. 56, No.669, pp. 583 –586, 1989
89. Casey; N.F, & Laura, P.A.A. "A Review of The Acoustic Emission Monitoring of Wire Rope" Ocean Engineering. Vol. 24, No.10, pp. 935 – 947, 1997
90. Laura; P.A.A & Matthews J.R "Monitoring the status of a mechanical cable while in operation by means of Acoustic Emission method" Ocean Engineering. Vol. 12, No.3, pp. 211 – 219, 1985
91. Woodward; R.J "Detecting fractures in steel cables" Wire Industry. Vol. 56, No.667, pp. 401 – 405, 1989
92. Harrop; I. & Summerscales; J. " Acoustic Emission Testing of the Structural integrity of Multi-core Cable" British Journal of NDT. Vol. 31, No.7, pp. 383 – 386, 1989
93. ASTM E976-84 "Standard guide for determining the reproducibility of Acoustic emission response" 1984
94. ASTM E650-85 "Standard guide for mounting piezoelectric Acoustic emission sensors" 1985
95. Rogers L.M "Structural and Engineering monitoring by Acoustic Emission methods - Fundamentals and Applications" 2001
96. Bridges, J: 2002
www.metal2models.btinternet.co.uk